# Probable Maximum Precipitation Study for Texas

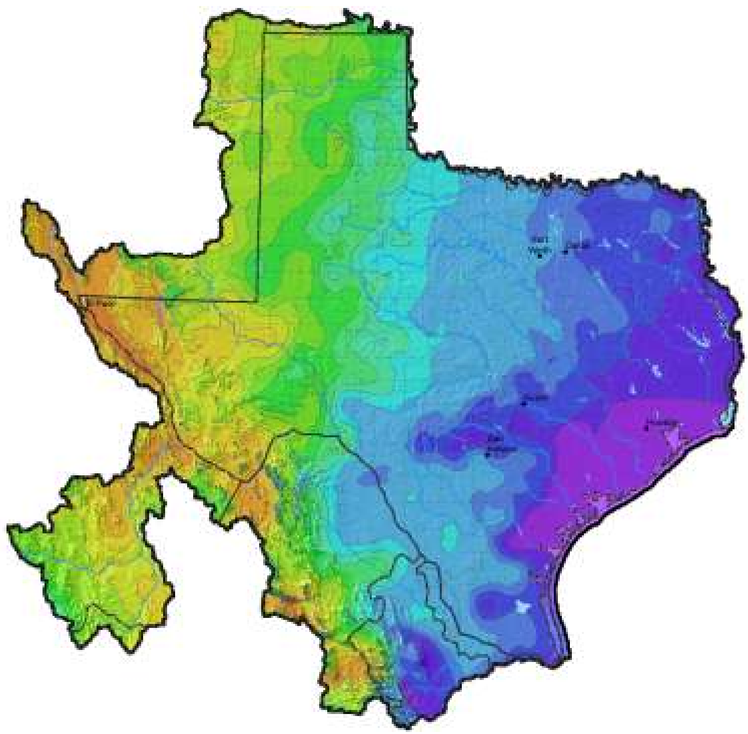

Prepared for

**Texas Commission on Environmental Quality**

Austin, TX 78711
(512) 239-5195
www.tceq.texas.gov/

Prepared by

**Applied Weather Associates, LLC**
PO Box 175, Monument, CO 80132
(719) 488-4311
www.appliedweatherassociates.com

Bill Kappel, Project Manager and Chief Meteorologist
Geoff Muhlestein, Senior GIS Analyst
Doug Hultstrand, Senior Hydrometeorologist
Dana McGlone, Staff Meteorologist
Kristi Steinhilber, Staff Meteorologist
Bryon Lawrence, Staff Meteorologist
Jacob Rodel, Staff GIS Analyst

**Setepmber 2016**

# Notice

This report was prepared by Applied Weather Associates, LLC (AWA). The results and conclusions in this report are based upon best professional judgment using currently available data. Therefore, neither AWA nor any person acting on behalf of AWA can: (a) make any warranty, expressed or implied, regarding future use of any information or method in this report, or (b) assume any future liability regarding use of any information or method contained in this report.

# Acknowledgements

The Texas Commission on Environmental Quality (TCEQ) would like to express sincere appreciation and thanks for the hard work and dedication of the entire staff of Applied Weather Associates, LLC.

The TCEQ would also like to acknowledge with much appreciation the review and feedback of the study's independent Technical Review Board comprised of Dr. John Nielsen-Gammon, Texas A&M University and Texas State Climatologist, Dr. William Asquith, United States Geological Society and Texas Tech University, Todd Marek, Natural Resources Conservation Service, and George Bomar, Texas Department of Licensing and Regulation and author of *Texas Weather*.  Important review and guidance was provided by Chuck McWilliams and Simeon Benson of the U.S. Army Corps of Engineers.

Furthermore, the TCEQ would like to express gratitude and thanks toward staff members from TCEQ Dam Safety Program.

Last but not least, the TCEQ would like to thank the Federal Emergency Management Agency for their financial contributions that made this study possible.

# Table of Contents

## List of Figures

# List of Tables

# Executive Summary

Applied Weather Associates (AWA) completed a statewide Probable Maximum Precipitation (PMP) study for Texas and immediately surrounding regions in New Mexico and Mexico. This study produced gridded PMP values for the project domain at a spatial resolution of .025 decimal degrees by .025 decimal degrees (approximately 2.5-square miles, on average). Variations in topography, climate, and storm types across the region were explicitly taken into account. A large set of storm data were analyzed for use in developing the PMP values. These values replace those provided in Hydrometeorological Reports (HMRs) 51 and 55A. The PMP values are valid for all times of the year, with no seasonality adjustment necessary for rainfall only scenarios. However, the tropical storm PMP will only occur from June through October, and local storm type producing PMP-level rainfall will only occur from April through October. General storm types producing PMP-level rainfall can occur anytime of the year.

Results of this analysis reflect the most current practices used for defining PMP, including comprehensive storm analyses procedures, extensive use of geographical information systems (GIS), explicit quantification of geographic effects, updated maximum dew point and sea surface temperature climatologies for storm maximization and transposition, and an updated understanding of the weather and climate throughout the region.

The approach used in this study follows the same philosophy used in the numerous site-specific, statewide, and regional PMP studies that AWA has completed since the early 1990's, utilizing the storm based approach to derive the PMP values. This also followed the general procedures used by the National Weather Service (NWS) in the development of the HMRs and the World Meteorological Organization (WMO) Manual for PMP determination. The storm based approach identified extreme rainfall events that have occurred in regions considered transpositionable to locations in the project domain. These are storms that had meteorological and topographical characteristics similar to extreme rainfall storms that could occur over any location within the project domain. Detailed storm analyses and adjustments were completed for the largest of these rainfall events. The adjusted storms were then transpositioned to appropriate regions across the project domain and used to define PMP.

Data, assumptions, and analysis techniques used in this study have been reviewed by the Project Review Board, the Texas Commission on Environmental Quality, the U.S. Army Corps of Engineers, and the Natural Resources Conservation Service (NRCS), all part of this study. Although this study produced deterministic values, it must be recognized that there is some subjectivity associated with the PMP development procedures. Examples of decisions where scientific judgment and uncertainty were employed include the determination of storms used for PMP development, maximization factors calculated for each storm, storm transposition limits, assumptions about maximum storm efficiency, and use of precipitation frequency climatology in the transposition calculations. For areas where uncertainties in data analysis results were recognized, conservative assumptions or choices were applied. All data and information supporting decisions in the PMP development process have been documented so that results can be reproduced and verified.

Sixty-eight extreme rainfall centers were identified as having characteristics representative of PMP-type rainfall that could potentially control PMP values at various locations within the project domain. Several storm events had multiple Depth-Area-Duration (DAD) zones (also referred to as Storm Precipitation Analysis DAD zones) that were used in the PMP determination process. This includes 25 general storm rainfall centers, 18 tropical storm rainfall centers, 19 local storm rainfall centers, three storm centers that were applied as both general and local storms, and three storm centers that were applied as both tropical and local storms. In total, 56 unique storms were included in the scope of this study.

Each individual storm center was analyzed using the Storm Precipitation Analysis System (SPAS), which produced several standard products, including hourly gridded rainfall, DAD values, mass curves, and total storm isohyetal patterns. National Weather Service (NWS) Next Generation Weather Radar (NEXRAD) data were used in storm analyses when available (generally for storms that occurred after the mid-1990's).

Standard procedures were applied for in-place maximization and horizontal moisture transposition adjustments (e.g., HMR 51 Section 2.3 and HMR 55A Section 5 and Section 8). New techniques and new datasets were used when justified in other procedures to increase accuracy and reliability by utilizing advancements in technology and meteorological understanding, while adhering to the basic approach used in the HMRs and in the WMO Manual. Updated precipitation frequency analyses were completed for this study. These were used with NOAA Atlas 14 precipitation frequency values where available to calculate the Geographic Transposition Factors (GTFs) for each storm. The GTF procedure replaces the so-called storm separation method (SSM) used by the NWS in the most recent HMRs. The GTF procedure, through its correlation process, provides quantifiable and reproducible analyses of the effects of terrain on rainfall by comparing precipitation frequency values at two locations. Results of these three factors (maximization, moisture transposition, and geographic transposition) were applied for each storm at each of the grid points for each of the area sizes and durations used in this study to define the PMP values.

Maximization factors were computed for each of the analyzed storm events using an updated dew point or sea surface temperature (SST) climatology representing the maximum moisture that could have been associated with each rainfall event. This climatology included the maximum average 3-, 6-, 12-, and 24-hour 100-year return frequency values for dew points and the +2 sigma (standard deviations) monthly average SST. The most appropriate duration consistent with the duration of the storm rainfall was used when applying the dew point climatology, a significant improvement over the use of the 12-hour persisting dew point process used in the HMRs. HYSPLIT model trajectories and NWS weather maps were used as guidance in identifying the storm representative moisture source regions.

To house, analyze, and produce results from the large datasets developed in the study, the PMP calculation information was stored and analyzed in individual Excel spreadsheets and a GIS geodatabase. This combination of Excel and GIS was used to query, calculate, and derive PMP values for each grid point for each duration for each storm type. For local/MCS storms, the durations pre-run and analyzed were 1-, 2-, 3-, 4-, 5-, 6-, 12-, 24-, 48-, and 72-hours. For general and tropical storms, the durations pre-run and analyzed were 1-, 2-, 3-, 6-, 12-, 24-, 48-, 72-, 96-, and 120-hours. Area sizes analyzed were 1-, 10-, 25-, 50-, 100-, 200-, 300-, 500-, and 1,000-square miles for local storms and 1-, 10-, 50-, 100-, 200-, 500-, 1000-, 10,000-, and 20,000-square miles for general and tropical storms. Although these specific durations and area sizes were analyzed, the geodatabase does allow PMP to be calculated at any area size and/or duration available in the underlying SPAS data.

When compared to previous PMP values provided in HMRs 51 and 55A, the updated values from this study resulted in a wide range of reductions at most area sizes and durations, with some regions resulting in minor increases. PMP values were highest near the coast and along the Balcones Escarpment in south-central Texas. These regions have exhibited past extreme rainfall accumulations that are the result of both moisture availability and topographic enhancement. Regions along and near the coast are also affected by coastal convergence processes which act to enhance lift and provide an additional mechanism for enhanced rainfall production versus other locations in the study domain. Minimum values were seen in the regions farthest from the moisture source regions (i.e. Gulf of Mexico and Gulf of California) and in areas with the least frequent frontal passages and infrequent tropical storm activity.

Region-wide on average, PMP values in areas covered by HMR 51 resulted in an 11% reduction after averaging all area sizes and durations. In regions covered by HMR 55A, the average reduction using 17 control points within the HMR 55A domain was 35%. Table E.1 provides the average percent difference from HMR 51 across each of the transposition regions analyzed within the HMR 51 domain. Figure E.1 provides a map of the transposition zones used in this study. Table E.2 provides the same comparison against HMR 55A values and Figure E.2 provides the control point locations used.

**Table E.1 Transposition zone average PMP percent difference from HMR 51 PMP at common area sizes and durations. Negative values represent a reduction from HMR 51. Reds signify reductions, greens signify increases.**

| Average PMP Percent Change from HMR 51 (by transposition zone) | | | | | | | | | | |
|---|---|---|---|---|---|---|---|---|---|---|
| Duration | Area | Zone 3 | Zone 4 | Zone 5 | Zone 7 | Zone 8 | Zone 9 | Zone 10 | Zone 11 | Zone 12 |
| 6-hour | 10-sqmi | -18% | -10% | -11% | -31% | -16% | -15% | -28% | -28% | -20% |
| 6-hour | 200-sqmi | -14% | -8% | -3% | -30% | -15% | -11% | -31% | -27% | -19% |
| 6-hour | 1,000-sqmi | -13% | -7% | -11% | -35% | -20% | -12% | -37% | -33% | -23% |
| 6-hour | 5,000-sqmi | -10% | -5% | 3% | -39% | -15% | -2% | -51% | -47% | -20% |
| 6-hour | 10,000-sqmi | -18% | -14% | -3% | -40% | -23% | -7% | -47% | -42% | -27% |
| 6-hour | 20,000-sqmi | -19% | -11% | -7% | -38% | -25% | -9% | -49% | -38% | -30% |
| 12-hour | 10-sqmi | -9% | -4% | -3% | -34% | -18% | -7% | -37% | -33% | -21% |
| 12-hour | 200-sqmi | -9% | -2% | -5% | -26% | -10% | -5% | -29% | -24% | -11% |
| 12-hour | 1,000-sqmi | -18% | -10% | -10% | -25% | -14% | -8% | -25% | -21% | -13% |
| 12-hour | 5,000-sqmi | -4% | 0% | 9% | -29% | -12% | 9% | -41% | -34% | -16% |
| 12-hour | 10,000-sqmi | -4% | 2% | 11% | -35% | -10% | 11% | -44% | -37% | -16% |
| 12-hour | 20,000-sqmi | -7% | 0% | 7% | -28% | -11% | 5% | -43% | -33% | -15% |
| 24-hour | 10-sqmi | -9% | -3% | -4% | -33% | -15% | -4% | -33% | -27% | -15% |
| 24-hour | 200-sqmi | -10% | -2% | -8% | -18% | -2% | -4% | -15% | -10% | 2% |
| 24-hour | 1,000-sqmi | -10% | -3% | -16% | -10% | 4% | -7% | -3% | 2% | 13% |
| 24-hour | 5,000-sqmi | -13% | -3% | -2% | -17% | -7% | 2% | -12% | -8% | -1% |
| 24-hour | 10,000-sqmi | -4% | 8% | 8% | -17% | 2% | 12% | -29% | -20% | 3% |
| 24-hour | 20,000-sqmi | 7% | 18% | 21% | -9% | 11% | 21% | -36% | -14% | 12% |
| 48-hour | 10-sqmi | -8% | -5% | -9% | -23% | -5% | -8% | -22% | -16% | -3% |
| 48-hour | 200-sqmi | 4% | 10% | -4% | -5% | 15% | 6% | -3% | 4% | 19% |
| 48-hour | 1,000-sqmi | -1% | 6% | -4% | -2% | 13% | 2% | 1% | 8% | 21% |
| 48-hour | 5,000-sqmi | -12% | -5% | 4% | -15% | -4% | 4% | -10% | -7% | 1% |
| 48-hour | 10,000-sqmi | -9% | 1% | 4% | -22% | -5% | 7% | -21% | -19% | -6% |
| 48-hour | 20,000-sqmi | -2% | 8% | 12% | -16% | 2% | 14% | -30% | -18% | 1% |
| 72-hour | 10-sqmi | -14% | -9% | -15% | -25% | -10% | -13% | -25% | -19% | -8% |
| 72-hour | 200-sqmi | -6% | 0% | -9% | -10% | 5% | -3% | -6% | -1% | 12% |
| 72-hour | 1,000-sqmi | -10% | -4% | -1% | -10% | 2% | 0% | -4% | 1% | 11% |
| 72-hour | 10,000-sqmi | -20% | -8% | 4% | -22% | -9% | 3% | -18% | -14% | -6% |
| 72-hour | 10,000-sqmi | -23% | -11% | -1% | -27% | -11% | -1% | -29% | -25% | -9% |
| 72-hour | 20,000-sqmi | -20% | -10% | -4% | -25% | -13% | -4% | -34% | -23% | -12% |

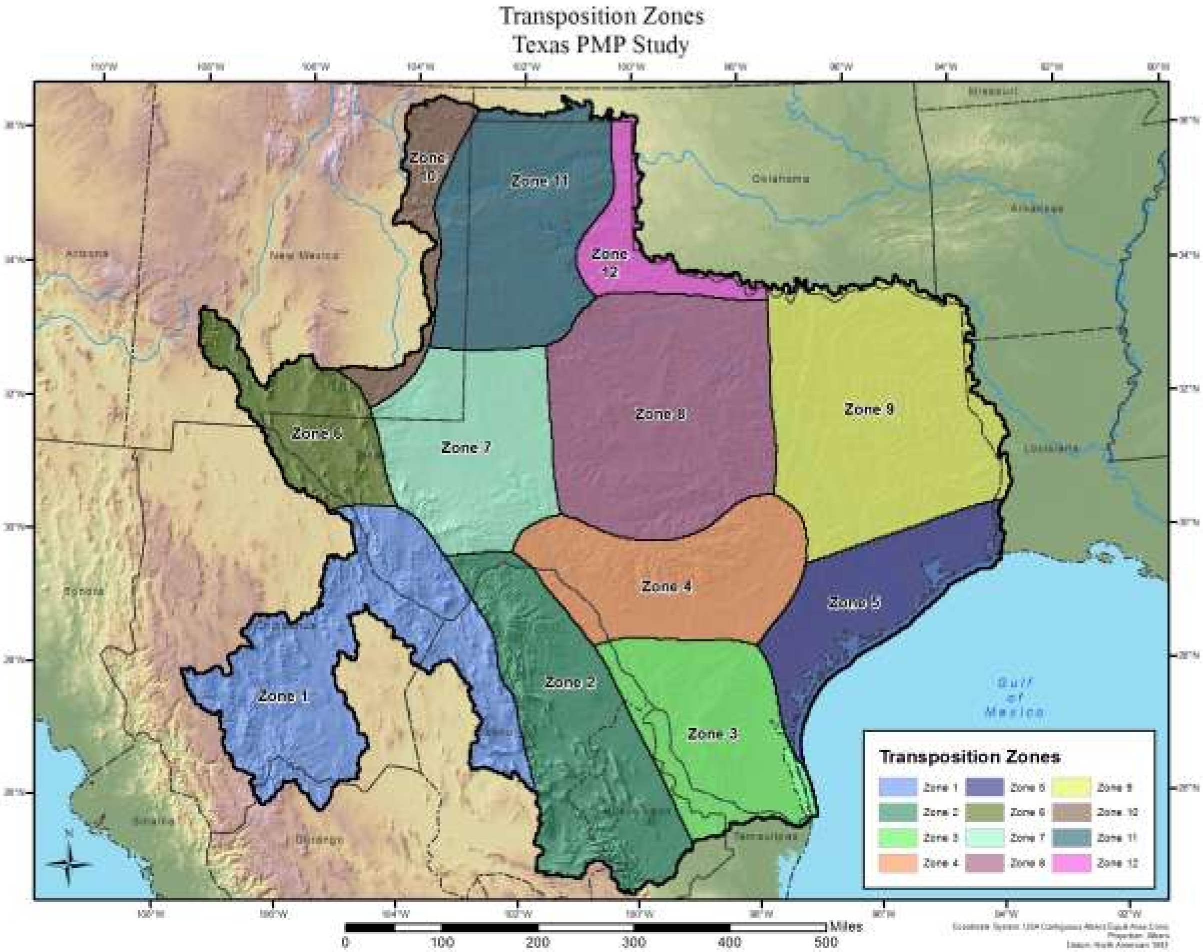


**Figure E.1 Transposition zones used during the PMP development process.**

**Table E.2 Control point PMP percent difference from HMR 55A PMP at common area sizes and durations. Negative values represent a reduction from HMR 55A.**

| Percent Change from HMR 55A PMP | | | | | | | |
|---|---|---|---|---|---|---|---|
| | | | | 1-hour | 6-hour | 24-hour | 72-hour |
| Point | Latitude | Longitude | Zone | 1-mi$^2$ | 10-mi$^2$ | 10-mi$^2$ | 10-mi$^2$ |
| 1 | 29.50° | -104.00° | 1 | -54.2% | -41.0% | -44.1% | -38.0% |
| 2 | 29.50° | -103.25° | 1 | -53.0% | -38.6% | -40.1% | -33.8% |
| 3 | 30.50° | -104.50° | 1 | -54.9% | -41.4% | -40.9% | -35.0% |
| 4 | 30.50° | -103.25° | 7 | -51.2% | -31.1% | -33.1% | -26.3% |
| 5 | 31.50° | -105.75° | 6 | -42.6% | -20.0% | -17.1% | -8.9% |
| 6 | 31.50° | -104.50° | 6 | -53.3% | -38.9% | -36.9% | -30.3% |
| 7 | 31.50° | -103.25° | 7 | -65.3% | -44.4% | -46.0% | -37.8% |
| 8 | 32.50° | -107.00° | 6 | -38.9% | -25.0% | -28.2% | -22.1% |
| 9 | 32.50° | -105.75° | 6 | -51.7% | -31.1% | -27.9% | -21.3% |
| 10 | 32.50° | -104.50° | 10 | -53.9% | -38.6% | -34.6% | -27.4% |
| 11 | 32.50° | -103.25° | 7 | -51.9% | -21.4% | -19.7% | -10.8% |
| 12 | 33.25° | -107.50° | 6 | -38.2% | -25.7% | -29.8% | -24.3% |
| 13 | 33.75° | -103.25° | 11 | -52.3% | -37.1% | -31.0% | -22.6% |
| 14 | 35.00° | -104.00° | 10 | -52.8% | -27.5% | -35.1% | -26.7% |
| 15 | 35.00° | -103.25° | 11 | -53.8% | -39.0% | -34.7% | -24.7% |
| 16 | 36.25° | -104.00° | 10 | -45.1% | -33.9% | -38.7% | -31.2% |
| 17 | 36.25° | -103.25° | 10 | -33.1% | -22.0% | -30.4% | -21.6% |

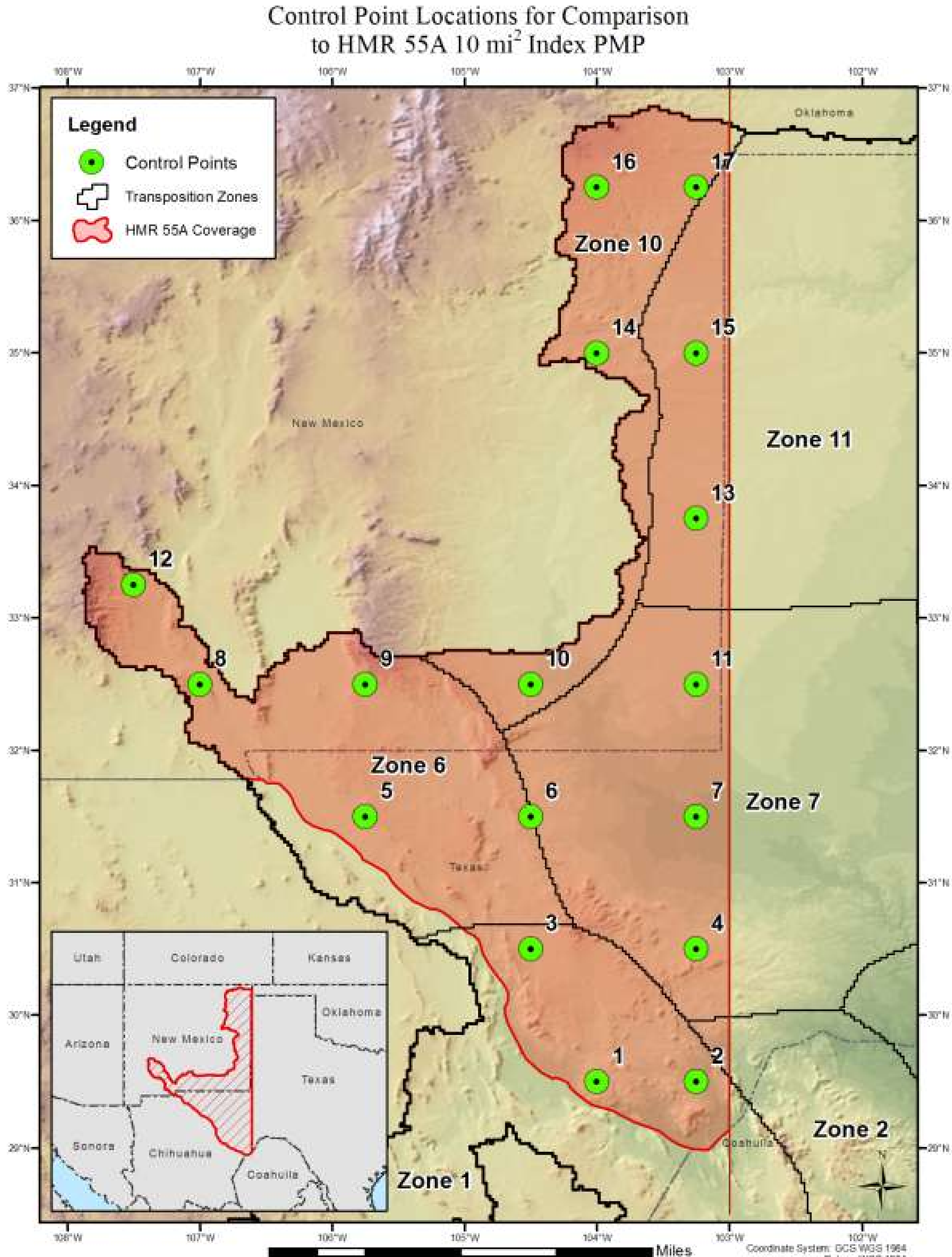


**Figure E.2 Control points used for PMP comparisons within the HMR 55A domain.**

# Glossary

**Adiabat:** Curve of thermodynamic change taking place without addition or subtraction of heat. On an adiabatic chart or pseudo-adiabatic diagram, a line showing pressure and temperature changes resulting from air rising with or without condensation of its water vapor: a line, thus, of constant equivalent potential temperature or constant potential temperature respectively.

**Adiabatic:** Referring to the process described by adiabat.

**Advection:** The process of transfer (of an air mass property) by virtue of motion. In particular cases, advection may be confined to either the horizontal or vertical components of the motion. However, the term is often used to signify horizontal transfer only.

**Air mass:** Extensive body of air approximating horizontal homogeneity, identified as to source region and subsequent modifications.

**Barrier:** A mountain range that inhibits the flow of warm humid air from a source of moisture to the basin under study.

**Convective rain:** Rainfall caused by the vertical motion of an ascending mass of air that is warmer than the environment and typically forms a cumulonimbus cloud. The horizontal dimension of such a mass of air is generally of the order of 12 miles or less, though it can be organized into larger-scale systems such as squall lines and hurricanes composed of many convective elements. Convective rain is typically of greater intensity than either of the other two main classes of rainfall (cyclonic and geographic) and is often accompanied by thunder. The term is more particularly used for those cases in which the precipitation covers a large area as a result of the agglomeration of cumulonimbus masses.

**Convergence:** Horizontal shrinking and vertical stretching of a volume of air, accompanied by net inflow horizontally and (when the convergence is near the ground) internal upward motion.

**Cooperative station:** A weather observation site where a volunteer maintains collects rainfall, temperatures, or other climatological data for the National Weather Service.

**Cyclone:** A distribution of atmospheric pressure in which there is a low central pressure relative to the surroundings. On large-scale weather charts, cyclones are characterized by a system of closed constant pressure lines (isobars), generally approximately circular or oval in form, enclosing a central low-pressure area. Cyclonic circulation is counterclockwise in the northern hemisphere and clockwise in the southern. (That is, the sense of rotation about the local vertical is the same as that of the earth's rotation).

**Depth-Area-Duration:** The precipitation values derived from Depth-Area and Depth-Duration curves at each time and area size increment analyzed for a PMP evaluation.

**Depth-Area-Duration Curve:** A curve showing the relation between an averaged areal rainfall depth and the area over which it occurs, for a specified time interval, during a specific rainfall event.

**Depth-Area-Duration values:** The combination of depth-area and duration-depth relations. Also called depth-duration-area.

**Dew point:** The temperature to which a given parcel of air must be cooled at constant pressure and constant water vapor content for saturation to occur.

**Envelopment:** A process for selecting the largest value from any set of data. In estimating PMP, the maximum and transposed rainfall data are plotted on graph paper, and a smooth curve is drawn through the largest values.

**Explicit transposition:** The movement of the rainfall amounts associated with a storm within boundaries of a region throughout which a storm may be transposed with only relatively minor modifications of the observed storm rainfall amounts. The area within the transposition limits has similar, but not identical, climatic and topographic characteristics throughout.

**Front:** The interface or transition zone between two air masses of different consistencies. The parameters describing the air masses are temperature and dew point.

**Geographic Transposition Factor (GTF):** A factor representing the relationship between climatological precipitation depths (at rarer return frequencies) between two locations. The GTF is primarily used to quantify the differences in the effects of topography on rainfall between the source and target locations, particularly for transposition within orographic regions. The GTF may also include a component of non-orographic (convergence only) effects on rainfall inherent in the precipitation frequency climatology.

**General storm:** A storm event that produces precipitation over areas in excess of 500-square miles, has a duration longer than 6 hours, and is associated with a major synoptic weather feature.

**Hydrologic Unit:** A hydrologic unit is a drainage area delineated to nest in a multi-level, hierarchical drainage system. Its boundaries are defined by hydrographic and topographic criteria that delineate an area of land upstream from a specific point on a river, stream or similar surface waters. A hydrologic unit can accept surface water directly from upstream drainage areas, and indirectly from associated surface areas such as remnant, non-contributing, and diversions to form a drainage area with single or multiple outlet points. Hydrologic units are only synonymous with classic watersheds when their boundaries include all the source area contributing surface water to a single defined outlet point.

**HYSPLIT:** Hybrid Single-Particle Lagrangian Integrated Trajectory. A complete system for computing parcel trajectories to complex dispersion and deposition simulations using either puff or particle approaches. Gridded meteorological data, on one of three conformal (Polar, Lambert, or Mercator latitude-longitude grid) map projections, are required at regular time intervals.

Calculations may be performed sequentially or concurrently on multiple meteorological grids, usually specified from fine to coarse resolution.

**Isohyets:** Lines of equal value of precipitation for a given time interval.

**Isohyetal pattern:** The pattern formed by the isohyets of an individual storm.

**Jet Stream:** A strong, narrow current concentrated along a quasi-horizontal axis (with respect to the earth's surface) in the upper troposphere or in the lower stratosphere, characterized by strong vertical and lateral wind shears. Along this axis it features at least one velocity maximum (jet streak). Typical jet streams are thousands of kilometers long, hundreds of kilometers wide, and several kilometers deep. Vertical wind shears are on the order of 10 to 20 mph per kilometer of altitude and lateral winds shears are on the order of 10 mph per 100 kilometer of horizontal distance.

**Local storm:** A storm event that occurs over a small area in a short time period. Precipitation rarely exceeds 6 hours in duration and the area covered by precipitation is less than 500 square miles. Frequently, local storms will last only 1 or 2 hours and precipitation will occur over areas of up to 200 square miles. Precipitation from local storms will be isolated from general-storm rainfall. Often these storms are thunderstorms.

**Low Level Jet stream:** A band of strong winds generally between 1,000 and 5,000 feet above ground level as contrasted with the jet streams of the upper troposphere.

**Mass curve:** Curve of cumulative values of precipitation through time.

**Mesoscale Convective Complex (MCC):** For the purposes of this study, a heavy rain-producing storm with horizontal scales of 10 to 1000 kilometers (6 to 625 miles) which includes significant, heavy convective precipitation over short periods of time (hours) during some part of its lifetime.

**Mesoscale Convective System (MCS):** A complex of thunderstorms that becomes organized on a scale larger than the individual thunderstorms, and normally persists for several hours or more. MCSs may be round or linear in shape, and include systems such as tropical cyclones, squall lines, and MCCs (among others). MCS often is used to describe a cluster of thunderstorms that does not satisfy the size, shape, or duration criteria of an MCC.

**Moist Adiabatic Laps Rate:** The rate of decrease of temperature with height along a moist adiabat. A rate of change of 2.7°F/1000 feet is applied in this study.

**Moisture maximization:** The process of adjusting observed precipitation amounts upward based upon the hypothesis of increased moisture inflow to the storm.

**One-hundred year rainfall event:** The point rainfall amount that has a one-percent probability of occurrence in any year.

**Polar front:** A semi-permanent, semi-continuous but not stationary front that separates tropical air masses from polar air masses.

**Precipitable water:** The total atmospheric water vapor contained in a vertical column of unit cross-sectional area extending between any two specified levels in the atmosphere; commonly expressed in terms of the height to which the liquid water would stand if the vapor were completely condensed and collected in a vessel of the same unit cross-section. The total precipitable water in the atmosphere at a location is that contained in a column or unit cross-section extending from the earth's surface all the way to the "top" of the atmosphere. The 30,000 feet level (approximately 300mb) is considered the top of the atmosphere in this study.

**Persisting dew point:** The dew point value at a station that has been equaled or exceeded throughout a period. Commonly durations of 12 or 24 hours are used, though other durations may be used at times.

**Probable Maximum Flood:** The flood that may be expected from the most severe combination of critical meteorological and hydrologic conditions reasonably possible in a particular drainage area.

**Probable Maximum Precipitation:** Theoretically, the greatest depth of precipitation for a given duration that is physically possible over a given size storm area at a particular geographic location at a certain time of the year.

**Pseudo-adiabat:** Line on thermodynamic diagram showing the pressure and temperature changes undergone by saturated air rising in the atmosphere, without ice-crystal formation and without exchange of heat with its environment, other than that involved in removal of any liquid water formed by condensation.

**Saturation:** Upper limit of water-vapor content in a given space; solely a function of temperature.

**Spatial distribution:** The geographic distribution of precipitation over a drainage according to an idealized storm pattern of the PMP for the storm area.

**Storm transposition:** The hypothetical transfer, or relocation of storms, from the location where they occurred to other areas where they could occur. The transfer or the mathematical adjustment of storm rainfall amounts from the storm site to another location is termed "explicit transposition." The areal, durational, and regional smoothing done to obtain comprehensive individual drainage estimates and generalized PMP studies is termed "implicit transposition" (WMO, 1986).

**Synoptic:** Showing the distribution of meteorological elements over an area at a given time (e.g., a synoptic chart). Use in this report also means a weather system that is large enough to be a major feature on large-scale maps (e.g., of the continental U.S.).

**Temporal distribution:** The time order in which incremental PMP amounts are arranged within a PMP storm.

**Tropical Storm:** A cyclone of tropical origin that derives its energy from the ocean surface.

**Total storm area and total storm duration:** The largest area size and longest duration for which depth-area-duration data are available in the records of a major storm rainfall.

**Transposition limits:** The outer boundaries of the region surrounding an actual storm location that has similar, but not identical, climatic and topographic characteristics throughout. The storm can be transpositioned within the transposition limits with only relatively minor modifications to the observed storm rainfall amounts.

**Undercutting:** The process of placing an envelopment curve somewhat lower than the highest rainfall amounts on depth-area and depth-duration plots.

## Acronyms and Abbreviations used in the report

**AMS:** Annual maximum series

**AWA:** Applied Weather Associates

**DAD:** Depth-Area-Duration

**dd:** decimal degrees

**EPRI:** Electric Power Research Institute

**F:** Fahrenheit

**GCS:** Geographical coordinate system

**GEV:** Generalized extreme value

**GIS:** Geographic Information System

**GRASS:** Geographic Resource Analysis Support System

**GTF:** Geographic Transposition Factor

**HMR:** Hydrometeorological Report

**HYSPLIT:** Hybrid Single Particle Lagrangian Integrated Trajectory Model

**IPMF:** In-place Maximization Factor

**mb:** millibar

**MCS:** Mesoscale Convective System

**MCC:** Mesoscale Convective Complex

**MTF:** Moisture Transposition Factor

**NCDC:** National Climatic Data Center (now National Centers for Environmental Information)

**NCEI:** National Centers for Environmental Information (formerly National Climatic Data Center)

**NEXRAD:** Next Generation Radar

**NOAA:** National Oceanic and Atmospheric Administration

**NWS:** National Weather Service

**NRCS:** Natural Resources Conservation Service

**PMF:** Probable Maximum Flood

**PMP:** Probable Maximum Precipitation

**PRISM:** Parameter-elevation Relationships on Independent Slopes

**PW:** Precipitable Water

**SPAS:** Storm Precipitation and Analysis System

**TAF:** Total Adjustment Factor

**TCEQ:** Texas Commission on Environmental Quality

**USACE:** U.S. Army Corps of Engineers

**USBR:** U.S. Bureau of Reclamation

**USGS:** United States Geological Survey

**WMO:** World Meteorological Organization

# 1. Introduction

This study provides Probable Maximum Precipitation (PMP) values for any drainage basin within Texas, including regions adjacent to the state that provide runoff into Texas from New Mexico and Mexico (Figure 1.1). The PMP values are valid for any month of the year, with preferred periods for each storm type. For local storms, the most likely period of PMP-type rainfall extends from April through October. For tropical storms, the period extends from June through October. For general storms, the period can be any time of the year, although this storm type is least likely in July and August. This results from frontal activity causing general storms to weaken and become less frequent in the summer season while local and tropical storms become more likely. The PMP values are used in the computation of the Probable Maximum Flood (PMF). PMP values provided in this study supersede PMP values from Hydrometeorological Reports (HMRs) for locations in Texas. These are HMR 51 (Schreiner and Riedel, 1978) and HMR 55A (Hansen et al., 1988).

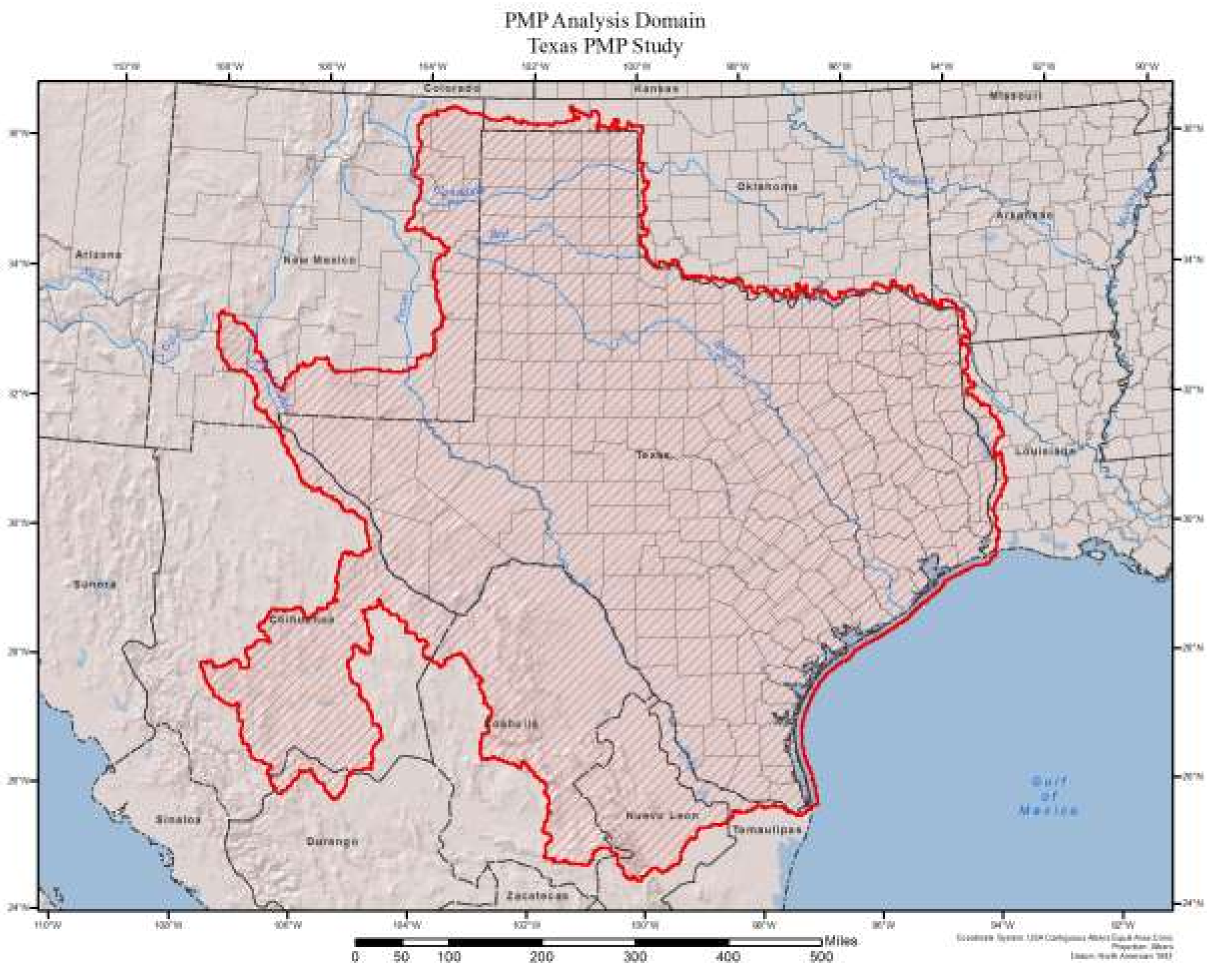


**Figure 1.1: Coverage of PMP domain used for this study.**

## 1.1 Background

Definitions of PMP are found in most of the HMRs issued by the National Weather Service (NWS). The definition used in the most recently published HMR is "theoretically, the greatest depth of precipitation for a given duration that is physically possible over a given storm area at a particular geographical location at a certain time of the year" (HMR 59, p. 5) (Corrigan et al., 1999). Since the early 1940s, several government agencies have developed methods to calculate PMP for various regions of the United States. The NWS (formerly the U.S. Weather Bureau), the U.S. Army Corps of Engineers (USACE), and the U.S. Bureau of Reclamation (USBR) have been the primary Federal government agencies involved in this activity. PMP values presented in their reports are used to calculate the PMF, which, in turn, is often used for the design of significant hydraulic structures. It is important to acknowledge that the methods used to derive PMP and the hydrological procedures that use the PMP values need to adhere to the requirement of being "physically possible." In other words, various levels of conservatism and/or extreme aspects of storms that could not physically occur in a PMP storm environment should not be used to produce combinations of storm characteristics that are not physically consistent in determining PMP values or for the hydrologic applications of those values.

The generalized PMP studies currently in use in the conterminous United States include HMRs 49 (1977) and 50 (1981) for the Colorado River and Great Basin drainage; HMRs 51 (1978), 52 (1982) and 53 (1980) for the U.S. east of the 105th meridian; HMR 55A (1988) for the area between the Continental Divide and the 103rd meridian; HMR 57 (1994) for the Columbia River Drainage; and HMRs 58 (1998) and 59 (1999) for California (Figure 1.2). In addition to these HMRs, numerous Technical Papers and Reports deal with specific subjects concerning precipitation (e.g., NOAA Tech. Report NWS 25, 1980). Topics in these reports include maximum observed rainfall amounts for various return periods and specific storm studies. Climatological atlases (e.g., Technical Paper No. 40, 1961; NOAA Atlas 2, 1973; and NOAA Atlas 14, 2004-2015) are available for use in determining precipitation return periods. A number of site-specific, statewide, and regional studies (e.g., Tomlinson, 1993; Tomlinson et al., 2002-2013; Kappel et al., 2012-2016) augment generalized PMP reports for specific regions included in the large areas addressed by HMRs 51 and 55A. Recent site-specific PMP projects completed within the domain have demonstrated outdated procedures and data used to estimate PMP values. These include a subjective application of methods to derive PMP values and address the effects of topography, which cannot be reproduced, a lack of analyzed storm events, a lack of explanation and backup documentation, and an inaccurate methodology to maximize storms. PMP results from this study provide values that replace those derived from HMRs 51 and 55A.

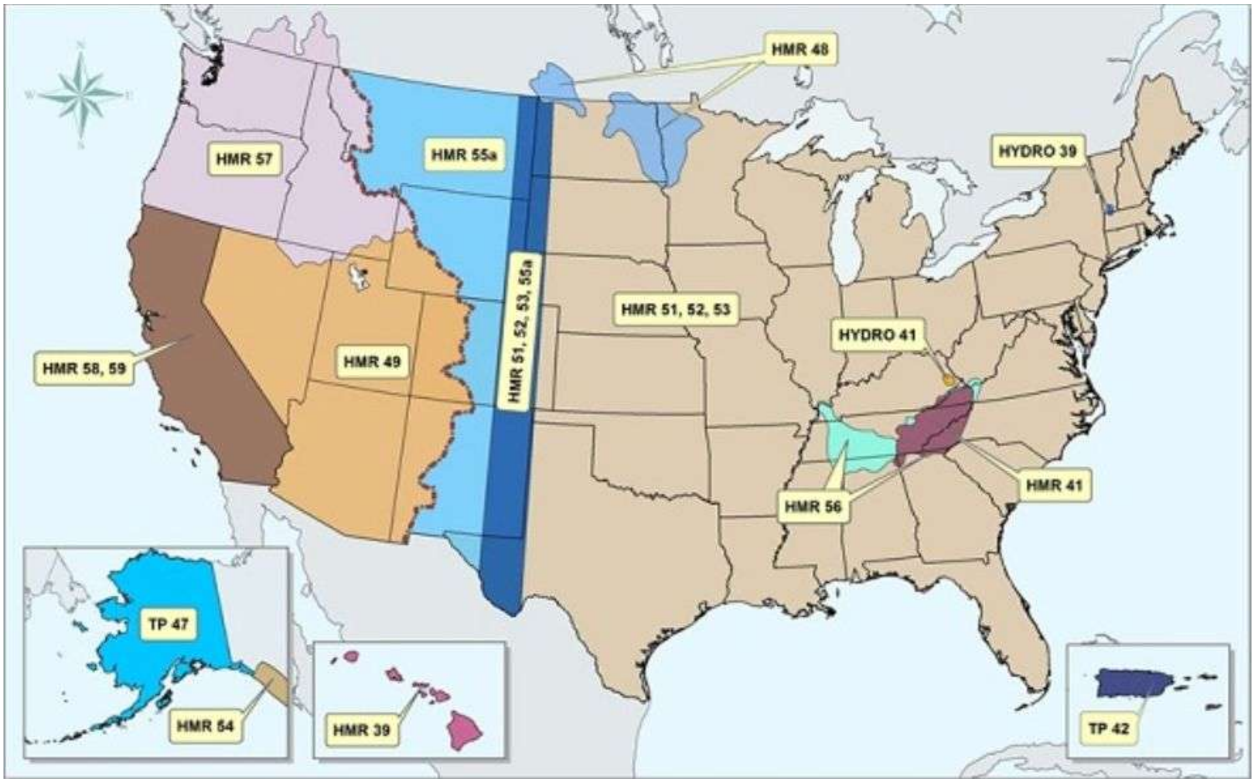


**Figure 1.2: Hydrometeorological Report coverages across the United States**

Texas is included within the domain covered by HMR 51 and 55A. These HMRs cover diverse regions that are not meteorologically and topographically similar. Texas contains many diverse regions which each exhibit unique rainfall characteristics that are a function of both distance from moisture sources and topography (Figure 1.3). In Texas, climate and terrain vary greatly. Because of the distinctive climate regions and topographic effects related to terrain and coastal interactions, the development of PMP values must account for the complexity of the meteorology and terrain throughout the state. This project incorporated the latest methods, technology, and data to address these complexities. Several major issues have been identified with the procedures used in the HMRs to developed PMP values. Important among these are the limited number of analyzed storm events, no inclusion of storms that have occurred since the 1980's, a non-reproducible and subjective process used to address geographic effects, inconsistent data and procedures used among the HMRs, and the outdated procedures used to derive PMP.

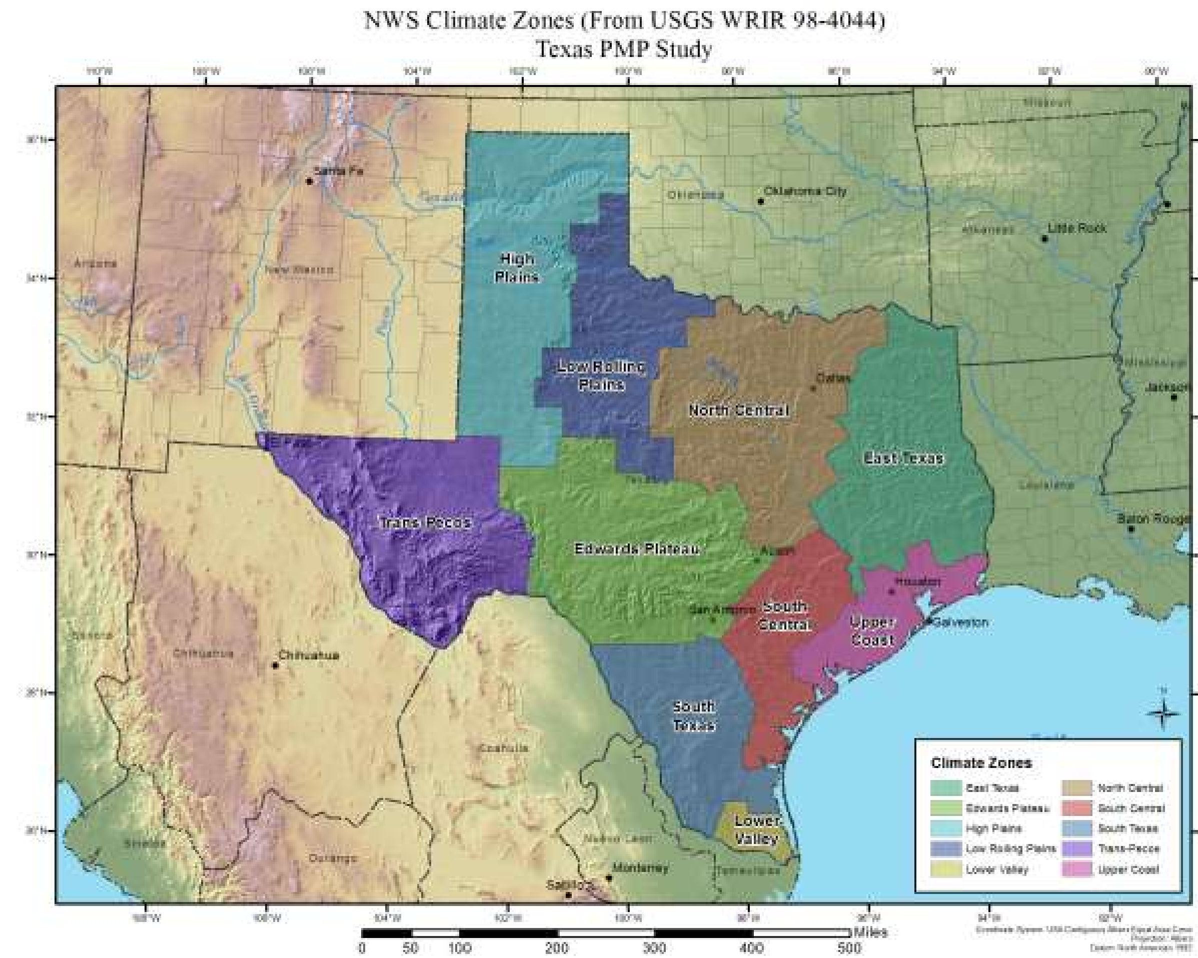


**Figure 1.3: National Weather Service climate zones within Texas.**

Previous site-specific, statewide, and regional PMP projects completed by AWA provide examples of PMP studies that explicitly consider the unique topography of the area being studied and characteristics of historic extreme storms over meteorologically and topographically similar regions surrounding the area. The procedures incorporate the most up-to-date sets, techniques, and applications to derive PMP. All completed AWA PMP studies are formally published after having received extensive review and after the results have been successfully applied to computing the PMF for the watersheds. This study follows similar procedures employed in those studies while making improvements where advancements in computer-aided tools and transposition procedures have become available.

Several PMP studies have been completed by AWA within the region covered by HMRs 51 and 55A, which are directly relevant to Texas (Figure 1.4). Each of these studies provided PMP values that have superseded those from HMR 51 and 55A. These are examples of PMP studies that explicitly consider the meteorology and topography of the study location along with characteristics of historic extreme storms over climatically similar regions. Information, experience, and data from these PMP studies were utilized in this study. These included use of previously analyzed storm events using the SPAS program, previously derived storm lists, previously derived in-place storm maximization factors, climatologies, and explicit understanding of the meteorology of the region. In addition, comparisons to these previous studies provided sensitivity and context with results of this study. These regional and site-specific PMP studies received extensive review and were accepted by the appropriate regulatory agencies, including the Federal Energy Regulatory Commission (FERC), state dam safety regulators, and the Natural Resources Conservation Service (NRCS). Results have been used in computing the PMF for individual watersheds. This study followed the same procedures used in those studies to determine PMP values. These procedures, together with SPAS rainfall analyses, were used to compute PMP values following standard procedures outlined in HMR 51.

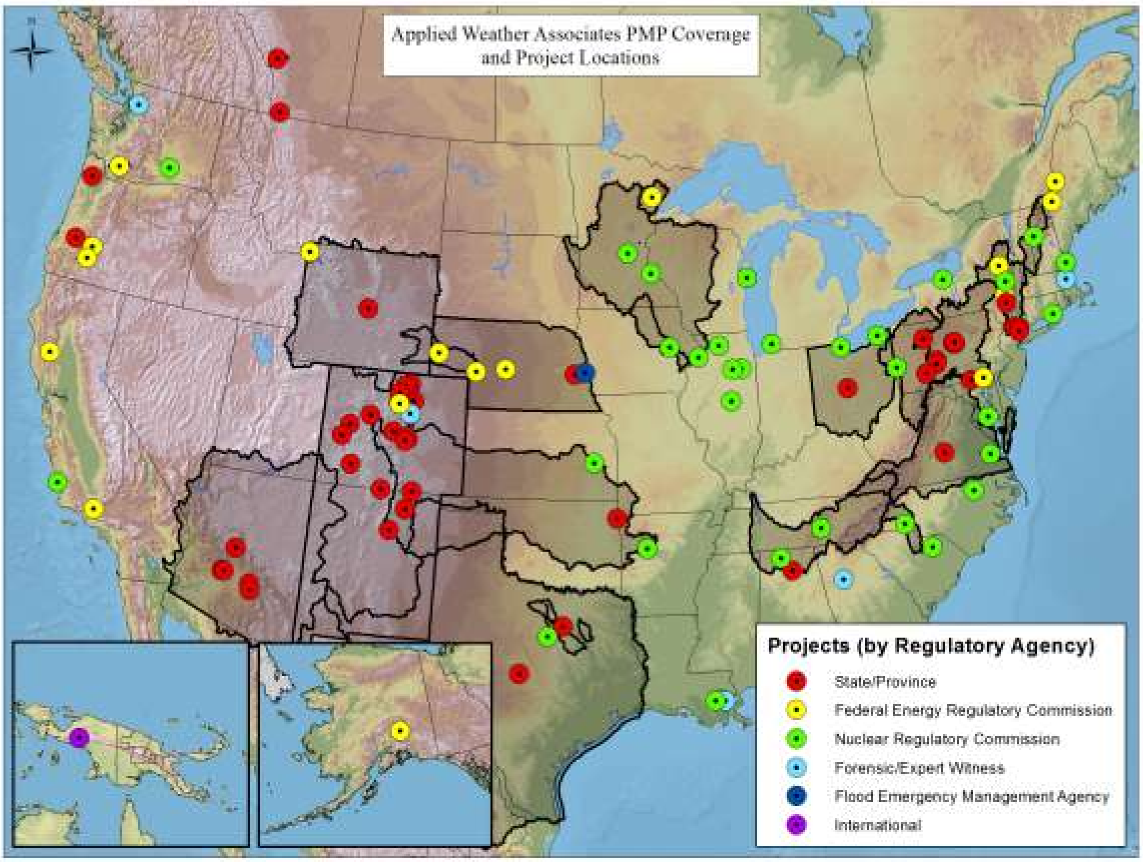


**Figure 1.4 Locations of AWA PMP studies as of June 2016.**

## 1.2 Objective

This study determines reliable and reproducible estimates of PMP values for use in computing the PMF for all watersheds in the state and within the overall project domain. The most reliable methods and data available were used, with updates to methods and data used in HMRs applied where appropriate.

## 1.3 Approach

The approach used in this study followed the procedures used in the development of the HMRs, with updated procedures used where appropriate. This includes updates AWA implemented in several recently completed PMP projects as well as updates developed during this study. These updated procedures were applied with a consideration for meteorology, terrain, and their interactions within the project domain. The weather and climate of the region are discussed in Section 2. Section 3 explains the effects of topography on rainfall and PMP within Texas. Section 4 describes the development of the updated dew point climatologies whereas Section 5 provides information on the updated precipitation frequency climatologies developed for this study. The initial steps of identifying extreme storms and the development of the final list of storms used to derive PMP are in Section 6. Adjustments for storm maximization, storm transposition, and calculation of final PMP values are provided in Sections 7, 8, and 9 respectively. The process for using the GIS PMP calculation tool to produce gridded and basin average PMP is discussed in Section 10. Discussions on sensitivities are provided in Sections 11 and 12, and recommendations for application are presented in Section 13.

A goal of this study was to maintain consistency, whenever appropriate, with the general methods used in recent HMRs, the World Meteorological Organization (WMO) manual for PMP (WMO, 2009), and the previous PMP studies completed by AWA. Deviations were incorporated when justified by developments in meteorological analyses and available data. The approach identifies major storms that occurred within the region considered transpositionable to any location within the overall project domain. Each of the main storm types producing extreme rainfall was identified and investigated. The main storm types include local storms, tropical storms, and general storms. The moisture content of each of these storms was maximized to provide worst-case rainfall estimations for each storm at the location where it occurred. Storms were then transpositioned to each grid point with regions of similar topography and meteorological conditions. Adjustments were applied to each storm as it was transpositioned to each grid point to represent the amount of rainfall that storm would have produced at the new location versus what it produced at the original location. These adjustments were combined to produce the total adjustment factor (TAF) for each storm for each grid point. The TAF is a product of the in-place maximization factor (IPMF), the moisture transposition factor (MTF), and the geographic transposition factor (GTF). Section 9 provides a more detailed discussion on this process and application.

$$\text{Total Adjustment Factor} = \text{IPMF} * \text{MTF} * \text{GTF} \qquad \text{Equation 1.1}$$

Advanced computer-based technologies, Weather Service Radar WSR-88D next-generation radar (NEXRAD), and the Storm Precipitation Analysis System (SPAS) were used in the storm analyses along with new meteorological data sources. New technologies, such as HYSPLIT model trajectories and data were incorporated into the study when they provided improved reliability, while maintaining as much consistency as possible with previous studies. An example is the updated maximum dew point climatology used in the IPMF and MTF calculations and the updated precipitation frequency climatologies used in GTF calculations.

For some applications such as storm maximization, storm transpositioning, defining PMP by storm type, and combining storms to create a PMP design storm, this study applied standard methods presented in previous publications (e.g., WMO Operational Hydrology Reports, 1986, 2009), whereas for other applications, new procedures were developed. Moisture analyses have historically used monthly maximum 12-hour persisting dew point values (3-hour persisting dew points were also used in HMR 57). For this project, an update to the maximum average dew point climatology (developed in previous studies for the 6-, 12-, and 24-hour duration periods) was used to better represent the atmospheric moisture for rainfall durations associated with the different storm types that affect Texas. Updated dew point data represent the 100-year recurrence interval return frequency values for 6-, 12-, and 24-hour duration periods. These recurrence interval durations better represent available atmospheric moisture used to maximize individual storms versus the persisting dew point process employed in the HMRs. The updated dew point climatology values replaced the 12-hour maximum persisting dew point values used in the HMRs. The resulting storm representative dew point values better represent the available atmospheric moisture that actually contributed to each storm's rainfall production. The maximum dew point climatologies used the most up-to-date periods of record, adding over 40 years of data to the datasets used in previous climatologies.

In addition to the updated dew point climatologies, the NOAA Optimum Interpolation (OI) SST v.2 (Reynolds, R.W et al., 2002) climatologies were used to maximize storms whose moisture source region originated from the Atlantic Ocean. This provides a significant improvement from HMR 51, which did not have a process to quantify this moisture source in the in-place maximization process. The NOAA OI SST v.2 datasets were provided by the NOAA/OAR/ESRL PSD, Boulder, Colorado, USA, from their Web site at http://www.esrl.noaa.gov/psd/. These SST climatologies replaced the Marine Climate Atlas of the World (U.S. Navy, 1981) that were used in the HMRs. This updated climatology dataset utilized monthly means from January, 1981 through December, 2013. SST plus 2σ (two standard deviations) datasets were produced for each month for use in moisture calculations (see Section 7.3). The spatial resolution for these data is 1.0 x 1.0 decimal degrees, prompting the decision to use a bilinear spatial interpolation when extracting climatological SST values. In conjunction with the climatology maps, daily SST maps based on ship and buoy reports as well as satellite data (after 1979) were used in deriving the storm representative SST values for each storm event where the moisture source originated over water (Kent et al., 2007; Reynolds et al., 2007; and Worley et al., 2005). The use of SST climatology as a surrogate to maximize storms was employed consistently starting with HMR 57 (Section 4.3, Hansen et al., 1994).

A reanalysis of transposition limits explicitly evaluated the effects of coastal convergence, topographical effects on storm structure, and moisture availability to determine which storms were transpositionable to any location within the domain. Extensive discussions with the study participants defined which storms would ultimately be used for PMP development. This re-analysis of the transposition limits provided precise guidance and constraints on the regions of influence for individual storms on a site-specific basis.

Environmental Systems Research Institute's (ESRI) ArcGIS Desktop GIS software was extensively used to evaluate topography and climatological datasets; analyze spatial relations; store, organize, and process the large amounts of spatial data; design, implement, and execute the

PMP database; and to provide visualization and mapping support throughout the process. SPAS used gridded storm analysis techniques to provide both spatial and temporal analyses for extreme rainfall storm events (see Appendix G for a complete description of SPAS).

## 1.4 PMP Analysis Domain

The project domain was defined to cover the entire state of Texas as well as watersheds that extended beyond state boundaries that included runoff into Texas. This study allows for gridded PMP values to be determined for each grid cell within the project domain. The full PMP analysis domain is shown in Figure 1.1.

## 1.5 PMP Analysis Grid Setup

A uniform grid covering the PMP project domain provides a spatial framework for the analysis. The PMP grid resolution for this study was 0.025 x 0.025 decimal degrees (dd), or 90 arc-seconds, using the Geographic Coordinate System (GCS) spatial reference with the World Geodetic System of 1984 (WGS 84) datum. This resulted in 154,998 grid cells with centroids within the domain shown in Figure 1.1. The grid cells have an approximate area ranging from 2.4 square miles for the southernmost grid cells to 2.7 square miles at the northernmost grid cells. The grid network placement is essentially arbitrary. However, the placement was oriented in such a way that the grid cell centroids are centered over whole number coordinate pairs and then spaced evenly every 0.025 dd (fraction of a degree). For example, there is a grid cell centered over 32°N and 99°W with the adjacent grid point to the west at 32°N and 99.025°W. As an example, the PMP analysis grid over the Lake Brownwood drainage basin is shown in Figure 1.5.

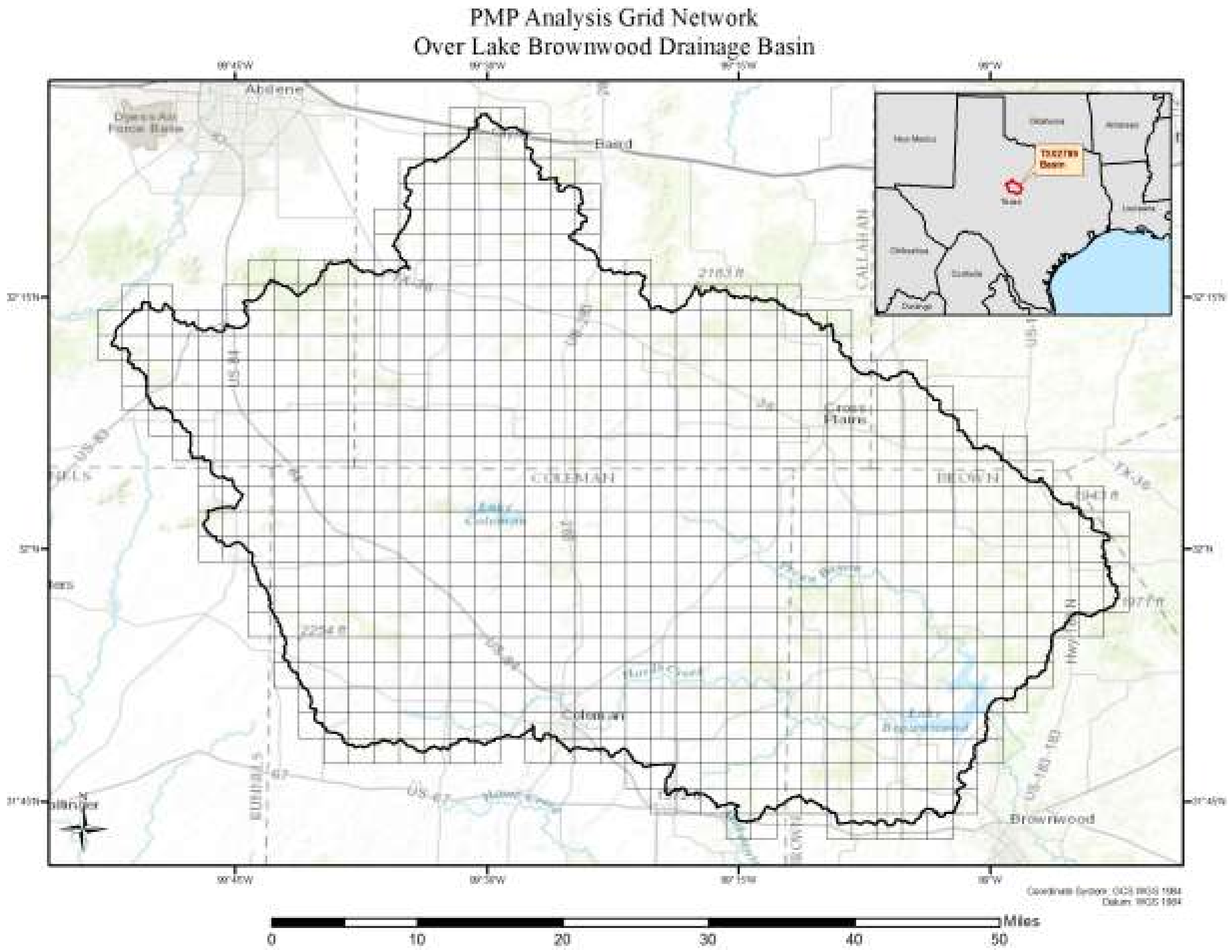


**Figure 1.5: PMP analysis grid placement over the Lake Brownwood drainage basin.**

# 2. Weather and Climate of the Region

This section describes the general weather patterns and climate of Texas and how they relate to the development of PMP for this project. More detailed descriptions of the climate of Texas and each of the storm types can be found in the references, including Bomar (1983), Lanning-Rush et al., (1998), Nielsen-Gammon et al., (2005), and Burnett (2008). These references provide additional information and more detailed analysis of the weather and climate of Texas than is included in this document.

## 2.1 General Climate of Texas

The region is influenced by several factors that can potentially contribute to extreme rainfall. First is the proximity of the region to the Gulf of Mexico. This allows high amounts of moisture to move directly into the region. The lift required to convert these high levels of moisture into rainfall on the ground is provided in several ways to the project domain. Secondarily, the eastern North Pacific Ocean supplies mid-level moisture, which can be substantial particularly during the tropical cyclone season, or from late May until early November.

Numerous large-scale weather systems with their associated fronts traverse the region, especially from fall through spring. These are most common in regions further to the north and east of approximately 100°W. The fronts (boundaries between two different air masses) can be a focusing mechanism providing upward motion in the atmosphere. These are often locations where heavy rainfall is produced. A front typically will move through with enough speed that no given area receives excessive amounts of rainfall. However, some of these fronts will stall or move very slowly across the region, allowing heavy amounts of rainfall to continue for several days in the same general area, which can lead to extreme widespread flooding.

Another mechanism, which creates lift in the region, is heating of the surface and lower atmosphere by the sun. This creates warmer air below cold air resulting in atmospheric instability and leads to rising motions. This will often form ordinary afternoon and evening thunderstorms. However, in unique circumstances, the instability and moisture levels in the atmosphere can reach very high levels and stay over the same region for an extended period of time. This can lead to intense thunderstorms and very heavy rainfall. If these storms are focused over the same area for a long period, flooding rains can be produced. This type of storm produces some of the largest point rainfall recorded, but often does not affect larger areas with extreme rainfall amounts.

Remnant tropical moisture and circulations associated with decaying tropical systems are another mechanism than can produce heavy rainfall in the region. This often leads to very heavy rainfall production and, when the storm become cut off from the main flow, these storms may stay over the same region for an extended period of time, producing devastating rainfall and flooding.

The impact of these mechanisms can be enhanced by the effects of topography, both coastal convergence and elevated terrain. Most prominent of these features is the Balcones Escarpment in south-central Texas. This region of elevation terrain just north of San Antonio is home to some of the largest recorded rainfalls in the world. This is an example of the effect of topography on an already moist, unstable air mass. Much research has been completed to demonstrate the effect of this region in producing uniquely heavy rainfall events (e.g., Lott, 1953; Texas Water Development Board, 1966; Baker, 1975; Patton and Baker, 1977; Caracena and Fritsch, 1983; Asquith, 1998; Clayton et al., 2015; and Nielsen et al., 2016).

## 2.2 Air Mass Type Related to Heavy Rainfall

There are four main air mass types that affect the weather and climate of the project domain. Major influences in the colder half of the year are the continental polar (cP) and continental Arctic (cA) air masses with origins north of the Arctic Circle. This air mass is most common in the winter and early spring and is often associated with the "blue norther" cold front passage and stratiform rainfall/snowfall events and cold temperatures. When this air mass type arrives, it often collides with a more humid air mass from warmer regions to the south. Low pressure (rising air) often results, and when combined with strong winds aloft, severe thunderstorms and flood producing rainstorms can result.

The second type of air mass observed in the region is the maritime polar (mP) which originates in the Gulf of Alaska and Pacific Ocean. This air mass often arrives on strong winds from the west and northwest, but is usually devoid of significant amounts of low-level moisture because it has traveled across several mountain ranges. After producing precipitation at these upwind locations far removed from Texas, this storm type is devoid of low-level moisture by the time it reaches northern and central Texas. These systems can produce a line of strong to severe thunderstorms, but they are usually fast moving and therefore do not produce PMP level rainfalls.

The third type of air mass that affects the region is comprised of warm, dry air that originates from the high plateaus to the southwest in Arizona, New Mexico, and northern Mexico. This air mass, called continental tropical (cT), is often accompanied by a cap on the atmosphere 5,000 to 10,000 feet above the surface. This serves to bottle up large amounts of potential energy which when released, can result in explosive growth of thunderstorms and heavy rain. The leading edge of this air mass is delineated by a dry line often found moving from eastern New Mexico into west and central Texas from the spring through the fall. Along this boundary, large damaging storms often form, and when enough moisture is present, can lead to floods.

The fourth type of air mass common to the region originates from the Gulf of Mexico and contains copious amounts of atmospheric moisture in a conditionally unstable atmosphere. This type of air mass is called maritime tropical (mT). This is most directly responsible for producing heavy rainfall in the region, especially when this air mass interacts with a frontal boundary in the area and/or is lifted by underlying terrain. Figure 2.1 shows the general source regions for the air masses described above.

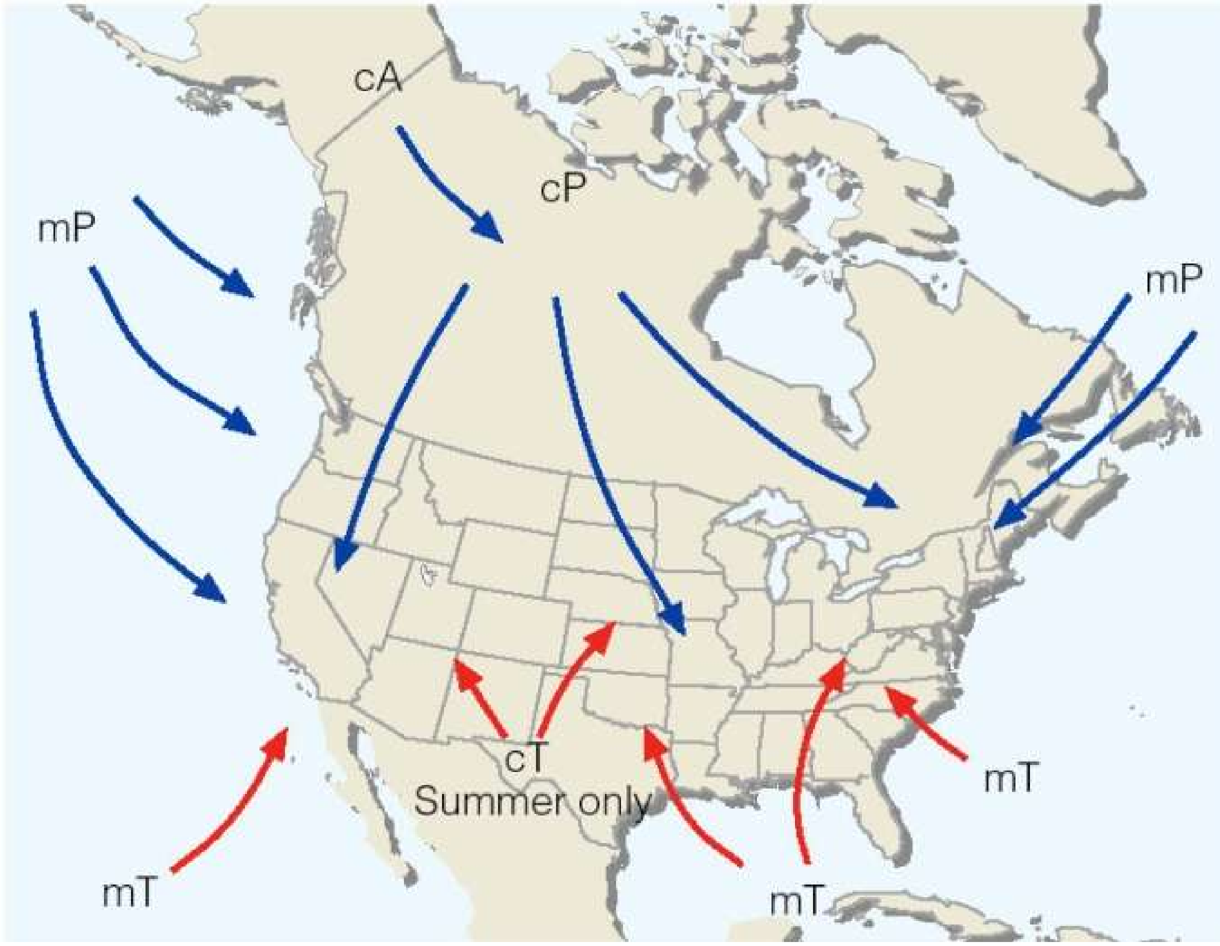


**Figure 2.1: Air mass source regions affecting the project domain (from Ahrens, 2007).**

The movement and general location of these air masses, along with access to moisture and interaction with terrain, create a general pattern of decreasing mean annual precipitation from east to west across Texas. Figure 2.2 displays the mean annual precipitation across Texas; a general rule of thumb is annual precipitation decreases one inch for each 15-mile displacement from east to west. This is important because it is expected that the same mechanisms resulting in the general pattern would occur to some extent with PMP-type storms. As a result, there is an expectation of generally decreasing PMP depths moving east to west across the project domain. Variations would occur where terrain overcomes the lack of moisture and generates relatively high rainfall accumulations in otherwise drier regions (e.g., the Balcones Escarpment and the elevated terrain in the Trans Pecos-Basin and Range region in southwest Texas, southern New Mexico, and Mexico).

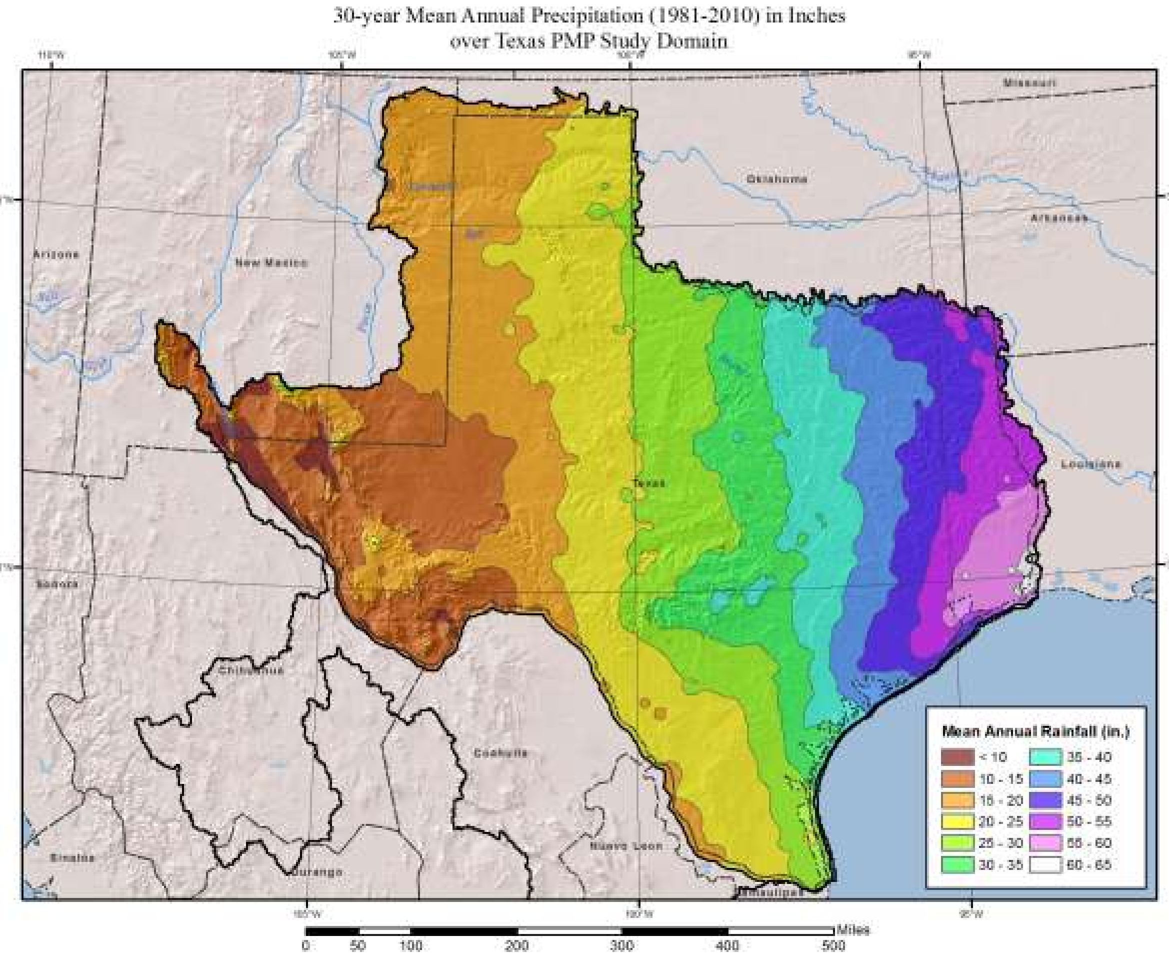


**Figure 2.2: PRISM 30-year mean annual precipitation across the state of Texas, in inches.**

## 2.3 PMP Storm Types

The project domain has a very active and varied weather regime throughout the year. Consequently, heavy rainfall events at both short and long durations are observed irrespective of season. By far, the most bountiful moisture available for precipitation over the region comes from the Gulf of Mexico, the Caribbean Sea, and tropical Atlantic Ocean. The major types of extreme precipitation events in the region are produced by Mesoscale Convective Systems (MCSs) (short durations and small area sizes), synoptic events/fronts (large areas sizes and longer durations), remnant tropical systems, or a combination of these storm types.

### 2.3.1 Local Thunderstorms and Mesoscale Convective Systems

Localized thunderstorms and MCSs are capable of producing extreme amounts of precipitation for short durations and over small area sizes, generally 12 hours or less over area sizes of 500 square miles or less. Meteorological understanding of MCS type storms has progressed significantly in recent decades with the advent of satellite technology starting in the 1970s and early 1980s. The current name of Mesoscale Convective Complex (MCC) was first applied in the late 1970s to these types of "flood producing", strong thunderstorm complexes

(Maddox, 1980). Mesoscale systems are so named because they are small in areal extent (10s to 100s of square miles), whereas synoptic storm events are hundreds to thousands of square miles. MCSs also exhibit a distinctive signature on satellite imagery highlighted by rapidly growing cirrus cloud shields with very high cloud tops. Furthermore, satellite images of the cirrus shield show nearly circular patterns as large as the size of the state of Iowa marked by constantly regenerating thunderstorms fed by moist low-level jet inflow.

MCCs are included in the more general definition of MCSs, which include a wider variety of mesoscale-sized storm systems, such as squall lines, tropical cyclones, and MCCs that do not fit the strict definition of size, duration, and/or appearance on satellite imagery. Climatologically, MCCs primarily form during the season months of April through October, but have been known to occur any month of the year.

The vast majority of MCSs have distinctive features and evolve in a standard pattern. A typical MCS begins as an area of thunderstorms over the western High Plains or Front Range of the Rocky Mountains. As these storms begin to form early in the day, the predominantly westerly winds aloft move them in a generally eastward direction. As the day progresses, the rain-cooled air below and around the storms begins to form a mesoscale area of high-pressure. This mesoscale high moves along with the area of thunderstorms. During nighttime hours, the MCS undergoes rapid development as it encounters increasingly warm and humid air from the Gulf of Mexico, usually associated with the low-level jet (LLJ) 3,000-5,000 feet above the ground. The area of thunderstorms will often form a ring around the leading edge of the mesoscale high and continue to intensify, producing heavy rain, damaging winds, hail, and/or tornadoes. An MCS will often remain at a constant strength as long as the low-level moisture transport continues to provide an adequate supply of moisture. Once the mesoscale environment begins to change, the storms weaken, usually around sunrise, but may persist into the early daylight hours.

Many of the storms previously analyzed by the USACE and NWS Hydrometeorological Branch in support of pre-1979 PMP research have features that indicate they were most likely MCCs or MCSs. However, this nomenclature had not yet been introduced into the scientific literature, nor were the events understood to the extent they are presently. The original name, Mesoscale Convective Complex (MCC), was first described by Maddox (1980) in the article "Mesoscale convective complexes". These are very important storms for determining PMP values for small area sizes and short durations across the project domain.

#### 2.3.2 General Storms-Synoptic Fronts

The polar front and jet stream, which separate cool, dry Canadian air to the north from warm, moist air to the south are often responsible for heavy rainfall over large areas for extended periods. They contribute large amounts of energy and storm dynamics to the atmosphere as fronts move through the region. These features are strongest and most active over the area from early autumn until late spring. A common type of occurrence with the polar front is an overrunning storm event. Frontal overrunning occurs when warm, humid air carried northward around the western edge of the Bermuda High circulation encounters the frontal zone and is forced to rise over the cooler, drier air mass to the north of the front. This forced ascent condenses moisture in the air mass into clouds and precipitation, while releasing latent heat. This process most often results in widespread rainfall over longer durations but can also help enhance convection. Air that arrives at the frontal location is conditionally unstable, in which the lower layers are much warmer and more humid than the air above. This conditionally unstable air mass awaits a mechanism to initiate lifting of the air mass to begin energy release, which will foster more instability and further uplift.

A stationary polar front will often provide the impetus necessary for this warm, humid air mass to release its convective potential. When this occurs, rainfall is produced, sometimes associated with embedded areas of convection and extremely heavy rainfall. The pockets of heavy rain are usually associated with a minor wave riding along the frontal boundary, called a shortwave. These are not strong enough to move the overall large-scale pattern, but instead add to the storm dynamics and energy available for producing precipitation.

This type of storm environment (synoptic frontal) will usually not produce the highest rainfall rates over short durations, but it instead leads to flooding situations as heavy to moderate rain continues to fall over the same regions for an extended period of time.

### 2.3.3 Tropical Storms

Tropical storms can affect any location in the project domain and are responsible for some of the greatest rainfall depths. Because of their reliance on warm water from the Gulf of Mexico along with supporting synoptic and upper level weather patterns, these storms only form from June through October in the region. In addition, direct tropical storm landfall is only possible along the immediate Gulf of Mexico coastline and up to a few hundred miles inland. After these storms move inland, both far enough removed in time and distance from the Gulf of Mexico, they quickly lose their pure tropical characteristics (warm core, no fronts, latent heat release from the warm Gulf of Mexico water, etc.) and transition into remnant tropical storms. However, the remnant air mass from a tropical system can add high levels of moisture and potential convective energy to the atmosphere, while circulations associated with the original tropical system continue to persist at diminished levels within the atmosphere. When these systems move slowly over a region, large amounts of rainfall can be produced both in convective bursts and over longer durations. These already extreme rainfall events are often enhanced further when interacting with the elevated terrain of the Balcones Escarpment and the Trans-Pecos Basin and Range region of southwest Texas, southern New Mexico, and Mexico.

### 2.3.4 Hybrid Storms

Often, heavy rainfall events throughout the region incorporate characteristics of more than one storm type described in the previous sections of this report. A common scenario includes a frontal boundary stalled out over central or northern Texas that becomes a focusing mechanism as tropical moisture moves north into the region from the Gulf of Mexico. The energy associated with the high levels of moisture and latent heat release is then focused along the frontal boundary and the rainfall mechanisms are enhanced. This can cause widespread heavy rainfall or local bursts of intense convection. If this scenario is positioned over the same region for an extended period, very high rainfall amounts can result. Another common scenario is associated with remnant outflow boundaries and moisture from decaying MCSs interacting with a frontal boundary to re-generate enhanced convection along that boundary, then continuing to “train” thunderstorms along that boundary for an extended period of time. This storm type contains characteristics of both synoptic frontal storms and intense convection. Generally, this type of storm lasts for a duration of at least 24 hours, but includes periods of intense rainfall for shorter durations. The bursts of rainfall are associated with strong imbedded convective cells within the overall storm environment that produce large amounts of rain over smaller areas within the larger storm environment.

# 3. Topographic Effects on PMP Rainfall

The terrain across Texas varies from sea level along the Gulf Coast gradually rising from the coastline inland and from east to west, not reaching above 1,000 feet until nearly a 1/3rd of the way across the state. This very gradual rise is an extension of a very gently-sloping continental shelf in the western Gulf of Mexico. North of San Antonio and west of Austin, elevation rises abruptly along the Balcones Escarpment, reaching to nearly 3,000 feet in a short distance. West of the Dallas-Fort Worth Metroplex, elevations rise gradually through the high plains, reaching 4,000 feet along the New Mexico border. The most significant topographic changes occur in the Trans Pecos-Basin and Range region of southwest Texas, west of 103°W and south of the Mexico border. This highly variable topography continues west of the Rio Grande into Mexico and north into southern New Mexico (Figure 3.1).

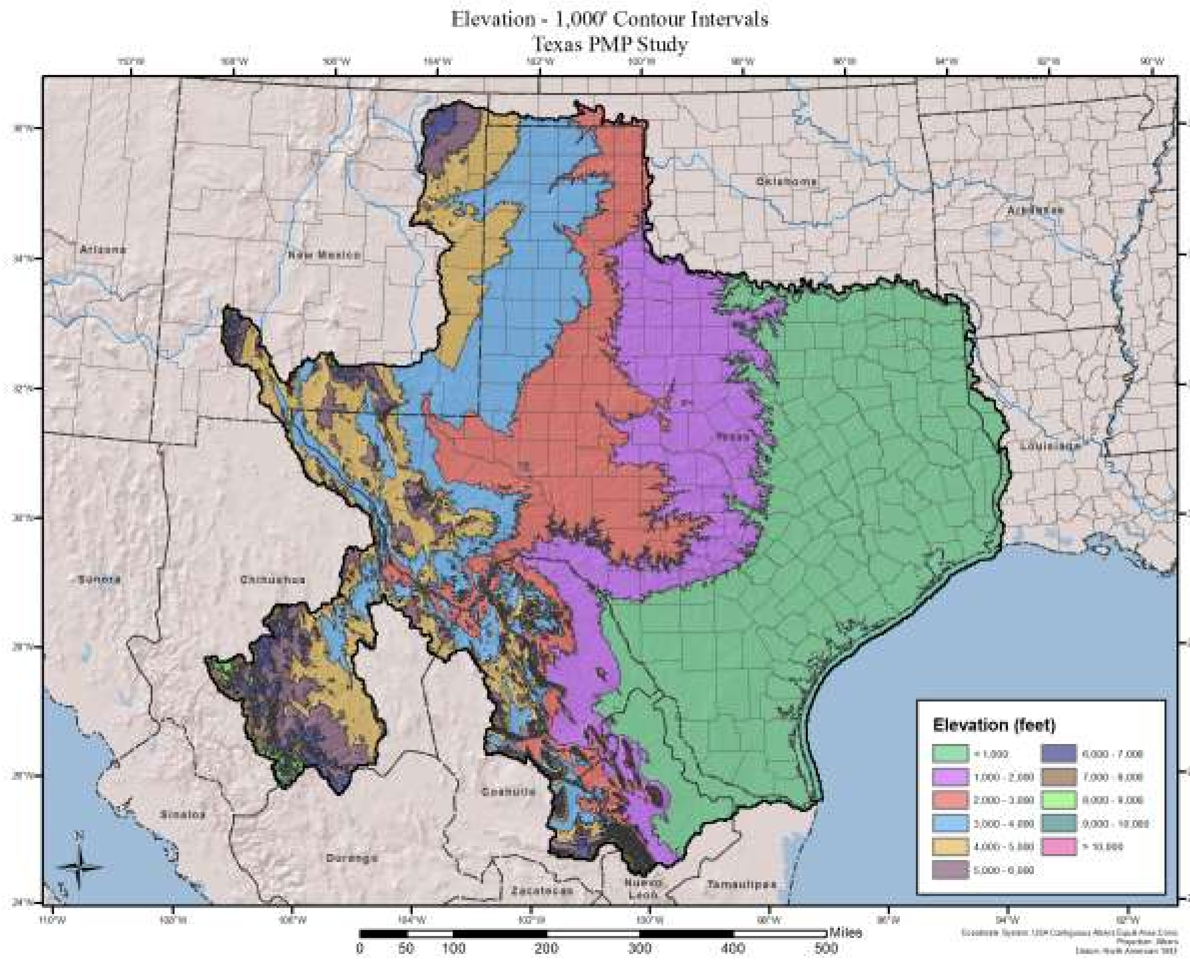


**Figure 3.1: Elevation contours at 1,000 feet intervals over the Texas PMP domain**

To account for the enhancements and reductions of precipitation by terrain features such as the Balcones Escarpment, coastal convergence, and mountainous terrain in the western project domain (called orographic effects), explicit evaluations were performed using precipitation frequency climatologies. These included NOAA Atlas 14, Volume 1 (Bonnin et al., 2004), NOAA Atlas 14, Volume 2 (Bonnin et al., 2004), NOAA Atlas 14, Volume 8 (Perica et al., 2013), NOAA Atlas 14 Volume 9 (Perica et al., 2013), and the Texas precipitation frequency climatologies developed as part of this study (see Section 5 and Appendix C). These climatologies were used to derive the Geographic Transposition Factors (GTFs). This approach is similar to that used in HMRs 55A, 57, and 59 that used the Storm Separation Method (SSM) to quantify geographic effects in topographically significant regions and as suggested in the WMO PMP Manual Section 3.1.4 (2009). In contrast to the SSM methodology, the GTF procedure is significantly more objective and reproducible. In Appendix J, a detailed example of the subjectivity and issues associated with the use of the SSM is provided. In Appendix J, AWA tried to replicate the SSM process and data using information provided in HMRs 55A, 57, and 59. The results of that analysis showed that the SSM method is not reproducible and highly subjective.

The GTF process used in this study reduces the amount of subjectivity involved and provides information that is reproducible. By evaluating rainfall values for a range of recurrence intervals at both locations, a relation between the two locations was established. For this study, gridded precipitation frequency climatologies from this study and NOAA Atlas 14 were used to develop the precipitation frequency relations and quantify orographic and other terrain effects. In previous studies, variations of the GTF method were called the orographic transposition factor (OTF) and were developed originally for highly orographic regions (e.g., Cascade and Rocky Mountains) as a way to replace the HMR SSM method. However, because the calculations are relying on relations between precipitation frequency climatologies between two locations considered transpositionable, the process can be applied in non-orographic regions. The validity of the GTF process for use in calculating PMP in both orographic and non-orographic regions and for each storm type analyzed (local, general, and tropical) has been extensively reviewed during previous AWA PMP studies (e.g., Tomlinson et al., 2011; Tomlinson et al., 2013; Kappel et al., 2014; Kappel et al., 2015) and again during this study. Each of the independent review boards agreed that it was a reasonable process to use in all meteorological scenarios.

## 3.1 Terrain Effects

Orographic and other geographically influenced effects on rainfall are captured in climatological analyses that use precipitation data from historical record. These observed rainfall amounts include precipitation that would have accumulated without topography, together with the amount of additional precipitation or decreased precipitation that accumulated because of the effects of topography at an observation site and in regions upwind of the observation site. Although the terrain effects at a particular location may vary from storm to storm, the overall effect of the topographic influence is inherently included in the climatology of precipitation that occurred at that location, assuming that the climatology is based on storms of the same type.

For Texas, extreme storm events (PMP-type storms) include local storms (both individual thunderstorms and MCSs), general storms, and tropical storms. Local storms are the primary controlling storm type of the precipitation frequency climatology at durations of 6 hours or less, while the general and tropical storms are responsible for the precipitation frequency climatology values for durations of 24 hours and greater. Hence, climatological analysis of the rainfall data associated with these storm types adequately reflects the differences in topographic influences at different locations when evaluated by storm type and duration, thereby reducing potential effects of mixed populations.

The procedure used in this study to account for terrain effects determines the differences between the climatological information at the in-place storm location and the individual grid point. This is a departure from the SSM used in HMRs 55A, 57, and 59. The SSM used in the HMRs is highly subjective and is not reproducible. There are unknown variables involved in the computation; specifically, the amount of rainfall that would have accumulated without the topography (convergence only or free atmospheric forced precipitation, e.g., HMR 55A Section 7.1). A detailed description of the HMR SSM process and an attempt to replicate/validate the process is provided in Appendix J.

It is important to ensure that non-orographic storms are not transpositioned into orographic regions and vice versa because the precipitation frequency relations and resulting GTF values would no longer be representative of the same storm types. This was recognized by the WMO 2009 Section 3.1.4 as well, where it is stated "since precipitation-frequency values represent equal probability, they can also be used as an indicator of the effects of topography over limited regions. If storm frequency, moisture availability, and other precipitation-producing factors do not vary, or vary only slightly, over an orographic region, differences in precipitation-frequency values should be directly related to variations in orographic effects." Therefore, by applying appropriate transposition limits, analyzing by storm type, and utilizing duration for storm type, we are ensuring the storms being compared using the precipitation frequency data are of similar moisture availability and other precipitation-producing factors.

The precipitation frequency estimates utilize information from the mean annual maximum grids developed using the Oregon State University Climate Group's PRISM system to help spatially distribute the values between observational data locations (Perica et al., 2013). PRISM is a peer-reviewed modeling system that combines statistical and geospatial concepts to evaluate gridded rainfall with particular effectiveness in geographic areas (Daly et al., 1994). The precipitation frequency estimates used in this study implicitly express terrain controls through the adoption of the PRISM system. A major component of the GTF process is the assumption that the relation between precipitation frequency values in areas of similar meteorology and topography (transpositionable regions) are a reflection of the difference in terrain effect between the two locations being compared. It is also assumed that the influence of terrain is the primary contributing factor to the variability in the relation between precipitation climatology values at two distinct point locations of interest.

Although the precipitation frequency climatologies developed for this study and the NOAA Atlas 14 climatologies are all useful for developing the GTF relation, the relation can vary slightly depending on which durations and return frequencies are used. Therefore it is important to apply the duration and return frequency that best represents the effects that are intended to be captured with the GTF for a given storm type. The 6-hour duration was determined to best represent local/MCS type storms, whereas the 24-hour duration was used to represent the tropical and general type events. Some local/MCS storms used in this study are considered hybrid events with characteristics of local and general storms or local and tropical storms. For hybrid events, the GTF is calculated separately for both storm types using the appropriate precipitation frequency climatology duration and applied to the PMP calculation for the given storm type.

The precipitation climatologies range in return frequencies up to 1,000-years. Many of the analyzed storms in this study have maximum rainfalls that greatly exceed the 1,000-year return frequency. The 1,000-year return frequencies provide a lower level of confidence than shorter frequencies (i.e. 100-year) and attempting to extrapolate beyond 1,000-years is highly speculative. For this study, the 100-year return frequency climatology provided magnitudes and a spatial distribution representative of extreme storms at a reasonable level of confidence. In previous studies, linear regression was used to predict the climatological precipitation depth at the storm's calculated return frequency based on the 10-year through 1,000-year depths. This method has been effective when transposing storms within a single precipitation climatology region where the data are proportional. However, in this study, some storms were transposed great distances into Texas (e.g., Douglasville, Georgia 2009 and Warner Park, Tennessee 2010) from NOAA Atlas 14 climatologies where the data series may not correlate as effectively with the Texas precipitation climatology. For these reasons, the 100-year return frequency was chosen as the representative dataset to determine the GTF ratio.

The GTF for a storm at a target (grid point) location was calculated by determining the relation between the climatological 100-year recurrence interval precipitation depth at the source storm center location as determined by the SPAS total storm rainfall gridded data and the corresponding depth at the target location grid point centroid. The geographic effect on rainfall is quantified as the GTF and defined as the ratio of the 100-year 24-hour climatological precipitation depth at the target grid point location to the storm center location (Equation 3.1). A description of the GTF calculation process is given in Section 9.4 and an example is provided in Section 9.6.4.

$$GTF = \frac{P_t}{P_s} \qquad \text{Equation 3.1}$$

where,

$P_t$ = climatological 100-year precipitation depth at the target location
$P_s$ = climatological 100-year precipitation depth at the source storm center location

# 4. Dew Point Climatology Development

This study incorporated updated procedures and data analysis methods used in other PMP studies completed by AWA. This section describes the development of the updated dew point climatologies used for storm maximizations and PMP development. The maximum average dew point climatology derived during this study included portions of northern Mexico, as this was a moisture region for some of the storm events evaluated in this study. This followed the same process as the dew point climatologies developed by AWA over the contiguous United States (e.g., Tomlinson et al., 2008; Tomlinson et al., 2013; Kappel et al., 2014) and extended those climatologies through this region.

## 4.1 3-, 6-, 12-, and 24-hour Maximum Average Dew Point Climatology Methodology

These updated dew point climatologies replace those provided in the HMRs and in other PMP studies in the region. The initial task in the development of the updated climatology involved a search of the National Climatic Data Center (NCDC) stations that record hourly dew point temperature data within a defined search domain (Figure 4.1). The dataset searched was DS472 (DL U.S. and Canada Surface Hourly Observations, daily from December 1976 to present, includes data for Mexico and Central America). This dataset contains hourly surface observational data for all of Mexico.

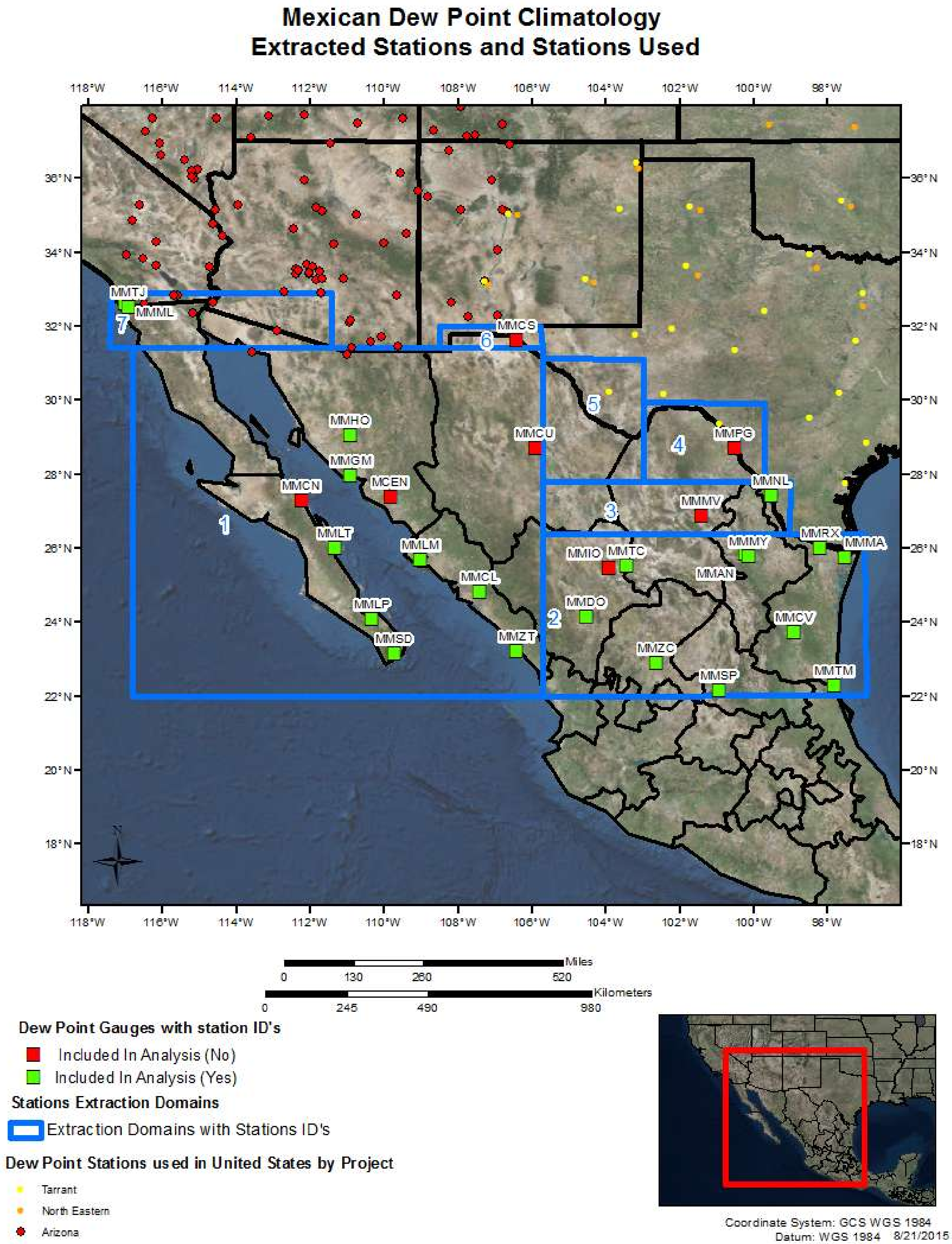


**Figure 4.1: Hourly dew point station locations used for the updated maximum dew point climatology development.**

Once stations were identified, AWA extracted the archived hourly datasets for the maximum average 3-hour, 6-hour, 12-hour, and 24-hour dew point temperatures for each reporting station. A total of 38 hourly stations were within the search domain. While initial quality control (QC) limited stations to 30 years or greater period-of-record, only 9 stations had more than 30-years record, so stations with less than 30 years were considered. Each annual maximum (AM) value was evaluated rather than imposing global thresholds and automatically keeping or omitting high AM values. Since high and low AM values can affect the distribution of annual maxima. Questionable AM values were carefully investigated and either validated, corrected, or removed from the series. Low outliers were often associated with years that had a significant percent of missing and/or accumulated data and hence presumed unreliable. If a year had less than 33% complete data and the AM was in the lowest 20% of ranked values, the AM was rejected. After QC procedures, 21 hourly stations were selected for the dew point temperature analysis (9 stations > 30-years record and 12 stations < 30-years record). These stations are listed in Table 4.1.

A script was written to extract each station's monthly maximum dew point temperatures for 3-, 6-, 12- and 24-hour durations for each year, providing annual maximum series (AMS) for that station. The AMS for each month for each station served as input to an R-statistical script that calculated L-moment statistics (Asquith, 2011a,b; Hosking, 2015a,b). Goodness-of-fit measures were evaluated for five candidate distributions: generalized logistic (GLO), generalized extreme value (GEV), generalized normal (GNO), Pearson type III (PE3), and generalized Pareto (GPA). An L-moment ratio diagram was also prepared based on L-Skewness and L-Kurtosis pairs for the collection of stations in each homogenous region. The regional weighted-average L-Skewness and L-Kurtosis pairing were found to be very near the GEV distribution. L-moment goodness-of-fit tests were conducted (Hosking and Wallis, 1997), and the GEV distribution was identified as the best-fit three-parameter probability distribution. Using the GEV distribution, the 20-year, 50-year, and 100-year return frequency dew point temperature values were calculated for each month for each station. The extracted dew point data were adjusted to the 15th of each month and adjusted to zero elevation (also described as 1000mb) from their original elevation.

The updated dew point climatologies replace the 12-hour maximum persisting dew point climatologies published by the U.S. Department of Commerce Environmental Data Service in the Climatic Atlas of the United States (Environmental Data Service, 1968) and those used in numerous PMP evaluations in the region. The 12-hour maximum persisting dew point climatologies were used to represent the maximum dew points for storm maximization procedures in the HMRs and other PMP studies in the region. The 12-hour maximum persisting dew point climatologies used were outdated, but more importantly they did not adequately represent the atmospheric moisture available in the PMP storm environment. The 12-hour persisting dew point values often missed or underestimated the atmospheric moisture available and resulted in in-place maximization values further from 1.00 than would have been calculated if more accurate data had been available (see Tomlinson et al., 2008 Section 8.1.1 and Kappel et al., 2014 Section 7.2.2).

The updated climatology more accurately represents the atmospheric moisture fueling storms by using average maximum dew point values observed over durations specific to each storm's rainfall duration. The average maximum dew point values for various durations replace the maximum 12-hour persisting dew point values.

**Table 4.1: Stations used to derive the maximum dew point climatology**

| No | Stid | Name | Province | Latitude | Longitude | Elevation (ft) | POR |
|---|---|---|---|---|---|---|---|
| 1 | MMCV | CIUDAD VICTORIA APT | MX | 23.7200 | -98.9000 | 781 | 36 |
| 2 | MMCL | CULIACAN CITY | MX | 24.8200 | -107.4000 | 128 | 36 |
| 3 | MMDO | DURANGO AIRPORT | MX | 24.1300 | -104.5000 | 6093 | 36 |
| 4 | MMGM | GUAYMAS INTL ARPT | MX | 27.9700 | -110.9000 | 89 | 36 |
| 5 | MMHO | HERMOSILLO INTL | MX | 29.0600 | -110.9000 | 692 | 16 |
| 6 | MMLP | LA PAZ INTL AIRPORT | MX | 24.0700 | -110.3000 | 69 | 36 |
| 7 | MMLT | LORETO | MX | 26.0100 | -111.3000 | 49 | 16 |
| 8 | MMLM | LOS MOCHIS AIRPORT | MX | 25.6800 | -109.0000 | 13 | 29 |
| 9 | MMMA | MATAMOROS_INTL | MX | 25.7600 | -97.5000 | 26 | 17 |
| 10 | MMZT | MAZATLAN | MX | 23.2000 | -106.4000 | 16 | 36 |
| 11 | MMML | MEXICALI INTL ARPT | MX | 32.6300 | -117.0000 | 72 | 16 |
| 12 | MMAN | MONTERREY INTL. | MX | 25.8600 | -100.2000 | 1470 | 36 |
| 13 | MMMY | MONTERREY/GEN_MARIA | MX | 25.7800 | -100.1000 | 1270 | 16 |
| 14 | MMNL | NUEVO LAREDO INTL | MX | 27.4300 | -99.5000 | 486 | 36 |
| 15 | MMRX | REYNOSA | MX | 26.0100 | -98.2000 | 128 | 16 |
| 16 | MMSD | SAN JOSE DEL CABO | MX | 23.1500 | -109.7000 | 358 | 16 |
| 17 | MMSP | SAN LUIS POTOSI | MX | 22.1500 | -100.9000 | 6243 | 16 |
| 18 | MMTM | TAMPICO | MX | 22.2800 | -97.8000 | 79 | 36 |
| 19 | MMTJ | TIJUANA INTL ARPT | MX | 32.5300 | -116.9000 | 499 | 16 |
| 20 | MMTC | TORREON AIRPORT | MX | 25.5300 | -103.4000 | 3688 | 16 |
| 21 | MMZC | ZACATECAS | MX | 22.9000 | -102.6000 | 7021 | 16 |

### 4.1.1 Procedure for Adjusting to the 15th of the Month

The station data were corrected to the 15th of each month using a linear relation between the previous month, current month, and following months. This follows the same procedure used in the HMR's when developing dew point climatological data sets (e.g., HMR 55A Section 4.3). The 15th adjustment was performed using a series of Excel macros. The steps are listed below:

1) Calculate the difference in days between the observed average date of the annual maximum series occurrence of the month being analyzed and the 15th.
2) Depending whether the difference in step 1 is positive or negative (direction of adjustment) calculate the ratio/difference between the non-adjusted dew point temperature (for the months of interest) and the number of days between the dates.
3) Apply the ratio calculated in step 2 to the difference calculated in step 1.
4) Check the adjusted dew point value with the previous and next month values, and the other two durations.
5) Calculate the difference between the original dew point value and the adjusted dew point value.
6) Create station plots of the duration and frequency for additional QC measure.
7) Create a list of the adjusted dew point values for each station in a GIS format.

### 4.1.2 1000mb Adjustment Procedures

A standard moist lapse rate (2.7°F/1,000 feet) was used to adjust the 15th of the month dew point temperature, at the station elevation, to elevation zero (i.e. sea level or 1000mb). A linear relation between elevation and lapse rate was created and applied to each station. For example, the June 24-hour maximum average dew point data for Monterrey, Mexico are shown in Table 4.2. The table shows the original station data, the data adjusted to the 15th, and the data adjusted to 1000mb.

**Table 4.2: Original 24-hour average dew point data, adjusted dew point data (to the 15th of the month), and the 1000mb dew point data for 20-year, 50-year, and 100-year frequencies at Monterrey, Mexico.**

| Monterrey, MX | 20-year | 50-year | 100-year |
|---|---|---|---|
| Station Data | 74.8°F | 75.6°F | 76.0°F |
| 15th Data | 74.6°F | 75.2°F | 75.3°F |
| 1000mb Data | 78.5°F | 79.1°F | 79.2°F |

### 4.1.3 Spatial Interpolation of Data

The adjusted dew point climatology data were interpolated between station locations using inverse distance weighting (IDW). IDW assigns to each interpolation location a weighted average of surrounding station values. The weights are inversely proportional to the distances to the stations (Isaaks and Srivastava, 1989), causing the nearest stations to have the greatest influence on the interpolated values. This weighting methodology has been used in previous similar analyses (e.g., Tomlinson et al., 2008; Tomlinson et al., 2013; Kappel et al., 2014). The interpolated values are calculated as:

$$\hat{z}(x_0) = \frac{\sum_{i=1}^{n} \frac{z(x_i)}{d_i^p}}{\sum_{i=1}^{n} \frac{1}{d_i^p}} \qquad \text{Equation 4.1}$$

where:

$\hat{z}(x_0)$ is the interpolated dew point value,

n is the total number of sample data values,

$z(x_i)$ is the $i$th data value,

$d_i$ denotes the separation distance between interpolated value and data value,

and exponent $p$ denotes the weighting power. The default weighting power is 2.0.

Creation of the final dew point maps used in this project was completed after applying the final step of manual interpretation by AWA meteorologists of the automated IDW algorithms. As part of the manual analysis, inconsistencies were removed and smoothing was applied where meteorological, climatological, and topographical factors warranted such actions. Further, judgment was used to compensate for the lack of spatial coverage in some sections of the domain and to ensure continuity between months and durations. Examples of the 100-year 24-hour dew point for June, July, August, and September are shown in Figures 4.2-4.5.

The northern Mexico dew point climatology datasets were merged with existing dew point climatologies created using procedures consistent with the other AWA PMP projects. The merged dew point climatologies created a seamless 6-, 12-, and 24-hour 100-year climatology for the continental United States east of the Cascade and Sierra Nevada mountain ranges. Note that the 3-hour dew point climatology developed in previous AWA studies only included regions west of the Continental Divide. As part of this work, the 3-hour climatology also covered all of Mexico bordering Texas. However, the 3-hour dew point climatology was not used in any of the storm adjustments in this study. This was because none of the storms used in the PMP development were best represented by the 3-hour climatology. Instead, all storm adjustments used in the development of PMP for this study used 6-, 12-, and 24-hour dew points or SST. Appendices A and B contain all the maps used in the development of PMP in this analysis.

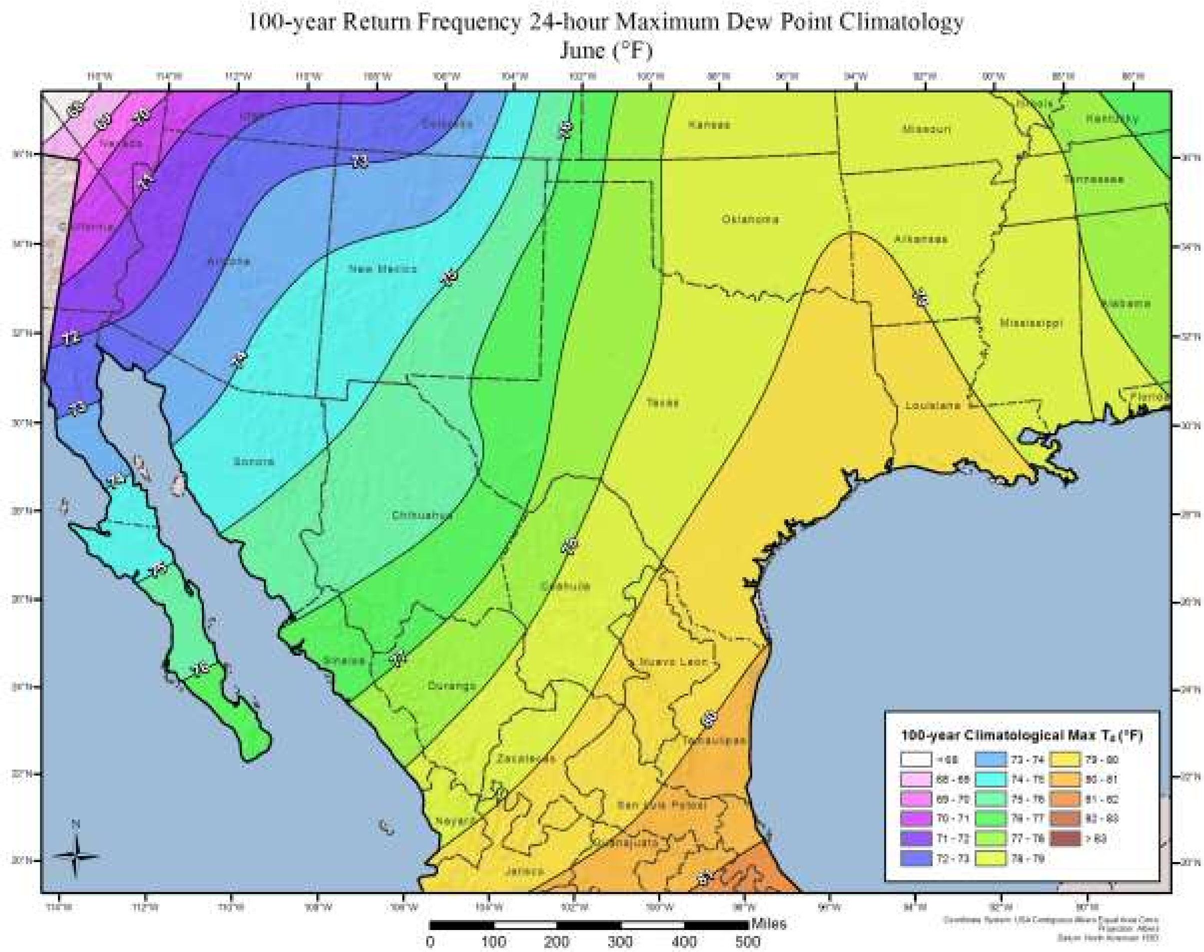


**Figure 4.2: June 100-year return frequency maximum average 24-hour 1000mb dew point map**

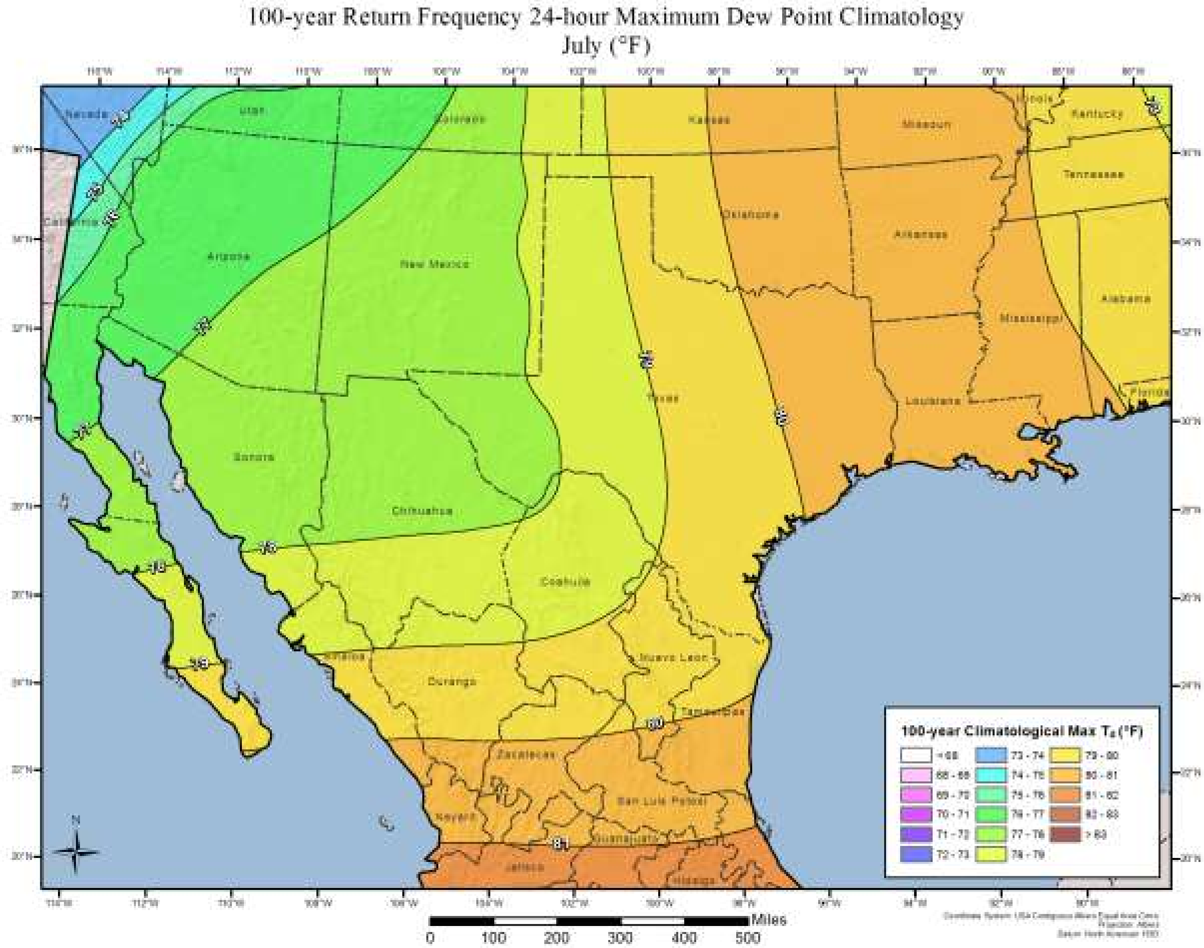


**Figure 4.3: July 100-year return frequency maximum average 24-hour 1000mb dew point map**

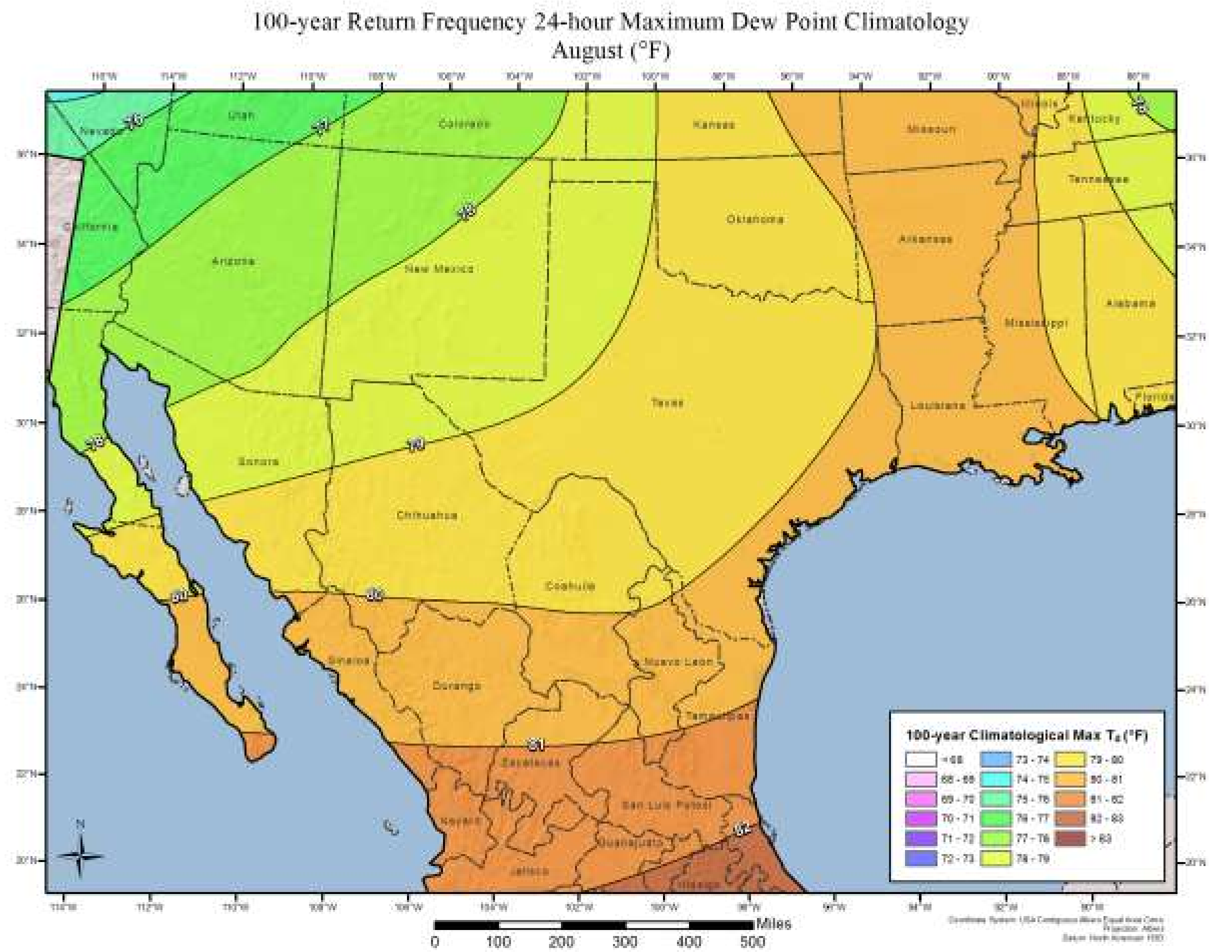


**Figure 4.4: August 100-year return frequency maximum average 24-hour 1000mb dew point map**

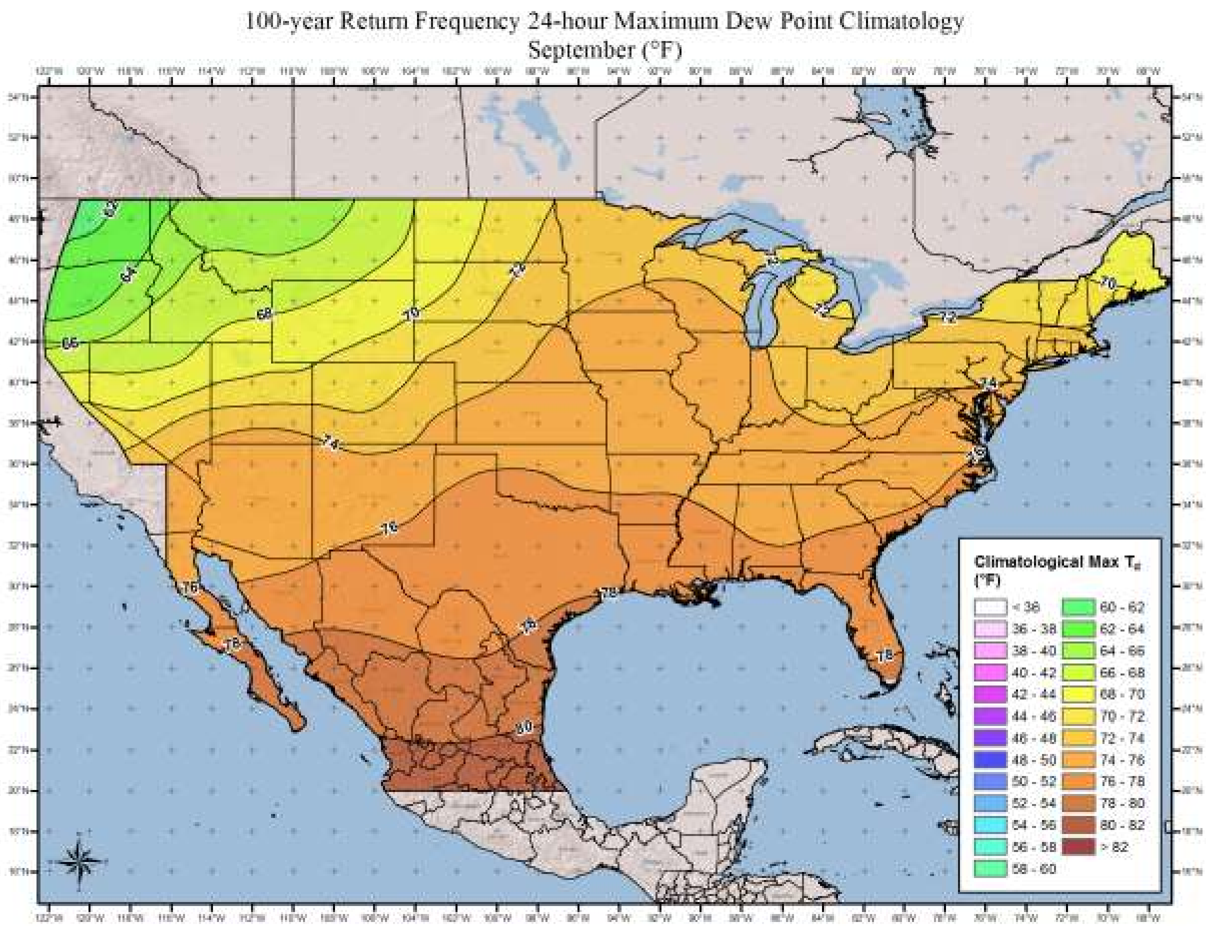


**Figure 4.5: September 100-year return frequency maximum average 24-hour 1000mb dew point map**

# 5. Precipitation and Rainfall Frequency Analyses

Precipitation frequency estimates are a necessary component of the GTF calculation process used in determining PMP values. Although precipitation frequency estimates existed as part of NOAA Atlas 2 Volume II (Miller, 1973), they were outdated, lacked accuracy across higher terrain, and did not incorporate over 40 years of additional precipitation data. In addition, several more recent updates to precipitation frequency climatologies have been completed for Texas (e.g., Faiers et al., 1997; Asquith and Roussel, 2004). This study produced an updated regional precipitation frequency analysis which included the entire state of Texas and much of northern Mexico. This was completed in order to add several years of data, incorporate enhancements in the statistical analysis process, include regions of northern Mexico required for PMP calculations, and produce the gridded precipitation frequency data required for PMP calculations. The result were precipitation frequency data covering the overall project domain for the 6- and 24-hour durations at average recurrence intervals (ARIs) of 2- through 1,000-years.

## 5.1 Regional 6- and 24-hour Precipitation Frequency Analysis

This document describes the methodology and results of an all-season regional rainfall frequency analysis for the 6- and 24-hour durations across the state of Texas and adjacent Probable Maximum Precipitation (PMP) domain. The purpose of this project was to produce 06- and 24-hour 2-, 5-, 10-, 25-, 50-, 100-, 200-, 500- and 1000-year Average Recurrence Interval (ARI) precipitation estimate maps/grids for Texas. The motivation of this project was to produce updated 100-year rainfall frequency estimates to optimize the calculation of the GTF used in the transposition of storms in this PMP study.

This project provides an update of the 6- and 24-hour estimates contained in *Update Atlas of Depth-Duration Frequency of Precipitation Annual Maxima for Texas* (Asquith and Roussel, 2004) that supersedes Technical Paper 40 (Hershfield, 1961). The 100-year 24-hour isohyets from Asquith and Roussel (2004) shown in Figure 5.1 are based on precipitation data collected through 1994 plus a modest difference in statistical processing that was used for the updated analysis of this PMP study. This PMP study project includes precipitation data collected through 2014, and this represents 20 years of additional data from that used by Asquith and Roussel (2004).

Table 5.1 shows the station counts between the two projects. Both projects used data from the National Weather Service, but this analysis also incorporated data from the United States Geological Survey (USGS), National Resources Conservation Service (NRCS), Texas Water Development Board (TWDB), Remote Automatic Weather Stations (RAWS), and data in Mexico. The USGS data were included to supplement the data density for the 6-hour duration (not the 24-hour) where an increase in station density was more necessary. The number of hourly stations used in the Asquith and Roussel (2004) study for the 24-hour duration may include hourly stations co-located with daily stations that are removed in the count of stations for this analysis. Therefore, the hourly station count for Asquith and Roussel's 24-hour duration is approximated.

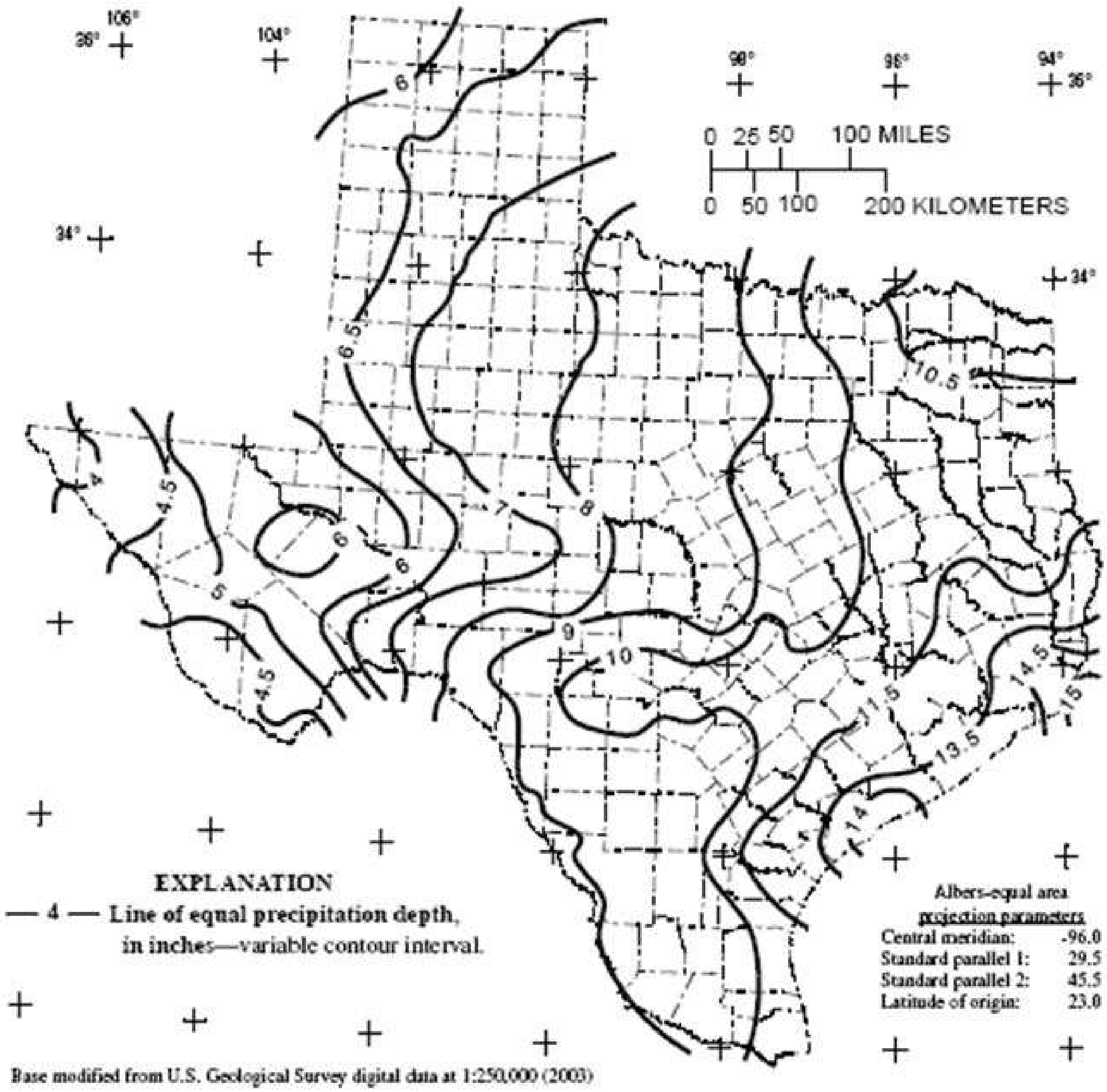


**Figure 5.1: Isopluvials of 100-year 24-hour precipitation in inches (Asquith and Roussel, 2004).**

**Table 5.1: Numbers of stations used in this analysis and in the previous study (Asquith, 1998).**

| Duration | Recording Increment | Asquith (1998) | This Analysis |
|---|---|---|---|
| 6-hour | Hourly | 274 | 493 |
| 24-hour | Hourly | ~274 | 249 |
| | Daily | 865 | 1082 |

The regional frequency analysis approach utilizes L-moments, which decrease the uncertainty of rainfall frequency estimates for rare events and dampens the influence of outlier precipitation amounts from extreme storms relative to other statistical fitting methods. Similar to

NOAA Atlas 14, a climatologically-aided spatial interpolation approach was used to distribute the at-site rainfall frequency estimates across Texas, thereby accounting for micro-climates, orographics, and other terrain driven spatial patterns of rainfall. Each of these important project elements is discussed in detail below. Please refer to Appendix C for more information.

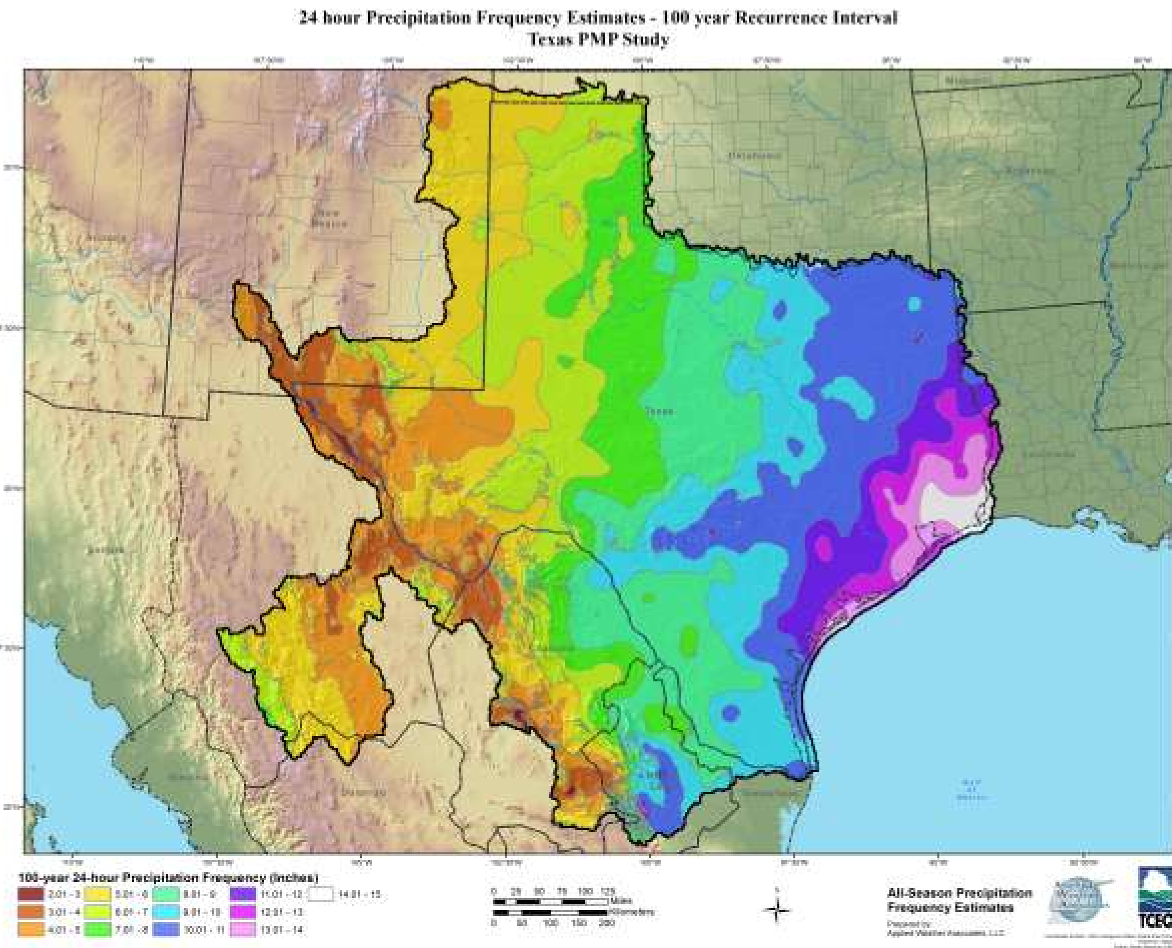


**Figure 5.2: 24-hour precipitation frequency estimates with an average recurrence interval of 100 years.**

## 5.2 Localized Precipitation Frequency Analysis

The GTF methodology requires rainfall frequency estimates to exist at (1) the location of the storm center associated with all of the SPAS DAD centers and (2) all points within the PMP project domain. The updated precipitation frequency analysis provided all necessary data for GTF analysis for all SPAS DAD centers with one exception, Gonzalez, Mexico October, 2000 (SPAS 1599). This storm center occurred just south of the overall region analyzed for the precipitation frequency development (Figure 5.3). To address this, a “mini” or localized regional precipitation frequency analysis was required. To ensure consistency among the rainfall frequency estimates, an approach consistent to that used in the Wyoming statewide analysis and in NOAA Atlas 14 was implemented, but on a smaller (i.e. “mini” or localized) scale.

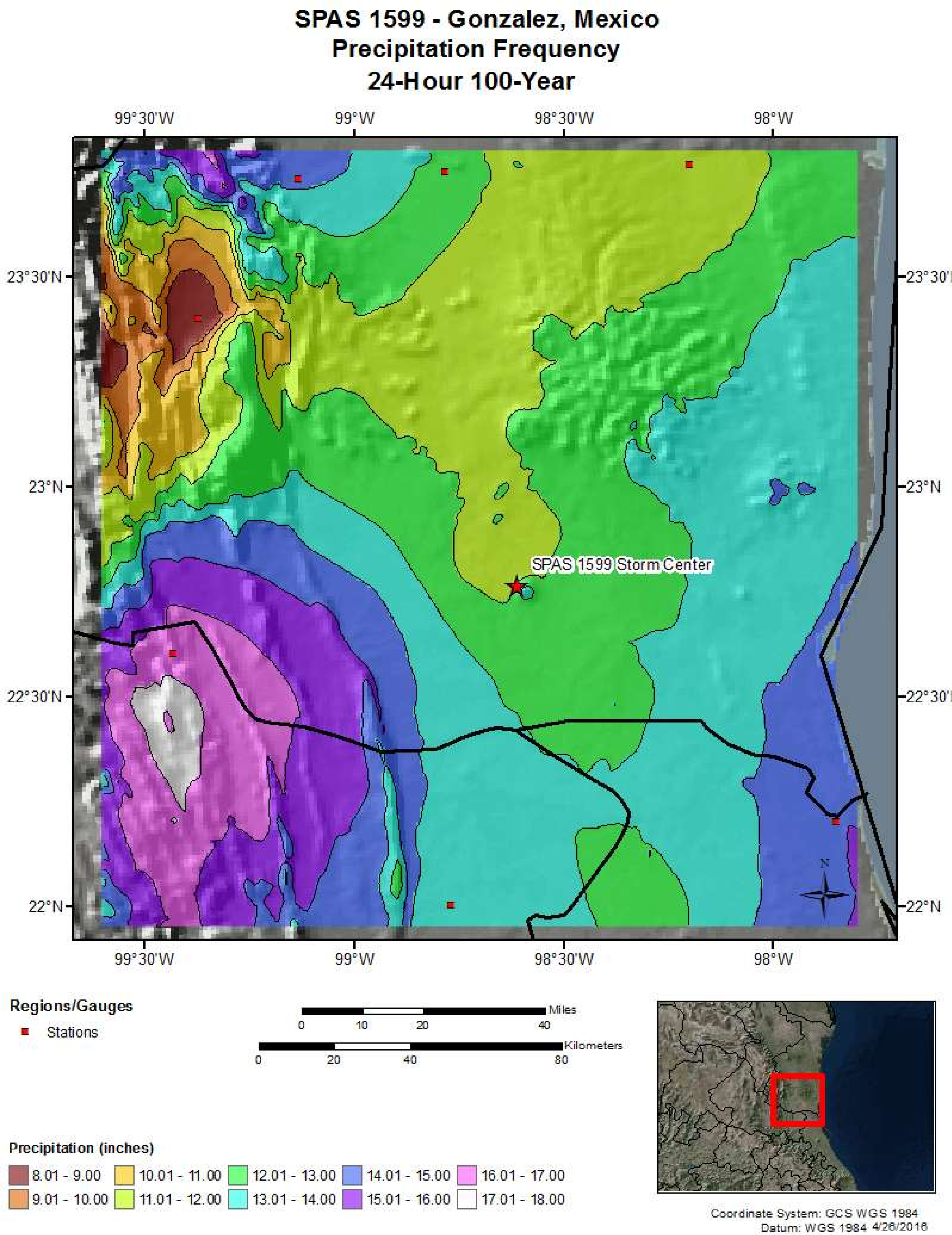


**Figure 5.3: SPAS 1599 frequency analysis, with the 100-year 24-hour precipitation frequency data within the localized domain provided.**

# 6. Extreme Storm Identification

## 6.1 Storm Search Area

A storm search was conducted using previous search results from several AWA PMP studies, all relevant HMRs, USACE Storm Studies, USGS reports, NWS reports, scientific journal articles, various weather books, and discussions with Review Board members. Previously used storm search domains were expanded to identify all storms that could potentially affect PMP values in the project domain used for the Texas PMP analysis. The search area covered an extensive region both east of the Continental Divide, through the Great Plains, south to the Gulf Coast, and east to the first upslopes of the Appalachians (Figure 6.1). This region included areas that were later determined not to be transpositionable to any point within the Texas PMP project domain. This large domain was needed to ensure that all storms which could potentially influence PMP values at any location within the project domain were included. Those storms and their limits of transpositionability were not known explicitly until extensive analysis was completed. Therefore, a large search area was used in the storm search to ensure all potential storms were included.

## 6.2 Data Sources

The storm search was conducted using a database containing rainfall data from several sources. The primary data sources are listed below:

1) Cooperative Summary of the Day / TD3200 through 2012. These data are published by the National Center for Environmental Information (NCEI), previously the National Climatic Data Center (NCDC). These are stored on AWA's database server and can be obtained directly from the NCEI.
2) Hourly Weather Observations published by NCEI, U.S. Environmental Protection Agency, and Forecast Systems Laboratory (now National Severe Storms Laboratory). These are stored on AWA's database server and can be obtained directly from the NCEI.
3) NCEI Recovery Disk. These are stored on AWA's database server and can be obtained directly from the NCEI.
4) Hydrometeorological National Weather Service Hydrometeorological Reports publication series. Each of which can be downloaded from the Hydrometeorological Design Studies Center website at http://www.nws.noaa.gov/oh/hdsc/studies/pmp.html
5) U.S. Corps of Engineers Storm Studies (USACE, 1973).
6) United States Geological Society (USGS) Flood Reports (e.g., Dalrymple et al., 1937; Dalrymple et al., 1939; Paulsen and Wells, 1952; Asquith and Slade, 1995; Asquith, 1998; Asquith, 1999; Juracek, 2001; Al-Asaadi, 2002; Asquith et al., 2004; Williams-Sether et al., 2004; and Costa and Jarrett, 2008).
7) Bureau of Reclamation storm data.

8) Other data published by NWS offices. These can be accessed from the National Weather Service homepage at http://www.weather.gov/.
9) Data from supplemental sources, such as Community Collaborative Rain, Hail, and Snow Network (CoCoRaHS), Weather Underground, Forecast Systems Laboratories, RAWS, and various Google searches.
10) Previous and ongoing PMP and storm analysis work (Tomlinson, 1993; Tomlinson et al., 2008-2012; Kappel et al., 2012-2016).
11) Flood and precipitation reports from members involved in the study (George Bomar, John Nielsen-Gammon, William Asquith, Todd Marek, and Simeon Benson).
12) Various Texas weather books (Bomar, 1983; Burnett, 2008).
13) Peer reviewed journals (e.g., McAuliffe, 1921; Jennings, 1950; Carr, 1951; Lott, 1952; Lott, 1953; Lott, 1954; Schoner and Molansky, 1956; Bosart, 1984; Moore and Riley, 1993; Keim and Faiers, 1999; Smith et al., 2000; Rogash et al., 2006; Furl et al., 2015; Clayton et al., 2015).

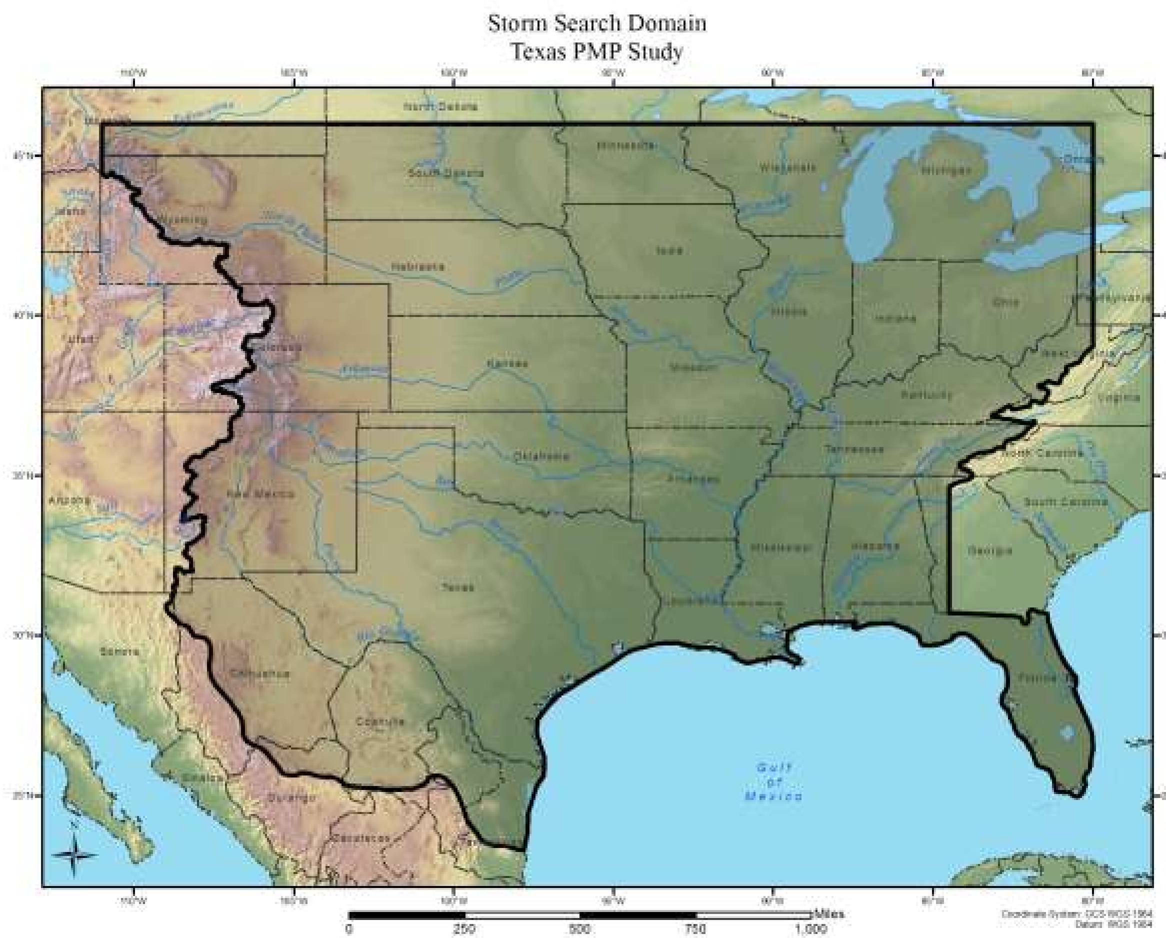


**Figure 6.1: Storm search domain**

## 6.3 Storm Search Method

The initial search began with identifying hourly and daily stations that have reliable rainfall data within the storm search domain. These stations were evaluated to identify the largest precipitation totals for various durations associated with each storm type: local storms, tropical storms, and general storms. Other reference sources such as HMRs, USGS reports, NWS reports, and climate center reports were reviewed to identify dates with large rainfall amounts for locations within the storm search domain. The threshold for storms to make the initial list of significant storms (referred to as the long storm list) were rainfall values that exceeded the 100-year return frequency value for specified durations at the station location or were associated with known extreme floods. The resulting long storm list was extensively quality controlled to ensure that only the highest storm rainfall values for each event were selected. Storms were then grouped by storm type, storm location, and duration for further analysis.

These storms were plotted and mapped using GIS to better evaluate the spatial coverage of the events throughout the region. Extensive discussions, evaluations, and comparisons of each storm were completed during several of the Review Board meetings. Table 6.1 provides an example of the long list as presented during Review Board meeting 3 hosted by TCEQ in Austin, Texas on July 29, 2015. From this initial long storm list, the potential storms to be analyzed were identified. Each storm was investigated in both published and unpublished references (NWS offices, USGS reports, other local Flood Reports, HMRs, AMS journals, etc.) to determine its significance in the storm and flood history of Texas and surrounding regions.

**Table 6.1: Example long list of storms used to derive the final short storm list.**

| Storm Name | State | Lat | Lon | Year | Month | Day | Maximum Rainfall in Inches | Precipitation Source |
|---|---|---|---|---|---|---|---|---|
| LARRABEE | IA | 42.8608 | -95.5453 | 1891 | 9 | 10 | 13.00 | MR 4-2 |
| GREELEY | NE | 41.5500 | -98.5333 | 1896 | 6 | 4 | 12.30 | MR 4-3 |
| LAMBERT | MN | 47.8000 | -96.0000 | 1897 | 7 | 18 | 8.00 | UMV 1-2 |
| HEARNE | TX | 30.8785 | -96.5931 | 1899 | 6 | 27 | 34.50 | GM 3-4 |
| EUTAW | AL | 32.8407 | -87.8875 | 1900 | 4 | 15 | 13.90 | LMV 2-5 |
| WOODBURN | IA | 41.0120 | -93.5991 | 1903 | 8 | 24 | 15.50 | MR 1-10 |
| ROCIADA | NM | 35.8667 | -105.3333 | 1904 | 9 | 26 | 7.90 | SW 1-6 |
| MEDFORD | WI | 45.1333 | -90.3333 | 1905 | 6 | 4 | 11.20 | GL 2-12 |
| BONAPARTE | IA | 40.7667 | -91.7500 | 1905 | 6 | 10 | 12.10 | UMV 2-5 |
| ELK | NM | 32.9432 | -105.3344 | 1905 | 7 | 21 | 13.30 | GM 3-13 |
| KNICKERBOCKER | TX | 31.2665 | -100.6232 | 1906 | 8 | 4 | 9.00 | GM 3-14 |
| AUSTIN | MS | 34.6500 | -90.4667 | 1906 | 11 | 17 | 19.40 | LMV 1-4 |
| MEEKER | OK | 35.5034 | -96.9028 | 1908 | 10 | 19 | 16.23 | SW 1-11 |
| BEAULIEU | MN | 47.3000 | -95.9000 | 1909 | 7 | 18 | 10.50 | UMV 1-11A |
| IRONWOOD | MI | 46.4500 | -90.1833 | 1909 | 7 | 21 | 13.20 | UMV 1-11B |
| GOLCONDA | IL | 37.3693 | -88.4843 | 1910 | 10 | 3 | 15.40 | OR 4-8 |
| FORT UNION | NM | 35.9360 | -105.0660 | 1913 | 6 | 6 | 7.90 | SW 1-14 |
| MONTELL | TX | 29.5380 | -100.0115 | 1913 | 6 | 27 | 20.60 | Texas Weather |
| MERRYVILLE | LA | 30.7543 | -93.5405 | 1914 | 3 | 24 | 12.90 | LMV 3-19 |
| CLAYTON | NM | 36.3333 | -103.1000 | 1914 | 4 | 29 | 9.60 | SW 1-16 |
| COOPER | MI | 42.3708 | -85.5875 | 1914 | 8 | 31 | 13.39 | SPAS 1426 |
| AUSTIN | TX | 30.2500 | -97.6833 | 1915 | 4 | 22 | 16.34 | GM 4-1 |
| TAJIQUE | NM | 34.7517 | -106.2878 | 1915 | 7 | 19 | 9.90 | SW 1-18 |
| LAKEWOOD | NM | 32.6323 | -104.3694 | 1916 | 8 | 7 | 6.00 | SW 1-20 |
| CONCEPTION | MO | 40.2428 | -94.6869 | 1919 | 5 | 2 | 6.20 | MR 2-20 |
| MEEK | NM | 33.6833 | -105.1833 | 1919 | 9 | 15 | 9.50 | GM 5-15B |
| PENROSE | CO | 38.4638 | -105.0705 | 1921 | 6 | 2 | 12.20 | SPAS 1294 |
| THRALL | TX | 30.5905 | -97.2970 | 1921 | 9 | 9 | 39.70 | GM 4-12 |
| BEAUMONT | TX | 30.0858 | -94.1017 | 1923 | 5 | 18 | 12.80 | John-Texas A&M |
| EAGLE PASS | TX | 28.7091 | -100.4995 | 1925 | 5 | 27 | 11.20 | GM 4-21 |
| NEOSHO FALLS | KS | 38.0820 | -95.7010 | 1926 | 9 | 12 | 14.00 | SW 2-1 |
| BOYDEN | IA | 43.1900 | -96.0100 | 1926 | 9 | 17 | 24.00 | MR 4-24 |
| WAKEENEY | KS | 39.0252 | -99.8796 | 1928 | 7 | 28 | 7.40 | MR 3-28 |
| ELBA | AL | 31.4167 | -86.0667 | 1929 | 3 | 12 | 29.60 | LMV 2-20 |
| PORTER | NM | 35.2000 | -103.2833 | 1930 | 10 | 9 | 9.90 | SW 2-6 |
| MEEKER | OK | 35.5034 | -96.9028 | 1932 | 6 | 2 | 12.40 | SW 2-7 |
| MOUNTAIN HOME | TX | 30.1746 | -99.3804 | 1932 | 6 | 30 | 35.60 | GM 5-1 |
| SONORA | TX | 30.5668 | -100.6435 | 1932 | 8 | 30 | 13.74 | USGS WRI 98-4099 |
| FAIRFIELD | TX | 31.6792 | -96.1292 | 1932 | 9 | 2 | 19.58 | SPAS 1428 |
| CHEYENNE | OK | 35.6100 | -99.6700 | 1934 | 4 | 3 | 23.00 | SW 2-11 |

Table 6.1: Example long list of storms used to derive the final short storm list (continued).

| Storm Name | State | Lat | Lon | Year | Month | Day | Maximum Rainfall in Inches | Precipitation Source |
|---|---|---|---|---|---|---|---|---|
| HERNANDO | MS | 34.8240 | -89.9937 | 1935 | 1 | 18 | 13.85 | LMV 1-19 |
| SIMMESPORT | LA | 30.9835 | -91.8001 | 1935 | 5 | 16 | 14.10 | LMV 4-21 |
| ELBERT | CO | 39.2375 | -104.4875 | 1935 | 5 | 30 | 24.00 | SPAS 1295 |
| HALE | CO | 39.6125 | -102.2625 | 1935 | 5 | 30 | 18.00 | SPAS 1295 |
| WOODWARD RANCH | TX | 29.3305 | -99.2798 | 1935 | 5 | 31 | 24.00 | GM 5-20 |
| SEGOVIA | TX | 30.4193 | -99.6704 | 1935 | 6 | 10 | 18.30 | GM 5-2 |
| BRACKETTVILLE | TX | 29.3100 | -100.4200 | 1935 | 6 | 14 | | USGS WSP 1455-B |
| NEWCOMERSTOWN | OH | 40.2723 | -81.6060 | 1935 | 8 | 6 | 12.70 | OR 9-11Thunder in the Heartland, |
| LAS CRUCES | NM | 32.3124 | -106.7779 | 1935 | 8 | 29 | 10.00 | HMR 55A storm 48, see Table 12.2 |
| BALLINGER | TX | 31.7382 | -99.9473 | 1935 | 9 | 2 | 12.30 | GM 5-3 |
| BEBE | TX | 29.3318 | -97.6816 | 1936 | 6 | 30 | 21.00 | GM 5-6 |
| BROOME | TX | 31.7596 | -100.8374 | 1936 | 9 | 13 | 30.00 | GM 5-7 |
| ROOSEVELT | TX | 30.4542 | -100.0375 | 1936 | 9 | 13 | 30.13 | SPAS 1582 |
| MCKENZIE | TN | 36.1326 | -88.5187 | 1937 | 1 | 5 | 22.60 | SPAS 1311 |
| SHARON SPRINGS | KS | 38.8978 | -101.7521 | 1938 | 5 | 30 | 10.00 | MR 3-29 |
| ELDORADO | TX | 30.8602 | -100.6010 | 1938 | 7 | 19 | 30.00 | GM 5-10 |
| GRANT TOWNSHIP | NE | 42.2400 | -96.5900 | 1940 | 6 | 3 | 13.00 | MR 4-5 |
| ENGLE | TX | 29.6810 | -97.0094 | 1940 | 6 | 29 | 22.70 | GM 5-11 |
| INDEX | AR | 33.5471 | -94.0419 | 1940 | 6 | 30 | 11.50 | LMV 4-25 |
| MILLER ISLAND | LA | 29.9000 | -91.9117 | 1940 | 8 | 6 | 37.50 | LMV 4-24 |
| HALLETT | OK | 36.2458 | -96.6125 | 1940 | 9 | 2 | 24.00 | SPAS 1429 |
| HEMPSTEAD | TX | 30.1292 | -96.0542 | 1940 | 11 | 22 | 21.29 | SPAS 1430 |
| PRAIRIEVIEW | NM | 33.1167 | -103.2000 | 1941 | 5 | 20 | 10.00 | GM 5-18 |
| HAYWARD | WI | 46.0130 | -91.4846 | 1941 | 8 | 28 | 15.00 | UMV 1-22 |
| MCCOLLEUM RANCH | NM | 32.1667 | -104.7333 | 1941 | 9 | 20 | 21.20 | GM 5-19 |
| TULAROSA | NM | 33.0740 | -106.0186 | 1941 | 9 | 27 | 7.50 | SW 3-1 |
| RANCHO GRANDE | NM | 34.9500 | -105.1000 | 1942 | 8 | 29 | 8.00 | SW 2-29 |
| WARNER | OK | 35.4792 | -95.3292 | 1943 | 5 | 6 | 25.24 | SPAS 1431 |
| MOUNDS | OK | 35.8458 | -96.0708 | 1943 | 5 | 16 | 19.27 | SPAS 1432 |
| SILVER LAKE | TX | 32.6700 | -95.5960 | 1943 | 6 | 5 | 16.50 | SW 3-3 |
| PORT ARTHUR | TX | 29.9271 | -93.9476 | 1943 | 7 | 27 | 17.76 | Texas Weather |
| STANTON | NE | 41.8670 | -97.0500 | 1944 | 6 | 10 | 17.30 | MR 6-15 |
| VAN | TX | 32.5248 | -95.6372 | 1945 | 3 | 28 | 17.40 | SW 3-5 |
| DANEVANG | TX | 29.0574 | -96.2075 | 1945 | 8 | 27 | 19.29 | Texas Weather |
| COLE CAMP | MO | 38.4600 | -93.2027 | 1946 | 8 | 12 | 19.40 | MR 7-2A |
| COLLINSVILLE | IL | 38.6708 | -90.0042 | 1946 | 8 | 12 | 19.07 | SPAS 1433 |
| SAN ANTONIO | TX | 29.1000 | -98.5000 | 1946 | 9 | 26 | 17.30 | GM 5-24 |
| GERING | NE | 41.8730 | -103.5942 | 1947 | 6 | 17 | 10.00 | MR 7-16 |
| HOLT | MO | 39.4542 | -94.3292 | 1947 | 6 | 18 | 17.62 | SPAS 1434 |
| FORT WORTH | TX | 32.7800 | -97.3000 | 1948 | 5 | 16 | 12.00 | Texas Weather |

Table 6.1: Example long list of storms used to derive the final short storm list (continued).

| Storm Name | State | Lat | Lon | Year | Month | Day | Maximum Rainfall in Inches | Precipitation Source |
|---|---|---|---|---|---|---|---|---|
| DEL RIO | TX | 29.3627 | -100.8968 | 1948 | 6 | 23 | 26.20 | HMR 51 storm 82 |
| YANKEETOWN | FL | 29.0300 | -82.7159 | 1950 | 9 | 3 | 45.20 | SA 5-8 |
| CONWAY | TX | 35.2070 | -101.3820 | 1951 | 5 | 13 | 15.00 | USGS WRI 98-4099 |
| DUMONT | IA | 42.7519 | -92.9755 | 1951 | 6 | 25 | 12.00 | UMV 3-29 |
| COUNCIL GROVE | KS | 38.6600 | -96.4900 | 1951 | 7 | 9 | 18.50 | MR 10-2 |
| MARSLAND | NE | 42.4439 | -103.2985 | 1951 | 7 | 27 | 7.00 | MR 10-7 |
| ALICE | TX | 27.7522 | -98.0697 | 1951 | 9 | 13 | 21.00 | USGS WSP 1227-D |
| KELSO | MO | 37.1906 | -89.5495 | 1952 | 8 | 11 | 13.00 | UMV 3-30 |
| JOHNSON CITY | TX | 30.2769 | 98.4116 | 1952 | 9 | 9 | 28.80 | SAT NWS top event last 100 yrs |
| CAMP POLK | LA | 31.0667 | -93.2000 | 1953 | 4 | 23 | 21.10 | LMV 5-3 |
| HARRISONBURG DAM | LA | 31.7875 | -91.8167 | 1953 | 5 | 11 | 25.35 | SPAS 1435 |
| RITTER | IA | 43.2441 | -95.8228 | 1953 | 6 | 7 | 11.00 | MR 10-8 |
| VIC PIERCE | TX | 30.3667 | -101.3833 | 1954 | 6 | 23 | 35.00 | SW 3-22, Hurricane Alice |
| LAKE MALOYA | NM | 37.0090 | -104.3410 | 1955 | 5 | 19 | 14.82 | SPAS 1251 |
| ROCKSPRINGS | TX | 30.0157 | -100.2054 | 1955 | 9 | 23 | 24.00 | USGS WRI 98-4099 |
| PARIS WATERWORKS | IN | 39.0500 | -87.7000 | 1957 | 6 | 27 | 12.40 | HMB-V18 |
| PRAGUE | NE | 41.3583 | -96.8794 | 1959 | 8 | 1 | 13.09 | SPAS 1031 |
| PORT LAVACA | TX | 28.6150 | -96.6261 | 1960 | 6 | 24 | 30.00 | USGS WRI 98-4099 |
| BIRMINGHAM | AL | 33.5612 | -86.7531 | 1961 | 2 | 19 | 13.58 | HYDRO 13 |
| IDA GROVE | IA | 42.3167 | -95.4667 | 1962 | 8 | 30 | 12.85 | EPRI |
| COLLEGE HILL | OH | 40.0854 | -81.6479 | 1963 | 6 | 3 | 19.39 | SPAS 1226 |
| DAVID CITY | NE | 41.2132 | -97.0710 | 1963 | 6 | 24 | 15.98 | SPAS 1030 |
| DEWEYVILLE | TX | 30.2977 | -93.7435 | 1963 | 9 | 18 | 20.60 | Texas Weather, Hurricane Cindy |
| MADISONVILLE | KY | 37.3458 | -87.4958 | 1964 | 3 | 8 | 11.67 | SPAS 1278 |
| LONGFELLOW | TX | 30.1424 | -102.3941 | 1965 | 6 | 11 | 11.00 | SAT NWS top event last 100 yrs |
| PLUM CREEK | CO | 39.1875 | -104.2958 | 1965 | 6 | 15 | 16.70 | SPAS 1293-Zone 3 |
| HOLLY | CO | 37.7125 | -102.4042 | 1965 | 6 | 16 | 19.18 | SPAS 1293 Zone 1 |
| EDGERTON | MO | 40.4125 | -95.5125 | 1965 | 7 | 18 | 20.76 | SPAS 1183 |
| GLADEWATER | TX | 32.8029 | -94.7050 | 1966 | 4 | 27 | 25.28 | SPAS 1181 |
| DELL CITY 10NW | TX | 32.0450 | -105.3257 | 1966 | 8 | 22 | 12.00 | HCLW ALL-NRCS document |
| SOMBRERETILLO | MX | 26.2000 | -99.9500 | 1967 | 9 | 19 | 34.90 | SW 3-24, Hurricane Beulah |
| DINERO | MX | 28.2542 | -97.9042 | 1967 | 9 | 19 | 35.01 | SPAS 1601 |
| WOOSTER | OH | 40.9146 | -81.9729 | 1969 | 7 | 4 | 14.95 | SPAS 1209 |
| KAFFIE RANCH | TX | 27.0759 | -98.6020 | 1971 | 9 | 12 | 21.02 | Texas Weather, Hurricane Fern |
| NEW BRAUNFELS | TX | 29.7000 | -98.1167 | 1972 | 5 | 11 | 16.00 | NRCS Survey |
| GLEN | MS | 34.8375 | -88.3958 | 1973 | 3 | 14 | 12.15 | SPAS 1357 |
| ENID | OK | 36.3805 | -97.8683 | 1973 | 10 | 10 | 19.45 | SPAS 1034 |
| TAYLOR RANCH | TX | 30.9732 | -98.9437 | 1976 | 7 | 3 | 17.83 | Texas Weather |
| CANYON | TX | 34.9799 | -101.9189 | 1978 | 5 | 26 | 10.00 | Texas Weather |

Table 6.1: Example long list of storms used to derive the final short storm list (continued).

| Storm Name | State | Lat | Lon | Year | Month | Day | Maximum Rainfall in Inches | Precipitation Source |
|---|---|---|---|---|---|---|---|---|
| MEDINA | TX | 29.7966 | -99.2466 | 1978 | 8 | 1 | 48.00 | Amelia |
| ALBANY | TX | 32.7260 | -99.3500 | 1978 | 8 | 3 | 32.50 | SPAS 1179 |
| WHITE SANDS | NM | 32.7833 | -106.1833 | 1978 | 8 | 19 | 10.00 | HMR 55A |
| LOUISVILLE | MS | 33.1167 | -89.0500 | 1979 | 4 | 12 | 22.07 | SPAS 1227 |
| ALVIN | TX | 29.4238 | -95.2441 | 1979 | 7 | 25 | 45.00 | NHC CLAUDETTE |
| CLEO | TX | 30.5050 | -99.7770 | 1980 | 9 | 5 | 25.00 | USGS WRI 98-4099, TS Danielle |
| FRIJOLE CREEK | CO | 37.0960 | -104.3790 | 1981 | 7 | 3 | 16.33 | SPAS 1247 |
| GONZALES | TX | 29.5016 | -97.4525 | 1981 | 8 | 31 | 16.31 | Texas Weather |
| CLYDE | TX | 32.4790 | -99.4790 | 1981 | 10 | 10 | 23.23 | SPAS 1184 |
| BIG FORK | AR | 35.8708 | -92.1208 | 1982 | 12 | 1 | 15.92 | SPAS 1219 |
| FOREST CITY | MN | 45.2394 | -94.5404 | 1983 | 6 | 20 | 17.00 | SPAS 1035 |
| BROWNSVILLE | TX | 25.9100 | -97.4900 | 1984 | 9 | 16 | 20.00 | USGS WRI 98-4099 |
| TAFT | TX | 27.9789 | -97.3986 | 1984 | 10 | 19 | 24.80 | John-Texas A&M |
| COLUMBUS | TX | 29.7066 | -96.5397 | 1984 | 11 | 11 | 20.87 | John-Texas A&M |
| BIG RAPIDS | MI | 43.6125 | -85.3125 | 1986 | 9 | 9 | 13.18 | SPAS 1206 |
| MINNEAPOLIS | MN | 44.8895 | -93.4021 | 1987 | 7 | 23 | 11.55 | SPAS 1210 |
| GILBERTSVILLE | KY | 36.9958 | -88.2625 | 1989 | 2 | 12 | 13.20 | SPAS 1277 |
| BOERNE | TX | 29.7953 | -98.7320 | 1991 | 12 | 18 | 14.00 | NWS |
| AMERICUS | GA | 32.0958 | -84.2292 | 1994 | 7 | 4 | 28.09 | SPAS 1317 |
| SPRING RANCH | TX | 29.5421 | -100.2535 | 1994 | 10 | 7 | 29.92 | SAT NWS top event last 100 yrs |
| CORRIGAN | TX | 30.2600 | -94.8900 | 1994 | 10 | 16 | 23.31 | SPAS 1185 |
| NECAISE | MS | 30.6019 | -89.4142 | 1995 | 5 | 8 | 27.50 | WEST PALM NWS REPORT |
| LEA COUNTY | NM | 32.9450 | -103.3490 | 1995 | 9 | 15 | 10.00 | NWS report |
| AURORA COLLEGE | IL | 41.4575 | -88.0699 | 1996 | 7 | 16 | 18.13 | SPAS 1286 |
| LOUISVILLE | KY | 38.1000 | -85.6700 | 1997 | 2 | 28 | 13.51 | SPAS 1244 |
| ART | TX | 30.7389 | -99.1119 | 1997 | 6 | 22 | 20.00 | NRCS Survey |
| DAUPHIN ISLAND | AL | 30.2593 | -88.1280 | 1997 | 7 | 19 | 37.75 | NWS RADAR ESTIMATED, DANNY |
| PAWNEE CREEK | CO | 40.7752 | -103.6253 | 1997 | 7 | 29 | 13.58 | SPAS 1036 |
| MUNSON | FL | 30.8578 | -86.8722 | 1998 | 9 | 24 | 38.46 | NHC MAP |
| NEW BRAUNFELS | TX | 29.7000 | -98.1167 | 1998 | 10 | 17 | 30.00 | SPAS 1180 |
| GONZALEZ | MX | 22.5000 | -98.2500 | 2000 | 10 | 5 | 24.55 | HURRICANE KEITH |
| HOUSTON | TX | 30.0500 | -94.3000 | 2001 | 6 | 5 | 40.68 | NHC ALLISON |
| DENISON DAM | TX | 33.8177 | -96.5708 | 2001 | 9 | 9 | 18.48 | John-Texas A&M |
| HELOTES | TX | 29.5780 | -98.6898 | 2002 | 6 | 30 | 33.75 | SAT NWS report |
| OGALLALA | NE | 41.1247 | -101.7166 | 2002 | 7 | 6 | 14.92 | SPAS 1033 |
| MONTGOMERY DAM | PA | 40.6625 | -80.3875 | 2004 | 9 | 18 | 8.80 | SPAS 1275 |
| JASPER | TX | 30.9210 | -93.9966 | 2005 | 9 | 23 | 17.92 | Simeon USACE |
| EL PASO | TX | 31.9350 | -106.5150 | 2006 | 8 | 1 | 10.25 | SPAS 1528 |
| KOUNTZE | TX | 30.3724 | -94.3108 | 2006 | 10 | 15 | 20.14 | Simeon USACE |

Table 6.1: Example long list of storms used to derive the final short storm list (continued).

| Storm Name | State | Lat | Lon | Year | Month | Day | Maximum Rainfall in Inches | Precipitation Source |
|---|---|---|---|---|---|---|---|---|
| SHERMAN | TX | 33.6350 | -96.6110 | 2007 | 6 | 18 | 12.00 | |
| MARBLE FALLS | TX | 30.5782 | -98.2728 | 2007 | 6 | 27 | 18.82 | NWS STP |
| FALL RIVER | KS | 37.6300 | -96.0500 | 2007 | 6 | 30 | 25.50 | SPAS 1228 |
| HOKAH | MN | 43.8125 | -91.3625 | 2007 | 8 | 18 | 18.32 | SPAS 1048 |
| ALLEY SPRING | MO | 37.1600 | -91.4500 | 2008 | 3 | 17 | 15.10 | SPAS 1242 |
| MENDOTA | TX | 35.7270 | -100.4790 | 2008 | 6 | 8 | 10.00 | NWS |
| KIRKSVILLE | MO | 40.1800 | -92.5800 | 2008 | 7 | 25 | 12.15 | ST LOUIS NWS |
| RUIDOSO | NM | 33.3531 | -105.6618 | 2008 | 7 | 26 | 7.00 | REMNANT OF DOLLY |
| THOMASVILLE | FL | 30.8300 | -83.9800 | 2008 | 8 | 21 | 27.50 | Melbourne, TS FAY |
| LARTO LAKE | LA | 31.2200 | -92.1300 | 2008 | 9 | 1 | 23.31 | SPAS 1182 |
| SPRING | TX | 30.0797 | -98.4172 | 2008 | 9 | 13 | 20.03 | Simeon USACE-Ike |
| DOUGLASVILLE | GA | 33.8700 | -84.7600 | 2009 | 9 | 19 | 25.37 | SPAS 1218 |
| WARNER PARK | TN | 36.0611 | -86.9056 | 2010 | 5 | 1 | 19.71 | SPAS 1208 |
| NEW BRAUNFELS | TX | 29.7779 | -98.2030 | 2010 | 6 | 8 | 11.30 | COCORAHS |
| SPEARMAN | TX | 36.2000 | -101.1900 | 2010 | 6 | 13 | | John report |
| ESTANZUELA/COAHUILA | MX | 25.5000 | -100.3000 | 2010 | 6 | 29 | 43.79 | HURRICANE ALEX |
| LUBBOCK | TX | 33.5890 | 101.8440 | 2010 | 7 | 4 | 8.00 | COCORAHS |
| GEORGETOWN | TX | 30.6333 | -97.6757 | 2010 | 9 | 8 | 17.00 | COCORAHS |
| DUBUQUE | IA | 42.4400 | 90.7500 | 2011 | 7 | 27 | 15.14 | SPAS 1220 |
| PENSICOLA | FL | 30.3258 | -87.4089 | 2012 | 6 | 10 | 27.72 | COCORAHS |
| LAKE CITY | FL | 30.1897 | -82.6393 | 2012 | 6 | 20 | 15.00 | TRMM REPORT |
| PASCAGOULA | LA | 30.4000 | -88.4800 | 2012 | 8 | 24 | 22.20 | NEW ORLEANS NWS |
| SAN ANTONIO | TX | 29.4692 | -98.5883 | 2013 | 5 | 25 | 11.82 | AUSTIN/SA NWS REPORT |
| OKLAHOMA CITY | OK | 35.4774 | -97.2887 | 2013 | 5 | 31 | 8.17 | NWS AEP 6-HR REPORT |
| MOUNTAIN GROVE | MO | 37.1306 | -92.2635 | 2013 | 7 | 29 | 15.00 | NWS REPORT |
| GUADALUPE PASS | TX | 32.0350 | -104.5550 | 2013 | 9 | 10 | 18.34 | SPAS 1530 |
| SUMNER LAKE | NM | 34.5950 | -104.4750 | 2013 | 9 | 10 | 9.63 | SPAS 1530 |
| CHAPARRAL | NM | 32.1450 | -105.9950 | 2013 | 9 | 10 | 11.94 | SPAS 1530 |
| GILLIS | LA | 30.3738 | -93.2001 | 2013 | 9 | 20 | 15.67 | LAKE CHARLES NWS REPORT |
| CRYSTAL CITY | TX | 28.6859 | -99.8185 | 2013 | 10 | 14 | 13.88 | COCORAHS |
| WIMBERLEY | TX | 30.0086 | -98.1769 | 2013 | 10 | 30 | 15.00 | AUSTIN/SA NWS REPORT |
| SILVERHILL | AL | 30.4880 | -87.8002 | 2014 | 4 | 29 | 21.80 | COCORAHS |
| BRACKETBILLE | TX | 29.3122 | -100.4428 | 2014 | 6 | 20 | 14.62 | COCORAHS |
| KOPPERL | TX | 32.1242 | -97.5976 | 2014 | 6 | 22 | 14.13 | COCORAHS |
| RED BLUFF DAM | TX | 31.9051 | -103.9105 | 2014 | 9 | 18 | 15.00 | NWS STP |
| GAIL | TX | 32.7704 | -101.4454 | 2014 | 9 | 21 | 10.79 | John-Texas A&M |
| TAHOKA | TX | 33.1664 | 101.7942 | 2015 | 5 | 5 | 9.10 | West TX Mesonet |
| KENDALIA | TX | 30.0078 | -98.5457 | 2015 | 5 | 23 | 12.32 | COCORAHS |
| ABILINE | TX | 32.4116 | -99.6800 | 2015 | 7 | 7 | 8.26 | GEORGE-BOMAR |

## 6.4 Developing the Short List of Extreme Storms

A multiple step process was followed to determine a list of storms that was comprehensive enough to ensure that major extreme-rain events were identified and facilitated the elimination of smaller events that would not be informative for determining PMP values at any area size or duration after standard adjustments were applied. The next step was to determine which of these storms would ultimately need to be fully analyzed using SPAS. Several steps were taken to compare the magnitude of each of the events with the magnitude of others on the list of potential storms. Storms were sorted by storm type and location for initial comparison. This helped eliminate several storms that occurred in the same climate region but were of significantly less magnitude compared with others of the same duration in similar locations. The remaining storms were further investigated using various flood reports, discussions with personnel familiar with the storm events, and examination of the synoptic environment surrounding the event. The storms that made it through these final evaluations were placed on the short storm list (Table 6.2 and Figure 6.2). Each of these storms was analyzed with SPAS and considered to potentially affect PMP values for one or more grid points analyzed in this study.

This list contained all the storms analyzed by AWA for this study, a total of 68 individual SPAS DAD zones. Ultimately, only some of these short list storms control PMP values, with most providing support for the PMP values. For example, Table 6.3 lists all of the local storms that control PMP at some point in the analysis domain at the 10 square mile area size. There were 25 local storm DAD centers transposed to the analysis domain. Of these, only 10 controlled PMP at the 6-hour duration, and even fewer at other durations. The controlling storm's SPAS ID can be determined using a GIS at any grid point from the PMP points feature class produced as part of the PMP tool output. The digital Appendix K contains the PMP point feature classes for all of the pre-run area-durations for the entire analysis domain. The reason more storms were analyzed than was ultimately required to derive the PMP values was to ensure no storms were omitted which could have affected PMP values after all adjustment factors were applied. The magnitude of the adjustment factors was unknown at the beginning of the process. In other words, a storm with large point rainfall values may have a relatively small total adjustment factor, while a storm with a relatively smaller but significant rainfall value may end up with a large total adjustment factor. The combination of these calculations may provide a total adjusted rainfall value for the smaller rainfall event that is greater than the larger rainfall event after all adjustments are applied.

Figures 6.2 through 6.5 display the locations of all the storms used for PMP development. Figure 6.2 shows the location of all the storms on the short storm list, while Figure 6.3 shows the locations of all the local/MCS storms, Figure 6.4 shows the locations of the tropical storms, and Figure 6.5 shows the locations of all the general storms.

Table 6.2: Short storm list used to derive PMP values (all storms were analyzed with SPAS).

| SPAS_ID | NAME | STATE | LAT | LON | YEAR | MONTH | DAY | MAX POINT RAIN | PMP_TYPE |
|---|---|---|---|---|---|---|---|---|---|
| SPAS_1591_1 | HEARNE | TX | 30.8400 | -96.5700 | 1899 | 6 | 27 | 34.50 | GENERAL |
| SPAS_1592_1 | THRALL | TX | 30.6292 | -97.3875 | 1921 | 9 | 9 | 39.90 | HYBRID (T/L) |
| SPAS_1428_1 | FAIRFIELD | TX | 31.6792 | -96.1292 | 1932 | 9 | 2 | 19.58 | GENERAL |
| SPAS_1494_1 | MOUNTAIN HOME | TX | 30.1708 | -99.3792 | 1932 | 6 | 30 | 35.56 | LOCAL |
| SPAS_1495_1 | CHEYENNE | OK | 35.6208 | -99.6792 | 1934 | 4 | 3 | 23.01 | LOCAL |
| SPAS_1295_3 | HALE | CO | 39.6125 | -102.2625 | 1935 | 5 | 30 | 18.00 | LOCAL |
| SPAS_1485_1 | LAS CRUCES | NM | 32.3042 | -106.7958 | 1935 | 8 | 30 | 10.03 | LOCAL |
| SPAS_1496_1 | WOODWARD RANCH | TX | 29.4792 | -99.3875 | 1935 | 5 | 31 | 21.93 | LOCAL |
| SPAS_1582_1 | BROOME | TX | 31.7875 | -100.8542 | 1936 | 9 | 13 | 30.34 | TROPICAL |
| SPAS_1582_2 | ROOSEVELT | TX | 30.4542 | -100.0375 | 1936 | 9 | 13 | 30.13 | TROPICAL |
| SPAS_1311_1 | MCKENZIE | TN | 36.4375 | -87.9125 | 1937 | 1 | 5 | 19.86 | GENERAL |
| SPAS_1430_1 | HEMPSTEAD | TX | 30.1292 | -96.0542 | 1940 | 11 | 22 | 21.29 | GENERAL |
| SPAS_1429_2 | HALLETT | OK | 36.2458 | -96.6125 | 1940 | 9 | 2 | 24.00 | LOCAL |
| SPAS_1596_1 | MILLER ISLAND | LA | 29.8542 | -92.2458 | 1940 | 8 | 6 | 37.85 | TROPICAL |
| SPAS_1486_1 | MCCOLLEUM RANCH | NM | 32.1458 | -104.7458 | 1941 | 9 | 20 | 21.81 | GENERAL |
| SPAS_1587_1 | PRAIRIEVIEW | NM | 33.1375 | -103.0792 | 1941 | 5 | 20 | 11.08 | GENERAL |
| SPAS_1431_1 | WARNER | OK | 35.4792 | -95.3292 | 1943 | 5 | 6 | 25.24 | GENERAL |
| SPAS_1432_1 | MOUNDS | OK | 35.8458 | -96.0708 | 1943 | 5 | 16 | 19.27 | LOCAL |
| SPAS_1583_1 | COUNCIL GROVE | KS | 38.6458 | -96.6208 | 1951 | 7 | 9 | 18.56 | GENERAL |
| SPAS_1560_1 | CONWAY | TX | 35.2208 | -101.3958 | 1951 | 5 | 13 | 15.21 | HYBRID (G/L) |
| SPAS_1435_1 | HARRISONBURG DAM | LA | 31.7875 | -91.8167 | 1953 | 5 | 11 | 25.35 | GENERAL |
| SPAS_1602_1 | VIC PIERCE | TX | 30.4042 | -101.4375 | 1954 | 6 | 23 | 35.79 | HYBRID (T/L) |
| SPAS_1251_1 | LAKE MALOYA | NM | 37.0090 | -104.3410 | 1955 | 5 | 19 | 14.82 | GENERAL |
| SPAS_1558_1 | ROCK SPRINGS | TX | 29.9120 | -99.9960 | 1955 | 9 | 23 | 24.09 | LOCAL |
| SPAS_1278_1 | MADISONVILLE | KY | 37.3458 | -87.4958 | 1964 | 3 | 8 | 11.67 | GENERAL |
| SPAS_1293_1 | HOLLY | CO | 37.7125 | -102.4042 | 1965 | 6 | 16 | 19.18 | LOCAL |
| SPAS_1181_1 | GLADEWATER | TX | 32.8029 | -94.7050 | 1966 | 4 | 27 | 25.28 | GENERAL |
| SPAS_1568_1 | CARLSBAD | NM | 32.2542 | -104.6125 | 1966 | 8 | 22 | 17.35 | HYBRID (G/L) |
| SPAS_1601_1 | SOMBRERETILLO | MX | 26.2792 | -99.9208 | 1967 | 9 | 19 | 35.87 | TROPICAL |
| SPAS_1601_2 | DINERO | MX | 28.2542 | -97.9042 | 1967 | 9 | 19 | 35.01 | TROPICAL |
| SPAS_1357_1 | GLEN | MS | 34.8375 | -88.3958 | 1973 | 3 | 14 | 12.15 | GENERAL |
| SPAS_1034_1 | ENID | OK | 36.3805 | -97.8683 | 1973 | 10 | 10 | 19.45 | LOCAL |
| SPAS_1487_1 | WHITE SANDS | NM | 32.3874 | -106.5292 | 1978 | 8 | 19 | 10.43 | LOCAL |
| SPAS_1179_1 | ALBANY | TX | 32.7260 | -99.3500 | 1978 | 8 | 3 | 32.50 | TROPICAL |

Table 6.2: Short storm list used to derive PMP values (all storms were analyzed with SPAS), continued.

| SPAS_ID | NAME | STATE | LAT | LON | YEAR | MONTH | DAY | MAX POINT RAIN | PMP_TYPE |
|---|---|---|---|---|---|---|---|---|---|
| SPAS_1600_1 | MEDINA | TX | 29.8875 | -99.3208 | 1978 | 8 | 1 | 48.97 | TROPICAL |
| SPAS_1227_1 | LOUISVILLE | MS | 33.1167 | -89.0500 | 1979 | 4 | 12 | 22.07 | GENERAL |
| SPAS_1463_1 | ALVIN | TX | 29.4292 | -95.2708 | 1979 | 7 | 25 | 45.49 | TROPICAL |
| SPAS_1247_1 | FRIJOLE CREEK | CO | 37.0960 | -104.3790 | 1981 | 7 | 3 | 16.33 | LOCAL |
| SPAS_1184_1 | CLYDE | TX | 32.4790 | -99.4790 | 1981 | 10 | 10 | 23.23 | TROPICAL |
| SPAS_1219_1 | BIG FORK | AR | 35.8708 | -92.1208 | 1982 | 12 | 1 | 15.92 | GENERAL |
| SPAS_1277_1 | GILBERTSVILLE | KY | 36.9958 | -88.2625 | 1989 | 2 | 12 | 13.20 | GENERAL |
| SPAS_1185_1 | CORRIGAN | TX | 30.2600 | -94.8900 | 1994 | 10 | 16 | 23.31 | LOCAL |
| SPAS_1317_1 | AMERICUS | GA | 32.0958 | -84.2292 | 1994 | 7 | 4 | 28.09 | TROPICAL |
| SPAS_1244_1 | LOUISVILLE | KY | 38.1000 | -85.6700 | 1997 | 2 | 28 | 13.51 | GENERAL |
| SPAS_1569_1 | DAUPHIN ISLAND | AL | 30.3150 | -88.0350 | 1997 | 7 | 19 | 45.27 | TROPICAL |
| SPAS_1180_1 | NEW BRAUNFELS | TX | 29.7750 | -98.0450 | 1998 | 10 | 17 | 35.43 | HYBRID (T/L) |
| SPAS_1593_1 | MUNSON | FL | 30.8550 | -87.7250 | 1998 | 9 | 24 | 24.92 | TROPICAL |
| SPAS_1599_1 | GONZALEZ | MX | 22.7626 | -98.6125 | 2000 | 10 | 5 | 24.83 | TROPICAL |
| SPAS_1464_1 | HOUSTON | TX | 29.7550 | -95.2750 | 2001 | 6 | 5 | 40.97 | TROPICAL |
| SPAS_1594_1 | HELOTES | TX | 29.8550 | -98.8850 | 2002 | 6 | 30 | 38.55 | HYBRID (G/L) |
| SPAS_1528_1 | EL PASO | TX | 31.9350 | -106.5150 | 2006 | 8 | 1 | 10.25 | LOCAL |
| SPAS_1228_1 | FALL RIVER | KS | 37.6300 | -96.0500 | 2007 | 6 | 30 | 25.50 | GENERAL |
| SPAS_1242_1 | ALLEY SPRING | MO | 37.1600 | -91.4500 | 2008 | 3 | 17 | 15.10 | GENERAL |
| SPAS_1182_1 | LARTO LAKE | LA | 31.2200 | -92.1300 | 2008 | 9 | 1 | 23.31 | TROPICAL |
| SPAS_1529_1 | SUNSPOT | NM | 33.3350 | -105.7950 | 2008 | 7 | 26 | 8.81 | TROPICAL |
| SPAS_1218_1 | DOUGLASVILLE | GA | 33.8700 | -84.7600 | 2009 | 9 | 19 | 25.37 | GENERAL |
| SPAS_1208_1 | WARNER PARK | TN | 36.0611 | -86.9056 | 2010 | 5 | 1 | 19.71 | GENERAL |
| SPAS_1595_1 | SPEARMAN | TX | 36.1350 | -101.4950 | 2010 | 6 | 13 | 13.89 | LOCAL |
| SPAS_1598_1 | ESTANZUELA_COAHUILA | MX | 25.5958 | -100.2042 | 2010 | 6 | 29 | 36.87 | TROPICAL |
| SPAS_1530_1 | GUADALUPE PASS | TX | 32.0350 | -104.5550 | 2013 | 9 | 10 | 18.34 | GENERAL |
| SPAS_1530_2 | SUMNER LAKE | NM | 34.5950 | -104.4750 | 2013 | 9 | 10 | 9.63 | GENERAL |
| SPAS_1530_4 | CHAPARRAL | NM | 32.1450 | -105.9950 | 2013 | 9 | 10 | 11.94 | GENERAL |
| SPAS_1597_1 | SILVERHILL | AL | 30.3750 | -87.5850 | 2014 | 4 | 29 | 25.42 | GENERAL |
| SPAS_1557_1 | GAIL | TX | 32.7250 | -101.4050 | 2014 | 9 | 21 | 13.96 | LOCAL |
| SPAS_1531_1 | THE BOWL | TX | 31.9350 | -104.8250 | 2014 | 9 | 21 | 10.83 | TROPICAL |
| SPAS_1588_1 | TAHOKA | TX | 33.1050 | -101.8250 | 2015 | 5 | 5 | 10.51 | LOCAL |
| SPAS_1589_1 | ABILENE | TX | 31.4350 | -99.1150 | 2015 | 7 | 7 | 10.91 | LOCAL |
| SPAS_1590_1 | DAWSON | TX | 31.8950 | -96.6450 | 2015 | 10 | 23 | 32.92 | LOCAL |

**Table 6.3: List of contributing local storms for 10-square mile PMP over the project domain.**

| Storm | 1-hour | 2-hour | 3-hour | 4-hour | 5-hour | 6-hour | 12-hour | 24-hour |
|---|---|---|---|---|---|---|---|---|
| FRIJOLE CREEK, CO 1981 (SPAS 1247) | X | X | X | X | X | X | X | |
| HALE, CO 1935 (SPAS 1295) | X | X | X | X | X | X | X | |
| HALLETT, OK 1940 (SPAS 1429) | | | | | | X | X | |
| MOUNDS, OK 1943 (SPAS 1432) | X | X | X | X | X | X | | |
| LAS CRUCES, NM 1935 (SPAS 1485) | X | X | X | X | X | X | | |
| WHITE SANDS, NM 1978 (SPAS 1487) | | | | | | X | X | |
| MOUNTAIN HOME, TX 1932 (SPAS 1494) | X | X | X | X | X | X | | |
| CHEYENNE, OK 1934 (SPAS 1495) | X | X | X | X | X | X | X | X |
| WOODWARD RANCH, TX 1935 (SPAS 1496) | X | | X | | | | | |
| CONWAY, TX 1951 (SPAS 1560) | | | X | X | X | X | X | X |
| VIC PIERCE, TX 1954 (SPAS 1602) | X | X | X | X | X | X | X | X |

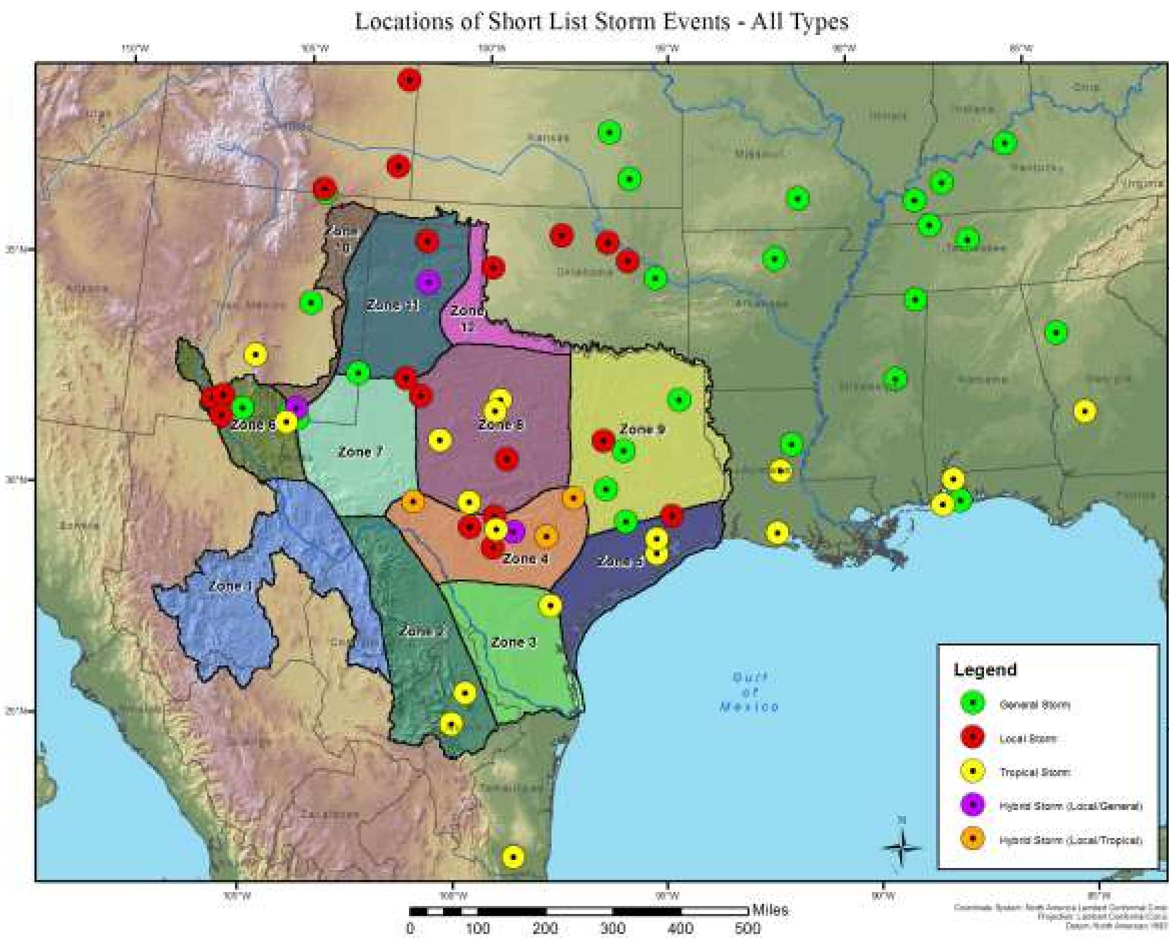


**Figure 6.2: Storm locations for storms on the short storm list**

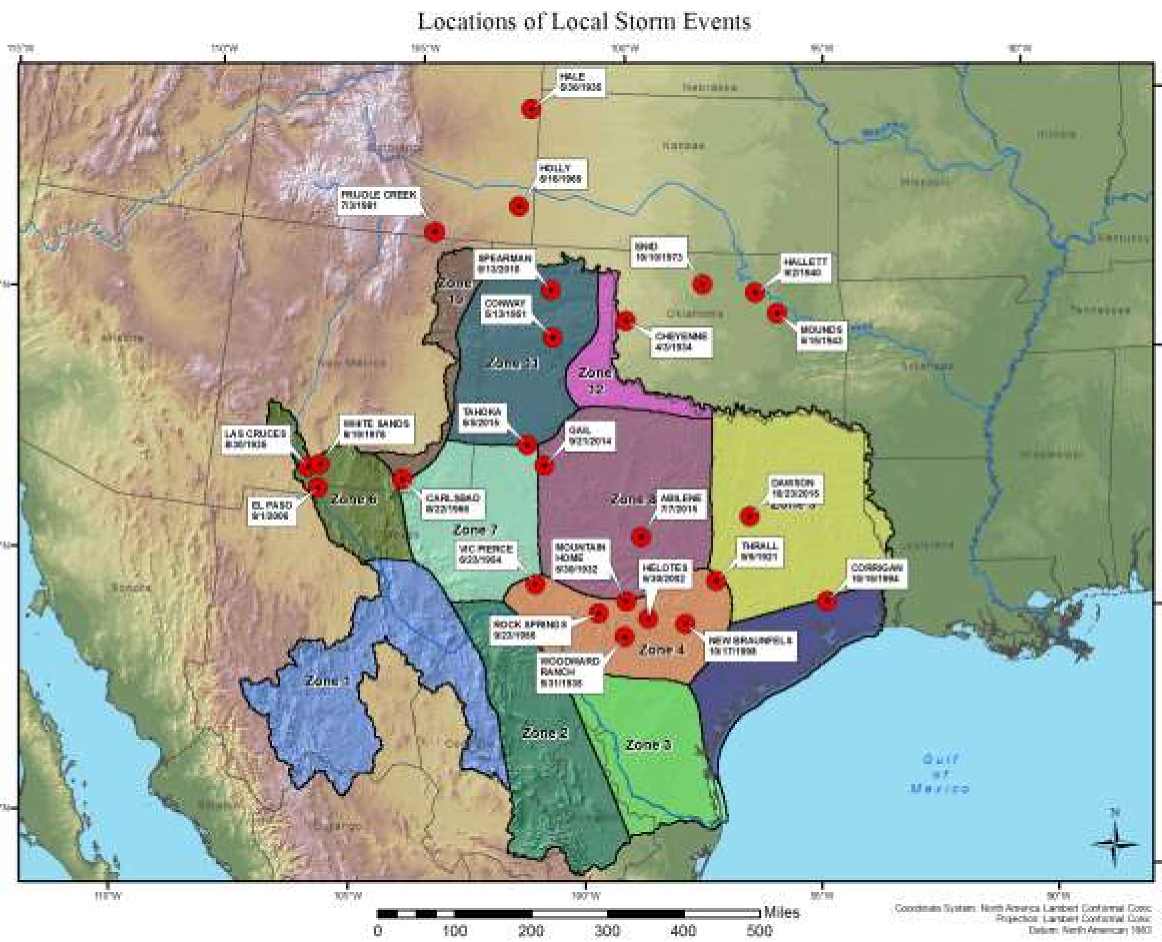


**Figure 6.3: Storm locations for local/MCS storms on the short storm list**

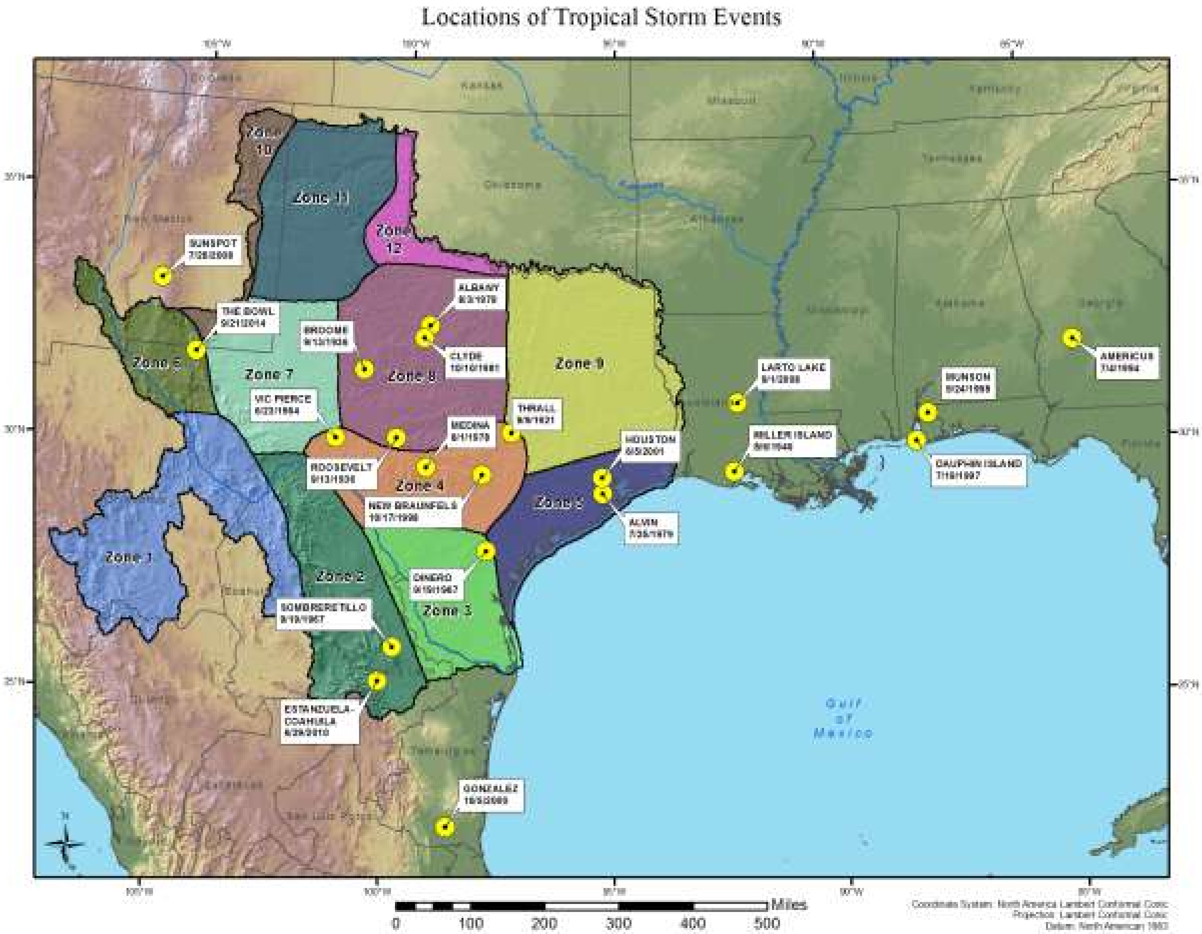


**Figure 6.4: Storm locations for tropical storms on the short storm list**

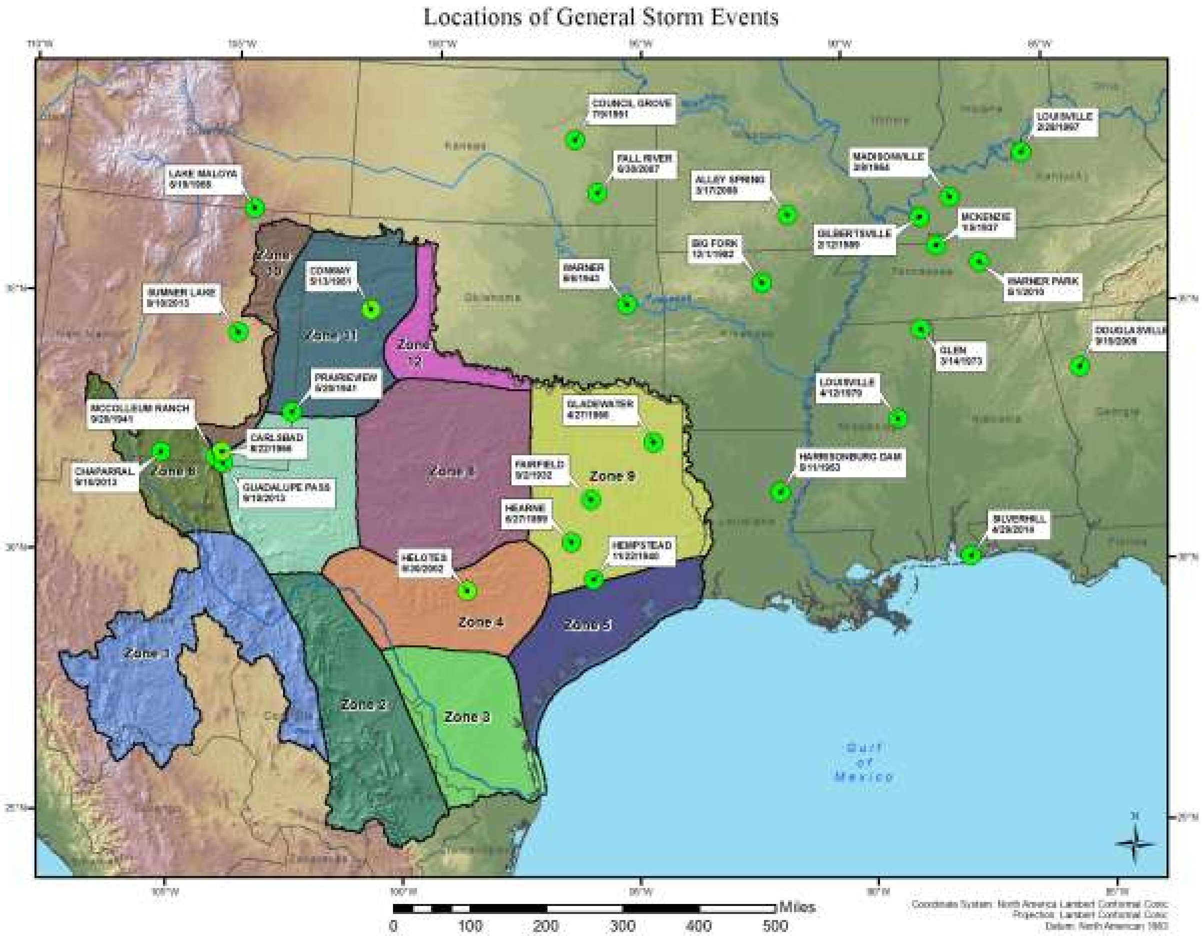


**Figure 6.5: Storm locations for general storms on the short storm list**

# 7. Storm Maximization

Storm maximization is the process of increasing rainfall associated with an observed extreme precipitation event under the potential condition that additional atmospheric moisture could have been available to the storm for rainfall production. This assumes that the storm dynamics, which convert that atmospheric moisture into precipitation remain constant and therefore an increase of available moisture would result in an increase in rainfall. Maximization is accomplished by increasing surface dew points or SSTs to a climatological maximum and calculating the enhanced rainfall amounts that could potentially be produced if the climatological maximum moisture had been available. An additional step in the process selects the climatological maximum dew point or SST for a date two weeks towards the season with higher amounts of moisture from the date that the storm actually occurred. This procedure assumes that the storm could have occurred with the same storm dynamics two weeks earlier or later in the year when maximum dew points or SSTs could be higher. This assumption follows HMR guidance and is consistent with procedures used to develop PMP values in all the current HMR documents (e.g., HMR 51 Section 2.3.4), the WMO manual (2009), as well as in all AWA PMP studies.

The in-place maximization and moisture transposition factors depend on the determination of storm representative dew points and SSTs, along with maximum historical dew points and SSTs. The magnitude of the maximization factor varies depending on the values used for the storm representative dew point or SST and the maximum dew point or SST value. Holding all other variables constant, the maximization factor is smaller for higher storm representative values as well as for lower maximum values. The maximization factor for a particular storm will change about 5% for every 1°F difference between the storm representative and maximum dew point values in the range of values used in this study.

For storm maximization, average dew point values for the appropriate duration that are most representative of the actual rainfall accumulation period for an individual storm (e.g., 6-, 12-, or 24-hour) are used to determine the storm representative dew point. This value is then maximized using the appropriate climatological value representing the 100-year return interval at the same location moved two weeks towards the season of higher climatological maximum values.

To determine which duration period was most appropriate for the storm representative value, the total accumulated precipitation during the duration of the storm was analyzed. The duration (6-, 12- or 24-hour) closest to when 90% of the rainfall had accumulated during the core precipitation period was used to specify the duration period. The HYSPLIT model (Draxler and Rolph, 2013) provides detailed analyses for assisting in the determination of the upwind trajectories of atmospheric moisture that was advected into the storm systems. HYSPLIT was developed to re-create past weather patterns based on all atmospheric data available. This allows the user to plot where moisture advected from, ending at the storm center location. Using these model results and trajectories, along with an analysis of the general synoptic weather patterns, the moisture source region is determined. The procedures followed to determine the storm representative location are similar to the approach used in HMRs. However, by utilizing the

HYSPLIT model, much of the subjectivity was eliminated. Further, details of each evaluation can be explicitly provided, and the HYSPLIT trajectory results based on the input parameters defined are reproducible. The tables presented in Appendix F list the moisture source region for each storm and dew point values used in the maximization calculations.

## 7.1 Use of Dew Point Temperatures

HMR and WMO procedures for storm maximization use a representative storm dew point as the parameter to represent available moisture to a historic storm. Storm precipitation amounts are maximized using the ratio of precipitable water for the maximum average dew point to precipitable water for the observed storm representative dew point.

Maximum dew point climatologies are used to determine the maximum atmospheric moisture that could have been available. Prior to the mid-1980s, maps of maximum dew point values from the *Climatic Atlas of the United States* (EDS, 1968) were the source for maximum dew point values. For the region covered by HMR 49, HMR 50 (Hansen and Schwartz, 1981) provided updated dew point climatologies. HMR 55A contained updated maximum dew point values for a portion of United States from the Continental Divide eastward into the Central Plains. HMR 57 updated the 12-hour persisting dew point values and added 3-hour persisting dew point climatology. The regional PMP study for Michigan and Wisconsin produced dew point return frequency maps representing the 50-year recurrence interval using the L-moments method. The Review Committee for that study included representatives from NWS, FERC, Bureau of Reclamation, and others. They agreed that the 50-year return frequency values were appropriate for use in PMP calculations. For the Nebraska statewide study, the Review Committee and FERC Board of Consultants agreed that the 100-year return frequency dew point climatology maps were appropriate because they afforded a layer of conservatism over the 50-year return period. This study, as in all prior PMP studies conducted by AWA, is again using the 100-year return frequency climatology constructed using data updated through 2016 (Figure 7.1).

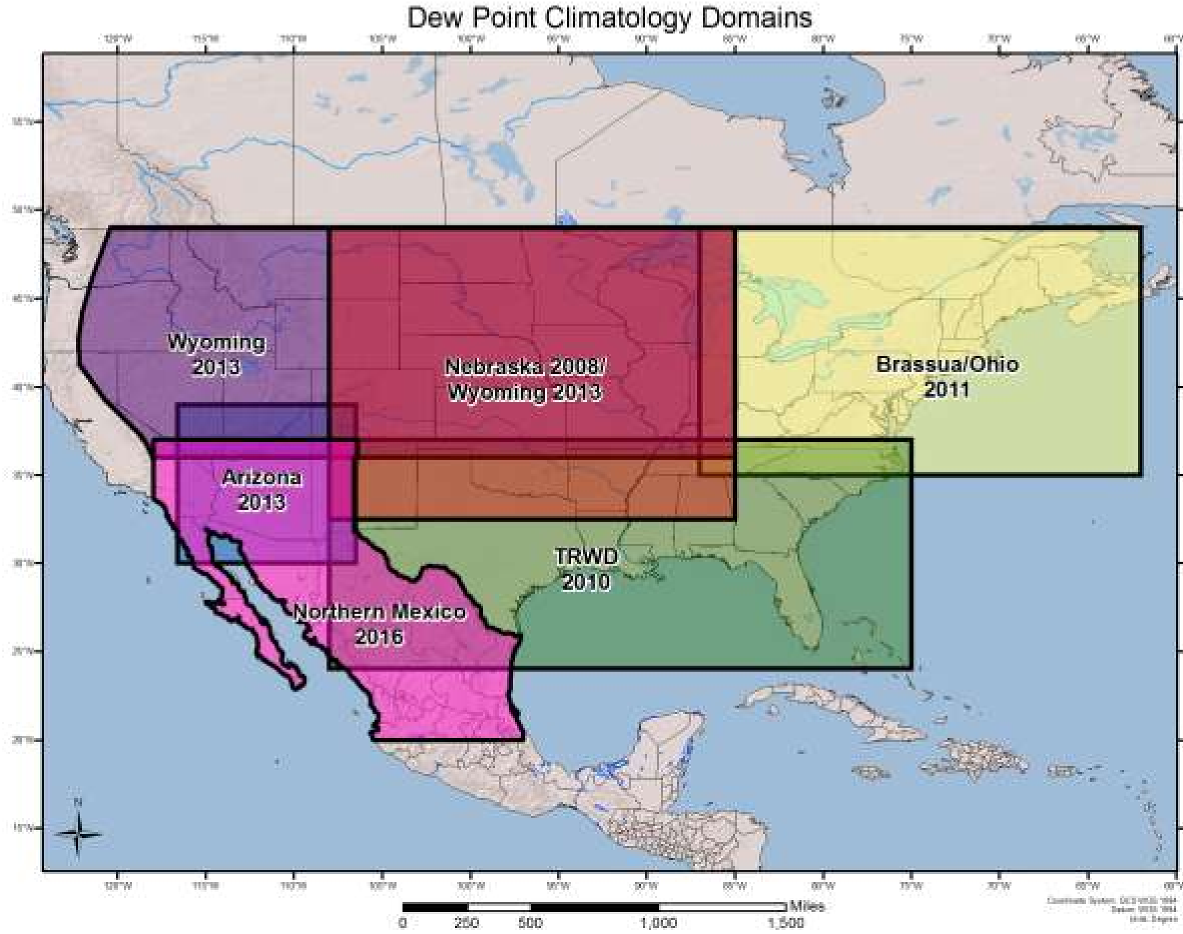


**Figure 7.1: Maximum dew point climatology development regions and dates of implementation**

Observed storm rainfall amounts are maximized using the ratio of precipitable water for the maximum dew point to precipitable water for the storm representative dew point, assuming a vertically saturated atmosphere. The ratio of the *maximum* precipitable water to the *actual* precipitable water associated with a storm event, called the in-place maximization factor (IPMF), is applied to the storm rainfall total to determine the storm's maximized rainfall total. By definition, maximization factors are always greater than or equal to 1. Following HMR (e.g., HMR 51 Section 3.2.2 and HMR 55A Section 8.4.1.1) and previous AWA PMP in-place storm maximization guidance, the in-place maximization value is capped at 1.50. This 1.50 limitation is somewhat ad hoc but is based on the consideration that if the moisture is increased beyond 50% (an IPMF of 1.50), the assumption that the moisture can be increased without altering the storm's dynamics is no longer valid (HMR 55A, Section 8.4.1.1). A further assumption is that properly analyzed and maximized storms should be some percent larger than the actual storm, but increases beyond certain limits (e.g., 50%) would change the characteristics of the storm.

## 7.2 Storm Representative Dew Point Determination Process

For storm maximization, average dew point values for the duration most consistent with the actual rainfall accumulation period for an individual storm (i.e. 6-, 12-, or 24-hour) were used to determine the storm representative dew point. To determine which time frame was most appropriate, the total rainfall amount was analyzed. The duration closest to when approximately 90% of the rainfall had accumulated was used to determine the duration used (e.g., 6-hour, 12-hour, or 24-hour).

The storm representative dew point was investigated for each of the storm events analyzed during this study. Once the general upwind location was determined, the hourly surface observations were analyzed for all available stations in the vicinity of the inflow vector. From these data, the appropriate durational dew point value was averaged for each station (6-, 12-, or 24-hour depending on the storm's rainfall accumulation). These values were then adjusted to zero elevation (also referred to as 1,000mb in previous AWA PMP studies as well as the HMRs) and the appropriate storm representative dew point and location were derived. The line connecting this point with the storm center location (point of maximum rainfall accumulation) is termed the moisture inflow vector. The information used and values derived for each storm's moisture inflow vector are included in Appendix F.

The HYSPLIT model developed by the NOAA Air Resources Laboratory (Draxler and Rolph, 2013) was used during the analysis of each of the rainfall events included on the short storm list when available (1948-present). Use of a trajectory model provides increased confidence in determining moisture inflow vectors and storm representative dew points. The HYSPLIT model trajectories have been used to analyze moisture inflow vectors in other PMP studies completed by AWA over the past several years. During these analyses, the model trajectory results were verified and the utility explicitly evaluated (e.g., Tomlinson et al., 2006-2013; Kappel et al., 2012-2015).

In determining the moisture inflow trajectories, the HYSPLIT model was used to compute the trajectory of the atmospheric moisture inflow associated with the storm's rainfall production, both location and altitude, for various levels in the atmosphere. The HYSPLIT model was run for trajectories at several levels of the lower atmosphere to capture the moisture source for each storm event. These included 700mb (approximately 10,000 feet), 850mb (approximately 5,000 feet), and the storm center location surface elevation. The HYSPLIT analysis utilized the NCEP-NCAR Reanalysis data (Kalnay et al., 1996). For the majority of the analyses, a combination of all three levels was determined to be most appropriate for use in evaluating the upwind moisture source location. It is important to note that the resulting HYSPLIT model trajectories are only used as a general guide to evaluate the moisture source for storms in both space and time. The final determination of the storm representative dew point and its location was determined following the standard procedures used by AWA in previous PMP studies (e.g., Tomlinson, 1993; Tomlinson et al., 2006-2013; Kappel et al., 2012-2015) and as outlined in the HMRs (e.g., HMR 51 Section 2.3) and WMO manual (Section 2.2).

The process involves deriving the average dew point (or SST) values at all stations with dew point (or SST) data in a large region along the HYSPLIT inflow vectors. Values representing the average 6-, 12-, and 24-hour dew points or daily SST are analyzed in Excel spreadsheets. The appropriate duration representing the storm being analyzed is determined and data are plotted to determine the storm representative dew point (or SST). This evaluation includes an analysis of the timing of the observed dew point (or SST) values to ensure they occurred in a source region where they would be advected into the storm environment at the time of the rainfall period. Several locations are investigated to find values that are of generally similar magnitude (within a degree or two Fahrenheit). Once these representative locations are identified, an average of the values to the nearest half °F is determined, and a location in the center of the stations is identified. This becomes the storm representative dew point (or SST) value and the location provides the inflow vector (direction and distance) connecting that location to the storm center location. This follows the approach used in HMR 51 Section 2, HMR 55A Section 5, and HMR 57 Section 4, with improvements provided by the use of HYSPLIT and updated maximum dew point and SST climatologies. Appendix F of this report contains each of the HYSPLIT trajectories analyzed as part of this study for each storm (when used). Figure 7.2 is an example map used to determine the storm representative dew point for the Dawson, Texas October 2015, SPAS 1590 storm event.

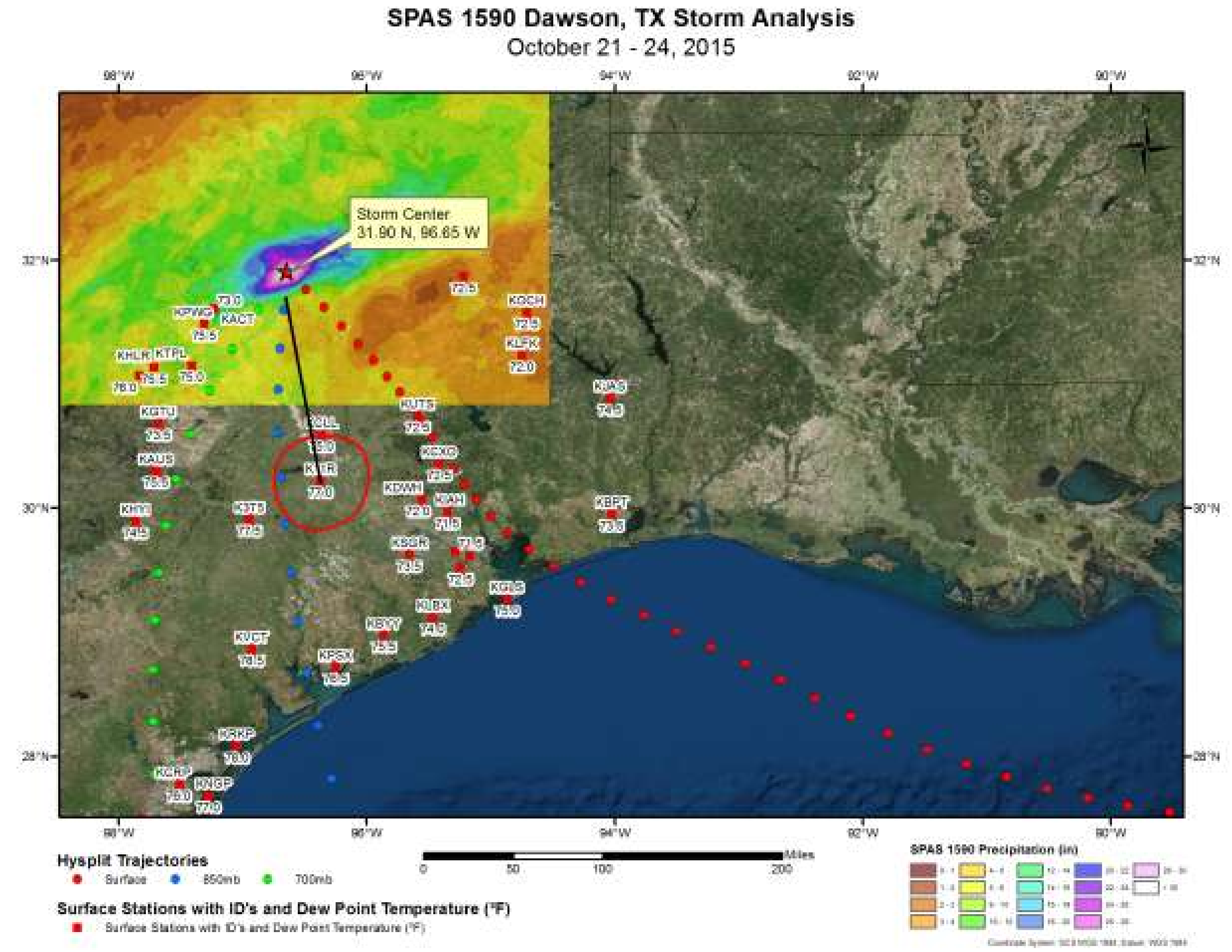


**Figure 7.2: Dew point values used to determine the storm representative dew point for Dawson, TX October, 2015, SPAS 1590 storm event. Note, the total storm isohyetal color contours represent precipitation depths as analyzed by SPAS. The values can be found in Appendix F.**

### 7.2.1 Storm Representative Dew Point Determination Example

As an example, Figure 7.3 shows the HYSPLIT trajectory model results used to analyze the inflow vector for the Holly, Colorado June, 1965 (SPAS 1293) storm. Note, in this HYSPLIT analysis, both the surface and 850mb inflow vectors (red and blue lines) are very similar in direction and distance, while the 700mb inflow vector (green line) is similar initially, then changes direction after the first 12 hours. In this case, surface dew point values were analyzed for a region starting at the storm center and extending southeastward into northern Texas and western Oklahoma. All the HYSPLIT inflow vectors showed a south to southeast inflow direction (the most common for storms in this region). The air mass source region supplying the atmospheric moisture for this storm was located over northern Texas and western Oklahoma some 12-36 hours prior to the rainfall occurring at Holly, Colorado and was advected into the rainfall region from the southeast. Surface dew points were analyzed over this source region, ensuring that the dew point observations were located outside of the area of rainfall to avoid compromising the dew points from evaporating rainfall. Figure 7.4 displays the stations analyzed and their representative 6-hour average dew point values. The region encircled in red is considered the moisture source region for this storm.

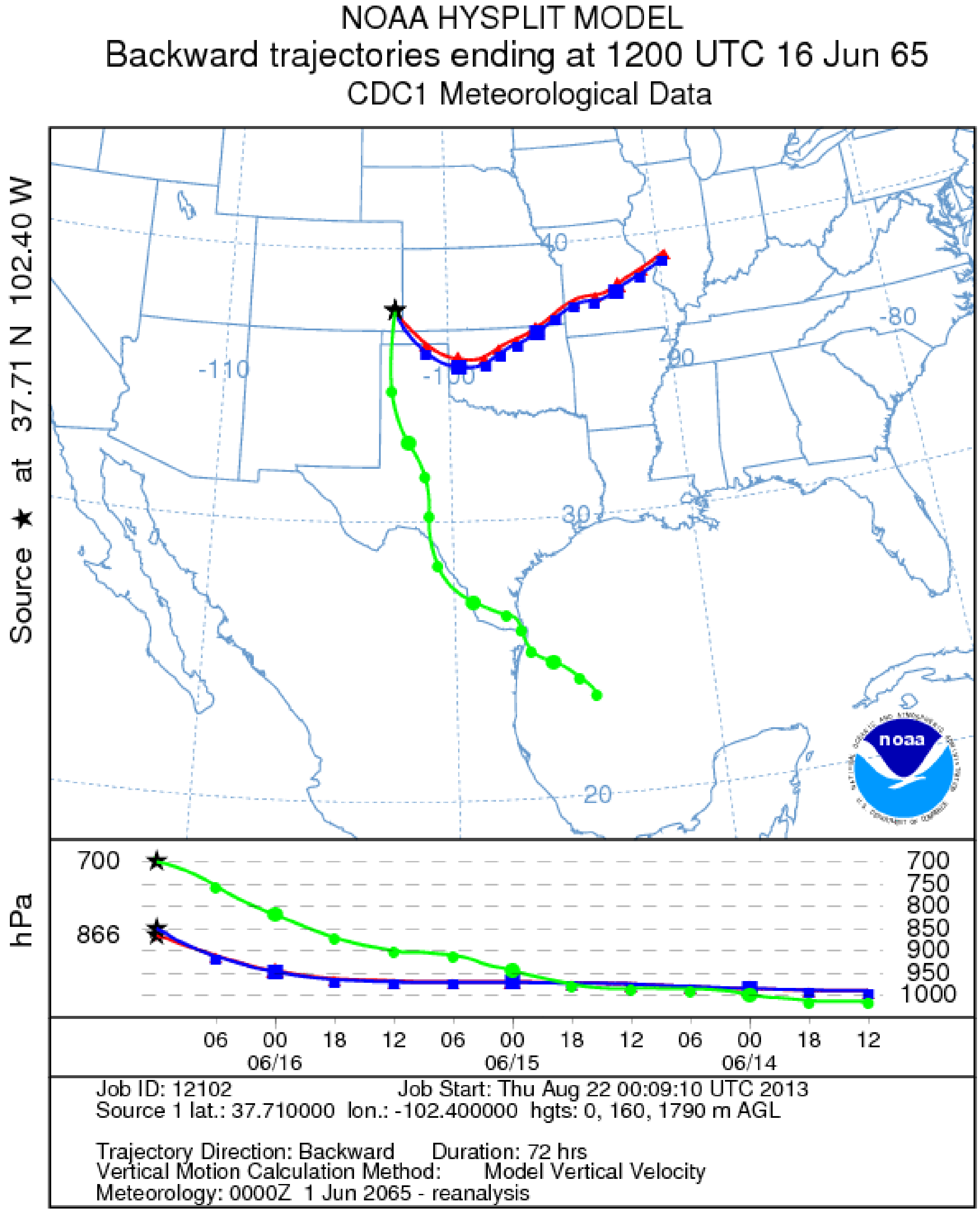


**Figure 7.3: HYSPLIT trajectory model results for the Holly, CO June 1965 storm**

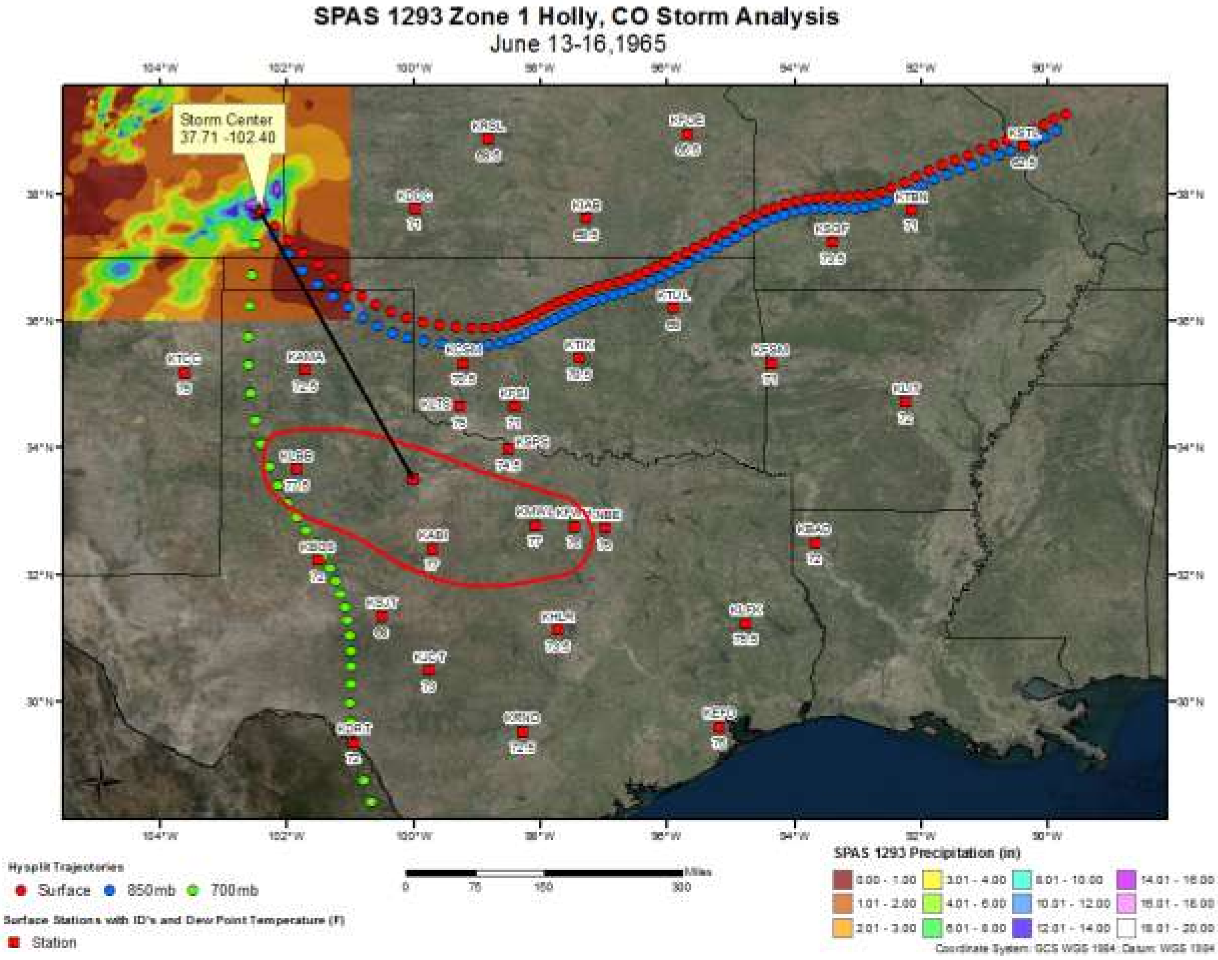


**Figure 7.4: Surface stations, 6-hour average dew points, and moisture source region, along with HYSPLIT trajectory model results for the Holly, CO June 1965 storm. Black line is the moisture source trajectory starting at storm center (star) and moving back toward the storm representative dew point location (red point). Red circle is the outline of stations used to calculate storm representative dew point temperature. Note, the total storm isohyetal color contours represent precipitation depths as analyzed by SPAS. The values can be found in Appendix F.**

### 7.2.2 Rationale for Using Average Dew Point Climatology

In previous storm analyses performed by the NWS and the USACE, a 12-hour persisting dew point was used for both the storm representative and maximum dew points. The 12-hour persisting dew point is the value equaled or exceeded at all observations during the 12-hour period (e.g., WMO, 2009). However, as was established in previous and ongoing AWA PMP studies, this dew point methodology tends to underestimate and not accurately reflect the available atmospheric moisture associated with the rainfall event.

An excellent example of this (from the Nebraska statewide PMP study but relevant for the storm types that affect eastern Texas) is illustrated by the David City, Nebraska 1963 storm. During this extreme storm event, a narrow tongue of moisture was advected into the region by strong southeasterly flow during a short time period. Most of the rain with this event (approximately 15 inches) accumulated in less than 6 hours. For this storm, hourly dew point data were collected from several locations near the rainfall event. These included Omaha, Nebraska; Des Moines, Iowa; Topeka, Kansas; and Kansas City, Missouri. Following standard procedures for determining storm representative dew point location, it was determined that Topeka, Kansas and Kansas City, Missouri were the two stations that best represented the air mass that produced the extreme rainfall. Hourly dew point data for these two stations clearly showed that use of 6-hour average dew point values better represented the atmospheric moisture available to the storm event than did use of 12-hour persisting dew point values. The 6-hour average dew point representing the moisture in the air mass associated with the rainfall was 71.5°F at Kansas City, Missouri and 71°F at Topeka, Kansas. Using these dew point values, a 1000mb 6-hour average dew point of 73.5°F was determined for Kansas City, Missouri and a dew point of 73°F was determined for Topeka, Kansas. Using the NWS approach, the 12-hour persisting dew point is 63°F (65°F at 1000mb) at Kansas City, Missouri and 66°F (68°F at 1000mb) at Topeka, Kansas for an average 12-hour persisting 1000mb adjusted value of 66.5°F (Table 7.1).

**Table 7.1: Comparison of 6-hour average storm representative dew point vs. 12-hour persisting storm representative dew point for the David City, NE 1963 storm**

| Observed Dew Point Values for David City, NE 1963 | | | | | | | | | | | | | | | | | | | | | | | | |
|---|---|---|---|---|---|---|---|---|---|---|---|---|---|---|---|---|---|---|---|---|---|---|---|---|
| **Kansas City, MO** | | | | | | | | | | | | | | | | | | | | | | | | |
| **Hour** | 00Z | 01Z | 02Z | 03Z | 04Z | 05Z | 06Z | 07Z | 08Z | 09Z | 10Z | 11Z | 12Z | 13Z | 14Z | 15Z | 16Z | 17Z | 18Z | 19Z | 20Z | 21Z | 22Z | 23Z |
| **Dew Point** | 58 | 61 | 62 | 62 | 63 | 63 | *63* | 64 | 66 | 68 | 69 | **71** | **72** | **72** | **72** | **71** | **71** | 69 | 68 | 67 | 67 | 67 | 67 | 67 |
| | | | | | | | | | | | | **Air Mass Supplying Rainfall Event** | | | | | | | | | | | | |
| **12-Hour Persisting Td 63 ( 65 reduced to 1000mb)** | | | | | | | ***12 Hour Persisting Td Timeframe*** | | | | | | | | | | | | | | | | | |
| **6-Hour Average Td 71.5 (73.5 reduced to 1000mb)** | | | | | | | | | | | | **6 Hour Average Td timeframe** | | | | | | | | | | | | |
| **Topeka, KS** | | | | | | | | | | | | | | | | | | | | | | | | |
| **Hour** | 00Z | 01Z | 02Z | 03Z | 04Z | 05Z | 06Z | 07Z | 08Z | 09Z | 10Z | 11Z | 12Z | 13Z | 14Z | 15Z | 16Z | 17Z | 18Z | 19Z | 20Z | 21Z | 22Z | 23Z |
| **Dew Point** | 61 | 62 | 64 | 65 | 65 | 65 | *66* | 66 | 67 | 68 | 69 | **72** | **71** | **71** | **71** | **70** | **70** | 70 | 69 | 70 | 69 | 68 | 66 | 69 |
| | | | | | | | | | | | | **Air Mass Supplying Rainfall Event** | | | | | | | | | | | | |
| **12-Hour Persisting Td 66 (68 reduced to 1000mb)** | | | | | | | ***12 Hour Persisting Td Timeframe*** | | | | | | | | | | | | | | | | | |
| **6-Hour Average Td 71 (73 reduced to 1000mb)** | | | | | | | | | | | | **6 Hour Average Td timeframe** | | | | | | | | | | | | |

The 12-hour persisting dew point analysis included dew point values from a 6-hour period not associated with the rainfall. The hourly dew point value that provides the 12-hour persisting dew point occurred outside of the rainfall period after adjustment for advection time from the dew point observing station to the storm location.

### 7.2.3 Rationale for Adjusting Persisting Dew Point Values

In some cases, (e.g. storms on the short storm list previously analyzed in the USACE Storm Studies and used in NWS HMRs), an adjustment factor was applied to provide consistency in storm maximization while utilizing the updated dew point climatology. The adjustment factor was determined using the same procedure used in the FERC Michigan/Wisconsin study and subsequent AWA PMP studies.

Results from the dew point analyses showed consistent results for Local/MCS and General type storms for differences between the older method for determining 12-hour persisting storm representative dew points and the approach using average storm representative dew points. The following discussion from the FERC Michigan/Wisconsin report (Tomlinson, 1993) addresses these differences:

*The average difference between dew points for the synoptic storms was five degrees less than that for the MCS storms. This may be attributed to the greater homogeneity of inflow* *moisture associated with the synoptic events. With most of the modern MCS storms, limited-area, short-duration pockets of relatively moist air were found within the inflow moisture at one or two locations. The analyses may indicate that for MCS events, bubbles of extremely moist air interact with storm catalysts to create extreme rainfall events of short duration. A warm humid air mass over a broad area with small moisture gradients more aptly describes the synoptic inflow moisture. Several stations within the air mass may have the same or similar dew points. Much smaller variations in dew points along the inflow moisture vector are expected.*

*Large spatial and temporal variations in moisture associated with MCS-type storms are not represented well with 12-hour persisting dew points, especially when only two observations a day are available. Average dew point values, temporally consistent with the duration of the storm event provide a much improved description of the inflow moisture available for conversion to precipitation. The more homogeneous moist air masses associated with synoptic storms result in smaller differences between average and persisting values.*

*This analysis has provided correlations between 12-hour persisting storm dew points and average storm dew points for both MCS and synoptic storms. Despite the small sample size, the consistent results tend to support the reliability of the analysis. However, the small sample size has been considered in making recommendations for adjusting the old storm representative dew points for use in determining PMP estimations. The eight degree difference for MCS-type storms has been decreased to five degrees to provide a conservative adjustment. A similar consideration is made for synoptic-type storms. The three-degree difference is decreased to two degrees to provide a conservative adjustment. The adjusted representative storm dew points are used with the new maximum average dew point climatology to maximize storms.*

Similar analyses were completed in the Nebraska, Ohio, and Wyoming statewide PMP studies. These analyses, which investigated additional modern storms, confirmed what had been found in previous studies, with an average difference of 7°F between the average and 12-hour persisting dew points for local/MCS storms and an average difference of 2°F for tropical and general storms. Table 7.2 provides recent examples of this validation that were completed as part of the Wyoming statewide study (2014). Therefore, results of the more recent analyses were very consistent with the FERC Michigan/Wisconsin regional PMP report. This validated the process of adjusting the 12-hour persisting dew points to achieve compliance with using the average dew point climatology.

**Table 7.2: Storms used to evaluate average vs. persisting dew point values.**

| | Local Storms | | | | |
|---|---|---|---|---|---|
| **Storm Event** | **Date** | **Avg. 12-hr Persisting Td** | **Avg. Td** | **Avg. Delta** | **Duration Analzyed** |
| Big Thompson Canyon, CO | July 31, 1976 | 59.0 | 78.5 | 19.5 | 6hr |
| Bluff, UT | August 14, 2001 | 58.0 | 76.5 | 18.5 | 6hr |
| Cedar City, UT | July 31, 2006 | 69.0 | 74.0 | 5.0 | 6hr |
| Morgan, UT | August 18, 1958 | 66.0 | 72.5 | 6.5 | 6hr |
| Ogallala, NE | July 6-7, 2002 | 74.5 | 76.5 | 2.0 | 6hr |
| Ft Collins, CO | July 28-29, 1997 | 74.0 | 77.5 | 3.5 | 6hr |
| Cheyenne, WY | August 1-2, 1985 | 71.0 | 77.0 | 6.0 | 6hr |
| Frijole Creek, CO | July 3, 1981 | 75.0 | 77.0 | 2.0 | 6hr |
| Rapid City, SD | July 8-10, 1972 | 71.5 | 78.5 | 7.0 | 6hr |
| | | | **Average** | **7.8** | |
| | **General Storms** | | | | |
| **Storm Event** | **Date** | **Avg. 12-hr Persisting Td** | **Avg. Td** | **Avg. Delta** | **Duration Analzyed** |
| Big Elk Meadows, CO | May 3-8, 1969 | 63.5 | 65.0 | 1.5 | 24hr |
| Gibson Dam, MT | June 6-9, 1964 | 61.0 | 66.0 | 5.0 | 24hr |
| Waterton Dam, AB | June 18-20, 1975 | 68.0 | 71.0 | 3.0 | 24hr |
| Lake Maloya, NM | May 18-20, 1955 | 69.0 | 70.5 | 1.5 | 24hr |
| Deer Creek, UT | October 23-25, 2010 | 59.0 | 59.0 | 0.0 | 24hr |
| | | | **Average** | **2.2** | |

## 7.3 Storm Representative Sea Surface Temperatures (SSTs) Calculation Example

The value for the maximum SST was determined using the mean +2-sigma (two standard deviations warmer than the mean) SST for that location. The use of the +2-sigma (two standard deviations) value follows the same procedure used in the HMRs (see HMR 57 Section 4.3). SSTs were substituted for dew points in this study for many storms where the inflow vector originated over the Gulf of Mexico and/or when rain at the coastline disqualified surface dew points from being used for analysis. For storm maximization, the value for the maximum SST was determined using the mean +2-sigma SST for that location for a date two weeks before or after the storm date (which ever represents the climatologically warmer SST period). Storm representative SSTs and the mean +2-sigma SSTs were used in the same manner as storm representative dew points and maximum dew point climatology representing the 15th of the month values in the maximization and transpositioning procedure. Figure 7.5 is an example of a daily SST map used to determine the storm representative SST for the Houston, Texas June, 2001 SPAS 1464 storm event.

In this example, the first effort involved determining whether surface dew points were available to derive the storm representative dew point. However, this was not possible for this storm because of rainfall at the coastline, thereby negating the use of those dew point readings along the inflow pathway for moisture advecting in from the Gulf of Mexico. Next, SSTs were investigated to determine regions of homogenous temperatures in a region that was appropriate in time and space according to the HYSPLIT trajectories. Several regions were possibilities in this case. Next, the track of the hurricane and its relation to advecting moisture into the storm center was considered. This better matched the HYSPLIT trajectory very well. Finally, sensitivity calculations were performed using several couplets of storm representative SST values versus the +2-sigma climatological maximum values to ensure the range of maximizations was within a reasonable range (i.e. greater than 1.00). Upon completing these determinations, the storm representative location of 25.0°N and 95.0°W was chosen. This was an average of several of the SST values within the red-circled area of Figure 7.5 on June 8, 2001.

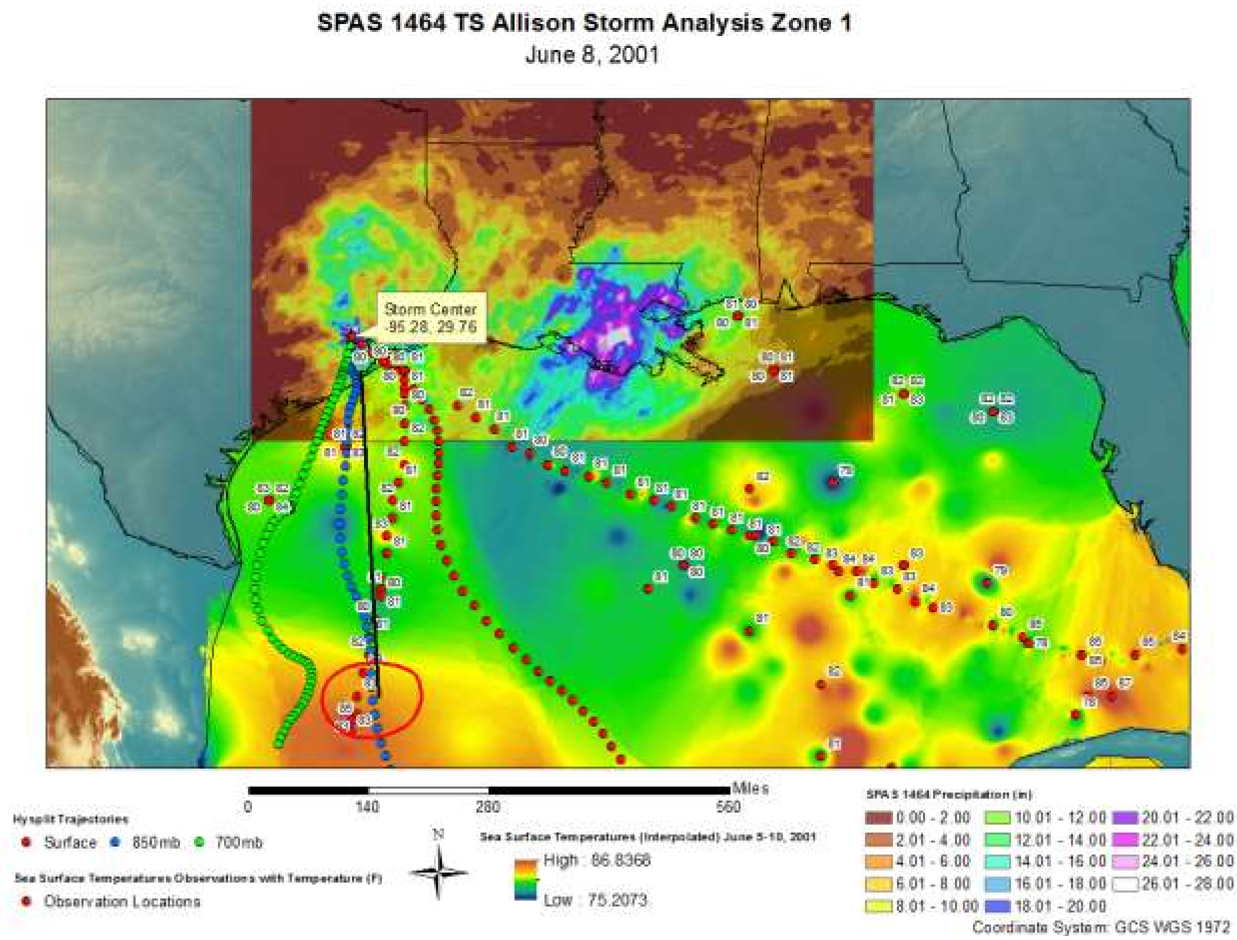


**Figure 7.5: Daily SST observations used to determine the storm representative SST value for the Houston, TX June, 2001 SPAS 1464 storm event. Note, the total storm isohyetal color contours represent precipitation depths as analyzed by SPAS. The values can be found in Appendix F. The colors over water correspond to temperature in degree F and are a simple IDW based on the observed point values plotted.**

# 8. Transposing Storms

Extreme rain events in a meteorologically homogeneous region surrounding a location are a very important part of the historical evidence on which a PMP estimate for that location is based. Since most locations have a limited period of record for rainfall data, the number of extreme storms that have been observed at or near a location is limited. Historic storms that have been observed within similar meteorological and topographic regions are analyzed and adjusted to provide information describing the storm rainfall as if that storm had occurred over the location being studied. Transfer of a storm from where it occurred to a new location that is meteorologically and geographically similar is called storm transpositioning. The underlying assumption is that storms transposed to the new location could have occurred under similar meteorological conditions as those found at the original location. To properly relocate such storms, it is necessary to address issues of similarity as they relate to meteorological conditions, moisture availability, and topography. In this study, adjustment factors used in transposing a storm are quantified by using the GTF and MTF, each of which are discussed in detail in Section 9.

The search for extreme rainfall events identified storms that occurred throughout the region discussed in Section 6 (see Figure 6.1). This region was considered meteorologically and geographically similar to one or more locations within the Texas project domain. All storms in this study region were fed with low-level atmospheric moisture primarily from the Gulf of Mexico and local moisture sources. These air masses cannot cross the North American Cordillera without significant loss of moisture content. Therefore, storm transposition was limited to the east side of the Continental Divide and eastward. Transposition limits were defined in part by dividing the project domain into 12 transposition zones. Each transposition zone was delineated after careful consideration of criteria including; physiographic and climatic provinces (defined by both the NWS and the USGS), climatological zones defined by NCDC, variations in topography, and ecological regions. The 6-hour and 24-hour L-moment statistical station regions defined in the precipitation frequency analysis (Section 5) were also evaluated as delineation criteria. The final delineation was agreed upon after extensive discussion with the Review Board (Figure 8.1). It is recognized that these boundaries are not discrete boundaries in nature, but transitional zones. However, for the purpose of this study, these zones provide a good estimation of acceptable transpositionable extents for each storm that can be used for classification and comparison purposes.

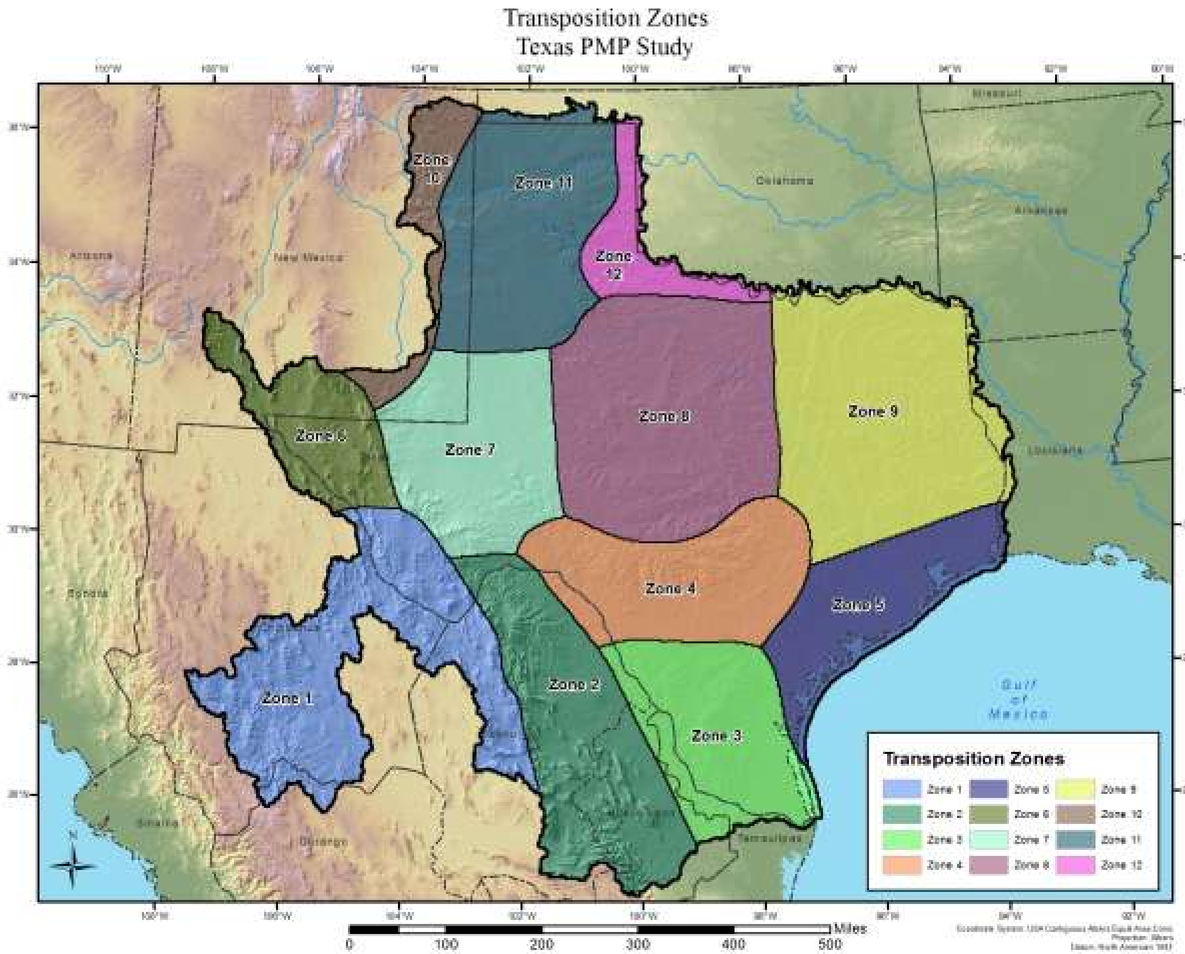


**Figure 8.1: Transposition zones used to define transposition limits for individual storms**

The 68 SPAS storm centers on the short storm list were individually evaluated to determine their unique transposition limits. Initially, general transposition limits were placed on all storms and their individual DAD zones based on subjective judgments of the meteorology associated with each, the moisture source regions, and the interaction with topography at the original location versus other areas being considered for transpositioning. Initial results were presented at the 4th Review Board meeting and the limits were refined prior to and during the 5th Review Board meeting. During the meetings, extensive discussions with all members present took place to explicitly define transposition limits for each of the storms.

Each storm's meteorological characteristics were evaluated, including the storm type, the seasonality, the storm isohyetal patterns, and the storm's moisture source. These factors were evaluated for each storm to provide a rationale for the extent to which the storm could be transpositioned. Spatial transposition limits were assigned to each storm. These limits were defined using constraints on elevation, latitude, longitude, transposition factors, and/or one or more of the 12 transposition zones across the study domain. For two storms; Hale, Colorado of May, 1935 (SPAS 1295 DAD Zone 3) and Guadalupe Pass, Texas of September, 2013 (SPAS 1530 DAD Zone 1), the transposition limits were defined, in part, manually using guidance resulting from discussions occurring at the 5th Review Board meeting. This included evaluation of the synoptic meteorology associated with each event, elevation constraints related to the original storm location, and hydrologic boundary considerations. It should be noted that conservative transposition limits were employed (i.e., moving storms to larger regions than may be justified) unless there was justification for a more refined analysis. This is because the transposition process involves some subjectivity, and although it produces a binary answer (either a storm is transposable to a point or not), in actuality there are gradients in meteorology that need to be considered.

Initial transposition limits were assigned with the understanding that additional refinements would take place as the data were run through the PMP evaluation process. Numerous sensitivity runs were performed using the PMP database to investigate the results based on the initial transposition limits. Several storms were re-evaluated based on the results that showed inconsistencies and/or unreasonable values when compared to other similar storms and/or HMR values. Although somewhat subjective, decisions to adjust the transposition limits for a storm were based on the understanding of the contributing atmospheric conditions present during the storm event, similarity of topography between the two locations, access to moisture source, season of occurrence, and comparison to other similar storm events. Appendix I provides a description of the iterations and adjustments that were applied during each PMP version to arrive at the final values.

For all storms, the IPMF does not change during transposition process. The MTF and GTF change as a storm is moved from its original location to a new location. Further, because the MTF represents the horizontal difference in available moisture between the original location and the target location (i.e. no elevation difference component is applied when used with the GTF), this factor does not vary as much as the GTF across the region. Generally, most MTFs result in less than a +/-10% change. Therefore, the largest contributing factor to the spatial variation of PMP over a specific area in the transposition process is the GTF.

## 8.1 Moisture Transposition Factor Evaluations

Extensive evaluations were completed to try and quantify how much of the MTF was already accounted for, if at all, in the GTF process. It is not straightforward to separate the purely geographic component driving the spatial distribution of the precipitation frequency climatology (used to calculate GTF) from other components that might be inherent, such as changes in atmospheric moisture. An approach taken to analyze and quantify these non-geographic components was to apply the GTF calculation process to NOAA Atlas 14 precipitation frequency data in non-orographic regions, where the change in elevation and terrain is negligible between the source and target locations. GTF calculations were done using locations in non-orographic regions of the Midwest where it was assumed the GTF was 1.00 or close to 1.00. Most of the resulting GTFs were indeed 1.00 or close to 1.00, although in some cases, the GTF was larger than expected, suggesting that there were non-orographic components captured, albeit with a minor effect on rainfall spatial distribution. If the variations of GTF values closely matched those of the MTF values calculated for the same storm transposition, then it could be concluded with reasonable certainty that the GTF was adequately capturing the MTF. However, there are several potential reasons as to why no definitive conclusion could be determined. These include internal variability of the precipitation frequency data even in seemingly homogenous regions, the inability to isolate a specific atmospheric component that mirrors the spatial distribution of the dew point climatology, and variability within the dew point climatologies. It is likely that the GTF does account for some of the moisture differences between two locations, however the amount is unknown and would potentially differ for each discrete storm event. Because we are quantifying moisture and geographic effects for storms of the rarest occurrence, it is expected the moisture associated with them to also be rare. Utilizing an explicit analysis related to extreme moisture conditions (i.e. the 100-year recurrence interval climatology) more accurately reflects the unique characteristics of a given storm event. In addition, the calculation of the MTF allows the atmospheric component to be evaluated discretely to the geographic component, which is useful in determining the storm's transposition limits. This also allows the factor to be explicitly known and therefore corrected if necessary.

Questions regarding whether the MTF process is already accounted for (called "double counting") in the GTF calculation received extensive discussion. In previous PMP studies completed by AWA (e.g., Tomlinson et al., 2013; Kappel et al., 2014; Kappel et al., 2015), this question was also discussed extensively. During the Texas PMP study, further evaluation and discussion demonstrated that the MTF is most likely not being "double counted" in the PMP calculation process. This is because the MTF process is setting the moisture levels for all storms used to their climatological maximum level (using the 100-year recurrence interval climatological maps) in order to compare the difference between the two locations being analyzed, assuming all storms had occurred with their maximum moisture instead of what actually occurred. Evaluations of the MTF will continue in future studies. However, including it as a separate calculation was important as this allowed the effect to be explicitly delineated and will allow for explicit correction to be made if needed. Note that the GTF is comparing the differences of the rainfall resulting from both moisture and topography interactions at two locations. The moisture component in the GTF process does not represent the climatological maximum amount, but represents the actual amount of moisture associated with each given event that went into the development of the precipitation frequency climatologies.

As discussed in Section 8.3 below, the effects of combined GTF and MTF were examined for all storms during the PMP development process. In a few cases, the combined GTF and MTF did seem to produce unrealistic PMP values at locations far from the original storms. For such storms, a cap was placed on the GTF, as described below.

If future investigations into the MTF show that a correction should be applied, this will allow for revisions in a straightforward, quantifiable manner. It is recognized that there is uncertainty regarding which (if any) portion of the atmospheric component expressed by the MTF may also be accounted for within the GTF factor. However, until it can be adequately quantified, the practice of including the MTF as a separate input should remain.

## 8.2 Use of Geographic Transposition Factor in Transposition Limit Analyses

The spatial variations in the GTF were useful in making decisions on transposition limits for a storm. As described in Section 7, values larger than 1.50 for a storm's maximization factor exceed reasonable limits. In these situations, changing a storm by this amount is likely also changing the storm characteristics. The same concept applies to the GTF. GTF values greater than 1.50 indicate that transposition limits have most likely been exceeded. Similarly, values less than 0.50 suggest the same thing. Mapping the GTF and MTF values across the state provided visual guidance for defining transposition zones allowing areas of excessively large transposition factors to be defined as non-transposable. Therefore, storms were reevaluated for transpositionability in regions which results in a GTF greater than 1.50. In higher elevations with a lack of extreme rainfall data where the GTF was greater than 1.50, a cap of 1.50 was applied to be consistent with the IPMF cap.

From these analyses, refinements such as limiting a storm's transposition location using an elevation constraint or by a GTF amount were applied. An example of the Hearne, TX June 1899 SPAS 1591 GTF map is provided in Figure 8.2. This storm occurred near the boundary of zones 5 and 9 (see Figure 8.1). Broadly, the storm is considered to be transposable to all of zones 5 and 9 where it originally occurred. Elevation constraints are then applied as the storm is transpositioned westward into zones 2, 3, 4, 8, and 12. Elevation, terrain, moisture source, storm type, and distance are considered to further refine the transposition limits. Figure 8.2 shows the GTF values for the storm across the project domain. Note the storm was only considered transpositionable east of the brown line in Figure 8.2. Notice how the GTF values decrease markedly as one moves west through the project domain. This is a result of moving further away from the moisture source and an increase in topography relative to the original storm location. It is apparent that this storm could not be moved to zones 1, 6, 10, and portions of zones 2, 7, and 11 without significantly changing the storm's characteristics because of both differences in moisture and topography. Thereby, moving the storm to these locations would be violating the definition of transpositionability.

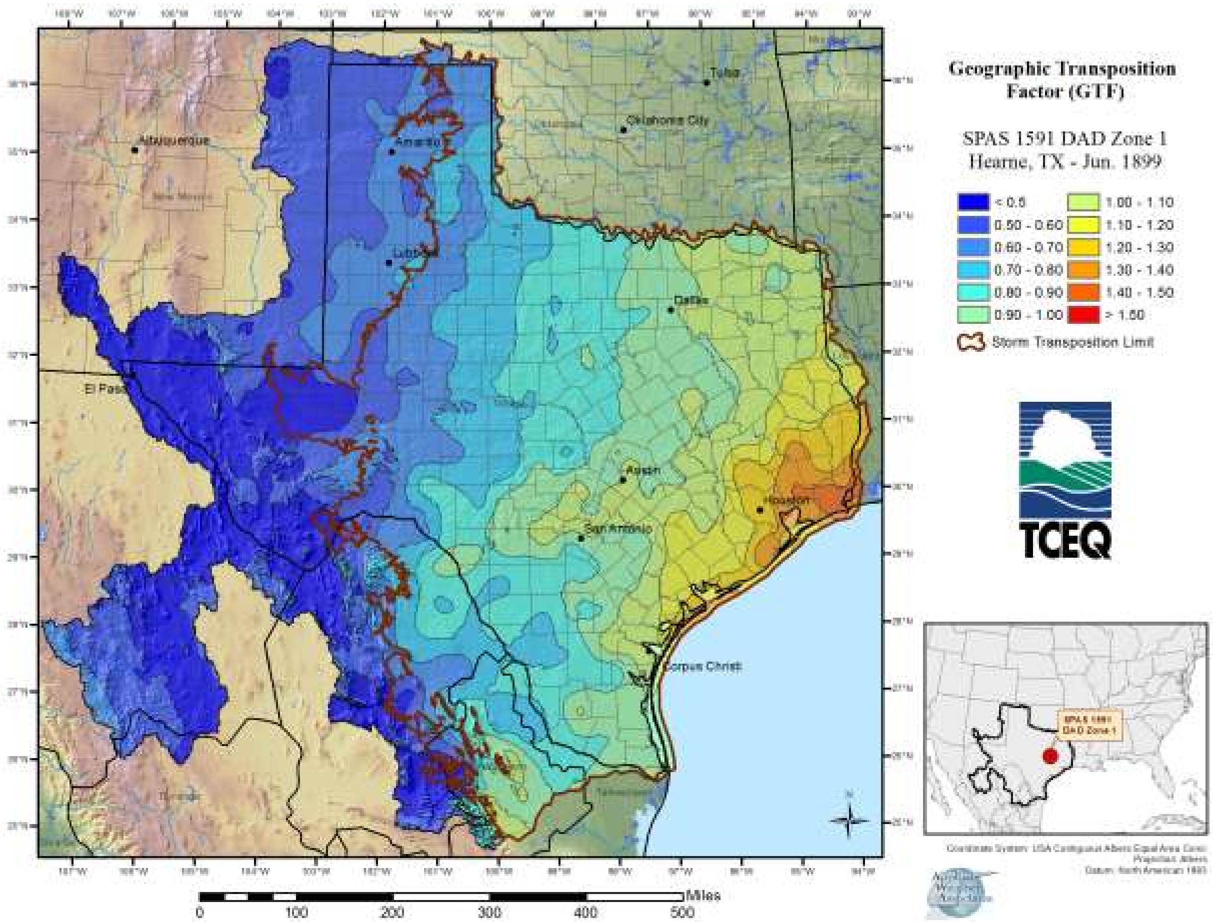


**Figure 8.2: Geographic Transposition Factors for Hearne, TX June 1899 SPAS 1591. The storm is only transpositioned to regions east of the brown line.**

## 8.3 Unique Adjustments Applied during the Transposition Process

The most difficult regions to define transposition limits occurred in relatively benign regions of topography going from zone 5 to zone 9 and from zone 9 to zones 8 and 12. In these regions, there were no sharp topographical or meteorological boundaries from which to draw explicit transposition limits. Therefore, numerous variations were applied to several storms important in the regions to try and create smooth PMP depth fields. Meteorological judgment was applied during this process to best represent what the PMP spatial pattern would be expected to look like given the meteorology and topography of the region. In these regions, sharp gradients in PMP depths were not justifiable given the meteorology of the region, similarity of terrain, and access to moisture. For tropical storms, an additional GTF cap was applied at 1.10 to provide for a more realistic spatial pattern of PMP depth across the region. For other PMP-controlling storms where the original analysis was deemed more unreliable than other, special considerations were applied. This was most important for Cheyenne, OK April 1943, SPAS 1495 and Vic Pierce, TX June 1954, SPAS 1602. In the case of SPAS 1495, the GTF was capped at 1.00 to allow for a more realistic fit with other storms of the same storm type in the same region.  SPAS 1602 was allowed to move into all transposition zones to allow for a more realistic spatial fit of PMP depth across the domain at the area sizes and durations where the storm was most influential.  All these decisions and adjustments are listed in Appendix I, which provides the transposition limits adjustment log as applied to each version of the PMP development process.

# 9. Development of PMP Values

Gridded PMP depths were calculated by comparing the total adjusted rainfall values for all transpositionable storm events over each grid point and taking the largest value. In this process, all transposable storms are considered independently at each grid point for the analyzed duration and area size. This approach provides a site-specific calculation for each grid point across the analysis project domain. During this process, durational envelopment occurs because the largest PMP depth for a given duration is identified after analyzing all the transposable storms for each grid point at each location for each duration at the area size(s) specific to the basin being analyzed. In addition, several storms can control the PMP depth for a given basin at various grid points and/or durations. This is similar to the process of envelopment, which encompasses several different storms for each area size.

The adjusted rainfall at a grid point, for a given storm event, was determined by applying a total adjustment factor (TAF) to the SPAS analyzed DAD value corresponding to the given area size (in square miles) at the appropriate duration. The TAF is the product of the three separate storm adjustment factors; the IPMF, the MTF, and the GTF. In-place maximization is described in Section 7, moisture transposition is described in Section 7 and Section 8.1, and geographic transposition is described in Section 3 and 8.2. These calculations were completed for all storms for every grid point analyzed over the entire domain. Several storms have multiple centers analyzed. Separate SPAS DAD zones were considered as independent events for the purpose of PMP calculation. In addition, six of the storm events were considered hybrid-type storms exhibiting characteristics of both local and tropical, or local and general-type events. In these situations, these events were analyzed as both types with separate PMP values developed for each scenario. In total there were 68 separate events analyzed.

An Excel storm adjustment spreadsheet was produced for each of the analyzed events. These spreadsheets are designed to perform the calculation of each of the three adjustment factors, along with the final TAF. The spreadsheet format allows for the large number of calculations to be performed correctly and consistently in an efficient template format. In addition to the IPMF, MTF, and GTF calculations, a Boolean transposition flag for each grid point is stored within the spreadsheets, allowing a conditional statement to determine if the given storm is transposable to the grid point based on predetermined criteria (see Section 8). Information such as the target grid point precipitation climatology values, coordinate pairs, grid point elevations, equations, and the precipitable water lookup table remain constant from storm to storm and remain static within the spreadsheet template. The spreadsheet contains a final adjusted rainfall tab with the adjustment factors, including the TAF, listed for each grid point. For each storm, this table was exported to a GIS feature class to be used as input for the PMP Evaluation Tool, a scripted GIS tool that automates the calculation and production of PMP gridded datasets. This approach, taken at any point in the future, enables new storm feature classes to be added, removed, or edited.

The PMP Evaluation Tool receives the storm TAF feature classes and the corresponding DAD tables for each of the storm events as input, along with a basin outline feature layer as a model parameter. The PMP Evaluation Tool then calculates and compares the total adjusted rainfall for each transposable storm at each grid point within the statewide analysis project domain and determines the PMP depth for each duration separately for all storm types. The tool was used to produce gridded PMP datasets for a range of durations and basin area sizes applicable to the study area for the entire analysis domain. The durations calculated for local/MCS storms PMP were 1-, 2-, 3-, 4-, 5-, 6-, 12-, 24-, 48-, and 72-hours. The durations calculated for tropical and general storms PMP were 1-, 2-, 3-, 6-, 12-, 24-, 48-, 72-, 96-, and 120-hours. The PMP area sizes calculated for local/MCS storms PMP were 1-, 10-, 25-, 50-, 100-, 200-, 300-, 500-, and 1,000-square miles. The PMP area sizes calculated for tropical and general storms PMP were 1-, 10-, 50-, 100-, 500-, 1,000-, 10,000-, and 20,000-square miles. The resulting PMP GIS datasets are included in the digital appendix K.

The following sections describe the procedure for calculating the IPMF, the MTF, the GTF, and the TAF for the creation of the storm adjustment feature classes. Examples of each of these calculations are presented, followed by discussion of the implementation and application of the PMP Evaluation Tool to calculate PMP.

## 9.1 Available Moisture at Source and Target Locations

The available atmospheric moisture, in terms of precipitable water depth, must be determined for the storm center location to calculate both the IPMF and MTF. The IPMF is determined by taking the ratio of the maximum precipitable water depth at the storm representative dew point/SST location to the storm representative precipitable water depth at the same point location. The MTF is determined by taking the ratio of the maximum precipitable water depth at the transposition dew point/SST location to the maximum precipitable water depth at the storm representative dew point/SST location. Identification of storm representative dew point/SST values and locations are described in Sections 7.2 and 7.3. The available moisture calculated for the IPMF and MTF differ in that the IPMF is calculated using the amount of precipitable water from the ground surface elevation to 30,000 feet and the MTF is calculated using the amount of precipitable water from sea level to 30,000 feet.

The precipitable water depth is obtained from a lookup table stored within the storm adjustment spreadsheets. The lookup table is a digital version of the precipitable water table found in Appendix C of HMR 55A and Annex I of the WMO PMP Manual (2009). The precipitable water tables provide an equivalent amount of precipitable water based on a dew point temperature starting at sea level through the top of the atmosphere. Values are provided for temperatures every 0.5°F through the entire atmospheric column, to represent the amount of precipitable water available for rainfall production (sea level through 30,000 feet).

To determine the temperatures to use from the precipitable water lookup table, ArcGIS was used to extract the values from the appropriate monthly climatological maximum dew point/SST raster files at the appropriate duration. ArcGIS was used to extract the dew point/SST temperatures to point features stored within shapefiles. For each storm there was a point feature at the storm center, and a series of 154,998 point features across the project domain. Before the dew point/SST extraction, each of these point features was shifted a distance in the *x* and *y* direction equivalent to the moisture inflow vector components for the given storm. This allows for the extraction of dew point/SST values that are representative of the moisture source location. The monthly maximum average dew point and +2 sigma SST values were linearly interpolated between the bounding monthly mean values according to the temporal transposition date. The moisture inflow vectors and temporal transposition date for each storm are in Appendix F.

Precipitable water was calculated for each event, within the storm adjustment spreadsheet, for the storm center grid cell and each of the target grid cells within the project domain using the lookup table with the storm center elevation. Storm center elevations were rounded to the nearest 100 feet, or nearest 500 feet for elevations above 5,000 feet, to coincide with the values in the precipitable water lookup table.

As described in Section 7, the precipitable water depths are adjusted for elevation for the IPMF calculation. This is done by determining the precipitable water depth present in the atmospheric column (from sea level to 30,000 feet) and subtracting the precipitable water depth that would be present in the atmospheric column between sea-level and the surface elevation at the storm location using Equation 9.1.

$$W_p = W_{p,30{,}000'} - W_{p,elev} \qquad \text{Equation 9.1}$$

where,

| | | |
|---|---|---|
| $W_p$ | = | precipitable water above the storm location (in.) |
| $W_{p,30{,}000'}$ | = | precipitable water, sea level to 30,000′ elevation (in.) |
| $W_{p,elev}$ | = | precipitable water, sea level to storm surface elevation (in.) |

## 9.2 In-Place Maximization Factor

In-place storm maximization is applied for each storm event using the methodology described in Section 7. Storm maximization is quantified by the IPMF using Equation 9.2.

$$IPMF = \frac{W_{p,max}}{W_{p,rep}} \qquad \text{Equation 9.2}$$

where,

| | | |
|---|---|---|
| $W_{p,max}$ | = | precipitable water for the maximum dew point (in.) |
| $W_{p,rep}$ | = | precipitable water for the representative dew point (in.) |

## 9.3 Moisture Transposition Factor

The change in available atmospheric moisture between the storm center location and the basin target grid point is quantified as the MTF. This MTF represents the change due to horizontal distance only and is calculated at the storm center elevation. The change due to vertical displacement is quantified inherently within the GTF, described in the next section. The MTF is calculated as the ratio of precipitable water for the maximum dew point at the target grid point location to precipitable water for the storm maximum dew point at the storm center location as described in Equation 9.3. Elevation is not considered in the MTF calculation;

therefore, the precipitable water depth is calculated for the entire atmospheric column, from sea level to 30,000'.

$$MTF = \frac{W_{p,trans}}{W_{p,max}} \qquad \text{Equation 9.3}$$

where,

| | | |
|---|---|---|
| $W_{p,trans}$ | = | maximum precipitable water, target location (in.) |
| $W_{p,max}$ | = | maximum precipitable water, storm center location (in.) |

## 9.4 Geographic Transposition Factor

Section 3.1 provides details on the methods used in this study to define the geographic effect on rainfall. The GTF is calculated by taking the ratio of transposed climatological precipitation to the in-place climatological precipitation.

$$GTF = \frac{P_t}{P_s} \qquad \text{Equation 9.4 (From Equation 3.1)}$$

where,

| | | |
|---|---|---|
| $P_t$ | = | climatological 100-year precipitation depth at the target location |
| $P_s$ | = | climatological 100-year precipitation depth at the source storm center |

The in-place climatological precipitation ($P_s$) was taken at the SPAS-analyzed total storm maximum rainfall center location. The corresponding transposed climatological precipitation ($P_t$) was taken discretely at each grid point location to which the storm was transposed. Texas' 100-year precipitation climatology was used for each transposed location and also for the in-place location for storm centers that occurred inside the PMP domain. For storm centers that occurred outside the domain, the appropriate NOAA Atlas 14 volume for that location was used. Six-hour climatologies were used for the local/MCS storms and 24-hour climatologies were used for the general and tropical storms.

## 9.5 Total Adjusted Rainfall

The TAF is a product of the linear multiplication of the IPMF, MTF, and GTF. The TAF is a combination of the total moisture and terrain differences on the SPAS analyzed rainfall after being maximized in-place and then transpositioned to the target grid point.

$$TAF = IPMF * MTF * GTF \quad \text{(from Equation 1.1)}$$

The TAF, along with other data relevant to each grid point, is exported and stored within the storm's adjustment factor feature class. The feature class includes a spatial component, a point feature at each grid cell centroid, and a table component as shown in Figure 9.1. For each feature, the table stores the grid point ID, the storm ID, the latitude and longitude coordinate pair, the transposition zone number, the elevation (in feet), the storm adjustment factors, and the transpositionability flag.

Table

SPAS_1242_1

| CNT | STORM | LON | LAT | ZONE | ELEV | IPMF | MTF | GTF | TAF | TRANS | Shape * |
|---|---|---|---|---|---|---|---|---|---|---|---|
| 95989 | 1242_1 | -99.075 | 31.800 | 8 | 1,476 | 1.28 | 1.18 | 1.14 | 1.72 | 1 | Point |
| 95990 | 1242_1 | -99.050 | 31.800 | 8 | 1,499 | 1.28 | 1.18 | 1.14 | 1.72 | 1 | Point |
| 95991 | 1242_1 | -99.025 | 31.800 | 8 | 1,486 | 1.28 | 1.18 | 1.14 | 1.72 | 1 | Point |
| 95992 | 1242_1 | -99.000 | 31.800 | 8 | 1,434 | 1.28 | 1.18 | 1.14 | 1.72 | 1 | Point |
| 95993 | 1242_1 | -98.975 | 31.800 | 8 | 1,378 | 1.28 | 1.18 | 1.13 | 1.71 | 1 | Point |
| 95994 | 1242_1 | -98.950 | 31.800 | 8 | 1,385 | 1.28 | 1.18 | 1.14 | 1.72 | 1 | Point |
| 95995 | 1242_1 | -98.925 | 31.800 | 8 | 1,447 | 1.28 | 1.18 | 1.14 | 1.72 | 1 | Point |
| 95996 | 1242_1 | -98.900 | 31.800 | 8 | 1,506 | 1.28 | 1.18 | 1.14 | 1.73 | 1 | Point |
| 95997 | 1242_1 | -98.875 | 31.800 | 8 | 1,578 | 1.28 | 1.18 | 1.15 | 1.73 | 1 | Point |
| 95998 | 1242_1 | -98.850 | 31.800 | 8 | 1,614 | 1.28 | 1.18 | 1.15 | 1.74 | 1 | Point |
| 95999 | 1242_1 | -98.825 | 31.800 | 8 | 1,663 | 1.28 | 1.18 | 1.15 | 1.74 | 1 | Point |
| 96000 | 1242_1 | -98.800 | 31.800 | 8 | 1,621 | 1.28 | 1.18 | 1.15 | 1.73 | 1 | Point |
| 96001 | 1242_1 | -98.775 | 31.800 | 8 | 1,647 | 1.28 | 1.18 | 1.14 | 1.73 | 1 | Point |
| 96002 | 1242_1 | -98.750 | 31.800 | 8 | 1,673 | 1.28 | 1.18 | 1.15 | 1.73 | 1 | Point |
| 96003 | 1242_1 | -98.725 | 31.800 | 8 | 1,716 | 1.28 | 1.18 | 1.15 | 1.73 | 1 | Point |
| 96004 | 1242_1 | -98.700 | 31.800 | 8 | 1,696 | 1.28 | 1.18 | 1.14 | 1.73 | 1 | Point |
| 96005 | 1242_1 | -98.675 | 31.800 | 8 | 1,765 | 1.28 | 1.18 | 1.14 | 1.73 | 1 | Point |
| 96006 | 1242_1 | -98.650 | 31.800 | 8 | 1,594 | 1.28 | 1.18 | 1.14 | 1.72 | 1 | Point |
| 96007 | 1242_1 | -98.625 | 31.800 | 8 | 1,608 | 1.28 | 1.18 | 1.13 | 1.71 | 1 | Point |
| 96008 | 1242_1 | -98.600 | 31.800 | 8 | 1,516 | 1.28 | 1.18 | 1.13 | 1.71 | 1 | Point |
| 96009 | 1242_1 | -98.575 | 31.800 | 8 | 1,444 | 1.28 | 1.18 | 1.13 | 1.71 | 1 | Point |
| 96010 | 1242_1 | -98.550 | 31.800 | 8 | 1,325 | 1.28 | 1.18 | 1.13 | 1.70 | 1 | Point |
| 96011 | 1242_1 | -98.525 | 31.800 | 8 | 1,371 | 1.28 | 1.18 | 1.13 | 1.71 | 1 | Point |
| 96012 | 1242_1 | -98.500 | 31.800 | 8 | 1,362 | 1.28 | 1.18 | 1.14 | 1.72 | 1 | Point |
| 96013 | 1242_1 | -98.475 | 31.800 | 8 | 1,312 | 1.28 | 1.18 | 1.14 | 1.72 | 1 | Point |

0 (1 out of 154998 Selected)

SPAS_1242_1

**Figure 9.1: Example of a storm adjustment factor feature class table. Grid point #96,000 (used in Section 9.6 sample calculations) is highlighted.**

For a grid point, the total adjusted rainfall depths for all storms of a given type transposable to that grid point are compared and the largest is stored as the PMP depth for that grid point location. It is important to understand that PMP depths are calculated for specific area sizes and are a representation of average PMP over that area size for a given duration and are not point rainfall values. *Therefore, no areal reduction factors should be applied to the calculated PMP depths*. The depth-area relationships in the PMP values are directly related to the gridded SPAS analyses from the controlling storm events.

## 9.6 Sample Calculations

The following sections provide sample calculations for the storm adjustment factors for the Alley Spring, MO March 2008 (SPAS 1242) general storm event when transposed to 31.8°N, 98.8°W (grid point ID #96,000). Figure 9.1 highlights the adjustment factors in the Total Adjustment Factor feature class table for the storm at this target grid point location. The target location is about 560 miles southwest of the storm location at an elevation of 1,600 feet in central Texas near Lake Brownwood and located in the east-central area of zone 8 (Figure 9.2).

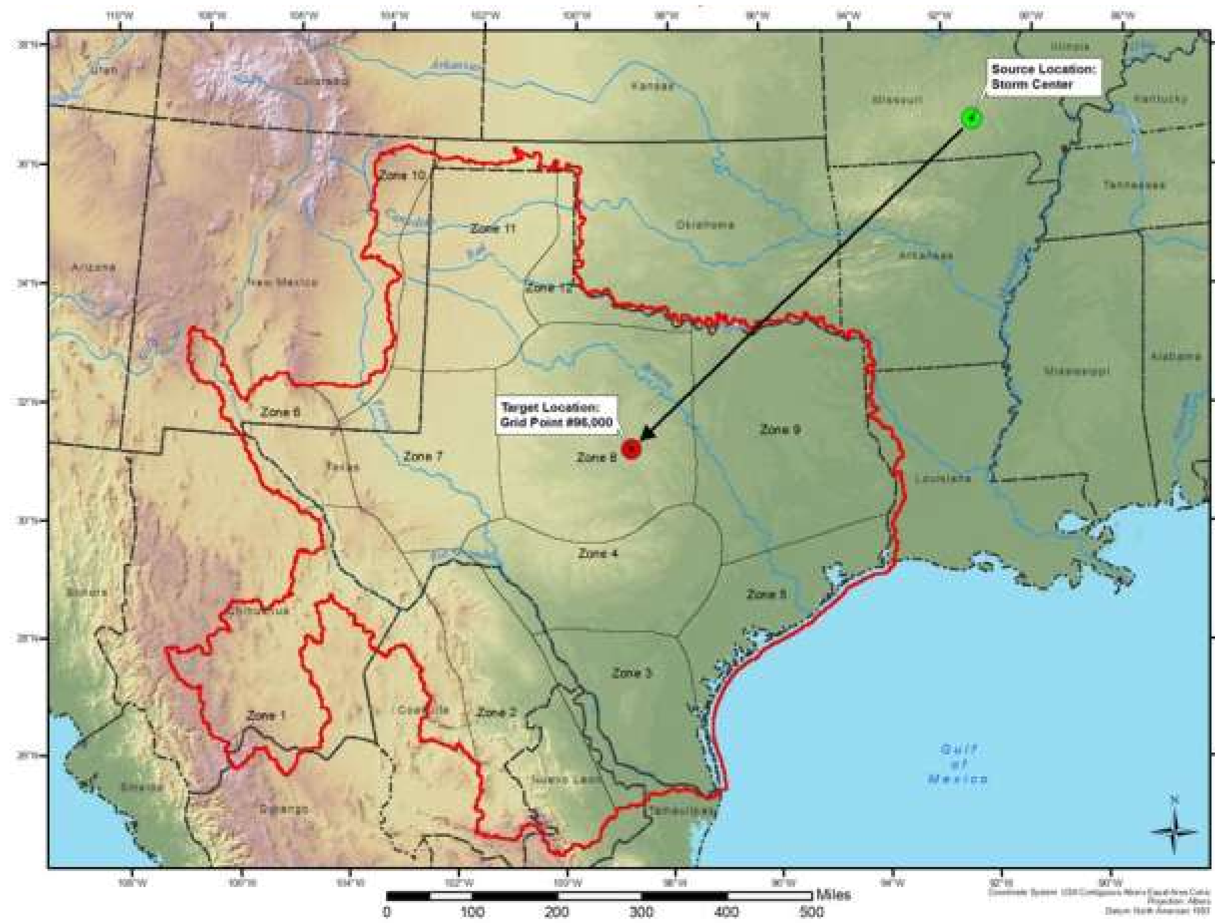


**Figure 9.2: Location of Alley Spring, MO March 2008, SPAS 1242 transposition to grid point #96,000**

### 9.6.1 Example of Precipitable Water Calculations

Using the storm representative dew point temperature and storm center elevation as input, the precipitable water lookup table returns the depth, in inches, used in Equation 9.1. The storm representative dew point temperature is 66 °F at the storm representative dew point location 500 miles southeast of the storm center (see Appendix F for the detailed storm maximization and analysis information). The storm center elevation is approximated at 900 feet at the storm center location of 37.16° N, 91.45° W. The storm representative available moisture ($W_{p,\ rep}$) is calculated using Equation 9.1:

$$W_{p,rep} = W(@66°)_{p,30{,}000'} - W(@66°)_{p,900'}$$

or,

$$W_{p,rep} = 1.86'' - 0.17''$$

$$\boldsymbol{W_{p,rep} = 1.69''}$$

The mid-March storm was adjusted 15 days toward the warm season to a temporal transposition date of April 1st. An average of the March and April 24-hour climatological maximum dew point temperatures was used for the April 1st temporal transposition date. The March climatological 100-year maximum 24-hour average dew point at the storm representative dew point location is 69.6°F and the April average is 72.2°F. The two monthly temperatures are averaged to a climatological maximum dew point temperature of 71°F. The in-place climatological maximum available moisture ($W_{p,\,max}$) is calculated.

$$W_{p,max} = W(@71°)_{p,30{,}000'} - W(@71°)_{p,900'}$$

$$W_{p,max} = 2.36" - 0.20"$$

$$\boldsymbol{W_{p,max} = 2.16"}$$

The climatological maximum available moisture was determined for the target grid point. The March climatological 100-year maximum 24-hour average dew point at the storm representative dew point location is 73.6°F and the April average is 75.6°F. The two monthly temperatures are averaged to 74.65°F and rounded to a climatological maximum dew point temperature of 74.5°F. The horizontally transposed climatological maximum available moisture ($W_{p,\,trans}$) is calculated.

$$W_{p,trans} = W(@74.5°)_{p,30{,}000'}$$

$$\boldsymbol{W_{p,trans} = 2.79"}$$

### 9.6.2 In-place Maximization Factor

Using Equation 9.2:

$$IPMF = \frac{W_{p,max}}{W_{p,rep}}$$

$$IPMF = \frac{2.16"}{1.69"}$$

$$\boldsymbol{IPMF = 1.28}$$

### 9.6.3 Moisture Transposition Factor

Using Equation 9.3:

$$MTF = \frac{W_{p,trans}}{W_{p,\max\,(30{,}000')}}$$

$$MTF = \frac{2.79"}{2.36"}$$

$$\boldsymbol{MTF = 1.18}$$

### 9.6.4 Geographic Transposition Factor

The ratio of the 100-year 24-hour climatological precipitation depth at the target grid point #96,000 location to the Alley Spring, MO 2008 storm center was evaluated to determine the storm's GTF at the target location. The 24-hour precipitation depth ($P_t$) of 8.59" was extracted at the grid point #96,000 location from the 100-year Texas precipitation climatology.

$$\boldsymbol{P_t = 8.59"}$$

Similarly, the 24-hour precipitation depth ($P_s$) of 7.49" was extracted at the storm center location from the 100-year NOAA Atlas 14 vol. 8 precipitation climatology.

$$\boldsymbol{P_s = 7.49"}$$

Equation 3.1 provides the climatological precipitation ratio to determine the GTF.

$$GTF = \frac{P_t}{P_s}$$

$$GTF = \frac{8.59"}{7.49"}$$

$$GTF = 1.15"$$

The GTF at grid #96,000 is 1.15, or a 15% rainfall increase from the storm center location due to the geographic effects captured within the precipitation climatology. The GTF is then considered to be a temporal constant for the spatial transposition between that specific source/target grid point pair, for that storm only, and can be applied to the other durations for that storm.

### 9.6.5 Total Adjustment Factor

$$TAF = IPMF * MTF * GTF$$

$$TAF = 1.28 * 1.18 * 1.15$$

$$\boldsymbol{TAF = 1.73}$$

The TAF for Alley Spring, MO March 2008, SPAS 1242 when moved to the grid point at 31.8°N, 98.8°W, representing storm maximization and transposition, is 1.73. This is an overall increase of 73% from the original SPAS analyzed in-place rainfall. The TAF can then be applied to the DAD value for a given area size and duration to calculate the total adjusted rainfall. If the total adjusted rainfall is greater than the depth for all other transposable storms, it becomes the PMP depth at that grid point for that duration.

# 10. PMP Calculation Process

To calculate PMP, the TAF for each storm must be applied to the storm's SPAS analyzed DAD value for the area size and duration of interest to yield a total adjusted rainfall value. The storm's total adjusted rainfall value is then compared with the adjusted rainfall values of every storm in the database transposable to the target grid point. This process must be repeated for each of the 154,998 grid points within the statewide domain for each duration and for each storm type.

## 10.1 PMP Tool Description and Usage

The PMP Evaluation Tool employed in this study uses a Python-based script designed to run within the ArcGIS environment. ESRI's ArcGIS 10.3 (or later) software (ESRI, 2012) is required to run the tool, and it is recommended that the user have a basic familiarity with the operation of this software. The tool provides gridded PMP values at a spatial resolution of 90 arc-seconds (equivalent to .025 x .025 dd) for a user-designated drainage basin or area at user-specified durations.

### 10.1.1 File Structure

The tool, source script, and all input data are stored within the 'PMP_Evaluation_Tool' project folder. The file and directory structure within the 'PMP_Evaluation_Tool' folder should be maintained as it is provided, as the script will locate various data based on its relative location within the project folder. If the subfolders or geodatabases within are relocated or renamed, then the script must be updated to account for these changes.

The file structure consists of only two subfolders: Input and Script. The 'Input' folder contains all input GIS files (Figure 10.1). There are three ArcGIS file geodatabase containers within the 'Input' folder: DAD_Tables.gdb, Storm_Adj_Factors.gdb, and Non_Storm_Data.gdb. The DAD_Tables.gdb contains the DAD tables (in file geodatabase table format) for each of the 68 SPAS analyzed storm DAD zones. The Storm_Adj_Factors.gdb contains a feature class for each analyzed event and stores the adjustment factors for each grid point as a separate feature. These feature classes are organized into feature datasets, according to storm type (General, Local, and Tropical). The storm adjustment factor feature classes share their name with their DAD Table counterpart. The naming convention is SPAS_XXXX_Y, where XXXX is the SPAS storm ID number and Y is the DAD zone number. Finally, the Non_Storm_Data.gdb contains spatial data not directly relating to the input storms: Grid_Points, a point feature class, and Vector_Grid, a polygon feature class representing the grid cells for each of the 154,998 grid points.

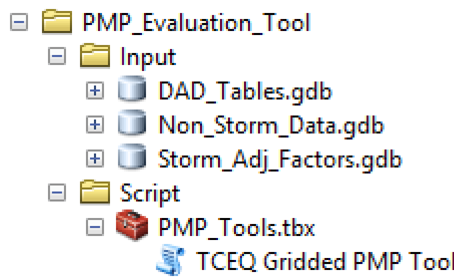


**Figure 10.1: PMP tool file structure.**

The 'Script' folder contains an ArcToolbox called PMP_Tools.tbx. The toolbox contains a script tool called 'TCEQ Gridded PMP Tool' that is used to calculate basin PMP. ArcGIS Desktop should be used for viewing the GIS tool file structure and interacting with the input and output geospatial data and metadata. A typical operating system's file browser does not allow access to the geodatabase containers and cannot be used to directly run the tool.

### 10.1.2 Python Script

Due to the large number of storm datasets and grid points within the project domain, a scripted process is necessary to compare each value efficiently and accurately for a given area of interest and make the necessary calculations. ArcGIS has integrated the Python scripting language to allow for the custom development of geoprocessing operations and toolsets. Python can be used to access the geoprocessing, data management, and looping functionality needed to process the PMP calculations for a basin. The gridded PMP analysis script has been added to an ArcToolbox and can be run as a tool within the ArcGIS environment. The script has been imported and stored internally within the TCEQ Gridded PMP Tool and all the parameters for the tool have been set. The script can be accessed by exporting it from the tool to a '.py' file. The Python code can be opened and edited within any text editor. A hardcopy version of the code is given in Appendix H.

The python script uses the arcpy, arcpy.analysis, arcpy.management, arcpy.conversion, and numpy modules. Python and these modules are included within the ArcGIS for Desktop package. The script is designed to run as efficiently as possible with a minimal amount of code and complexity. To achieve this, the script is organized into functions that are called as needed. The primary PMP analysis calculations are calculated within the pmpAnalysis() function which is called separately for each PMP storm type analyzed. Within the broader pmpAnalysis() function, several smaller functions are called to perform various tasks:

| | |
|---|---|
| **createPMPfc()** | Creates the PMP_Points feature class to store vector (point) results |
| **getAOIarea()** | Calculates the area of the input basin |
| **dadLookup()** | Gets the DAD value for the current storm based on basin area or Area of Interest (AOI) defined by the user |
| **updatePMP()** | Records the largest adjusted rainfall value (PMP) |

**outputPMP()** Produces output PMP GIS files and tables

**basinAve()** Calculates the basin average PMP

The tool contains some extra functionality for this project to add the PMP output feature classes and summary basin average table to the current mapping environment:

**outputBasAveTable()** Creates a basin average summary table

**addLayerMXD()** Adds a feature or table layer to the current map document

The presence of the addLayerMXD() function requires that the tool is run from an open ArcMap .mxd session. There is extensive documentation within the code in the form of '# comments'. These comments provide guidance toward its functionality and describe the code.

While the script performs many actions, its primary purpose is to iterate through both the storm list and the grid points within the area of interest (AOI), comparing each, and creating output based on the maximum values. To accomplish this, several layers of nested iterative "for" loops are used.

The following high-level algorithm broadly describes the script process:

- Calculate Basin Area (in $mi^2$)
- For each Storm Type (general, tropical, and local)
    - For each duration
        - For each storm in database
            - Lookup storm's depth-area-duration (DAD) value for AOI size
            - For each grid point in basin
                - Calculate total adjusted rainfall (TAR) by multiplying DAD value by total adjustment factor for the grid point
                - If TAR > PMP, the TAR becomes the new PMP value for that grid point
    - Create PMP point feature class for the storm type
    - Create PMP raster GRID files for each duration
    - Create basin average table
- Create summary table
- Add layers to map session

### 10.1.3 Usage

The 'TCEQ Gridded PMP Tool' stored within the PMP_Tools.tbx ArcToolbox opens and runs the script within the ArcGIS environment and should be run from ArcMap. In addition to running as a standalone tool, the tool can be incorporated into Model Builder or be called as a sub-function of another script.

To run the tool, the user navigates to the PMP_Tools.tbx toolbox, expands it, and opens the PMP tool. The dialogue window opens and the user populates input parameters (see Figure 10.2) and clicks the 'OK' button. The tool will run in the foreground and display text output in the Messages window. Processing time can vary greatly depending on AOI size, the number of durations selected, and computer hardware. Small to medium-sized basins generally take a few minutes to analyze depending on computer processing speed. The tool produces PMP output described in Section 10.1.5.

### 10.1.4 Input Parameters

The tool requires eight parameters as input to define the area and durations to be analyzed (Table 10.1).

**Table 10.1: Parameters for the PMP calculation tool.**

| Parameter # (in script) | Display Name | Data Type | Type | Direction | MultiValue |
|---|---|---|---|---|---|
| 0 | Input basin outline shapefile or feature class | Feature Layer | Required | Input | No |
| 1 | Location of "PMP_Evaluation_Tool' Folder | Folder | Required | Input | No |
| 2 | Output Folder | Folder | Required | Input | No |
| 3 | Local storm durations | String | Optional | Input | Yes |
| 4 | General storm durations | String | Optional | Input | Yes |
| 5 | Tropical storm durations | String | Optional | Input | Yes |
| 6 | Use Basin Area | Boolean | Required | Input | No |
| 7 | PMP Area (sqmi) | Double | Optional | Input | No |
| 8 | Apply weighted average to border grid cells | Boolean | Required | Input | No |
| 9 | Output Basin Average Summary Table | Table | Required | Output | No |

Figure 10.2 shows the tool dialogue window with each of the input parameters. The first parameter required by the tool dialogue is a feature layer, such as a basin shapefile or feature class, designed to outline the area of interest (AOI) for the PMP analysis. If the AOI dataset does not have a surface projection, the tool will apply the Albers Equal Area projection for the purpose of calculating the AOI area size. If the feature layer has multiple features (or polygons), the tool will use the combined area as the analysis region. Only the selected polygons will be used if the tool is run from the ArcMap environment with selected features highlighted. If the AOI shapefile extends beyond the project analysis domain, PMP will only be calculated for grid cells inside the project domain.

The second parameter requires the path of the 'PMP_Evaluation_Tool' folder. The default location of the folder is set within the tool parameters, but it can be changed if the user wishes to link the tool to another set of input datasets. The 'PMP_Evaluation_Tool' project folder should be stored locally at a location that can be accessed (both read/write) by ArcGIS desktop. The user will need to set the 'Output Folder' path which provides the tool with the location to create the output PMP files. The user must have read/write privileges for this folder location. The user then selects the durations to be run for each storm type. The next parameter allows the user the option to have the tool perform a weighted analysis on the grid cells underlying the AOI boundary. If this option is checked, each boundary grid cell depth will be weighted by the portion of the cell's area inside the basin for the purpose of the basin average

PMP table calculations. Finally, the user may override the default to use the input basin feature area size for the AOI and enter a custom area (in square miles). The tool calculates PMP for the area-size of the basin; a manually entered area-size will override the basin area-size in the PMP calculations (a larger area produces smaller depths).

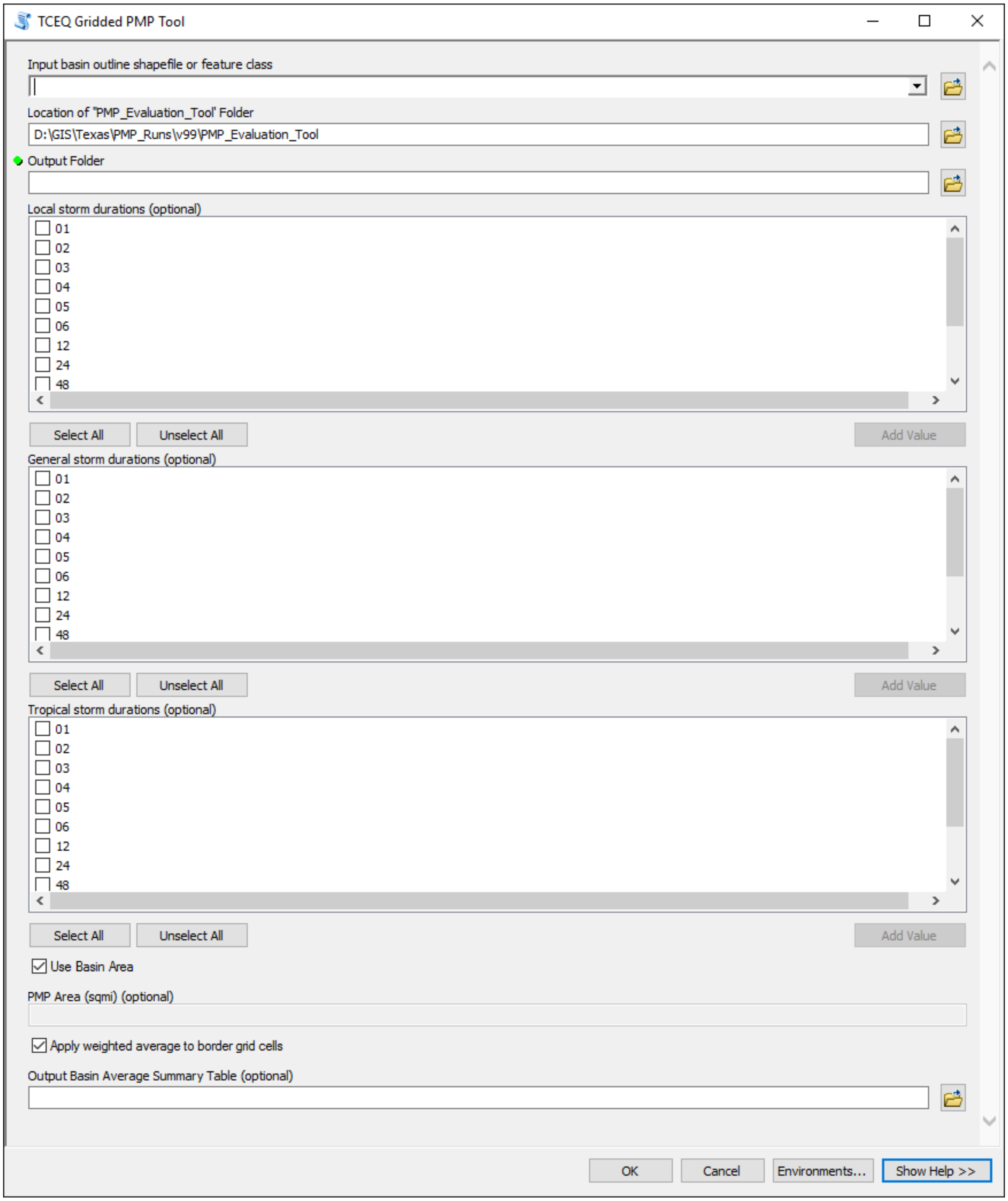


**Figure 10.2: The PMP Evaluation Tool input dialogue window**

Finally, the Validation tab of the tool properties contains some custom scripting to handle the input parameter formatting. This script is included at the end of Appendix H.

### 10.1.5 Tool Output

Once the tool has been run, the output file geodatabases will be populated with the model results. The GIS files can then be brought into an ArcMap, or other compatible GIS environments, for mapping and analysis. The tool is set to have overwrite capabilities; if output data exists, it will be overwritten the next time the tool is run, if the same output folder is used.

A separate output folder is created for each storm type and the output is organized within file geodatabases and named according to the input basin feature name and analyzed PMP area. Each output file geodatabase contains a feature class which stores each grid point centroid within the basin as a separate feature. Each feature has a field for the grid ID, latitude, longitude, analysis zone, elevation, PMP (for each duration), and the contributing storm ID (see Figure 9.1). The PMP raster files are also stored within the file geodatabase. The naming convention for the raster files is the storm type and duration (L for local/MCS, G for general, and T for tropical), followed by the input basin feature name, and ending with the basin area (in square miles). An example of the output file structure is shown in Figure 10.3.

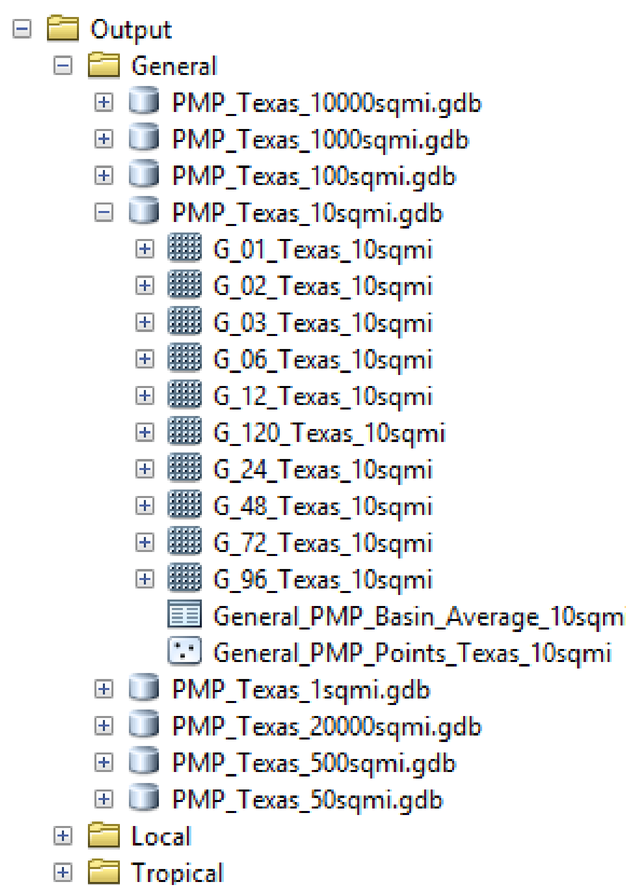


**Figure 10.3: Example of the PMP tool output file structure**

## 10.2 Project-wide PMP output datasets

Gridded PMP datasets were produced for the series of durations and areas listed below for the entire analysis domain of this project (Figure 1.1). The final PMP datasets are stored in geodatabase raster format and have been provided to TCEQ. All data are included as part of the digital Appendix K. Below are the datasets pre-run and analyzed during the study. Other durations and area sizes available from the native SPAS DADs can be run using the overall database included.

**Local Storm PMP Durations:**
1-, 2-, 3-, 4-, 5-, 6-, 12-, 24-, 48-, and 72-hour

**Local Storm PMP Area Sizes:**
1-, 10-, 25-, 50-, 100-, 200-, 300-, 500-, and 1,000-sq. miles

**General/Tropical Storm PMP Durations:**
1-, 2-, 3-, 6-, 12-, 24-, 48-, 72-, 96- and 120-hour

**General/Tropical Storm PMP Area Sizes:**
1-, 10-, 50-, 100-, 500-, 1,000-, 10,000-, and 20,000-sq. miles

## 10.3 Temporal Distribution of PMP Values

This study does not include guidance for applying temporal distributions to PMP values. The authors recognize that temporal distributions should vary with storm type and potentially basin size and location. Extensive work has already been completed in Texas by various agencies to provide guidance for temporal accumulation patterns of rainfall. Examples include Al-Asaadi, 2002; Asquith, 2003; Asquith et al., 2003; Asquith and Thompson, 2003; and Asquith et al., 2004. Current TCEQ guidance for temporal distributions is provided in the TCEQ *Hydrologic and Hydraulic Guidelines for Dams in Texas (TCEQ Publication GI-364, January 2007*). For this study, 68 storms were analyzed with SPAS at 1-hour or higher temporal resolutions, and mass curves were produced for each analyzed DAD zone. These individual temporal storm distributions could be applied in hydrologic models to greatly aid in the development of storm type specific and/or region specific temporal distribution patterns. The mass curves showing the accumulation of rainfall through time for each event are included in Appendix F of this report.

# 11. PMP Sensitivity and Comparisons

The PMP and intermediate data produced for this study was rigorously evaluated throughout the process. ArcGIS was used as a visual and numerical evaluation tool to assess gridded values to ensure they fell within acceptable ranges and met test criteria. Many iterations of maps were produced as visual aids to help identify potential issues with calculations, transposition limits, DAD values, or storm adjustment values. The maps also helped to define storm characteristics and transposition limits, as discussed previously. Over the entire PMP analysis domain, different storms control PMP values at different locations for a given duration and area size. In some instances, a discontinuity of PMP depths between adjacent grid point locations resulted. This occurs as a result of the binary transposition limits applied to the controlling storms, with no allowance for gradients of transpositionability. Therefore, different storms are affecting adjacent grid points and may result in a shift in values over a short distance. In reality, there would be some transition for a given storm, but the process and definition of transpositionability does not allow for this. It is important to note that these discontinuities make little difference in the overall basin average PMP values as applied for hydrologic analysis purposes for most basins. The discontinuities are only seen when analyzing data at the highest resolution (e.g., individual grid points). Any significant discontinuities would potentially have the most significant effect for small basins where there are a small number of grid points representing the drainage. In those instances, each grid point value would have an exaggerated effect on the basin average PMP.

Figures 11.1 through 11.3 display 6-hour local storm PMP for 10 square miles, 24-hour tropical storm PMP for 100 square miles, and 72-hour general storm PMP for 1,000 square miles, respectively, for the project-wide domain. Figures 11.4 through 11.6 display the controlling storms by storm type across the entire domain. The spatial variations of controlling storms in these map images can be a result of storm transposition limits, which can be defined by transposition zone, elevation, GTF values, and specific geographic extents, or they can be a result of rounding when multiple storms produce similar adjusted rainfall values in the same region.

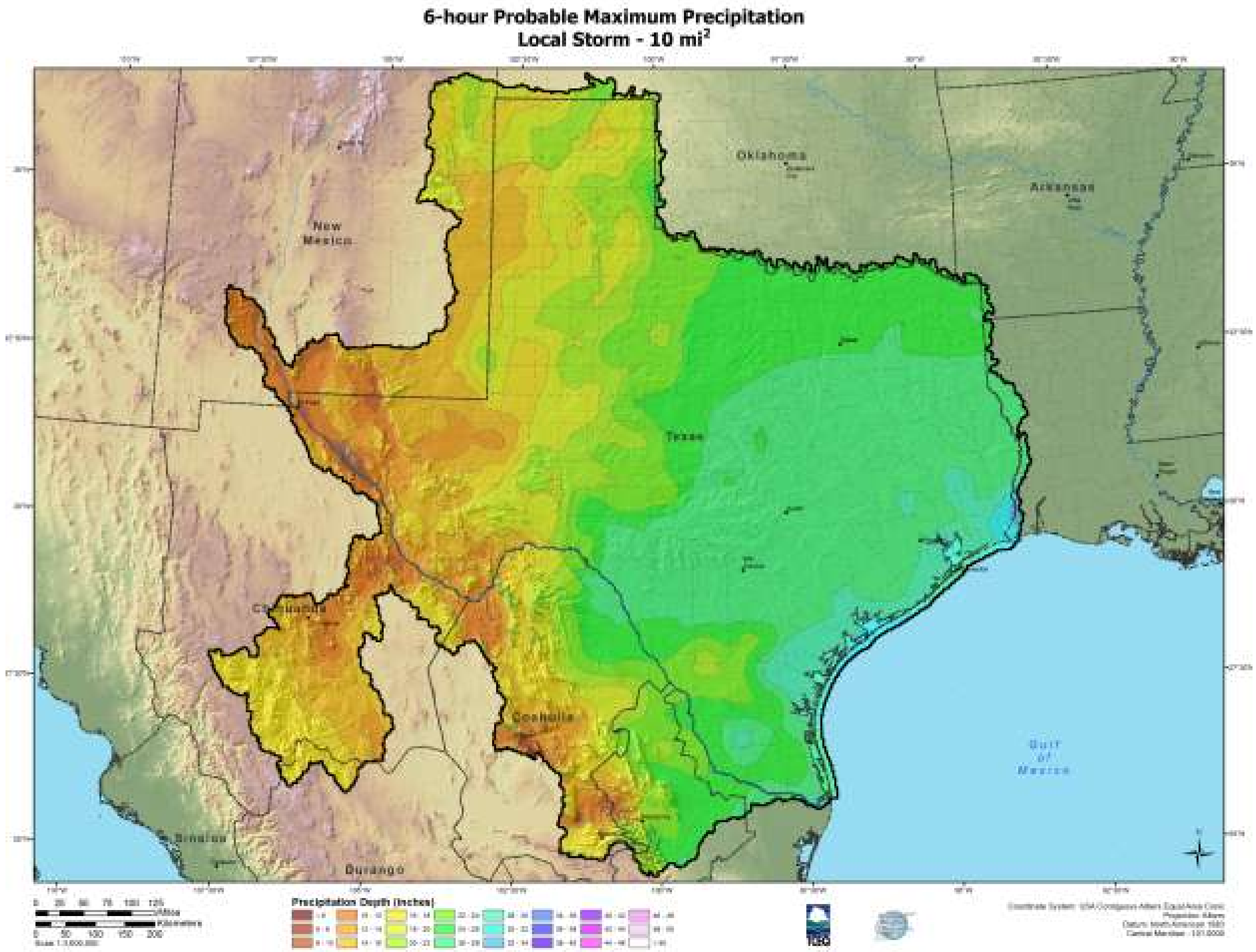


**Figure 11.1: Project domain map of the 6-hour, 10-square mile PMP values derived from local/MCS storms.**

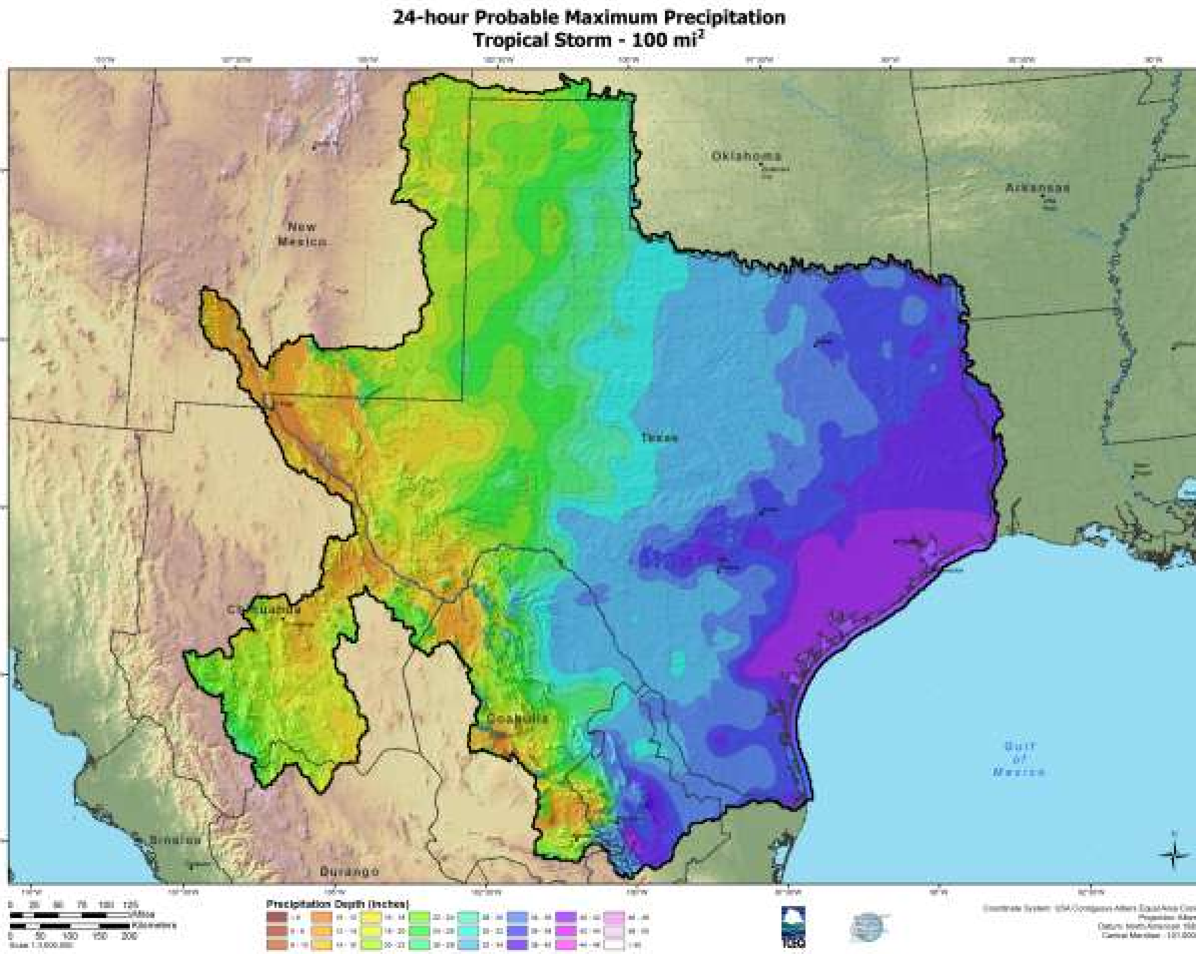


**Figure 11.2: Project domain map of the 24-hour, 100-square mile PMP values derived from tropical storms.**

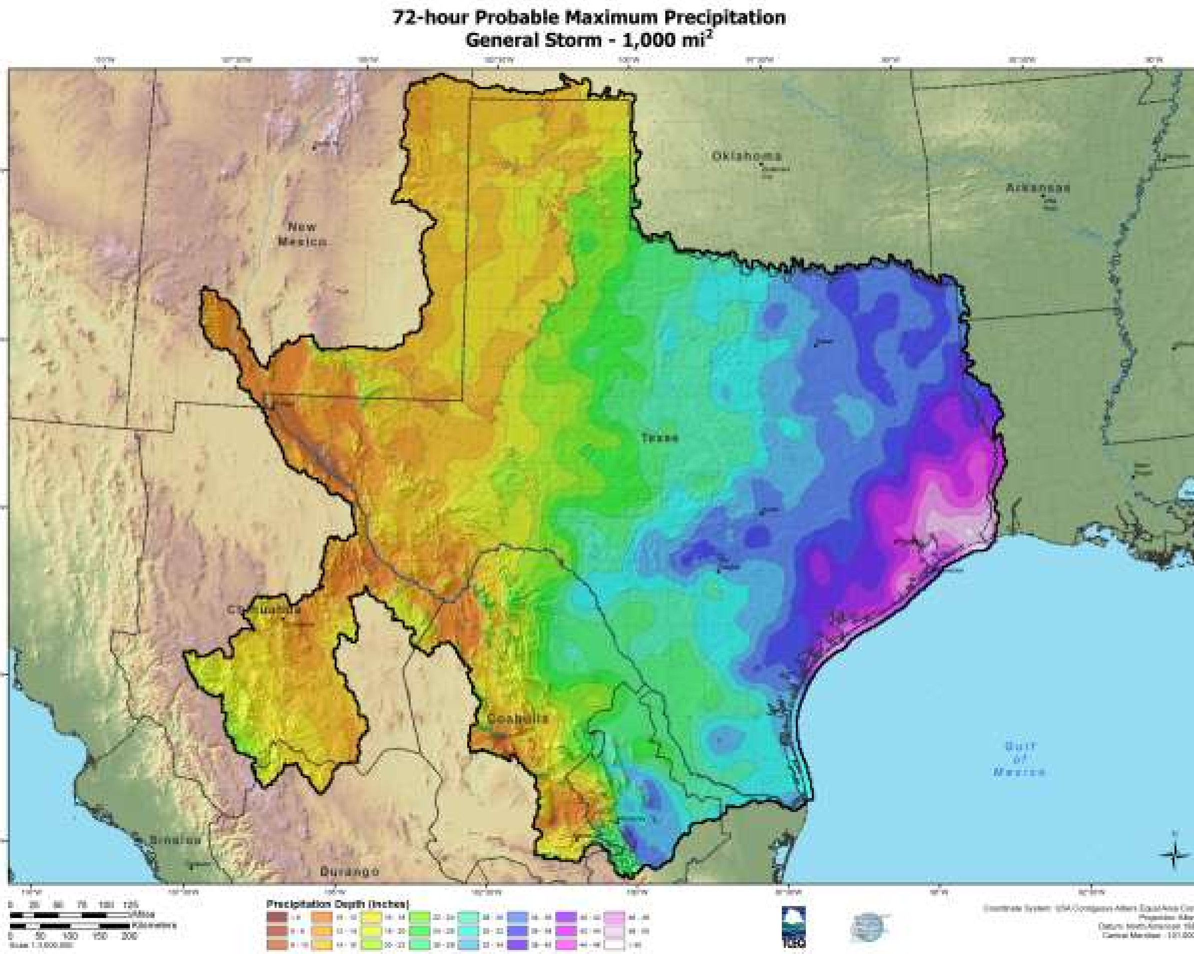


**Figure 11.3: Project domain map of the 72-hour, 1,000-square mile PMP values derived from general storms.**

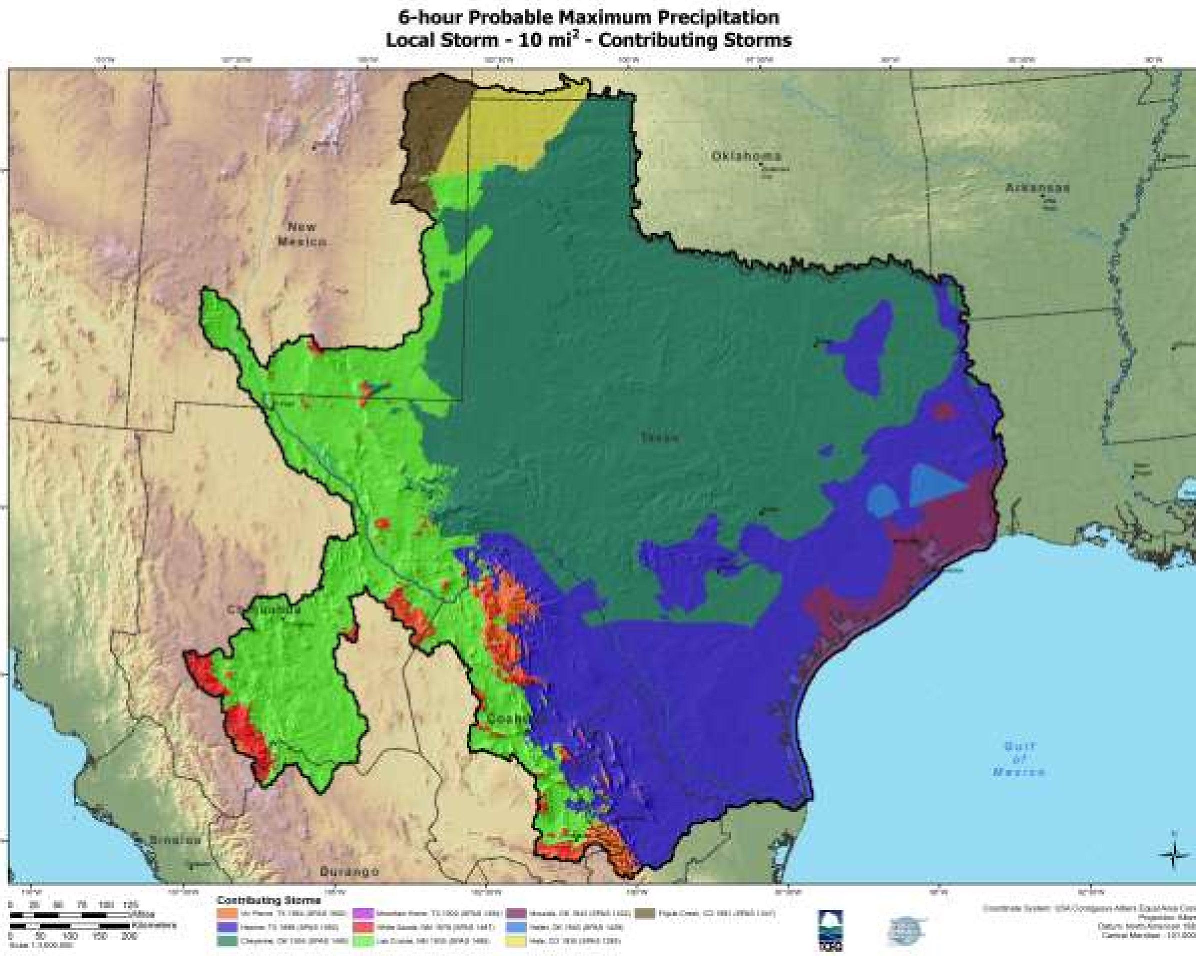


**Figure 11.4: Project domain map of the controlling storms of the local/MCS storm type for the 6-hour 10-square mile PMP.**

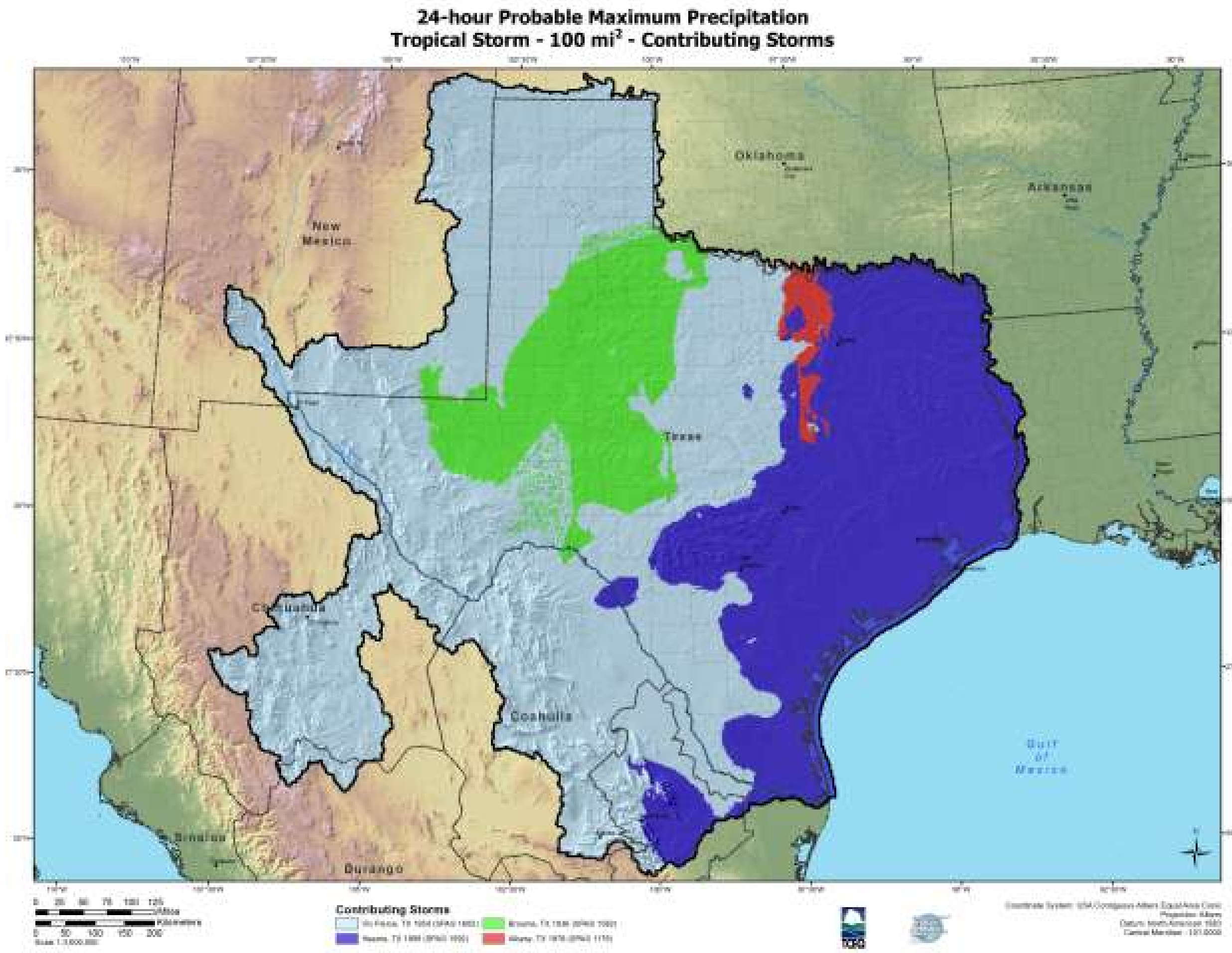


**Figure 11.5: Project domain map of the controlling storms of the tropical storm type 24-hour 100-square mile PMP.**

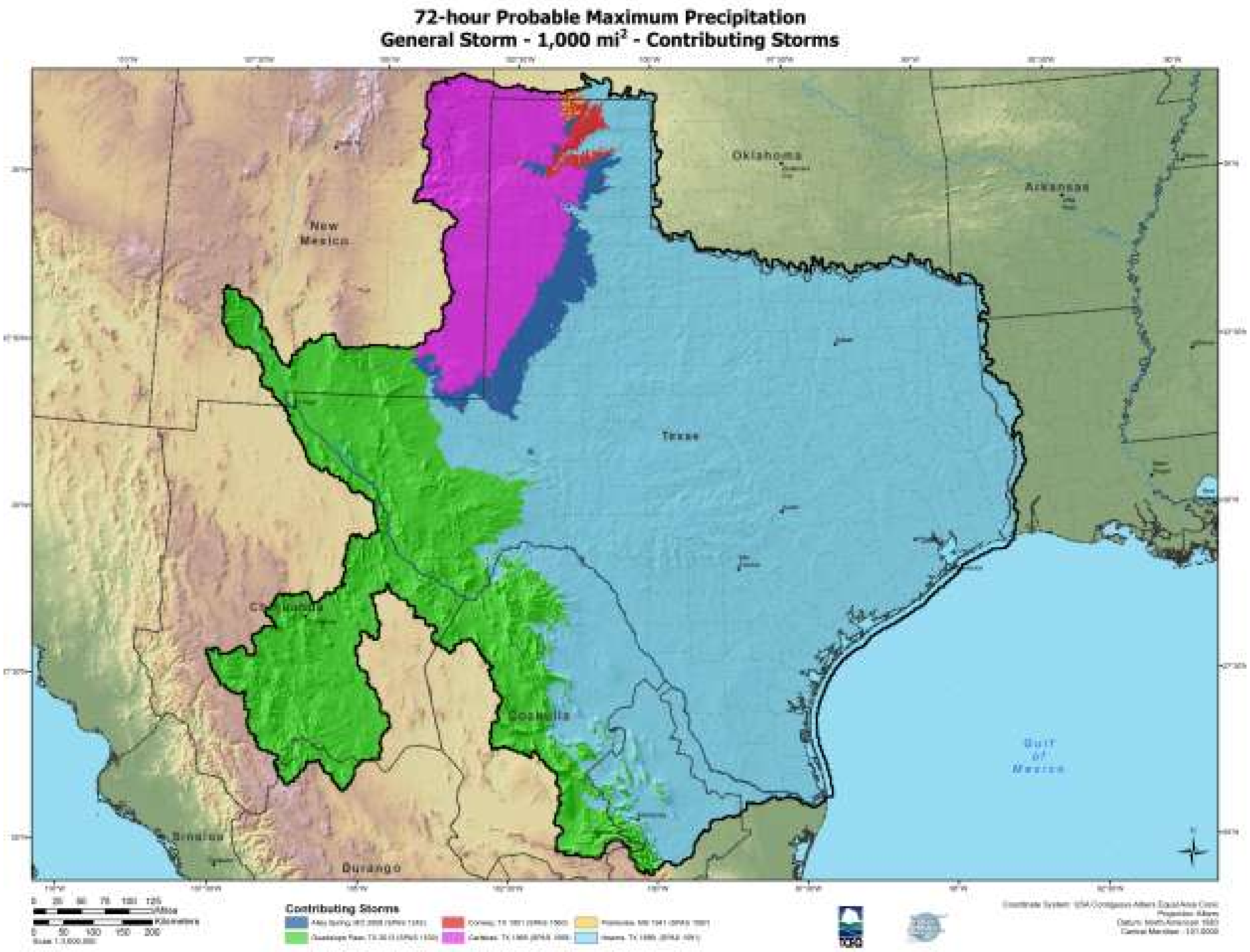


**Figure 11.6: Project domain map of the controlling storms of the general storm type 72-hour 1,000-square mile PMP.**

## 11.1 Evaluation of Basin-Specific PMP

PMP was calculated for three sample drainage basins: Basin #1913 is a 2,096 square mile basin located primarily in transposition zone 4 along the Guadalupe River drainage in South Texas, basin #2789 is a 1,565 square mile basin located in transposition zone 8 covering the Lake Brownwood drainage in west-central Texas, and basin #1952 is a 442 square mile basin located in transposition zone 1 along the Alamito Creek in West Texas. The basin locations are shown in Figure 11.7.

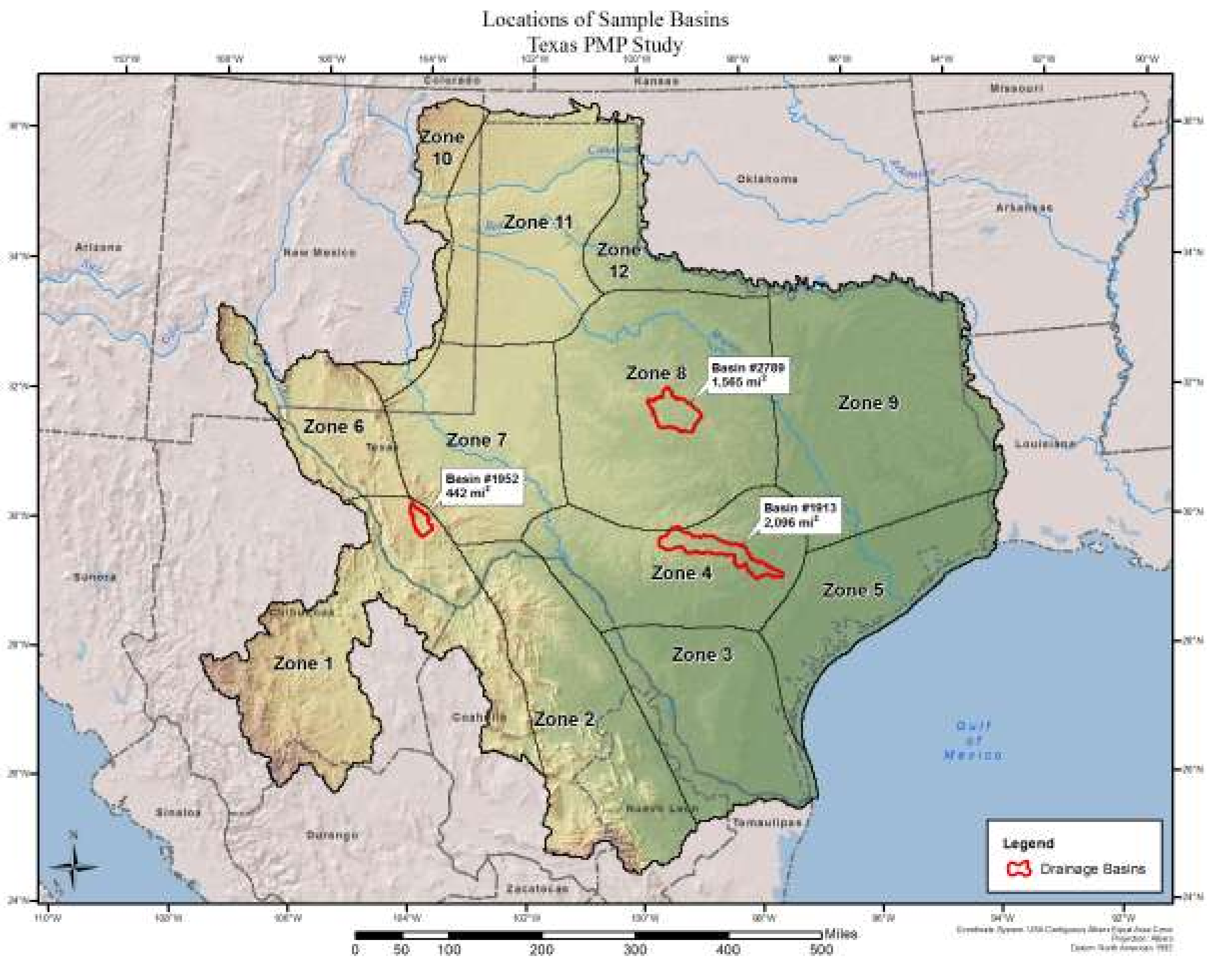


**Figure 11.7: Sample basin locations.**

Gridded PMP values were determined for each basin at their precise area sizes following the methods described in Section 10.1 using the 'TCEQ Gridded PMP Tool'. The basin average results for each storm type were tabulated for Basin #1913 PMP (Table 11.1), Basin #2789 PMP (Table 11.2), and Basin #1952 PMP (Table 11.3). The PMP magnitudes at all durations are within the reasonable range for each storm type. For durations shorter than 24-hours, local storm PMP provides the largest values, which is to be expected for basins at these locations and at these area sizes.

**Table 11.1: Basin average PMP values and controlling storms at 2,096 square miles for Basin #1913**

| Basin #1913 Average PMP (2,096 $mi^2$) | 1-hour | 2-hour | 3-hour | 6-hour | 12-hour | 24-hour | 48-hour | 72-hour | 96-hour | 120-hour |
|---|---|---|---|---|---|---|---|---|---|---|
| **Local Storm** | 3.7" | 7.4" | 11.1" | 13.4" | 16.7" | 23.8" | - | - | - | - |
| **General Storm** | 2.7" | 4.7" | 6.4" | 11.4" | 17.0" | 21.6" | 26.5" | 30.8" | 32.1" | 32.1" |
| **Tropical Storm** | 3.5" | 7.0" | 10.5" | 12.7" | 15.8" | 23.8" | 29.4" | 29.5" | 29.5" | 29.5" |
| **Max. (All Types)** | **3.7"** | **7.4"** | **11.1"** | **13.4"** | **17.0"** | **23.8"** | **29.4"** | **30.8"** | **32.1"** | **32.1"** |
| **Controlling Storm(s)** | Mounds, OK 1943 Thrall, TX 1921 | Thrall, TX 1921 | Thrall, TX 1921 | Thrall, TX 1921 | Warner Park, TN 2010 | Vic Pierce, TX 1954 | Vic Pierce, TX 1954 | Hearne, TX 1899 | Hearne, TX 1899 | Hearne, TX 1899 |

**Table 11.2: Basin average PMP values and controlling storms at 1,565 square miles for Basin #2789**

| Basin #2789 Average PMP (1,565 $mi^2$) | 1-hour | 2-hour | 3-hour | 6-hour | 12-hour | 24-hour | 48-hour | 72-hour | 96-hour | 120-hour |
|---|---|---|---|---|---|---|---|---|---|---|
| **Local Storm** | 3.4" | 6.4" | 9.7" | 11.7" | 15.2" | 24.5" | - | - | - | - |
| **General Storm** | 3.3" | 4.8" | 5.8" | 10.0" | 14.5" | 18.6" | 24.2" | 27.6" | 28.6" | 28.6" |
| **Tropical Storm** | 3.1" | 6.1" | 9.2" | 11.1" | 15.8" | 25.2" | 31.4" | 31.4" | 31.4" | 31.4" |
| **Max. (All Types)** | **3.4"** | **6.4"** | **9.7"** | **11.7"** | **15.8"** | **25.2"** | **31.4"** | **31.4"** | **31.4"** | **31.4"** |
| **Controlling Storm(s)** | Mounds, OK 1943 Thrall, TX 1921 Mountain Home. TX | Thrall, TX 1921 | Thrall, TX 1921 | Thrall, TX 1921 | Broome, TX 1936 | Vic Pierce, TX 1954 | Vic Pierce, TX 1954 | Vic Pierce, TX 1954 | Vic Pierce, TX 1954 | Vic Pierce, TX 1954 |

**Table 11.3: Basin average PMP values and controlling storms at 442 square miles for Basin #1952**

| Basin #1952 Average PMP (442 $mi^2$) | 1-hour | 2-hour | 3-hour | 6-hour | 12-hour | 24-hour | 48-hour | 72-hour | 96-hour | 120-hour |
|---|---|---|---|---|---|---|---|---|---|---|
| **Local Storm** | 3.2" | 5.2" | 6.1" | 8.5" | 13.2" | 19.0" | - | - | - | - |
| **General Storm** | 2.2" | 3.1" | 4.3" | 7.3" | 13.0" | 15.9" | 18.1" | 18.7" | 18.6" | 18.6" |
| **Tropical Storm** | 2.6" | 4.9" | 5.8" | 8.1" | 12.5" | 18.0" | 23.4" | 23.4" | 23.4" | 23.4" |
| **Max. (All Types)** | **3.2"** | **5.2"** | **6.1"** | **8.5"** | **13.2"** | **19.0"** | **23.4"** | **23.4"** | **23.4"** | **23.4"** |
| **Controlling Storm(s)** | Las Cruces, NM 1935 | Vic Pierce, TX 1954 | Vic Pierce, TX 1954 | Vic Pierce, TX 1954 | Vic Pierce, TX 1954 | Vic Pierce, TX 1954 | Vic Pierce, TX 1954 | Vic Pierce, TX 1954 | Vic Pierce, TX 1954 | Vic Pierce, TX 1954 |

The spatial distribution is consistent for all durations within a given storm type and is representative of the 100-year precipitation climatology. Figure 11.8 illustrates the 24-hour general storm PMP distributed over Basin #1913. The spatial distribution of PMP values reflects the terrain effects due to landforms such as the Balcones Escarpment, Edwards Plateau, and Llano Uplift, as considered implicitly in the GTF. Despite the color variations shown in Figure 11.8, the total PMP variation over the entire basin is less than 3.5 inches, which indicates a fairly constant spatial distribution. The initial spatial distribution of PMP over the basin is provided by the unique PMP depth at each grid point. Other spatial distributions can be implemented by applying actual storm patterns or other spatial patterns judged to be appropriate to the initial PMP depths. Care should be taken to ensure the alternate spatial distributions reflect a physically possible combination of topography and meteorology for the given basin and that the basin average depth is the same as the initial PMP values, at each analyzed duration. Figure 11.9 illustrates the 24-hour general storm PMP distributed over Basin #2789, Lake Brownwood. The terrain effect is even more static in this region resulting in a spatial variation of just over 2 inches for the entire basin. The variation is primarily controlled by the gentle rise in elevation from east to west and the increasing distance from the moisture source. Figure 11.10 illustrates the 24-hour local storm PMP distributed over Basin #1952. This is a smaller basin in the more orographically influenced basin and range western region of the study area with PMP more likely to be controlled by the local/MCS storm type. The spatial distribution is fairly constant over the majority of the relatively flat and protected basin, but it varies more rapidly along the northern and eastern fringes of the basin due to the orographic effects of the Puertacitas Mountains.

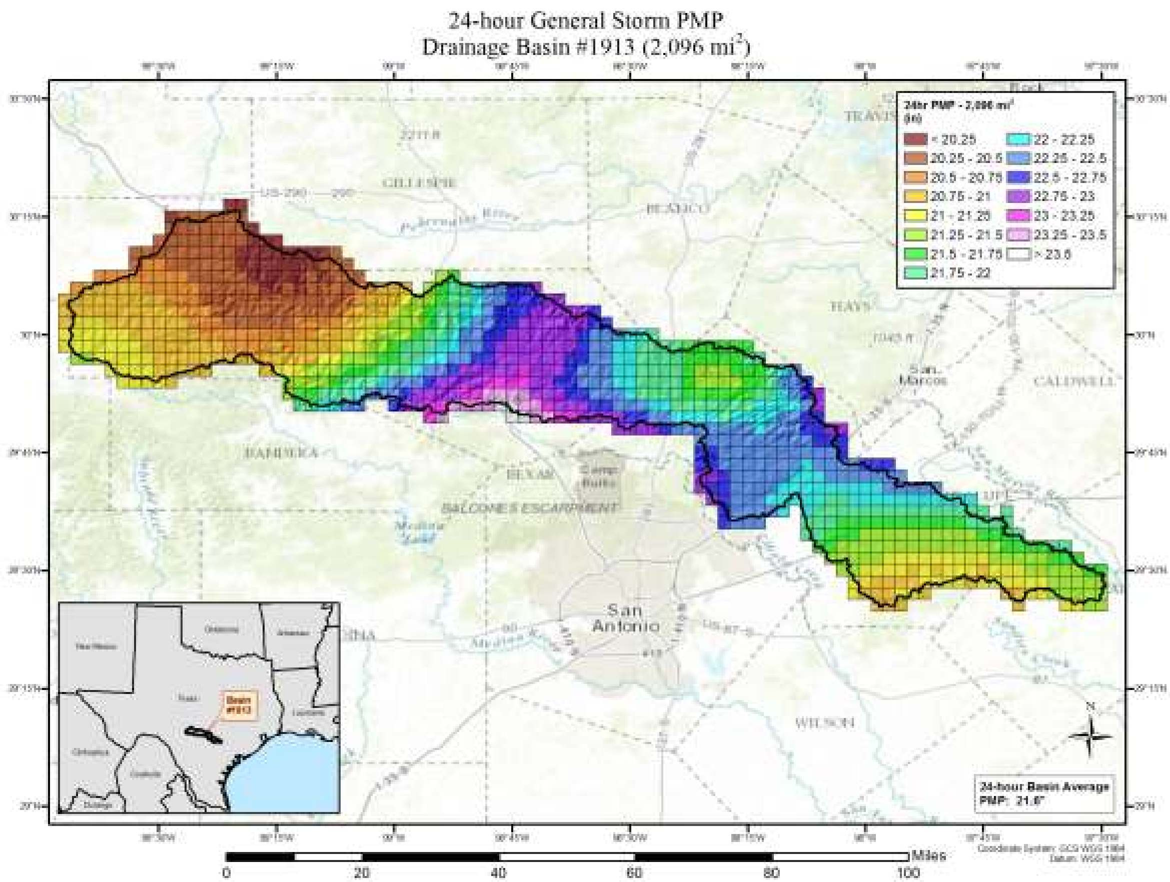


**Figure 11.8: Spatial distribution of the 24-hour general storm PMP over Basin #1913**

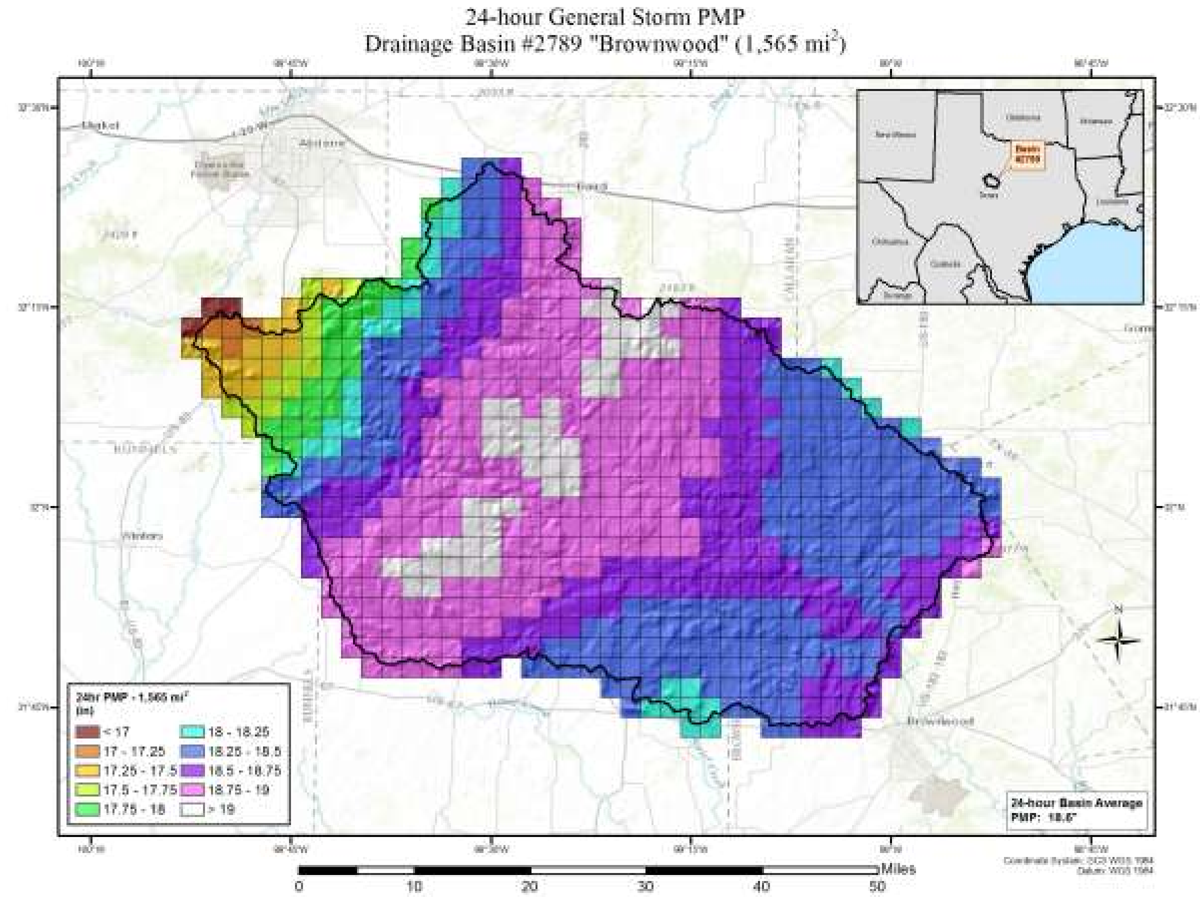


**Figure 11.9: Spatial distribution of the 24-hour general storm PMP over Basin #2789**

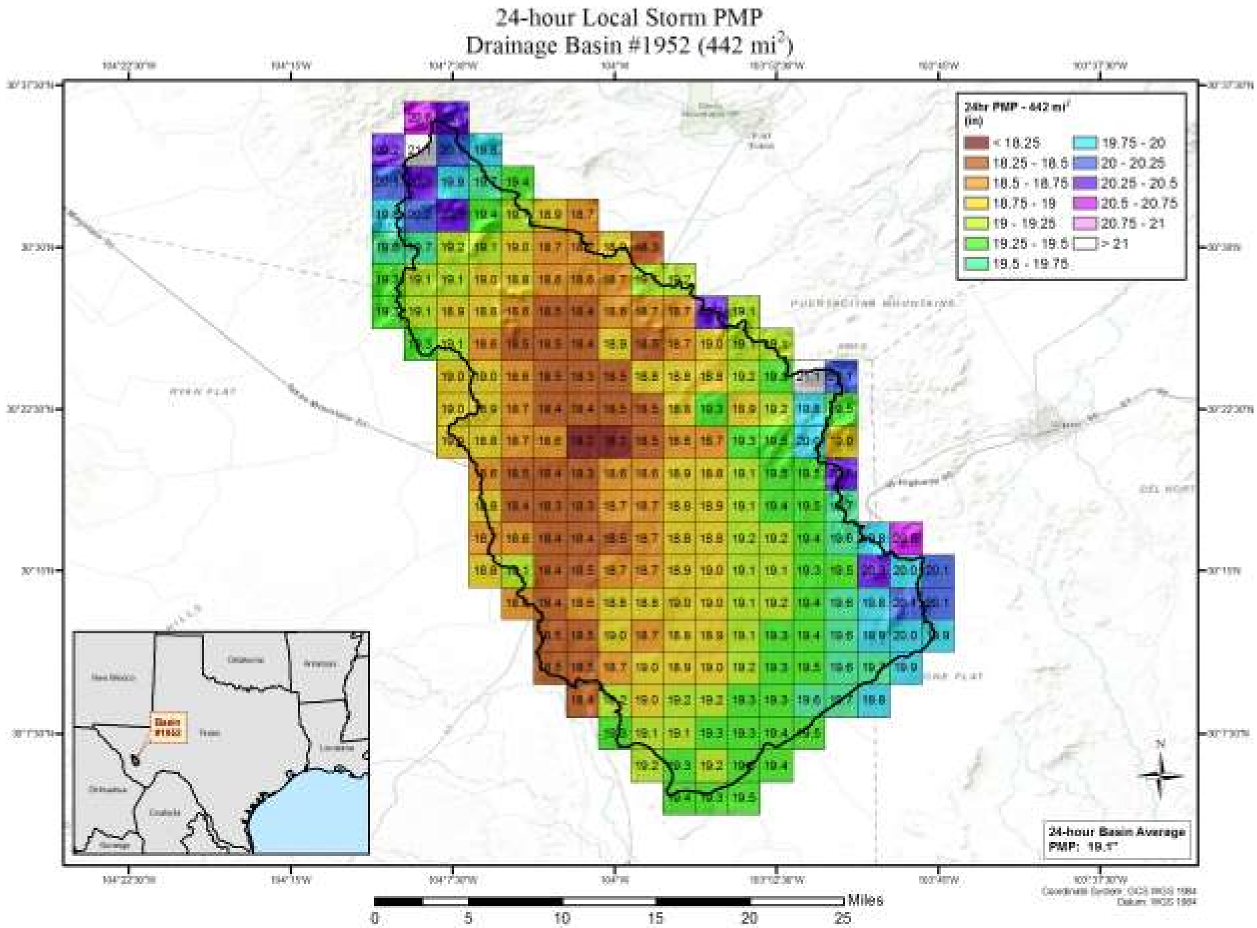


**Figure 11.10: Spatial distribution of the 24-hour local storm PMP over Basin #1952**

The basin average PMP was calculated by weighting the grid cells along the basin AOI boundary according to the proportion of their area inside the basin boundary. Note, the PMP for each storm type is calculated independently. Therefore, the PMP at a duration for a given storm type may be higher than the PMP at a longer duration for another storm type.

This occurs chiefly due to the Hybrid events used that are run as more than one storm type (e.g. Thrall, TX September, 1921 and Vic Pierce, TX June, 1954) which provide high local storm depths at 24 hours. The local and tropical depths at 24 hours (and greater) should be comparable, but might differ slightly due to the different precipitation frequency climatologies used to calculate the GTFs (6 hour for local vs 24 hour for tropical).

## 11.2 Comparison of the PMP Values with Climatological Precipitation Values

The ratio of the 10-square mile 24-hour PMP to 24-hour 100-year return period precipitation amounts is generally expected to range between two and four, with values as low as 1.7 and as high as 5.5 for regions east of 117° W found in HMRs 57 and 59 (Hansen et al., 1994; Corrigan et al., 1999). Further, as stated in HMR 59 "…*the comparison indicates that larger* *ratios are in lower elevations where short-duration, convective precipitation dominates, and smaller ratios in higher elevations where general storm, long duration precipitation is prevalent*" (Corrigan et al., 1999, p. 207).

For this study, the maximum 24-hour 10-square mile PMP was compared directly to the 100-year 24-hour precipitation frequency values on a grid-by-grid basis for the entire analysis domain using a GIS. The comparison was presented as a percent of PMP and ratio of PMP to precipitation, and it was determined for each grid point. Average zonal statistics were summarized for each transposition zone. Table 11.4 provides the statistics for the comparison with 100-year 24-hour precipitation. The PMP to 100-year return period precipitation ratios vary from 3.7 to 4.6. The values are in reasonable proportion expected for the study area and demonstrate the PMP values are at conservatively high levels.

**Table 11.4: Comparison of maximum 24-hour 10-square mile PMP with 100-year 24-hour precipitation values.**

| Gridded Average by Transposition Zone | | | | |
|---|---|---|---|---|
| Transposition Zone | 24hr 10mi$^2$ PMP (inches) | 100yr 24hr Precip (inches) | 100yr 24hr Precip Percent of PMP | Ratio of PMP to 100yr 24hr Precip |
| Zone 1 | 20.67 | 4.94 | 24% | 4.2 |
| Zone 2 | 31.78 | 7.09 | 22% | 4.5 |
| Zone 3 | 41.38 | 8.98 | 22% | 4.6 |
| Zone 4 | 41.29 | 9.24 | 22% | 4.5 |
| Zone 5 | 45.86 | 12.35 | 27% | 3.7 |
| Zone 6 | 16.89 | 4.19 | 25% | 4.0 |
| Zone 7 | 23.86 | 5.68 | 24% | 4.2 |
| Zone 8 | 33.88 | 8.09 | 24% | 4.2 |
| Zone 9 | 42.01 | 10.71 | 25% | 3.9 |
| Zone 10 | 21.58 | 5.48 | 25% | 3.9 |
| Zone 11 | 24.93 | 6.17 | 25% | 4.0 |
| Zone 12 | 31.31 | 7.60 | 24% | 4.1 |

## 11.3 Annual Exceedance Probability of Short List Storms

Annual Exceedance Probabilities (AEP) were estimated for each storm's unadjusted maximum rainfall, using the precipitation frequency climatologies developed for this study and the NOAA Atlas 14 precipitation frequency climatologies. The AEPs were calculated at the 6-hour duration for local storms and 24-hour and 72-hour durations for general and tropical storms. The SPAS analyzed maximum rainfall at the storm center location was compared to the Texas precipitation frequency data or NOAA Atlas 14 precipitation values (depending on the location of the actual storm center), which were obtained from the Precipitation Frequency Data Server (PFDS) at the same location. The AEP was estimated by locating the SPAS analyzed rainfall depth on the range of precipitation values reported on the PFDS and linearly interpolating between the two bounding average recurrence intervals. The reciprocal of the return period is the AEP. The precipitation frequency estimates are available up to the 1,000-year average recurrence interval. In many cases, the return period of the analyzed storms was beyond 1,000-years. When this occurred, the AEP was expressed as < 0.10%. Table 11.5 lists the AEP for each local storm, Table 11.6 lists the AEP for each general storm, and Table 11.7 lists the AEP for each tropical storm.

**Table 11.5: Annual Exceedance Probability for local storms**

| Storm Name | SPAS ID | State | Latitude | Longitude | Date | Precip. Climatology Source | SPAS 6-hour Rainfall | SPAS 24-hour Rainfall | SPAS 72-hour Rainfall | AEP (6-hour) | AEP (24-hour) | AEP (72-hour) |
|---|---|---|---|---|---|---|---|---|---|---|---|---|
| ENID | SPAS_1034_1 | OK | 36.38 | -97.87 | Oct-1973 | NA14 v8 | 11.22 | 19.02 | 19.38 | <0.10% | <0.10% | <0.10% |
| NEW BRAUNFELS | SPAS_1180_1 | TX | 29.78 | -98.05 | Oct-1998 | Texas | 19.45 | 30.96 | 35.42 | <0.10% | <0.10% | - |
| CORRIGAN | SPAS_1185_1 | TX | 30.26 | -94.89 | Oct-1994 | Texas | 16.93 | 22.91 | 29.82 | <0.10% | <0.10% | - |
| FRIJOLE CREEK | SPAS_1247_1 | CO | 37.10 | -104.38 | Jul-1981 | NA14 v8 | 16.27 | 16.30 | 16.33 | <0.10% | <0.10% | <0.10% |
| HOLLY | SPAS_1293_1 | CO | 37.71 | -102.40 | Jun-1965 | NA14 v8 | 13.66 | 16.45 | 18.90 | <0.10% | <0.10% | <0.10% |
| HALE | SPAS_1295_3 | CO | 39.61 | -102.26 | May-1935 | NA14 v8 | 18.00 | 18.00 | 18.00 | <0.10% | <0.10% | <0.10% |
| HALLETT | SPAS_1429_2 | OK | 36.25 | -96.61 | Sep-1940 | NA14 v8 | 18.42 | 24.00 | 24.00 | <0.10% | <0.10% | <0.10% |
| MOUNDS | SPAS_1432_1 | OK | 35.85 | -96.07 | May-1943 | NA14 v8 | 16.23 | 17.34 | 18.94 | <0.10% | <0.10% | <0.10% |
| LAS CRUCES | SPAS_1485_1 | NM | 32.30 | -106.80 | Aug-1935 | NA14 v1 | 9.87 | 10.03 | 10.03 | <0.10% | <0.10% | <0.10% |
| WHITE SANDS | SPAS_1487_1 | NM | 32.39 | -106.53 | Aug-1978 | NA14 v1 | 8.84 | 10.43 | 10.43 | <0.10% | <0.10% | <0.10% |
| MOUNTAIN HOME | SPAS_1494_1 | TX | 30.17 | -99.38 | Jun-1932 | Texas | 19.89 | 33.76 | 35.56 | <0.10% | <0.10% | - |
| CHEYENNE | SPAS_1495_1 | OK | 35.62 | -99.68 | Apr-1934 | NA14 v8 | 20.09 | 23.11 | 23.11 | <0.10% | <0.10% | <0.10% |
| WOODWARD RANCH | SPAS_1496_1 | TX | 29.48 | -99.39 | May-1935 | Texas | 21.93 | 21.93 | 21.93 | <0.10% | <0.10% | - |
| EL PASO | SPAS_1528_1 | TX | 31.94 | -106.52 | Aug-2006 | Texas | 6.83 | 10.25 | 10.25 | <0.10% | <0.10% | - |
| GAIL | SPAS_1557_1 | TX | 32.73 | -101.41 | Sep-2014 | Texas | 13.07 | 13.96 | 13.96 | <0.10% | <0.10% | - |
| ROCK SPRINGS | SPAS_1558_1 | TX | 29.91 | -100.00 | Sep-1955 | Texas | 14.65 | 24.05 | 24.09 | <0.10% | <0.10% | - |
| CONWAY | SPAS_1560_1 | TX | 35.22 | -101.40 | May-1951 | Texas | 8.23 | 12.23 | 15.21 | <0.10% | <0.10% | - |
| CARLSBAD | SPAS_1568_1 | NM | 32.25 | -104.61 | Aug-1966 | Texas | 7.52 | 13.35 | 17.33 | <0.10% | <0.10% | <0.10% |
| TAHOKA | SPAS_1588_1 | TX | 33.11 | -101.83 | May-2015 | Texas | 9.16 | 10.51 | 10.51 | <0.10% | <0.10% | - |
| ABILENE | SPAS_1589_1 | TX | 31.44 | -99.12 | Jul-2015 | Texas | 9.61 | 10.91 | 10.91 | <0.10% | 0.23% | - |
| DAWSON | SPAS_1590_1 | TX | 31.90 | -96.65 | Oct-2015 | Texas | 18.67 | 28.05 | 32.92 | <0.10% | <0.10% | - |
| THRALL | SPAS_1592_1 | TX | 30.63 | -97.39 | Sep-1921 | Texas | 23.50 | 38.36 | 39.90 | <0.10% | <0.10% | - |
| HELOTES | SPAS_1594_1 | TX | 29.86 | -98.89 | Jun-2002 | Texas | 9.55 | 17.52 | 29.41 | 0.32% | <0.10% | - |
| SPEARMAN | SPAS_1595_1 | TX | 36.14 | -101.50 | Jun-2010 | Texas | 8.13 | 13.89 | 13.89 | <0.10% | <0.10% | - |
| VIC PIERCE | SPAS_1602_1 | TX | 30.40 | -101.44 | Jun-1954 | Texas | 17.47 | 27.69 | 35.79 | <0.10% | <0.10% | - |

**Table 11.6: Annual Exceedance Probability for general storms**

| Storm Name | SPAS ID | State | Latitude | Longitude | Date | Precip. Climatology Source | SPAS 6-hour Rainfall | SPAS 24-hour Rainfall | SPAS 72-hour Rainfall | AEP (6-hour) | AEP (24-hour) | AEP (72-hour) |
|---|---|---|---|---|---|---|---|---|---|---|---|---|
| GLADEWATER | SPAS_1181_1 | TX | 32.80 | -94.71 | Apr-1966 | Texas | 9.17 | 14.53 | 21.04 | 0.21% | 0.21% | - |
| WARNER PARK | SPAS_1208_1 | TN | 36.06 | -86.91 | May-2010 | NA14 v2 | 15.31 | 18.39 | 19.71 | <0.10% | <0.10% | <0.10% |
| DOUGLASVILLE | SPAS_1218_1 | GA | 33.87 | -84.76 | Sep-2009 | NA14 v9 | 17.36 | 22.82 | 25.37 | <0.10% | <0.10% | <0.10% |
| BIG FORK | SPAS_1219_1 | AR | 35.87 | -92.12 | Dec-1982 | NA14 v9 | 6.75 | 14.58 | 15.92 | 0.50% | <0.10% | <0.10% |
| LOUISVILLE | SPAS_1227_1 | MS | 33.12 | -89.05 | Apr-1979 | NA14 v9 | 9.32 | 20.06 | 22.07 | 0.11% | <0.10% | <0.10% |
| FALL RIVER | SPAS_1228_1 | KS | 37.63 | -96.05 | Jun-2007 | NA14 v8 | 9.12 | 14.91 | 25.43 | 0.23% | <0.10% | <0.10% |
| ALLEY SPRING | SPAS_1242_1 | MO | 37.16 | -91.45 | Mar-2008 | NA14 v8 | 6.18 | 13.32 | 15.09 | 0.20% | <0.10% | <0.10% |
| LOUISVILLE | SPAS_1244_1 | KY | 38.10 | -85.67 | Feb-1997 | NA14 v2 | 5.42 | 10.94 | 13.51 | 0.49% | <0.10% | <0.10% |
| LAKE MALOYA | SPAS_1251_1 | NM | 37.01 | -104.34 | May-1955 | NA14 v1 | 3.98 | 11.90 | 14.82 | 1.08% | <0.10% | <0.10% |
| GILBERTSVILLE | SPAS_1277_1 | KY | 37.00 | -88.26 | Feb-1989 | NA14 v2 | 5.14 | 9.41 | 13.06 | 1.19% | 0.33% | 0.12% |
| MADISONVILLE | SPAS_1278_1 | KY | 37.35 | -87.50 | Mar-1964 | NA14 v2 | 3.90 | 8.71 | 11.59 | 4.66% | 0.51% | 0.40% |
| MCKENZIE | SPAS_1311_1 | TN | 36.44 | -87.91 | Jan-1937 | NA14 v2 | 4.04 | 6.33 | 12.94 | 4.58% | 3.57% | 0.15% |
| GLEN | SPAS_1357_1 | MS | 34.84 | -88.40 | Mar-1973 | NA14 v9 | 4.78 | 10.36 | 12.15 | 3.78% | 0.47% | 0.71% |
| FAIRFIELD | SPAS_1428_1 | TX | 31.68 | -96.13 | Sep-1932 | Texas | 10.04 | 18.58 | 19.58 | 0.12% | <0.10% | - |
| HEMPSTEAD | SPAS_1430_1 | TX | 30.13 | -96.05 | Nov-1940 | Texas | 8.85 | 18.88 | 21.29 | 0.49% | <0.10% | - |
| WARNER | SPAS_1431_1 | OK | 35.48 | -95.33 | May-1943 | NA14 v8 | 10.09 | 17.77 | 25.24 | <0.10% | <0.10% | <0.10% |
| HARRISONBURG DAM | SPAS_1435_1 | LA | 31.79 | -91.82 | May-1953 | NA14 v9 | 9.43 | 18.02 | 20.46 | 0.93% | 0.14% | 0.19% |
| MCCOLLEUM RANCH | SPAS_1486_1 | NM | 32.15 | -104.75 | Sep-1941 | Texas | 10.88 | 12.07 | 21.81 | <0.10% | <0.10% | <0.10% |
| GUADALUPE PASS | SPAS_1530_1 | TX | 32.04 | -104.56 | Sep-2013 | Texas | 8.14 | 17.47 | 20.09 | <0.10% | <0.10% | <0.10% |
| SUMNER LAKE | SPAS_1530_2 | NM | 34.60 | -104.48 | Sep-2013 | NA14 v1 | 2.98 | 5.28 | 8.28 | 4.84% | 0.87% | 0.19% |
| CHAPARRAL | SPAS_1530_4 | NM | 32.15 | -106.00 | Sep-2013 | Texas | 4.05 | 6.50 | 9.61 | 0.27% | <0.10% | <0.10% |
| CONWAY | SPAS_1560_1 | TX | 35.22 | -101.40 | May-1951 | Texas | 8.23 | 12.23 | 15.21 | <0.10% | <0.10% | - |
| CARLSBAD | SPAS_1568_1 | NM | 32.25 | -104.61 | Aug-1966 | Texas | 7.52 | 13.35 | 17.33 | <0.10% | <0.10% | <0.10% |
| COUNCIL GROVE | SPAS_1583_1 | KS | 38.65 | -96.62 | Jul-1951 | NA14 v8 | 5.11 | 9.35 | 18.56 | 2.84% | 0.29% | <0.10% |
| PRAIRIEVIEW | SPAS_1587_1 | NM | 33.14 | -103.08 | May-1941 | Texas | 3.86 | 6.01 | 10.57 | 4.24% | 1.32% | 0.19% |
| HEARNE | SPAS_1591_1 | TX | 30.84 | -96.57 | 6/1899 | Texas | 7.20 | 24.15 | 34.44 | 1.15% | <0.10% | - |
| HELOTES | SPAS_1594_1 | TX | 29.86 | -98.89 | Jun-2002 | Texas | 9.55 | 17.52 | 29.41 | 0.32% | <0.10% | - |
| SILVERHILL | SPAS_1597_1 | AL | 30.38 | -87.59 | Apr-2014 | NA14 v9 | 15.52 | 24.34 | 25.42 | <0.10% | 0.38% | 0.32% |

**Table 11.7: Annual Exceedance Probability for tropical storms**

| Storm Name | SPAS ID | State | Latitude | Longitude | Date | Precip. Climatology Source | SPAS 6-hour Rainfall | SPAS 24-hour Rainfall | SPAS 72-hour Rainfall | AEP (6-hour) | AEP (24-hour) | AEP (72-hour) |
|---|---|---|---|---|---|---|---|---|---|---|---|---|
| ALBANY | SPAS_1179_1 | TX | 32.73 | -99.35 | Aug-1978 | Texas | 21.94 | 30.54 | 32.50 | <0.10% | <0.10% | - |
| ALVIN | SPAS_1463_1 | TX | 29.43 | -95.27 | Jul-1979 | Texas | 20.52 | 43.08 | 45.48 | <0.10% | <0.10% | - |
| AMERICUS | SPAS_1317_1 | GA | 32.10 | -84.23 | Jul-1994 | NA14 v9 | 12.76 | 21.20 | 27.53 | <0.10% | <0.10% | <0.10% |
| BROOME | SPAS_1582_1 | TX | 31.79 | -100.85 | Sep-1936 | Texas | 13.79 | 27.18 | 30.34 | <0.10% | <0.10% | - |
| CLYDE | SPAS_1184_1 | TX | 32.48 | -99.48 | Oct-1981 | Texas | 10.44 | 18.64 | 23.00 | <0.10% | <0.10% | - |
| DAUPHIN ISLAND | SPAS_1569_1 | AL | 30.32 | -88.04 | Jul-1997 | NA14 v9 | 20.75 | 37.07 | 45.27 | <0.10% | <0.10% | <0.10% |
| DINERO | SPAS_1601_2 | MX | 28.25 | -97.90 | Sep-1967 | Texas | 13.80 | 19.36 | 34.30 | <0.10% | <0.10% | - |
| ESTANZUELA-COAHUILA | SPAS_1598_1 | MX | 25.60 | -100.20 | Jun-2010 | Texas | 7.95 | 17.99 | 35.47 | 0.13% | <0.10% | - |
| GONZALEZ | SPAS_1599_1 | MX | 22.76 | -98.61 | Oct-2000 | 24hr Mini-Analysi | 11.76 | 21.36 | 24.83 | - | <0.10% | - |
| HOUSTON | SPAS_1464_1 | TX | 29.76 | -95.28 | Jun-2001 | Texas | 20.98 | 29.41 | 29.89 | <0.10% | <0.10% | - |
| LARTO LAKE | SPAS_1182_1 | LA | 31.22 | -92.13 | Sep-2008 | NA14 v9 | 11.34 | 16.55 | 23.31 | 0.27% | 0.40% | 0.18% |
| MEDINA | SPAS_1600_1 | TX | 29.89 | -99.32 | Aug-1978 | Texas | 20.90 | 31.00 | 48.97 | <0.10% | <0.10% | - |
| MILLER ISLAND | SPAS_1596_1 | LA | 29.85 | -92.25 | Aug-1940 | NA14 v9 | 8.26 | 23.24 | 37.85 | 1.91% | <0.10% | <0.10% |
| MUNSON | SPAS_1593_1 | FL | 30.86 | -87.73 | Sep-1998 | NA14 v9 | 10.27 | 20.69 | 24.92 | 0.63% | 0.22% | 0.29% |
| NEW BRAUNFELS | SPAS_1180_1 | TX | 29.78 | -98.05 | Oct-1998 | Texas | 19.45 | 30.96 | 35.42 | <0.10% | <0.10% | - |
| ROOSEVELT | SPAS_1582_2 | TX | 30.45 | -100.04 | Sep-1936 | Texas | 15.06 | 23.33 | 30.13 | <0.10% | <0.10% | - |
| SOMBRERETILLO | SPAS_1601_1 | MX | 26.28 | -99.92 | Sep-1967 | Texas | 7.97 | 16.54 | 30.38 | 0.31% | <0.10% | - |
| SUNSPOT | SPAS_1529_1 | NM | 33.34 | -105.80 | Jul-2008 | NA14 v1 | 4.08 | 7.16 | 8.81 | 1.30% | <0.10% | 0.10% |
| THE BOWL | SPAS_1531_1 | TX | 31.94 | -104.83 | Sep-2014 | Texas | 5.24 | 9.00 | 10.83 | 1.07% | 0.35% | - |
| THRALL | SPAS_1592_1 | TX | 30.63 | -97.39 | Sep-1921 | Texas | 23.50 | 38.36 | 39.90 | <0.10% | <0.10% | - |
| VIC PIERCE | SPAS_1602_1 | TX | 30.40 | -101.44 | Jun-1954 | Texas | 17.47 | 27.69 | 35.79 | <0.10% | <0.10% | - |

## 11.4 Comparison of the PMP Values with HMR PMP Values

This study employs a variety of improved methods when compared to previous HMR studies. These methods include: a far more robust storm analysis system with a higher temporal and spatial resolution; improved dew point/SST and precipitation climatologies that provide an increased ability to maximize and transpose storms; gridded PMP calculations which result in higher spatial and temporal resolutions; and a greatly expanded storm record. Because of the number and degree of changes from these past studies, there is limited usefulness in making direct PMP comparisons. Unfortunately, working papers and notes from the HMRs are not available in most cases. Therefore, direct PMP comparisons between the HMRs and the values from this study are somewhat limited. Furthermore, due to the generalization of the regionally-based HMR studies, comparisons to the detailed gridded PMP of this study can vary greatly over short distances. However, comparisons were made for sensitivity purposes where data allowed. The PMP values in this study resulted in a wide range of both reductions and increases as compared to the HMRs.

Comparisons were made using the largest PMP-depth from all three storm types by zonal average for all regions covered by HMR 51, at all HMR 51 standard area sizes and durations. For the region covered by HMR 55A, comparisons were made at 17 grid points for the durations available in HMR 55A. Figure 11.11 shows the coverage of the HMRs in relation to the overall project domain, and Figure 11.12 provides the locations of the 17 grids points used for comparisons to HMR 55A. Table 11.8 provides the results of the comparisons against HMR 51. Table 11.9 provides the results of the comparisons against the HMR 55A values.

Overall, in the region covered by HMR 51, there is an 11% reduction in PMP values. However, there is a large range of both positive and negative differences from HMR 51. In general, the largest reductions are in the westernmost zones and at relatively higher elevations. This makes sense given that this is also the transition area between HMR 51 and HMR 55A, where the authors of HMR 51 pointed out they had very little confidence in those values. In addition, the reductions are similar to the magnitude seen at the 17 grid points used for comparison against HMR 55A. In the regions where there were increases compared to HMR 51 values, the increases were most common at larger area sizes (e.g., greater than 5,000 $mi^2$) or at longer durations (e.g., 48- and 72-hours). This is most likely reflective of two factors; the inclusion of several significant extreme rainfall events that are important for large area sizes and long durations that were not included in HMR 51 (e.g., Alvin 1979, Allison 2001, Alley Spring 2008, and Warner Park 2010), and a more accurate representation of the Hearne, TX June, 1899 storm. Note that the authors of HMR 51 chose to undercut the Hearne storm by 2% in-place (see HMR 51 Table 4). AWA did not undercut any storm data that was considered valid, including this storm.

For the PMP in the region covered by HMR 55A, values appear to be far too high compared to maximized storm data. This is most likely the result of a lack of storm data and the highly subjective process used to quantify the effects of topography (the HMR 55A Storm Separation Method or SSM). Similar findings of significant reductions from HMR 55A have been realized in other AWA studies (e.g., Kappel et al., 2014). In this region, the GTF process more accurately accounts for the lack of moisture available to storms, where topography has a significant influence on low-level moisture access. In these situations, the HMR 55A SSM process does not allow for values less than 1 and therefore, does not properly represent a physically possible storm in these regions where terrain affects would decrease rainfall.

Finally, note that there were limited PMP-type storms in zone 2, and the meteorological and topographic conditions for heavy rain in zone 2 are not similar to most locations in the United States. Further, there is no previous HMR PMP data in that region to provide explicit comparisons. The sensitivities provided using the precipitation frequency climatologies do demonstrate that the PMP values are in the expected range, similar to other transposition zones. However, given the lack of PMP analysis for zone 2, the PMP values in this region should be considered uncertain and treated as such.

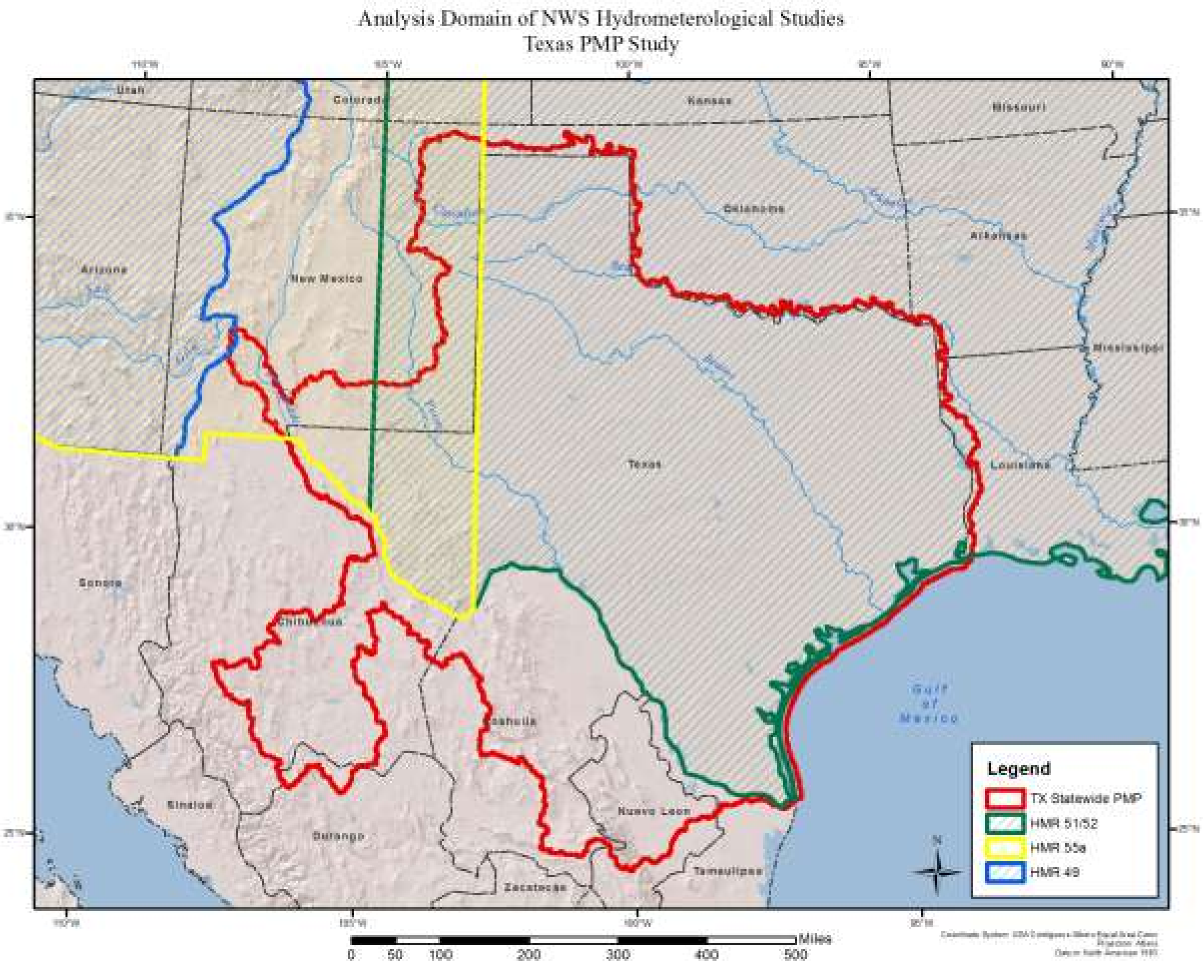


**Figure 11.11: HMR coverage over the overall project domain**

Control Point Locations for Comparison to HMR 55A 10 $mi^2$ Index PMP

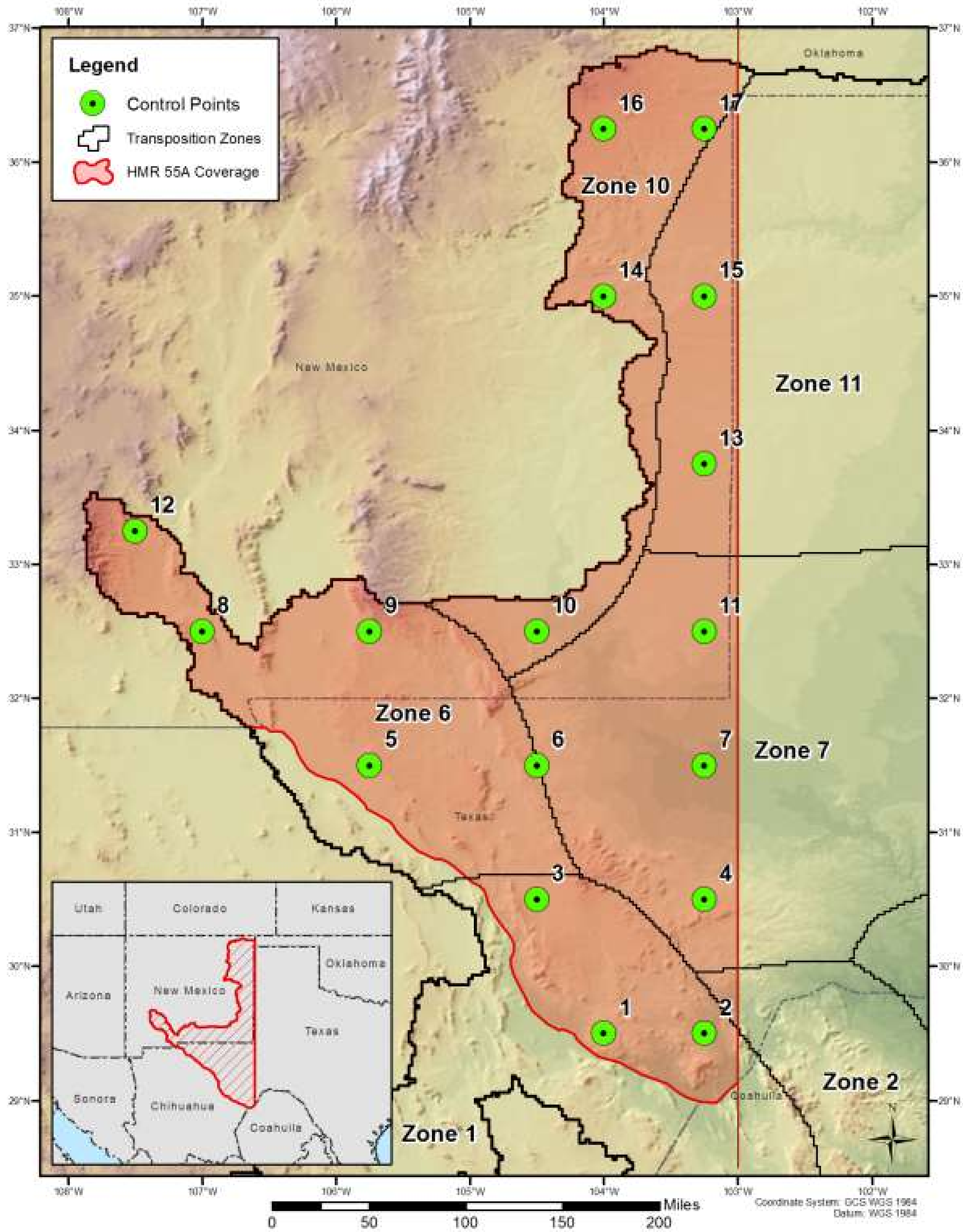


Figure 11.12: Grid point locations used for HMR 55A comparisons

**Table 11.8: Comparisons of PMP values versus HMR 51 at standard area sizes and durations. Values represent zonal average. Refer to Figure 8.1 for transposition zone locations.**

| Average PMP Percent Change from HMR 51 (by transposition zone) | | | | | | | | | | |
|---|---|---|---|---|---|---|---|---|---|---|
| Duration | Area | Zone 3 | Zone 4 | Zone 5 | Zone 7 | Zone 8 | Zone 9 | Zone 10 | Zone 11 | Zone 12 |
| 6-hour | 10-sqmi | -18% | -10% | -11% | -31% | -16% | -15% | -28% | -28% | -20% |
| 6-hour | 200-sqmi | -14% | -8% | -3% | -30% | -15% | -11% | -31% | -27% | -19% |
| 6-hour | 1,000-sqmi | -13% | -7% | -11% | -35% | -20% | -12% | -37% | -33% | -23% |
| 6-hour | 5,000-sqmi | -10% | -5% | 3% | -39% | -15% | -2% | -51% | -47% | -20% |
| 6-hour | 10,000-sqmi | -18% | -14% | -3% | -40% | -23% | -7% | -47% | -42% | -27% |
| 6-hour | 20,000-sqmi | -19% | -11% | -7% | -38% | -25% | -9% | -49% | -38% | -30% |
| 12-hour | 10-sqmi | -9% | -4% | -3% | -34% | -18% | -7% | -37% | -33% | -21% |
| 12-hour | 200-sqmi | -9% | -2% | -5% | -26% | -10% | -5% | -29% | -24% | -11% |
| 12-hour | 1,000-sqmi | -18% | -10% | -10% | -25% | -14% | -8% | -25% | -21% | -13% |
| 12-hour | 5,000-sqmi | -4% | 0% | 9% | -29% | -12% | 9% | -41% | -34% | -16% |
| 12-hour | 10,000-sqmi | -4% | 2% | 11% | -35% | -10% | 11% | -44% | -37% | -16% |
| 12-hour | 20,000-sqmi | -7% | 0% | 7% | -28% | -11% | 5% | -43% | -33% | -15% |
| 24-hour | 10-sqmi | -9% | -3% | -4% | -33% | -15% | -4% | -33% | -27% | -15% |
| 24-hour | 200-sqmi | -10% | -2% | -8% | -18% | -2% | -4% | -15% | -10% | 2% |
| 24-hour | 1,000-sqmi | -10% | -3% | -16% | -10% | 4% | -7% | -3% | 2% | 13% |
| 24-hour | 5,000-sqmi | -13% | -3% | -2% | -17% | -7% | 2% | -12% | -8% | -1% |
| 24-hour | 10,000-sqmi | -4% | 8% | 8% | -17% | 2% | 12% | -29% | -20% | 3% |
| 24-hour | 20,000-sqmi | 7% | 18% | 21% | -9% | 11% | 21% | -36% | -14% | 12% |
| 48-hour | 10-sqmi | -8% | -5% | -9% | -23% | -5% | -8% | -22% | -16% | -3% |
| 48-hour | 200-sqmi | 4% | 10% | -4% | -5% | 15% | 6% | -3% | 4% | 19% |
| 48-hour | 1,000-sqmi | -1% | 6% | -4% | -2% | 13% | 2% | 1% | 8% | 21% |
| 48-hour | 5,000-sqmi | -12% | -5% | 4% | -15% | -4% | 4% | -10% | -7% | 1% |
| 48-hour | 10,000-sqmi | -9% | 1% | 4% | -22% | -5% | 7% | -21% | -19% | -6% |
| 48-hour | 20,000-sqmi | -2% | 8% | 12% | -16% | 2% | 14% | -30% | -18% | 1% |
| 72-hour | 10-sqmi | -14% | -9% | -15% | -25% | -10% | -13% | -25% | -19% | -8% |
| 72-hour | 200-sqmi | -6% | 0% | -9% | -10% | 5% | -3% | -6% | -1% | 12% |
| 72-hour | 1,000-sqmi | -10% | -4% | -1% | -10% | 2% | 0% | -4% | 1% | 11% |
| 72-hour | 10,000-sqmi | -20% | -8% | 4% | -22% | -9% | 3% | -18% | -14% | -6% |
| 72-hour | 10,000-sqmi | -23% | -11% | -1% | -27% | -11% | -1% | -29% | -25% | -9% |
| 72-hour | 20,000-sqmi | -20% | -10% | -4% | -25% | -13% | -4% | -34% | -23% | -12% |

**Table 11.9: Comparisons of PMP values versus the HMR 55A. Refer to Figure 11.11 for grid point locations.**

| Percent Change from HMR 55A PMP | | | | | | | |
|---|---|---|---|---|---|---|---|
| Point | Latitude | Longitude | Zone | 1-hour 1-mi² | 6-hour 10-mi² | 24-hour 10-mi² | 72-hour 10-mi² |
| 1 | 29.50° | -104.00° | 1 | -54.2% | -41.0% | -44.1% | -38.0% |
| 2 | 29.50° | -103.25° | 1 | -53.0% | -38.6% | -40.1% | -33.8% |
| 3 | 30.50° | -104.50° | 1 | -54.9% | -41.4% | -40.9% | -35.0% |
| 4 | 30.50° | -103.25° | 7 | -51.2% | -31.1% | -33.1% | -26.3% |
| 5 | 31.50° | -105.75° | 6 | -42.6% | -20.0% | -17.1% | -8.9% |
| 6 | 31.50° | -104.50° | 6 | -53.3% | -38.9% | -36.9% | -30.3% |
| 7 | 31.50° | -103.25° | 7 | -65.3% | -44.4% | -46.0% | -37.8% |
| 8 | 32.50° | -107.00° | 6 | -38.9% | -25.0% | -28.2% | -22.1% |
| 9 | 32.50° | -105.75° | 6 | -51.7% | -31.1% | -27.9% | -21.3% |
| 10 | 32.50° | -104.50° | 10 | -53.9% | -38.6% | -34.6% | -27.4% |
| 11 | 32.50° | -103.25° | 7 | -51.9% | -21.4% | -19.7% | -10.8% |
| 12 | 33.25° | -107.50° | 6 | -38.2% | -25.7% | -29.8% | -24.3% |
| 13 | 33.75° | -103.25° | 11 | -52.3% | -37.1% | -31.0% | -22.6% |
| 14 | 35.00° | -104.00° | 10 | -52.8% | -27.5% | -35.1% | -26.7% |
| 15 | 35.00° | -103.25° | 11 | -53.8% | -39.0% | -34.7% | -24.7% |
| 16 | 36.25° | -104.00° | 10 | -45.1% | -33.9% | -38.7% | -31.2% |
| 17 | 36.25° | -103.25° | 10 | -33.1% | -22.0% | -30.4% | -21.6% |

# 12. Sensitivity Discussions Related to PMP Derivations

In the process of deriving PMP values, various assumptions and meteorological judgments were made. Additionally, various parameters and derived values were used in the calculations which are standard to the PMP development process. It is of interest to assess the sensitivity of PMP values to assumptions that were made and to the variability of parameter values.

## 12.1 Assumptions

### 12.1.1 Saturated Storm Atmosphere

The atmospheric air masses that provide available moisture to both the historic storm and the PMP storm are assumed to be saturated through the entire depth of the atmosphere and to contain the maximum moisture possible based on the surface dew point. This assumes moist pseudo-adiabatic temperature profiles for both the historic storm and the PMP storm. Limited evaluation of this assumption in the EPRI Michigan/Wisconsin PMP study (Tomlinson, 1993) and the Blenheim Gilboa study (Tomlinson et al., 2008) indicated that historic storm atmospheric profiles are generally not entirely saturated and contain somewhat less precipitable water than is assumed in the PMP procedure. It follows that the PMP storm (if it were to occur) would also have somewhat less precipitable water available than the assumed saturated PMP atmosphere would contain. The *ratio* of precipitable water associated with each storm is used in the PMP calculation procedure. If the precipitable water values for each storm are both slightly overestimated, the ratio of these values will be essentially unchanged. For example, consider the case where instead of a historic storm with a storm representative dew point of 70°F having 2.25 inches of precipitable water and assuming a saturated atmosphere, it actually had 90% of that value or about 2.02 inches. The PMP procedure assumes the same type of storm with similar atmospheric characteristics for the maximized storm but with a higher dew point, say 76°F. The maximized storm, having similar atmospheric conditions, would have about 2.69 inches of precipitable water instead of the 2.99 inches associated with a saturated atmosphere with a dew point of 76°F. The maximization factor computed, using the assumed saturated atmospheric values, would be 2.99/2.25 = 1.33. If both storms were about 90% saturated, the maximization factor would be 2.69/2.02 = 1.33. Therefore, any potential inaccuracy of assuming saturated atmospheres (whereas the atmospheres may be somewhat less than saturated) should have a minimal impact on storm maximization and subsequent PMP calculations.

### 12.1.2 Maximum Storm Efficiency

The assumption is made that if a sufficient period of record is available for rainfall observations, at least a few storms would have been observed that attained or came close to attaining the maximum efficiency possible in nature for converting atmospheric moisture to rainfall for regions with similar climates and topography. The further assumption is made that if additional atmospheric moisture had been available, the storm would have maintained the same efficiency for converting atmospheric moisture to rainfall. The ratio of the maximized rainfall amounts to actual rainfall amounts would be the same as the ratio of precipitable water in the atmosphere associated with each storm.

There are two issues to be considered. First relates to the assumption that a storm has a rainfall efficiency close to the maximum possible. Unfortunately, state-of-the-science in meteorology does not support a theoretical evaluation of storm efficiency. However, if the period of record is considered (generally over 100 years), along with the extended geographic region with transpositionable storms, it is accepted that there should have been at least one storm with dynamics that approached the maximum efficiency for rainfall production.

The other issue pertains to the assumption that storm efficiency does not change if additional atmospheric moisture is available. Storm dynamics could potentially become more efficient or possibly less efficient depending on the interaction of cloud microphysical processes with the storm dynamics. Offsetting effects could indeed lead to the storm efficiency remaining essentially unchanged. For the present, the assumption of no change in storm efficiency seems acceptable.

## 12.2 Parameters

### 12.2.1 Storm Representative Dew Point and Maximum Dew Point

The maximization factor depends on the determination of storm representative dew points, along with maximum historical dew point values. The magnitude of the maximization factor varies depending on the values used for the storm representative dew point and the maximum dew point. Holding all other variables constant, the maximization factor is smaller for higher storm representative dew points as well as for lower maximum dew point values. Likewise, larger maximization factors result from the use of lower storm representative dew points and/or higher maximum dew points. The magnitude of the change in the maximization factor varies depending on the dew point values. For the range of dew point values used in most PMP studies, the maximization factor for a particular storm will change about 5% for every 1°F difference between the storm representative and maximum dew point values. The same sensitivity applies to the transposition factor, with about a 5% change for every 1°F change in either the in-place maximum dew point or the transposition maximum dew point.

For example, consider the following case:

| | | | |
|---|---|---|---|
| Storm representative dew point: | 75°F | Precipitable water: | 2.85" |
| Maximum dew point: | 79°F | Precipitable water: | 3.44" |

Maximization factor = 3.44"/2.85" = 1.21

If the storm's representative dew point was 74°F with precipitable water of 2.73",
Maximization factor = 3.44"/2.73" = 1.26 (an increase of approximately 5%)

If the maximum dew point was 78°F with precipitable water of 3.29",
Maximization factor = 3.29"/2.85" = 1.15 (a decrease of approximately 5%)

### 12.2.2 Sensitivity of the Elevation Adjustment Factor to Changes in Storm Elevation

Elevated topographic features remove atmospheric moisture from an air mass as it moves over the terrain. When storms are transpositioned, the elevation of the original storm is used in this study to compute the amount of atmospheric moisture depleted from or added to the storm atmosphere. The absolute amount of moisture depletion or addition is somewhat dependent on the dew point values, but it is primarily dependent on the elevation at the original storm location and the elevation of the study basin. The elevation adjustment is slightly less than 1% for every 100 feet of elevation change between the original storm location and the study basin elevation.

For example, consider the following case:

| | |
|---|---|
| Maximum dew point: | 79$^{o}$F |
| Study basin elevation: | 100 feet |
| Historic storm location elevation: | 500 feet |
| Precipitable water between 1000mb and the top of the atmosphere: | 3.44 inches |
| Precipitable water between 1000mb and 100': | 0.03 inches |
| Precipitable water between 1000mb and 500': | 0.15 inches |

Elevation Adjustment Factor = (3.44"-0.03")/(3.44"-0.15") = 1.04 (about 1% per 100 feet)

If the historic storm location elevation were 1,000', the precipitable water between 1000mb and 1,000' is 0.28"
Elevation Adjustment Factor = (3.44"-0.03")/(3.44"-0.28") = 1.08 (about 1% per 100 feet)

# 13. Recommendations for Application

## 13.1 PMP Applications

The PMP values in this study quantify rainfall amounts for use in computing the Probable Maximum Flood (PMF). This study addressed several issues that could potentially affect the magnitude of the PMP storm over any drainage basin within the project domain covering the state of Texas and immediate surrounding regions. It is important to remember that the methods used to derive PMP, and subsequently the methods used to derive the PMF from those data, adhere to the caveat of being "physically possible" as described in the definition of PMP (see Section 1.1). In other words, various levels of conservatism and/or extreme aspects of storms that would not occur/co-occur in a PMP storm environment should not be compounded together to generate unrealistic results in either the PMP values or the hydrologic applications of those values to derive the PMF.

The storm search process and selection of storms analyzed in this study only considered events that occurred over areas that are both meteorologically and topographically similar to locations within the overall project domain. Each storm type (local, tropical, and general) that occurs in the overall project domain was analyzed. Therefore, results of this study should not be used for watersheds where meteorological and/or topographical parameters are different from those found within the project domain without further evaluation.

## 13.2 Future Work Requirements

Although this study was comprehensive in its development and calculation of PMP values, several related areas deserve further analysis and interpretation.

Temporal distributions can be thought of as the time order in which incremental PMP amounts are arranged within a PMP storm. Initial analysis of the temporal accumulations of the PMP rainfall began during this work. This is an important aspect for properly determining the PMF where PMP values are distributed over time and the total analysis duration in question. Analysis should continue using the storm data derived in this study to determine whether any adjustments to current guidelines are warranted. This could potentially be by storm type and storm location. The underlying principal would be that the guidelines would be storm-based using the storms in this study and, therefore, most accurately represent temporal distributions expected to occur with Texas PMP-type storms.

The field of paleohydrology can provide a valuable dataset of past flood peak and information on flood hydrology that can be used to bound PMP or as a sensitivity of PMP. Investigations should be undertaken to derive paleoflood data in as many regions of Texas as possible. This data would help support and put in context the PMP values derived in this study and supply an independent dataset which could be used in assessing the PMP values and expanding the historical storm record especially in high elevation and data-sparse regions.

Finally, increasing the number of meteorological and hydrological observation locations across the project domain is critical to capturing the rainfall and flood events that will occur in the future. This is especially relevant in the western portions of Texas, southern New Mexico, and Mexico where there is currently a lack of observation data points. These data are the foundation for being able to assess storms and floods in relation to PMP and to update and add to the database developed during this work.

# References


Ahrens, C.D., 2007: *Meteorology Today-An Introduction to Weather, Climate, and the Environment*. Thomson Brooks/Cole, Belmont, CA, 537 pp.

Al-Asaadi, Rawaa, 2002, Hyetograph estimation for the State of Texas: Lubbock, Texas, Texas Tech University, M.S. thesis, 96 p.

Asquith, W.H., and R.M. Slade, 1995: Documented and Potential Extreme Peak Discharges and Relation Between Potential Extreme Peak Discharges and Probable Maximum Flood Peak Discharges in Texas, U.S. Geological Survey Water Resources Investigations Report 95-4249, 63 pp.

Asquith, W.H., 1998, Depth-duration frequency of precipitation for Texas: U.S. Geological Survey Water-Resources Investigations Report 98–4044, 107 p.

Asquith, W.H., 1999: Areal-reduction Factors for the Precipitation of the 1-Day Design Storm in Texas, U.S. Geological Survey Water Resources Investigations Report 99-4267, 83 pp.

Asquith, W.H., 2003: Modeling of runoff-producing rainfall hyetographs in Texas using L-moments statistics: Austin, Texas, the University of Texas at Austin, Ph.D dissertation, 386 pp.

Asquith, W.H., Bumgarner, J.R., and Fahlquist, L.S., 2003: A triangular model of dimensionless runoff-producing rainfall hyetographs in Texas: Journal American Water Resources Association, v. 39, no. 4, p. 911-921.

Asquith, W.H., and Thompson, D.B, 2003: Modeling of runoff-producing rainfall hyetographs in Texas using L-moments: Texas Section, Spring Meeting, American Society of Civil Engineers, Corpus Christi, TX.

Asquith, W.H., Thompson, D.B., Cleveland, T.G., and Fang, Xing, 2004: Synthesis of rainfall and runoff data used for Texas Department of Transposition Research Projects 0-4193 and 0-4194: U.S. Geological Survey Open-File Report 2004-1035, 1,050 pp.

Asquith, W.H., and M.C., Roussel, 2004: Atlas of Depth-Duration Frequency of Precipitation Annual Maxima for Texas, U.S. Geological Survey Scientific Investigations Report 2004-5041, 106 pp.

Baker, V.R., 1975: Flood hazards along the Balcones Escarpment in central Texas, alternative approaches to their recognition, mapping, and management. Tex. Bur. Econ. Geol. Circ. 75-5, 22 pp.

Bomar, G.W., 1995: *Texas Weather*, University of Texas Press, Austin, TX, 275 pp.

Bonnin, G., D. Martin, B. Lin, T. Parzybok, M. Yekta, and D. Riley, 2004: NOAA *Atlas 14 Volume 1, Precipitation-Frequency Atlas of the United States, Semiarid Southwest*. NOAA, National Weather Service, Silver Spring, MD.

Bonnin, G., D. Martin, B. Lin, T. Parzybok, M. Yekta, and D. Riley, 2004: NOAA *Atlas 14 Volume 2, Precipitation-Frequency Atlas of the United States, Delaware, District of Columbia, Illinois, Indiana, Kentucky, Maryland, New Jersey, North Carolina, Ohio, Pennsylvania, South Carolina, Tennessee, Virginia, West Virginia.* NOAA, National Weather Service, Silver Spring, MD.

Bosart, L.F., 1984: The Texas Coastal Rainstorm of 17-21 September 1979: An Example of Synoptic-Mesoscale Interaction, *Monthly Weather Review*, Vol. 112, 1108-1133.

Burnett, J., 2008: *Flash Floods in Texas*, Texas A&M University Press, College Station, TX, 330 pp.

Caracena, F., and J. M. Fritsch, 1983: Focusing Mechanisms in the Texas Hill Country Flash FIOMS of 1978. *Mon. Wea. Rev.*, **111**, 2319–2332.

Carr, J.A., 1951: The Rains over Arizona, August 26–29, 1951. *Mon. Wea. Rev.*, **79**, 163.

Clayton, P., B. Cox, E. Rathje, A. Keene, J.R. Phillips, and C. Woodruff, 2015: The Geotechnical Aspects of the Central Texas Floods of May 23-25, 2015, GEER Association Report No. GEER-039, Ver. 1, 20 pp.

Corps of Engineers, U.S. Army, 1945-1973: Storm Rainfall in the United States, Depth-Area-Duration Data. Office of Chief of Engineers, Washington, D.C.

Corrigan, P., D.D. Fenn, D.R. Kluck, and J.L. Vogel, 1999: Probable Maximum Precipitation for California, *Hydrometeorological Report Number 59*, National Weather Service, National Oceanic and Atmospheric Administration, U. S. Department of Commerce, Silver Spring, Md, 392 pp.

Costa, J.E., and R.D. Jarrett, 2008: An Evaluation of Selected Extraordinary Floods in the United States Reported by the U.S. Geological Survey and Implications for Future Advancement of Flood Science, http://pubs.er.usgs.gov/usgspubs/sir/sir20085164/.

Dalrymple, T., and others, 1937: Major Texas Floods of 1936, U.S. Geological Survey Water Supply Paper 816, 146 pp.

Dalrymple, T., and others, 1939: Major Texas Floods of 1935, U.S. Geological Survey Water Supply Paper 796-G, 223-290.

Daly, C., R.P. Neilson, and D.L. Phillips, 1994: A Statistical-Topographic Model for Mapping Climatological Precipitation over Mountainous Terrain. *J. Appl. Meteor.*, **33**, 140–158.

Draxler, R.R. and Rolph, G.D., 2013: HYSPLIT (HYbrid Single-Particle Lagrangian Integrated Trajectory) Model access via NOAA ARL READY Website (http://ready.arl.noaa.gov/HYSPLIT.php), NOAA Air Resources Laboratory, Silver Spring, MD.

Environmental Data Service, 1968: Maximum Persisting 12-Hour, 1000mb Dew Points (°F) Monthly and of Record. *Climate Atlas of the United States*, Env. Sci. Srv. Adm., U.S. Dept of Commerce, Washington, D.C.

Faiers, G.E., Keim, B.D., and R.A. Muller, 1997: Rainfall Frequency/Magnitude Atlas for the South-Central United States, *SRCC Technical Report 97-1*, Dept of Geography and Anthropology, Louisiana St University, Baton Rouge, LA, 41 pp.

Furl, Chad, Hatim O. Sharif, Almoutaz El Hassan, Newfel Mazari, Daniel Burtch, and Gretchen L. Mullendore, 2015: Hydrometeorological Analysis of Tropical Storm Hermine and Central Texas Flash Flooding, September 2010. *J. Hydrometeor*, **16**, 2311–2327.

GRASS (Geographic Resources Analysis Support System) GIS is an open source, free software GIS with raster, topological vector, image processing, and graphics production functionality that operates on various platforms. http://grass.itc.it/.

Hansen, E.M., L.C. Schreiner and J.F. Miller, 1982: Application of Probable Maximum Precipitation Estimates – United States East of the 105$^{th}$ Meridian. *Hydrometeorological Report No. 52*, U.S. Department of Commerce, Washington, D.C., 168 pp.

Hansen, E.M, F.K. Schwarz, and J.T Reidel, 1977: Probable Maximum Precipitation Estimates. Colorado River and Great Basin Drainages. *Hydrometeorological Report No. 49*, NWS, NOAA, U.S. Department of Commerce, Silver Spring, Md, 161 pp.

Hansen, E.M, and F.K. Schwartz, 1981: Meteorology of Important Rainstorms in the Colorado River and Great Basin Drainages. *Hydrometeorological Report No. 50*, National Weather Service, National Oceanic and Atmospheric Administration, U.S. Department of Commerce, Silver Spring, MD, 167 pp.

Hansen, E.M, Schwarz, F.K., and J.T. Riedel, 1994: Probable Maximum Precipitation- Pacific Northwest States, Columbia River (Including portion of Canada), Snake River, and Pacific Drainages. *Hydrometeorological Report No. 57*, National Weather Service, National Oceanic and Atmospheric Administration, U.S. Department of Commerce, Silver Spring, MD, 353 pp.

Hansen, E.M, Fenn, D.D., Schreiner, L.C., Stodt, R.W., and J.F., Miller, 1988: Probable Maximum Precipitation Estimates, United States between the Continental Divide and the 103$^{rd}$ Meridian, *Hydrometeorological Report Number 55A*, National weather Service, National Oceanic and Atmospheric Association, U.S. Dept of Commerce, Silver Spring, MD, 242 pp.

Hershfield, D.M., 1961: *Rainfall frequency atlas of the United States for durations from 30 minutes to 24 hours and return periods from 1 to 100 years*. Weather Bureau Technical Paper No. 40, U.S. Weather Bureau, Washington, D.C., 115 pp.

Hosking, J.R.M. (1992). "Moments or L moments? An example comparing two measures of distributional shape". The American Statistician. **46** (3): 186–189. doi:10.2307/2685210. JSTOR 2685210.

Hosking, J. R. M., and Wallis, J. R. (1997). *Regional frequency analysis: an approach based on L-moments*. Cambridge University Press, Cambridge, U.K.

Hosking, J.R.M, 2015a. L-moments. R package, version 2.5. URL: http://CRAN.R-project.org/package=lmom.

Hosking, J.R.M, 2015b. Regional frequency analysis using L-moments. R package, version 3.0-1. URL: http://CRAN.R-project.org/package=lmomRFA.

Isaaks, E.H, R.M. Srivastava, 1989. *An introduction to applied geostatistics*, Oxford University Press: New York, 592 pp.

Jennings, A.H., 1950: World's Greatest Observed Point Rainfalls, *Monthly Weather Review*, Vol. 78:1, 4-5.

Jennings, A.H., 1952: Maximum 24-hour Precipitation in the United States, *Technical Paper Number 16*, U.S. Weather Bureau, U.S. Department of Commerce, Washington, DC, 284 pp.

Juracek, K.E., C.A. Perry, and J.E. Putnam, 2001: The 1951 Floods in Kansas Revisited, U.S. Geological Survey Fact Sheet 041-01, 6 pp.

Kalnay, E., M. Kanamitsu, R. Kistler, W. Collins, D. Deaven, L. Gandin, M. Iredell, S. Saha, G. White, J. Woollen, Y. Zhu, A. Leetmaa, R. Reynolds, M. Chelliah, W. Ebisuzaki, W. Higgins, J. Janowiak, K. Mo, C. Ropelewski, J. Wang, R. Jenne, and D. Joseph, 1996: The NCEP/NCAR 40-Year Reanalysis Project. *Bull. Amer. Meteor. Soc.*, **77**, 437–471.

Kappel, W.D., Hultstrand, D.M., Tomlinson, E.M., and G.A., Muhlestein, August 2012: Site-Specific Probable Maximum Precipitation (PMP) Study for the Tarrant Regional Water District-Benbrook and Floodway Basins, Ft Worth, TX.

Kappel, W.D., Hultstrand, D.M., Tomlinson, E.M., Muhlestein, G.A., and T.P. Parzybok, September 2012: Site-Specific Probable Maximum Precipitation (PMP) Study for the Quad Cities Nuclear Generating Station, Quad Cities, IA.

Kappel, W.D., Hultstrand, D.M., Muhlestein, G.A., and D. McGlone, March 2014: Site-Specific Local Intense Precipitation (LIP) Study for the Columbia Power Station, Washington.

Kappel, W.D., Hultstrand, D.M., Muhlestein, G.A., Tomlinson, E.M., and D. McGlone, April 2014: Site-Specific Probable Maximum Precipitation (PMP) Study for the North Umpqua Basin, Oregon, prepared for PacifiCorp.

Kappel, W.D., Hultstrand, D.M., Muhlestein, G.A., Steinhilber, K., and D. McGlone, July 2014: Site-Specific Probable Maximum Precipitation (PMP) Study for the College Lake Basin, Colorado, prepared for Colorado State University.

Kappel, W.D., Hultstrand, D.M., Muhlestein, G.A., Steinhilber, K., McGlone, D., Parzybok, T.W, and E.M. Tomlinson, December 2014: Statewide Probable Maximum Precipitation (PMP) Study for Wyoming.

Kappel, W.D., Hultstrand, D.M., Muhlestein, G.A., Steinhilber, K., McGlone, D., Lovisone, S., and B. Lawrence, April 2015: Site-specific Probable Maximum Precipitation for the Thomson Dam Basin, Minnesota.

Kappel, W.D., Hultstrand, D.M., Muhlestein, G.A., Steinhilber, K., McGlone, D., Lovisone, S., and B. Lawrence, June 2015: Site-specific Probable Maximum Precipitation for the Elbow River Basin, Alberta, Canada.

Kappel, W.D., Hultstrand, D.M., Muhlestein, G.A., Steinhilber, K., McGlone, D., Parzybok, T.W., Tomlinson, E.M., and B. Lawrence, August 2015: Regional Probable Maximum Precipitation for the Tennessee Valley Authority.

Kappel, W.D., Hultstrand, D.M., Muhlestein, G.A., Steinhilber, K., and McGlone, D, August 2015: Site-Specific Probable Maximum Precipitation for the Altoona Water Authority.

Kappel, W.D., Hultstrand, D.M., Muhlestein, G.A., Steinhilber, K., McGlone, D., Parzybok, T.W., and B. Lawrence, November 2015: Statewide Probable Maximum Precipitation for Virginia.

Kappel, W.D., Hultstrand, D.M., Muhlestein, G.A., Steinhilber, K., McGlone, D., Tomlinson, E.M., and B. Lawrence, June 2015: Site-specific Probable Maximum Precipitation for the Conowingo Dam Basin, MD.

Kappel, W.D., Hultstrand, D.M., Muhlestein, G.A., Steinhilber, K., and McGlone, D, February 2016: Site-Specific Probable Maximum Precipitation for Hebgen Dam, MT.

Kappel, W.D., Hultstrand, D.M., Muhlestein, G.A., Steinhilber, K., and McGlone, D, February 2016: Site-Specific Probable Maximum Precipitation for Sylvan Dam, CO.

Kappel, W.D., Hultstrand, D.M., Muhlestein, G.A., Steinhilber, K., and McGlone, D, May 2016: Site-Specific Probable Maximum Precipitation for Warren Ohl, Upper Castanea, and Boyd Keller Dams, City of Lock Haven, PA.

Kappel, W.D., Hultstrand, D.M., Muhlestein, G.A., Steinhilber, K., and McGlone, D, February 2016: Site-Specific Probable Maximum Precipitation for North Fork Dam, PA.

Keim, B. D., and G.E. Faiers, 1999: A Comparison of Techniques to Produce Quantile Estimates of Heavy Rainfall in Air and Mountainous Environments: A Test Case in Western Texas, *J. Arid Environ.*, **44**, 267-275.

Lanning-Rush, J., Asquith, W.H. , and R.M. Slade, 1998: Extreme Precipitation Depths for Texas Excluding the Trans-Pecos Region, U.S. Geological Survey Water Resources Investigations Report 98-4099, 42p

Lott, G.A., 1952: Rain Storm of September 9–10, 1952. *Mon. Wea. Rev.*, **80**, 161–163.

Lott, G.A., 1953: The Unparalleled Thrall, Texas Rainstorm. *Mon. Wea. Rev.*, **81**, 195–203.

Lott, G.A., 1954: The World-Record 42-Minute Holt, Missouri, Rainstorm. *Mon. Wea. Rev.*, **82**, 50–59.

Maddox, R. A., Canova, F., and L. R. Hoxit, 1980: Meteorological Characteristics of Flash Flood Events over the Western United States, *Monthly Weather Review*, Vol. 108, 1866-1877.

Mcauliffe, J. P., 1921: Excessive Rainfall and Flood at Taylor, Tex. *Mon. Wea. Rev.*, **49**, 496–498.

Mesinger, F., G. DiMego, E. Kalnay, K. Mitchell, P.C. Shafran, W. Ebisuzaki, D. Jović, J. Woollen, E. Rogers, E.H. Berbery, M.B. Ek, Y. Fan, R. Grumbine, W. Higgins, H. Li, Y. Lin, G. Manikin, D. Parrish, and W. Shi, 2006: North American Regional Reanalysis. *Bull. Amer. Meteor. Soc.*, **87**, 343–360.

MGS Software, LLC, 2011: L-moments Regional Analysis Program (LRAP) Users Manual.

Miller, J.F., R.H. Frederick and R.S. Tracey, 1973: *NOAA Atlas 2, Precipitation: Frequency Atlas of the Western United States*. U.S. Dept. of Commerce, NOAA, National Weather Service, Washington DC.

Moore, James N. and Ray C. Riley, 1993: Comparison of Temporal Rainfall Distributions for Near Probable Maximum Precipitation Storm Events for Dam Design. Proceedings of the 1993 annual conference of the Association of State Dam Safety Officials, Minneapolis, MN.

National Climatic Data Center (NCDC). NCDC TD-3200 and TD-3206 datasets - Cooperative Summary of the Day

National Climatic Data Center (NCDC) Heavy Precipitation Page http://www.ncdc.noaa.gov/oa/climate/severeweather/rainfall.html#maps

National Oceanic and Atmospheric Association, Forecast Systems Laboratory FSL Hourly/Daily Rain Data, http://precip.fsl.noaa.gov/hourly_precip.html

Natural Resources Conservation Service (NRCS), Conservation Engineering Division. (2005, July). *Earth Dams and Reservoirs, TR-60.*

Nielsen, Erik R., Russ S. Schumacher, and Alexandra M. Keclik, 2016: The Effect of the Balcones Escarpment on Three Cases of Extreme Precipitation in Central Texas. *Mon. Wea. Rev.*, **144**, 119–138.

Nielsen-Gammon, J.W., F. Zhang, A.M. Odins, and B. Myoung, 2005: Extreme Rainfall in Texas: Patterns and Predictability, *Physical Geography*, Vol. 26, Is. 5.

Parzybok, T. W., and E. M. Tomlinson, 2006: A New System for Analyzing Precipitation from Storms, *Hydro Review*, Vol. XXV, No. 3, 58-65.

Patton, P. C., & Baker, V. R., 1977: Geomorphic response of central Texas stream channels to catastrophic rainfall and runoff. In D. O. Doehring (Ed.), *Geomorphology in arid regions. Proc. 8th Binghamton symposium in geomorphology, 1977.* (pp. 189-217). Allen & Unwin.

Paulsen, C.G., and J.V.B. Wells, 1952: Kansas-Missouri Floods of July 1951, U.S. Geological Survey Water Supply Paper 1139, 250 pp.

Perica, S. Martin, D., Pavlovic, S., Roy, I., Laurent, M.S., Trypaluk, C., Unruh, D., Yekta, M., and G. Bonnin, 2013: *NOAA Atlas 14 Volume 8 version 2, Precipitation-Frequency Atlas of the United States, Midwestern States* NOAA, National Weather Service, Silver Spring, MD.

Perica, S. Martin, D., Pavlovic, S., Roy, I., Laurent, M.S., Trypaluk, C., Unruh, D., Yekta, M., and G. Bonnin, 2013: *NOAA Atlas 14 Volume 9 version 2, Precipitation-Frequency Atlas of the United States, Southeastern States* NOAA, National Weather Service, Silver Spring, MD.

PRISM Mapping Methodology http://www.ocs.oregonstate.edu/prism/index.phtml

Remote Automated Weather Stations RAWS, http://www.raws.dri.edu/index.html

Reynolds, R.W., N.A. Rayner, T.M. Smith, D.C. Stokes, and W. Wang, 2002: An improved in situ and satellite SST analysis for climate. J. Climate, 15, 1609-1625.

Reynolds, R.W., T.M. Smith, C. Liu, D.B. Chelton, K.S. Casey, and M.G. Schlax, 2007: Daily High-resolution Blended Analysis for Sea Surface Temperature. *J. Climate.*, **20**, 5473-5496.

Riedel, J.T., and L.C. Schreiner, 1980: Comparison of Generalized Estimates of Probable Maximum Precipitation with Greatest Observed Rainfalls, *NOAA Technical Report NWS 25*, US Department of Commerce, NOAA, Silver Spring, Md, 46 pp.

Rogash, J., M. Hardiman, D. Novlan, T. Brice, and V. MacBlain, 2009: Meteorological Aspects of the 2006 El Paso Texas Metropolitan Area Floods. *National Weather Digest*, Vol. 33, No. 1, 78-103.

Schreiner, L.C., and J.T. Riedel, 1978: Probable Maximum Precipitation Estimates, United States East of the $105^{th}$ Meridian. *Hydrometeorological Report No. 51*, U.S. Department of Commerce, Silver Spring, Md, 242 pp.

Schoner, R. W., and S. Molansky, 1956: National Hurricane Research Project No. 3: Rainfall Associated With Hurricanes (and Other Tropical Disturbances). United States Department of Commerce.

Smith, J.A., M.L. Baeck, J.E. Morrison, and P. Sturdevant-Rees, 2000: Catastrophic Rainfall and Flooding in Texas. *J. Hydrometeor.*, **1**, 5–25.

Storm Studies – Pertinent Data Sheets, and Isohyetal Map, U.S. Department of Interior, Bureau of Reclamation, Denver, CO.

Texas Water Development Board, 1966; Symposium on Consideration of Some Aspects of Storms and Floods in Water Planning, Technical Papers presented at the Oct 7-9, 1965 ASCE, Texas Section Meeting, 170 pp.

Tomlinson, E.M., 1993: Probable Maximum Precipitation Study for Michigan and Wisconsin, Electric Power Research Institute, Palo Alto, CA, TR-101554, V1.

Tomlinson, E.M., Ross A. Williams, and Parzybok, T.W., September 2002: Site-Specific Probable Maximum Precipitation (PMP) Study for the Upper and Middle Dams Drainage Basin, Prepared for FPLE, Lewiston, ME.

Tomlinson, E.M., Ross A. Williams, and Parzybok, T.W., September 2003: Site-Specific Probable Maximum Precipitation (PMP) Study for the Great Sacandaga Lake / Stewarts Bridge Drainage Basin, Prepared for Reliant Energy Corporation, Liverpool, New York.

Tomlinson, E.M., Ross A. Williams, and Parzybok, T.W., September 2003: Site-Specific Probable Maximum Precipitation (PMP) Study for the Cherry Creek Drainage Basin, Prepared for the Colorado Water Conservation Board, Denver, CO.

Tomlinson, E.M., Kappel W.D., Parzybok, T.W., Hultstrand, D., Muhlestein, G., and B. Rappolt, May 2008: Site-Specific Probable Maximum Precipitation (PMP) Study for the Wanahoo Drainage Basin, Prepared for Olsson Associates, Omaha, Nebraska.

Tomlinson, E.M., Kappel W.D., Parzybok, T.W., Hultstrand, D., Muhlestein, G., and B. Rappolt, June 2008: Site-Specific Probable Maximum Precipitation (PMP) Study for the Blenheim Gilboa Drainage Basin, Prepared for New York Power Authority, White Plains, NY.

Tomlinson, E.M., Kappel W.D., and Parzybok, T.W., February 2008: Site-Specific Probable Maximum Precipitation (PMP) Study for the Magma FRS Drainage Basin, Prepared for AMEC, Tucson, Arizona.

Tomlinson, E.M., Kappel W.D., Parzybok, T.W., Hultstrand, D., Muhlestein, G., and P. Sutter, December 2008: Statewide Probable Maximum Precipitation (PMP) Study for the state of Nebraska, Prepared for Nebraska Dam Safety, Omaha, Nebraska.

Tomlinson, E.M., Kappel, W.D., and Parzybok, T.W., July 2009: Site-Specific Probable Maximum Precipitation (PMP) Study for the Scoggins Dam Drainage Basin, Oregon.

Tomlinson, E.M., Kappel, W.D., and Parzybok, T.W., February 2009: Site-Specific Probable Maximum Precipitation (PMP) Study for the Tuxedo Lake Drainage Basin, New York.

Tomlinson, E.M., Kappel, W.D., and Parzybok, T.W., February 2011: Site-Specific Probable Maximum Precipitation (PMP) Study for the Magma FRS Drainage Basin, Arizona.

Tomlinson, E.M., Kappel, W.D., and Parzybok, T.W., March 2011: Site-Specific Probable Maximum Precipitation (PMP) Study for the Tarrant Regional Water District, Texas.

Tomlinson, E.M., Kappel, W.D., Hultstrand, D.M., Muhlestein, G.A., and Parzybok, T.W., November 2011: Site-Specific Probable Maximum Precipitation (PMP) Study for the Lewis River basin, Washington State.

Tomlinson, E.M., Kappel, W.D., Hultstrand, D.M., Muhlestein, G.A., and Parzybok, T.W., December 2011: Site-Specific Probable Maximum Precipitation (PMP) Study for the Brassua Dam basin, Maine.

Tomlinson, E.M., Kappel, W.D., Hultstrand, D.M., Muhlestein, G.A., S. Lovisone, and Parzybok, T.W., March 2013: Statewide Probable Maximum Precipitation (PMP) Study for Ohio.

U.S. Navy Marine Climate Atlas of the World (NAVAIR50-1C-65), 1981: Volume IX, Naval Oceanographic Command Detachment, Asheville, NC.

U.S. Weather Bureau, 1946: Manual for Depth-Area-Duration analysis of storm precipitation. *Cooperative Studies Technical Paper No. 1*, U.S. Department of Commerce, Weather Bureau, Washington, D.C., 73pp.

U.S. Weather Bureau, 1951: Tables of Precipitable Water and Other Factors for a Saturated Pseudo-Adiabatic Atmosphere. *Technical Paper No. 14*, U.S. Department of Commerce, Weather Bureau, Washington, D.C., 27 pp.

U.S. Weather Bureau, 1952. *Maximum 24-Hour Precipitation in the United States*. Technical Paper No. 16, U.S. Department of Commerce, Hydro-meteorological Section.

Weather Underground, http://www.wunderground.com/stationmaps/

Williams-Sether, Tara, Asquith, W.H., Thompson, D.B., Cleveland, T.G., and Fang, Xing, 2004, Empirical, dimensionless, cumulative-rainfall hyetographs developed from 1959–86 storm data for selected small watersheds in Texas: U.S. Geological Survey Scientific Investigations Report 2004–5057, 132 p.

World Meteorological Organization, 1986: Manual for Estimation of Probable Maximum Precipitation, *Operational Hydrology Report No 1*, 2nd Edition, WMO, Geneva, 269 pp.

World Meteorological Organization, 2009: Manual for Estimation of Probable Maximum Precipitation, *Operational Hydrology Report No 1045*, WMO, Geneva, 259 pp.

Worley, S.J., S.D. Woodruff, R.W. Reynolds, S.J. Lubker, and N. Lott, 2005: ICOADS Release 2.1 data and products. *Int. J. Climatol. (CLIMAR-II Special Issue)*, **25**, 823-842.